Identification of the underlying mechanism of the c.192G>C mutation in the *DJ-1* gene and functional characterisation in patient-based cellular models of Parkinson's disease *ex vivo*

Dissertation

zur Erlangung des Grades eines
Doktors der Naturwissenschaften

der Mathematisch-Naturwissenschaftlichen Fakultät
und
der Medizinischen Fakultät
der Eberhard-Karls-Universität Tübingen

vorgelegt
von

Carolin Obermaier

aus Sindelfingen, Deutschland

Mai 2015

DISSERTATION

Defense held on 13/07/2015 in Tübingen, Germany

to obtain the degree of

DOCTEUR DE L'UNIVERSITÉ DU LUXEMBOURG

EN *BIOLOGIE*

AND

DOKTOR DER EBERHARD-KARLS-UNIVERSITÄT TÜBINGEN

IN *NATURWISSENSCHAFTEN*

by

Carolin OBERMAIER
Born on 19 July 1985 in Sindelfingen (Germany)

IDENTIFICATION OF THE UNDERLYING MECHANISM OF THE C.192G>C MUTATION IN THE *DJ-1* GENE AND FUNCTIONAL CHARACTERISATION IN PATIENT-BASED CELLULAR MODELS OF PARKINSON'S DISEASE *EX VIVO*.

Date of oral exam: 13th of July 2015

President of the University of Tübingen: Prof. Dr. Bernd Engler

…..………………………………………………

Chairman of the Doctorate Board of the University of Tübingen: Prof. Dr. Mathias Jucker

…..………………………………………………

Dekan der Math.-Nat. Fakultät: Prof. Dr. W. Rosenstiel

…..………………………………………………

Dekan der Medizinischen Fakultät: Prof. Dr. I. B. Autenrieth

…..………………………………………………

President of the University of Luxembourg: Prof. Dr. Rainer Klump

…..………………………………………………

Supervisor from Luxembourg: Prof. Dr. / PD Dr. / Dr. Rejko Krüger

…..………………………………………………

Supervisor from Tübingen: Prof. Dr. / PD Dr. / Dr. Bernd Wissinger

……………………………………………………

Dissertation Defence Committee:

Committee members: Prof. Dr. / PD Dr. / Dr. Bernd Wissinger…………………………………………..

Prof. Dr. / PD Dr. / Dr. Olaf Riess……………………………………………….…

Prof. Dr. / PD Dr. / Dr. Rejko Krüger…………………………………………….…

Prof. Dr. / PD Dr. / Dr. Rudi Balling………………………………………………

Prof. Dr. / PD Dr. / Dr. Daniela Vogt-Weissenhorn……………………………….

Prof. Dr. / PD Dr. / Dr. Marco Baralle………………………………………………

Affidavit / Declaration:

I hereby declare that I have produced the work entitled "Identification of the underlying mechanism of the c.192G>C mutation in the *DJ-1* gene and functional characterisation in patient-based cellular models of Parkinson's disease *ex vivo*.", submitted for the award of a doctorate, on my own (without external help), have used only the sources and aids indicated and have marked passages included from other works, whether verbatim or in content, as such. I swear upon oath that these statements are true and that I have not concealed anything. I am aware that making a false declaration under oath is punishable by a term of imprisonment of up to three years or by a fine.

Luxembourg, the ....

                                Date   Signature

Acknowledgements

Table of Contents

III

List of abbreviations

AA	Ascorbic acid		**MEF**	Mouse embryonic fibroblasts
AD	Autosomal dominant		**MIM**	Mendelian inheritance in man
ALP	Autophagy lysosomal pathway		**MMP**	Mitochondrial membrane potential
AR	Autosomal recessive		**mtDNA**	Mitochondrial DNA
BBB	Blood-brain barrier		**MTT**	Thiazolyl blue tetrazolium bromide
B.C.	Before Christ		**NGS**	Next generation sequencing
cDNA	Complimentary deoxyribonucleic acid		**OMM**	Outer mitochondrial membrane
CNS	Central nervous system		**PCR**	Polymerase chain reaction
D. melanogaster	*Drosophila melanogaster*		**PD**	Parkinson's disease
DA	Dopaminergic		**PEG**	Polyethylene glycol
DMSO	Dimethyl sulfoxide		**PORN**	Poly-DL-ornithine hydrobromide
ESC	Embryonic stem cells		**pre-mRNA**	Precursor mRNA
ETC	Electron transport chain		**qPCR**	Real-time PCR
SpeU1	Specific U1 snRNP		**ROS**	Reactive oxygen species
FA	Formaldehyde		**rtPCR**	Reverse transcription PCR
FD	Familial Dysautonomia		**Rv**	Reverse
Fwd	Forward		**SDS-PAGE**	One-dimensional discontinuous sodium lauryl sulfate polyacrylamide gel electrophoresis
GWAS	genome-wide association study			
H₂O₂ H_2O_2	Hydrogen peroxide		**smNPCs**	Small molecule neural precursor cells
HEK cells	Human embryonic kidney cells		**SNCA**	α-synuclein
hnRNPs	Heterogeneous nuclear ribonucleo-proteins		**snRNA**	Small nuclear RNA
ICC	Immunocytochemistry		**SR proteins**	Serine/arginine-rich proteins
Intron	Intervening sequence		**TALEN**	Transcription activator-like effector nuclease
iPSC	Induced pluripotent stem cells		**TMRE**	Tetramethylrhodamine, methyl ester
LRRK2	Leucine-rich repeat kinase 2		**UPS**	Ubiquitin proteasome system
LTD	Long-term depression		**U snRNP**	Uridine-rich small nuclear ribonucleoproteins
LTP	Long-term potentiation		**Wt**	Wildtype
mDA neurons	Midbrain dopaminergic neurons		**ZFN**	Zinc finger nuclease

Abstract/Summary

Parkinson's disease (PD) is the second most common neurodegenerative disease and characterised by a progressive loss of dopaminergic neurons in the *substantia nigra pars compacta* and in other brain regions. Homozygous loss-of-function mutations in the *DJ-1* gene (*PARK7*) are a rare cause of familial early-onset PD.

The protein encoded by *PARK7* is involved in a variety of biological processes including transcriptional regulation, chaperone-like functions, oxidative stress response and mitochondrial protection.

In the present study, we deciphered novel molecular mechanisms underlying the pathogenicity of the c.192G>C *DJ-1* mutation previously predicted to lead to a p.E64D amino acid exchange in the DJ-1 protein.

To analyse the c.192G>C *DJ-1* mutation, we generated and characterised different *ex vivo* patient-based cellular models including patient-derived primary fibroblasts, immortalised fibroblasts, induced pluripotent stem cells (iPSCs), iPSC-derived small molecule neuronal precursor cells (smNPCs) as well as iPSC-derived midbrain-specific dopaminergic (mDA) neurons.

Analyses of DJ-1 expression in these patient-derived model systems from homozygous carriers of the c.192G>C *DJ-1* mutation unexpectedly revealed that this mutation leads to the loss of DJ-1 protein in these cell types. Further experiments using qPCR and an *in vitro* splicing assay showed a splicing defect causing complete skipping of the mutation-carrying exon 3 in the pre-mRNA. After deciphering the pathogenic mechanism, we developed a targeted genetic rescue strategy of the pathological skipping of exon 3. This was performed by using a specific U1 snRNA that specifically binds to the mutated *DJ-1* pre-mRNA and allows for the re-induction of physiological splicing.

In addition, we extended our strategy by first candidate approaches aiming at a pharmacological rescue that may offer novel causative treatment options in patients carrying the c.192G>C *DJ-1* mutation as well as for other diseases caused by the same mutational mechanism.

Beyond the molecular genetic characterisation, we developed different patient-based cellular models and addressed the functional effects of loss of DJ-1 protein in different patient-derived cells carrying the c.192G>C *DJ-1* mutation (human fibroblasts, iPSC-derived mDA neurons).

These analyses revealed mitochondrial impairments upon loss of DJ-1 protein in fibroblasts, including fragmentation and reduced branching of mitochondria as well as a reduced mitochondrial membrane potential compared to healthy controls. The results correlate with our observations in primary cells from DJ-1 knockout mice and support the idea of a conserved role of DJ-1 in maintaining mitochondrial function. Moreover, mDA neurons of the index patient carrying the homozygous c.192G>C *DJ-1* mutation showed increased lesion rates of mtDNA and no increase in mtDNA copy numbers, suggesting a lack of compensatory capacity.

Our data substantially contribute to the understanding of mechanisms and functions of *DJ-1* mutations in PD pathogenesis, in particular focusing on mitochondrial phenotypes upon loss of DJ-1 in different human *ex vivo* models. This underlines the role of DJ-1 as an important key player in the response to oxidative stress and the maintenance of proper mitochondrial function and homeostasis.

Overall, we show that the fibroblasts with an inherited c.192G>C *DJ-1* mutation, mDA neurons differentiated from iPSCs of these human fibroblasts and the DJ-1 knockout mice constitute excellent knockout model systems to further dissect the role of *DJ-1* in neurodegeneration in PD. This also offers human DJ-1 knockout models for future isogenic control experiments with a restituted endogenous DJ-1 background. Sequentially, it is possible to test whether disease related phenotypes might be rescued by reintroducing DJ-1 or correcting the defective splicing.

Finally, the discovery of the underlying mechanism of the c.192G>C *DJ-1* mutation opens up novel opportunities for a first genetic and maybe even pharmacological causative treatment for PD.

1 Introduction

1.1 Parkinson's disease

Parkinson's disease (PD) is the second most common neurodegenerative brain disease after Alzheimer's disease. The characteristic motor symptoms including rigidity, imbalance and uncontrollable shaking are all familiar to the general public. To date, there is no cure for PD and motor symptoms can only be alleviated to increase the quality of life of patients. Overall, 2% of the world's population over 65 suffers from this debilitating disease and the incidence of PD is set to double in the next 20 years due to the demographic development of the population (people are living longer and the world's population is growing) (Elbaz et al., 2002, Van Den Eeden et al., 2003).

Amongst other famous people like Muhammad Ali, Johnny Cash, Adolf Hitler and Pope John Paul II who suffered from PD, is Michael J. Fox - who developed the disease very early in life. He established the Michael J. Fox Foundation, which raises money for research through which we will hopefully be able to eventually decipher the cause of the disease.

1.1.1 History of PD

By the time James Parkinson formally described PD in 1817, the illness had been known for centuries and single cardinal symptoms had been mentioned in many different old texts (Stern, 1989). The oldest records about PD symptoms like palsies and tremor are from 2500 B.C. They are found in ancient Indian texts about Ayurvedic medicine by Agnivesha (Stern, 1989). But also an old Egyptian papyrus from 1200 B.C. mentions "Parkinsonian" dribbling (Stern, 1989). Later, around 500 B.C., PD symptoms are also mentioned in an old Chinese medical text (Zheng, 2009). The writings of the Greek physician Galen who had a lot of influence in ancient times, mention tremor and gait disorders, he writes about "troubled limbs" (Stern, 1989). Tremor was also described by Leonardo da Vinci who writes about involuntary movements "without permission of the soul" (Calne et al., 1989). It was in 1690 when the Hungarian doctor Ferenc Pápai Páriz in his work "Pax corporis" describes the four cardinal symptoms of PD in Hungarian for lay public (Bereczki, 2010). In his monograph entitled "An essay on the Shaking Palsy", James Parkinson writes about 6 patients suffering from the "Shaking Palsy", but he also acknowledges earlier descriptions of the symptoms by other people like Boissier de Sauvage who wrote about compulsive tremor in 1768 and Sylvius de la Böe who already mentions tremor in 1680 (Stern, 1989). Interestingly, James Parkinsons' essay combines early symptoms with a late stage of the disease "The disease is of long duration: to connect, therefore, the symptoms which occur

in its later stages with those which mark its commencement, requires a continuance of observation of the same case, or at least a correct history of its symptoms even for several years" (Parkinson, 2002). Interestingly as well is that he also describes enteric symptoms already. In 1861, Jean-Martin Charcot rewarded Parkinsons' work by calling PD "Maladie de Parkinson". The French physician completed the work with a comprehensive description of the symptoms (Charcot, 1877). Approximately 100 years after James Parkinson described PD, it was Frederic Lewy who reported on one of the main characteristics of PD, which is now named Lewy bodies. He described intraneuronal inclusions in neurons of the brain of PD patients during autopsy (Lewy, 1912). Seven years later, Constantin Tretiakoff writes about the involvement of the *substantia nigra* in PD (Tretiakoff, 1919). In 1957 and 1958 Carlsson descirbes that akinetik effects can be reversed by an intravenous injection of the dopamine (and noradrenaline) precursor, 3,4-dihydroxyphenylalanine (DOPA) (Carlsson et al., 1957, Carlsson et al., 1958). Only one year went by from the discovery that levels of the neurotransmitter dopamine are reduced in the brain of PD patients, or more specifically the striatum (Ehringer and Hornykiewicz, 1960), to the first treatment with L-dopa, which is a metabolic precursor of dopamine (Birkmayer and Hornykiewicz, 1961). In the beginning, L-dopa was administered intravenously (Birkmayer and Hornykiewicz, 1961), however the oral administration as PD treatment has been established since 1968 (Cotzias et al., 1969). Since that time, the treatment has not changed markedly, however several new important findings were made. In 1983, William Langston reported about young patients who suddenly acquired PD symptoms after having taken drugs with an impurity (Langston et al., 1983). This neurotoxin 1-methyl-4-phenyl-1, 2, 3, 6-tetrahydropyridine (MPTP) is the first described environmental factor causing PD symptoms. The first genetic cause of PD was found in 1997 by Polymeropoulos and colleagues who described the first PARK gene *α-synuclein* (*SNCA*) (Polymeropoulos, 1997). PARK2 was found one year later (Kitada, 1998) as a cause of autosomal recessive PD and in 2003, PARK7 encoding DJ-1 was published as a cause of early-onset PD autosomal PD (Bonifati, 2003). To date, there are 21 PARK genes published. Current methods for the identification of PD genes like next-generation sequencing allowed to identify new monogenic forms of PD (Chartier-Harlin et al., 2011, Edvardson et al., 2012, Quadri et al., 2013). With the increasing use of large genome-wide association study (GWAS) meta-analyses in 2011, new putative genes associated with PD have been identified (Nalls, 2011).

Today, we celebrate the World Parkinson's Day on April 11th - James Parkinson's birthday – and wear the red James Parkinson tulip as a symbol for PD.

1.1.2 **Epidemiology** (Greek: *epi -* on, *demos -* people, *logos -* study of) **of Parkinson's disease**

The major issues of analysing and comparing different epidemiological studies are the huge heterogeneity of the cohorts, differences in the evaluation of diagnostic criteria as well as the methodology of the various studies. This accounts not only for the high variation between different studies with regards to prevalence and incidence (Muangpaisan et al., 2011, von Campenhausen et al., 2005), but also to morbidity and mortality (Macleod et al., 2014). In PD, the prevalence increases with age. In the age group of 40 to 49 years, the prevalence is 41 per 100,000, this increases to 428 per 100,000 in individuals between 60 and 69 years of age and that further increases significantly to 1,903 per 100,000 in the group of people over 80 (worldwide) (Pringsheim et al., 2014). The overall worldwide prevalence (over age 40) is 315 per 100,000 (Pringsheim et al., 2014). If these statistics are applied to the world's population of people over age 40 from 2012 one gets to 7.5 million people in the world suffering from PD (Ross and Abbott, 2014). When comparing the prevalence of different continents, a geographic variation can be seen. Indeed, Asia has a lower prevalence than South America, Europe, North America and Australia (Ross and Abbott, 2014). Interestingly, a recent study comparing the differences in prevalence between men and women showed that the prevalence in women was not lower in all age groups (Twelves et al., 2003). However, it could be concluded that the incidence in men is slightly higher than in women. Additionally, men seem to have an earlier age of onset of disease (Twelves et al., 2003) while women usually show more benign phenotypes and disease progression is slower (Haaxma et al., 2007).

In a study where projections were made to calculate the number of people with PD in Western Europe's five most and the world's ten most populous nations, the authors concluded that 8.7 to 9.3 million people will be suffering from PD by 2030 (Dorsey et al., 2007).

Another interesting aspect is the effect of environmental factors. The most replicated environmental factor, which reduces the risk of getting PD, is smoking. It is also the most consistent factor, which impressively reduces the risk of developing PD by 60 % (Ross and Abbott, 2014). Other factors that are thought to be protective include coffee, tea, vitamin D and exercise (Ross et al., 2000). On the other hand, exposure to pesticides such as the insecticides rotenone and permethrin and the herbicides paraquat and 2, 4- dichlorophenoxyacetic acid as well as some organochlorines and metals such as high dose manganese increase the risk of getting the disease (Abbott et al., 2003, Kalantzi et al., 2001).

Although the overall mortality in PD patients is reduced, it is difficult to estimate an overall number of PD deaths. A recent review came up with mortality ratios between 1.2 and 2.4 (Macleod et al., 2014). Interestingly, the main causes of death are similar to the ones in the healthy population, including cardiovascular diseases (Ho et al., 1989). The biggest concern for patients and their relatives is not an early death but rather reduced quality of life. Instead of increasing longevity, they are more interested in being able to live independently and not suffer from depression and other non-motor symptoms such as sleep disturbances, constipation or smell impairment (Ross and Abbott, 2014).

1.1.3 Clinical features and treatment of the disease

Until to date there are no therapies available which slow or halt the underlying neurodegenerative process of this very common disease, as the loss of neurons cannot be stopped. At least a symptomatic treatment replacing the dopaminergic deficit or treating pathological oscillations of neuronal populations exist.

The mean age of onset of PD is 65 years (de Rijk et al., 2000) and the diagnosis is mainly based on the clinical investigation requiring structural and only rarely functional brain imaging (Hughes et al., 1992). Interestingly, years before the first symptoms appear the A9 dopaminergic pigmented neurons in the *substantia nigra pars compacta* start to die already (Ma et al., 1997). This can be seen by a white appearance of this region compared to a healthy brain. Only once 30 % of these neurons are gone the motor symptoms occur due to less dopamine in the striatum (Greffard et al., 2006, Ma et al., 1997). The reason is a compensatory increased release of dopamine of 50 % to 70 % in the remaining neurons (de la Fuente-Fernandez et al., 2011, Lee et al., 2000). There are even direct correlations between cell loss and motor dysfunction (Halliday et al., 2006, Jellinger and Paulus, 1992). The most common medications applied for treating motor symptoms in PD belong to four groups: Levodopa plus peripheral dopa decarboxylase inhibitors (Levodopa-PDDI), Dopamine agonists, monoamine oxidase type B inhibitors (MAOBIs) and catechol-O-methyl-transferase inhibitors (COMTIs).

Although the motor symptoms are most recognised by the public, surveys tell that patients suffer more from the non-motor symptoms (Breen and Drutyte, 2013). These symptoms have a brought range and can be classified in four groups:

1) Neuropsychiatric symptoms (for example depression and dementia),
2) Autonomic symptoms (for example Constipation and Nausea),
3) Sleep disturbances (for example vivid dreaming and insomnia) and
4) Sensory symptoms (like for example olfactory deficits and taste deficits).

The treatment of the nonmotor symptoms of course depends on the symptoms, therapies are available for most of the symptoms, but like for all therapies there are side effects. All treatments can be supported by physiotherapy, logopedics and occupational therapy.

Furthermore since in 1947 Spiegel and Wycis first used deep brain stimulation it is another option for treatment (Fukaya and Yamamoto, 2015). By implanting electrodes into the *nucleus subthalamicus* overactive neurons can be inhibited. The advantage of this method is that the complications of dopaminergic medication like motor fluctuations can be effectively treated and medication can be reduced together with improved motor abilities (Kleiner-Fisman et al., 2003, Deuschl et al., 2006).

1.1.4   Contribution of genes in Parkinson's disease

In 1997, the first genetic cause of PD was discovered (Polymeropoulos, 1997). Since then, 20 genetic causes have been identified (Table 1) and also approximately 28 risk loci for PD (Nalls et al., 2014). Even though most forms of PD are sporadic, analysing the genetics of the familial cases helped to get important insight into the etiology of the disease. About 11 % of all PD patients have a family history with one or more other PD mutation-carrying person in the family (Shino et al., 2010). The monogenic forms can be distinguished by inheritance between autosomal dominant (AD) and autosomal recessive (AR) forms (Table 1).

Mutations in *SNCA*, locus PARK1, are rare and include five point mutations which cause late onset PD and gene duplications and triplications which have been associated to an early onset of the disease (Corti et al., 2011).

Mutations in the leucine-rich repeat kinase 2 (*LRRK2*), locus PARK8, are the most common cause for an AD inherited PD (Biskup and West, 2009, Zimprich et al., 2004a, Zimprich et al., 2004b). The most common mutation in the Caucasian population is the G2019S mutation (Goldwurm et al., 2005). *LRRK2* is a large gene consisting of 51 exons. The protein contains a GTPase and a kinase domain as well as several protein-protein interaction domains (Gasser, 2009).

Homozygous mutations of the autosomal recessively inherited forms of PD cause an early onset of the disease.

The most common mutations in autosomal recessively inherited PD are in *Parkin*, locus PARK2, which was the second monogenic form identified (Lucking et al., 2000, Kitada, 1998). *Parkin* encodes for an E3 ubiquitin ligase.

Mutations in *PINK1*, PARK6 locus, are rare and account for 1 % to 8 % of the cases with early onset (Valente et al., 2004a). *PINK1* stands for phosphatase and tensin homologue

(PTEN) - induced putative kinase 1. The protein is a ubiquitously expressed kinase with a mitochondrial targeting sequence, a serine-threonine kinase domain and an autoregulation domain (Beilina et al., 2005, Sim et al., 2006, Valente et al., 2004b, Zhou et al., 2008). *PINK1* plays a role in outer mitochondrial membrane (OMM) integrity as well as mitophagy [*PINK1* function reviewed in (Bonifati et al., 2005, Li et al., 2005, Rogaeva et al., 2004)].

Table 1: **Monogenic causes of PD.**

The table shows the chromosomal location of the disease gene, the name of the gene, the type of mutations that have been found for the respective gene as well as when and by whom the gene has first been described. The locus names of the genes stand for Parkinson (PARK) and are numbered in the order the respective loci have been identified. MIM stands for mendelian inheritance in man and the MIM No. is part of a database for all known genetically inherited diseases.

(MIM No. = Mendelian Inheritance in Man; Chr. = Chromosome)

Locus	MIM No.	Inheritance	Chr.	Gene	Mutation	First described by
PARK1	601508	AD	4q21-23	*α-Synuclein*	PM	(Polymeropoulos, 1997)
PARK2	600116	AR	6q25.2-27	*Parkin*	Del/Ins/Dupl/ Tripl/PM	(Kitada, 1998)
PARK3	602404	AD	2p13	-	-	(Gasser et al., 1998)
PARK4	605543	AD	4q21-23	*α-Synuclein*	Dupl, Tripl	(Singleton et al., 2003)
PARK5	191342	AD	4p14	*UCH-L1*	PM	(Leroy et al., 1998)
PARK6	605909	AR	1p35-36	*PINK-1*	PM	(Valente et al., 2004b)
PARK7	606324	AR	1p36	*DJ-1*	Del, PM	(Bonifati et al., 2002)
PARK8	607060	AD	12cen	*LRRK2*	PM	(Zimprich et al., 2004a)
PARK9	606693	AR	1p36	*ATP13A2*	PM	(Ramirez et al., 2006)
PARK10	606852	AD	1p32	-	-	(Hicks et al., 2002)
PARK11	607688	AD	2q36-37	*GIGYF2*	PM	(Lautier et al., 2008)
PARK12	300557	nd	Xq21-25	-	-	(Pankratz et al., 2002)
PARK13	610297	AD	2p12	*Omi/HtrA2*	PM	(Strauss et al., 2005)
PARK14	610297	AR	22q13	*PLA2G6*	PM	(Gregory et al., 1993)
PARK15	610297	AR	22q12-13	*FBXO7*	PM	(Di Fonzo et al., 2009)
PARK16	613164	AR	1q32	-	-	(Satake et al., 2009)
PARK17	614203	AD	16q13	*VPS35*	PM	(Zimprich et al., 2011)
PARK18	614251	AD	3q27.1	*EIF4G1*	PM	(Chartier-Harlin et al., 2011)
PARK19	615528	AR	1p31.3	*DNAJC6*	Del, PM	(Edvardson et al., 2012)
PARK20	615530	AR	21q22.11	*SYNJ1*	PM	(Quadri et al., 2013)
PARK21	614334	AD	3q22.1	*DNAJC13*	PM	(Vilarino-Guell et al., 2014)

Mutations in *ATP13A2*, locus PARK9, *PLA2G6*, locus PARK14 and *FBXO7*, locus PARK15 encode even rarer forms of recessively inherited parkinsonism usually with an early onset of below 30 years and may be associated with atypical symptoms like spasticity, early dementia and predominant dystonia (Di Fonzo et al., 2009, Paisan-Ruiz et al., 2009, Ramirez et al., 2006).

VPS35, e*IF4G1*, *DNAJC6* and *SYNJ1* are more recently identified genes. Before the identification of new PD genes was based on analysing large pedigrees with multiple affected, linkage analysis and subsequent sequencing of candidate genes in the identified region. The new genes defining PARK7 to PARK20 loci however were identified making use of the new technique of next-generation sequencing allowing to directly sequence whole exomes in affected family members and controls (Singleton et al., 2013).

Another recent publication aimed to find novel PD genes by whole-genome and exome sequencing of a Japanese family with PD. In this study, a potential new autosomal dominantly inherited PD gene called *CHCHD2* has been identified (Funayama et al., 2015). Further genetic studies in independent cohorts and populations are warranted in order to confirm the pathogenicity of this new gene.

Genereally there is a fluent transition from monogenic forms, to risk factors and to common variants with a small effect size.

Monogenic forms are rare, but have a high effect size and account for Mendelian diseases. Variants with lower frequencies and intermediate effect can be distinguished from common variants with a low effect size which are mainly identified by genome wide association. Rare variants with a low effect size are very hard to indetify by genetic means, in contrast to common variants with a high effect, but these cases are only very rare (Manolio et al., 2009).

Some of the PARK loci do not only carry mutations which cause monogenic forms of PD, but also carry additional mutations in the coding or non-coding regions, that are associated with a higher risk for developing PD. Such as the p.G2385R mutation in *LRRK2* which has been found to cause an approximately 2-fold increase in risk for PD in the Asian population (Bonifati, 2007).

One example for a common variant with a small effect size is a polymorphism in the promoter region of *SNCA,* which was shown to increase the risk for developing PD and subsequently confirmed by unbiased genome-wide association studies (Kruger et al., 1999, Simon-Sanchez et al., 2009).

An example for a rare variant with a substantial effect is glucocerebrosidase (*GBA*), which causes an approximately 5-fold increase for PD in the presence of a single *GBA* mutation (Sidransky et al., 2009). There are also other genes, todate there are 28 known, which are not PARK loci that have been associated with an increased risk for PD using GWAS, examples are *MAPT*, *NAT2*, *INOS2A*, *GAK*, *HLA-DRA*, and *APOE* (Nalls et al., 2014).

1.1.5 Pathophysiological pathways of Parkinson's disease

PD is seen as a heterogenous disease and there is no common pathophysiological pathway for all PARK loci, because there are too many gaps in our current knowledge. There are, however, several pathways shared by at least some PD genes (Hardy et al., 2006, Antony et al., 2013). These hallmark pathways include

- synaptic dysfunction including exo- and endocytosis:

PD includes motor and cognitive symptoms, which are known to be impaired due to the progressive loss of dopaminergic neurons. In order to work efficiently, motor and cognitive functions require the synapse to be modified based on the activity, such as long-term depression (LTD) and long-term potentiation (LTP). LTD and LTP are controlled by the release of dopamine at the synaptic terminals (Picconi et al., 2012). Different PD genes play a role at the presynaptic site. For example, the release of dopamine into the synaptic cleft depends amongst other things on the transport of the vesicle.

SNCA seems to have a critical function by modulating neurotransmitter vesicle function (Bisaglia et al., 2005, Ulmer et al., 2005). But also LRRK2 regulates the release of vesicles as well as axonal polarity (Trinh and Farrer, 2013).

- protein degradation including proteolytic degradation and autophagy as well as protein misfolding:

A hallmark of PD is Lewy body pathology. These inclusion bodies are aggregates of mainly α-synuclein and if they are found in neurites they are referred to as Lewy neurites. These abnormal aggregates are a sign of impaired degradation of either misfolded or altered proteins (Spillantini et al., 1997). The ubiquitin proteasome system (UPS) as well as the autophagy lysosomal pathway (ALP) are systems to remove these types of proteins. The PD gene *ATP13A2* for example is known to play a role in the APL including impaired lysosomal acidification, decreased proteolytic processing of lysosomal enzymes, reduced degradation of lysosomal substrates and diminished lysosomal-mediated clearance of autophagosomes (Dehay et al., 2012). A-synuclein is known to easily misfold and the UPS (largely under physiological conditions) and

ALP (upon increased/pathological conditions) contribute to the clearance of α-synuclein aggregates, fibrils and oligomers [reviewed in (Ebrahimi-Fakhari et al., 2012)].

- <u>mitochondrial dysfunction through oxidative stress (ROS and metals) and neuroinflammation as well as calcium homeostasis (see 1.1.6).</u>

1.1.6 Mitochondrial involvement in PD

MPTP was the first environmental factor described in literature that was shown to cause PD symptoms (Langston et al., 1983). Unlike the typical slow and progressive disease development in typical sporadic PD, MPTP-induced PD occurs via an acute toxic insult. MPTP itself does not appear to be toxic, but its oxidised form MPP^+. Both are able to cross the blood-brain barrier (BBB) and MPP^+ is taken up by dopaminergic (DA) neurons (Nicklas et al., 1985). There, it inhibits mitochondrial respiration by reducing complex I, which is a NADH ubiquinone oxidoreductase of the electron transport chain (ETC) leading to dysfunctional mitochondria and increased oxidative stress (Dauer and Przedborski, 2003).

Not only environmental toxins hinted at a mitochondrial involvement in neurodegeneration in PD, but also biochemical and pathoanatomical studies of PD brains showed an approximately 30 % reduced complex I activity in the *substantia nigra* and frontal cortex of post mortem PD brains (Parker et al., 2008, Schapira et al., 1989, Janetzky et al., 1994, Mann et al., 1994, Schapira et al., 1990).

Additionally, PD-associated genes such as *PINK1* and *Parkin* encoding mitochondrial proteins linked impaired mitochondrial function to neurodegeneration in PD (Schapira, 1999, Strauss et al., 2005, Valente et al., 2004b).

Mitochondrial can be affected at different instances in neurodegeneration in PD (Figure 1):

1) Complex I activity,
2) Oxidative stress,
3) Bioenergetics,
4) Quality control and clearance,
5) Homeostasis,
6) Dynamics and biogenesis and
7) Transport
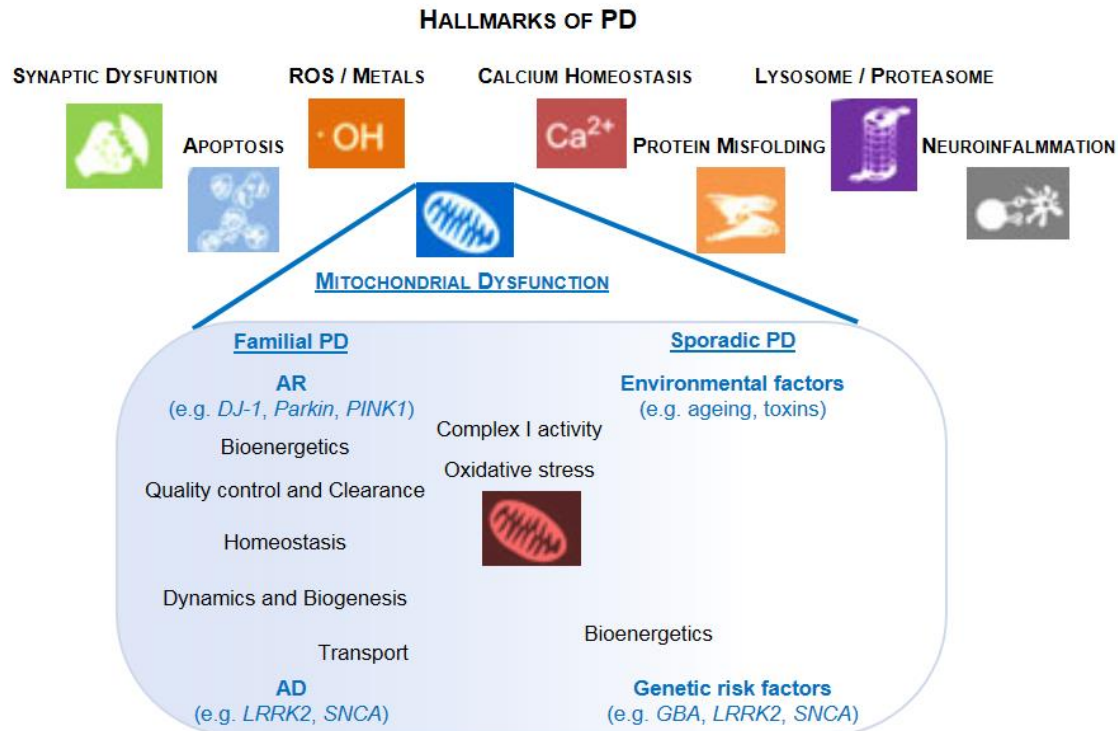
Figure 1: **Hallmarks and aetiology of PD and possible links to mitochondrial features.**

PD is characterised by certain hallmarks and is characterised by different cellular dysfunctions which may be shared amongst the indicated hallmarks. Familial PD is caused by autosomal dominantly or autosomal recessively inherited mutations in different PD genes. These mutations influence different mitochondrial features such as bioenergetics, quality control, dynamics and transport and homoeostasis. Sporadic PD is a complex disease, which is caused by an interplay of genetic risk factors and environmental factors like toxins but also aging. In this case, mitochondrial features are also affected.

Figure modified from (Exner et al., 2012, Antony et al., 2013).

1) Complex I activity:

Beside MPTP, other toxins were used in animal models to define the impact of a complex I deficiency in PD. Rotenone for example not only inhibits complex I in the central nervous system (CNS) of mouse and rat models. Animal studies using rotenone showed that even a mild reduction of complex I activity can cause different hallmarks of PD in animal models such as the degeneration of the *substantia nigra pars compacta* and protein inclusions similar to Lewy bodies (Drolet et al., 2009). Another interesting finding linking mitochondrial ROS, mainly produced by complex I and III of the respiratory chain (Sugioka et al., 1988, Turrens and Boveris, 1980), to PD was the discovery that PD patients carry more mutations in the mitochondrial DNA (mtDNA) compared to age-matched controls (Bender et al., 2006). Thirteen genes encoding subunits of the respiratory chain are encoded by the mtDNA. The majority, seven, of them encode subunits of complex I, which makes this subunit particularly vulnerable to damage through point mutations and deletions [reviewed

in (Larsson, 2010, Reeve et al., 2008)]. Such mutations in the mtDNA can be inherited maternally or acquired over time through damage of the mtDNA by ROS or polymerase γ deficiency. The latter ones are more prone to occur in cells with a high-energy demand such as neurons and muscles.

Mutations in the human *POLG1* gene, encoding the DNA polymerase γ which exerts its functions in the mitochondria, co-segregate with parkinsonism [reviewed in (Orsucci et al., 2011)]. In support, mice expressing a mutant polymerase γ accumulate mtDNA mutations and show phenotypes of premature aging (Kujoth et al., 2005, Trifunovic et al., 2004).

2) <u>Oxidative stress:</u>

Oxidative stress can be caused by reactive oxygen species (ROS) and by dopamine. ROS are mainly produced by complex I and III of the ETC and under normal conditions function as signal transducers (Fomenko et al., 2011). Once a certain amount of ROS is exceeded, it cannot be compensated anymore and oxidative stress occurs. This stress can lead to damage of lipids, proteins and DNA and such oxidatively damaged molecules have been found in brains of PD patients (Alam et al., 1997, Dexter et al., 1989, Floor and Wetzel, 1998).

Interestingly, the neurotransmitter dopamine itself can also mediate an increase in oxidative stress and may explain part of the vulnerability of dopaminergic neurons in PD. Dopamine is metabolised by monoamine oxidase or by auto-oxidation which can lead to cytotoxic ROS followed by neuromelanin formation (Sulzer et al., 2000).

3) <u>Bioenergetics:</u>

Mitochondria are dynamic organelles and largely devoted to nutrient metabolism and bioenergetics. Different mitochondrial functions are regulated in response to different energy demands (Little et al., 2011) and bioenergetics dictate the response of mitochondria. Each cell type has a different bioenergetic status and it has been shown for example that fluctuations in energy demands lead to altered fission and fusion of mitochondria (Ding et al., 2010). By fission of mitochondria new mitochondria are created. During cell division this process makes sure that new cells have an adequate number of mitochondria. At the same time fission acts as quality control mechanism by which damaged mitochondria can be removed (Chen and Chan, 2010). Also fusion of mitochondria can help in case of not too severly damaged mitochondria by mixing contents of partially damaged mitochondria (Youle and van der Bliek, 2012). Both fission and fusion are important for mitochondrial quality control and need to be balanced. The bioenergetic status therefore is relevant for disease development (Van Laar and Berman, 2013).

4) Quality control and clearance:

Mitochondrial quality control and clearance are controlled at different instances, e.g. chaperones for intramitochondrial molecular quality control, and by the PD genes *PINK1*, *Parkin* and *DJ-1* for organellar quality control. Dysfunctional mitochondria are degraded by mitophagy, a pathway of lysosome-mediated organellar degradation that was defined by studies on *PINK1* and *Parkin* by (Narendra et al., 2008, Youle and van der Bliek, 2012). *PINK1* accumulates at the outer mitochondrial membrane of impaired or dysfunctional mitochondria (Narendra et al., 2010); this is followed by the recruitment and phosphorylation of Parkin (Narendra et al., 2008). Parkin ubiquitinates several outer mitochondrial membrane proteins, e.g. VDAC, Mfn2 or Miro1 (Sarraf et al., 2013). This step is followed by the recruitment of p62 to the mitochondria, which initiates autophagy via engulfment of dysfunctional organelles by autophagosomes (Geisler et al., 2010).

Loss of function of DJ-1 has been shown to lead to accumulation of dysfunctional mitochondria because of reduced lysosomal activity and impaired mitophagy (Krebiehl et al., 2010).

5) Homeostasis:

Loss of function mutations in the PD-associated genes *Parkin*, *PINK1*, *Omi/HtrA2* and *DJ-1* can lead to mitochondrial dysfunction *in vivo* and *in vitro* and the encoded proteins of these genes are therefore important to maintain the mitochondrial homoeostasis [reviewed in (Burbulla et al., 2010)].

Mitochondrial stressors can also induce an imbalance in calcium homoeostasis. Recent work indicated that homeostatic calcium stress could be a determinant of the selective vulnerability of the dopaminergic neurons of the *substantia nigra pars compacta* to PD (Chan et al., 2009).

6) Dynamics and biogenesis:

The fission and fusion process of mitochondria is indispensable for maintaining adequate metabolic function of mitochondria. It allows them to rapidly react to the requirements of the cell by renewing themselves, interact with each other and redistribute themselves (Knott and Bossy-Wetzel, 2008). Upon fusion, mitochondria form big interconnected networks whereas in case of fission, they change their size and shape to become more fragmented (Detmer and Chan, 2007). Again PD associated genes are involved in this process. Loss of function of *PINK1* leads to fragmented mitochondria in different cellular and animal models (Exner et al., 2007, Lutz et al., 2009). The same holds true for loss of *Parkin*

models (Lutz et al., 2009). In mice and human primary cells, the same effect of mitochondrial fragmentation was seen through the loss of DJ-1 (Blackinton et al., 2009, Krebiehl et al., 2010). An imbalance in either case can lead to the death of the cell.

7) Transport:

The mobility of mitochondria is extremely important and undergoes frequent changes depending on the metabolic demand and physiological changes in the neurons. Mitochondria can change direction, move rapidly or stay at the same place. Depending on the direction of the transport, anterograde transport is defined by mitochondria, but also other organelles, being transported towards the synaptic terminal of the axon. This aims at delivering mitochondria to regions with a high energy demand. Retrograde transport denotes the transport back to the cell body (Chang et al., 2006, Hollenbeck and Saxton, 2005, Li et al., 2004). In this way, aged or dysfunctional mitochondria can be degraded or recycled (Saxton and Hollenbeck, 2012). Loss of function mutations in *PINK1* have been associated with disturbed mitochondrial dynamics in *D. melanogaster* (Poole et al., 2008).

The mitochondrial contribution to sporadic as well as familial PD needs further investigation and better understanding of the underlying mechanism. This could serve for mitochondrial pathway-based therapeutic strategies that could intervene in disease progression.

1.2 DJ-1, a multifunctional protein

DJ-1 has a small 20kDa domain, which in solutions forms a dimer (Figure 2) to become active (Wilson et al., 2003). DJ-1 has multiple functions and is cytoprotective. The *DJ-1* gene was first described as an oncogene in 1997 (Nagakubo et al., 1997) and shortly thereafter *DJ-1* was found to regulate male fertility (Welch et al., 1998). In 2003, Bonifati and colleagues described four PD patients in a Dutch and three PD patients in an Italian family with mutations in *DJ-1* (Bonifati et al., 2003). *DJ-1* thereafter defined the PD locus *PARK7*.

1.2.1 Functions and structure of DJ-1

DJ-1 is composed of seven exons with exon 1 not coding. DJ-1 consists of 189 amino acids and belongs to the Thj1/Pfp1 superfamily. It is highly conserved among different species, homologues are found in all aerobic species from prokaryotes to eukaryotes and the amino acid residues are highly conserved, including the presumably most important residues for PD, namely C106, located in a nucleophile elbow, shown as ball and stick (Figure 2) (Bandyopadhyay and Cookson, 2004, Lucas and Marin, 2007). The cysteine in position 106 of the peptide sequence is highly oxidisable and responds to oxidative stress/ROS by forming a sulfinic acid (Honbou et al., 2003, Huai et al., 2003, Lee et al.,

2003, Wilson et al., 2003). DJ-1 with oxidised C106 is thought to be less stable and therefore becomes inactive (Hulleman et al., 2007, Zhou et al., 2006). Interestingly, when C106 was replaced with other amino acids, DJ-1 lost its neuro protective activity (Meulener et al., 2006). Only oxidised DJ-1 gets transported to the mitochondria where it acts mitoprotective (Canet-Aviles et al., 2004).
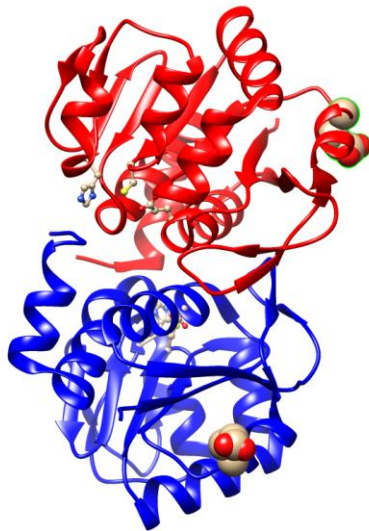
Figure 2: **Crystal structure of the DJ-1 dimer.**

One homomer is blue and one homomer is red. The side chains of residues C106 and L166 are shown as ball and stick. The c.192G>C mutation is shown as balls in white. The molecular model were drawn with Chimera (www.cgl.ucsf.edu/chimera) using the DJ-1 crystal structure data with PDB accession code 1PDW (Tao and Tong, 2003).

The precise biochemical functions of DJ-1 in PD, however, are unclear. One reason might be that no post mortem brain samples from PD patients with *DJ-1* mutations reached autopsy to study the pathology in these cases.

Another reason is the broad spectrum of publications describing different and partially quite vague functions of this small protein:

- DJ-1 affects ras-dependent transformation (Nagakubo et al., 1997),
- controls fertility (Wagenfeld et al., 1998),
- modulates androgen-receptor signalling via sumoylation (Takahashi et al., 2001, Tillman et al., 2007) and possibly through histone deacetylation (Niki et al., 2003);
- acts as a protein chaperone (Shendelman et al., 2004),
- acts as a protease (Koide-Yoshida et al., 2007, Olzmann et al., 2004),
- affects transcription (Taira et al., 2004a) including that of tyrosine hydroxylase (Xu et al., 2005),

- alters dopamine receptor signalling (Goldberg et al., 2005),
- suppresses apoptosis via an interaction with kinases (Junn et al., 2005, Sekito et al., 2006) and/or suppression of the phosphatase PTEN (Kim et al., 2005a),
- alters p53 signalling (Bretaud et al., 2007, Fan et al., 2008, Shinbo et al., 2005),
- alters Akt1 function (Yang et al., 2005),
- upregulates glutathione synthesis or heat shock proteins (Zhou and Freed, 2005),
- stabilizes antioxidant transcription factors (Clements et al., 2006),
- interacts with PINK1 (Tang et al., 2006) and Parkin (Moore et al., 2005), and
- acts similar to a peroxiredoxin (Andres-Mateos et al., 2007).
- It plays a role as well as glyoxalase (Lee et al., 2012b), as a metal sequestering protein (Bjorkblom et al., 2013) and
- it has been suggested as a regulator of mitochondrial fusion (Krebiehl et al., 2010).

DJ-1 is ubiquitously expressed. In the human brain, it is found in neurons and astrocytes. In sporadic PD patients, a strong expression is seen in reactive astrocytes, but it is not accumulating in the pathognomonic Lewy bodies (Bandopadhyay et al., 2004, Neumann et al., 2004, Rizzu et al., 2004).

1.2.2 DJ-1 protects mitochondria and is a sensor for oxidative stress

As described before, DJ-1 acts as a redox sensor through the C106 residue. DJ-1 itself contains no mitochondrial targeting sequences. Nevertheless, upon oxidation, DJ-1 translocates to the OMM (Canet-Aviles et al., 2004) and it was found in cytosolic fractions as well as inside the mitochondria after exposure to mitochondrial toxins (Zhang et al., 2005). It is under discussion if inside the mitochondria, DJ-1 colocalises with complex I and this colocalisation could be increased by oxidative stress (Zhang et al., 2005). It was shown that DJ-1 directly binds to NDFU4 and ND1, both subunits of complex I, thereby maintaining complex I activity (Hayashi et al., 2009). Interestingly, a reduction in mitochondrial complex I activity is also seen in PD patients (Mizuno et al., 1989, Schapira et al., 1990).

Upon loss of DJ-1, an increase in ROS was consistently shown in different *in vitro* and *in vivo* models and include altered mitochondrial dynamics (Irrcher et al., 2010). We were the first ones to show, that in primary cells, upon loss of DJ-1, dysfunctional mitochondria accumulated because of impaired autophagy (Krebiehl et al., 2010). (Irrcher et al., 2010) also showed altered mitochondrial morphology in the absence of DJ-1. Furthermore, a group observed the accumulation of LC3 near mitochondria in DJ-1 deficient cells (Thomas et al., 2011). Another study showed impaired Ca^{2+} uptake of mitochondria in DJ-1 deficient cells, an important factor to maintain proper cell physiology (Ottolini et al., 2013).

By acting as a transcriptional regulator, DJ-1 also protects against oxidative stress. DJ-1 sequesters kelch-like ECH-associated protein 1 (Keap1) in the event of oxidative stress. Sequestered Keap1 sets Nrf2 free, which subsequently translocates to the nucleus and regulates the transcription of genes, which protects the cell against ROS and detoxication (Clements et al., 2006). DJ-1 can also directly bind to the DNA binding domain of p53 to inhibit its transcriptional activity. This prevents p53 from inducing apoptosis under stress conditions (Fan et al., 2008, Kato et al., 2013).

DJ-1 shares mitochondria-related functions with two other PD genes: *PINK1* and *Parkin*. It has been shown that loss of DJ-1-related phenotypes can be partly reverted by introducing PINK1 or Parkin. DJ-1, however, cannot rescue loss of PINK1- or Parkin-related phenotypes (Exner et al., 2007, Irrcher et al., 2010, Krebiehl et al., 2010, Thomas et al., 2011).

1.2.3 Mutations in *DJ-1* are associated with PD

The number of mutations in *DJ-1* associated with PD is relatively low compared to the number of disease related mutations in *PINK1* and *Parkin*, two other autosomal recessively inherited PD genes. At present, there are 21 mutations published, see Table 2 for the type of mutation, the occurance, the population in which the mutation was found, the effect of the mutation if known as well as the reference.

Mutations in *DJ-1* cause approximately 1 % of all PD cases world-wide (Lockhart et al., 2004). However, there is a variation seen in the frequency of *DJ-1* mutations between different ethnic groups. Caucasians: 0.83 % in familial cases and 0.99 % in sporadic cases and 0.54 % copy number variations, Asians: 3.03 % in familial cases, Arabs: 0.74 % in sporadic cases and Ashkenazi Jews: 1.96 % in sporadic cases (Nuytemans et al., 2010). The mutations result in an early-onset with slow progression (except for the compound heterozygous c.317_322del:p.106_108del mutation (Jose M. Bras et al., 2014)) of the disease. For many of the mutations, the effect is still unknown including the previously described p.E64D mutation (Hering et al., 2004). Others cause a decreased protein stability and the 14kb deletion even causes loss of DJ-1 protein (Bonifati, 2003). Some are also predicted to lead to an altered transcript (Table 1).

The mutations can be found in a homozygous, a compound heterozygous and a heterozygous state. Mutational mechanisms include missense mutations as well as copy number variations (Table 2).

The p.E64D mutation was first found in a male Turkish patient. He developed PD symptoms at the age of 34. His sister who is also a homozygous carrier of the mutation, however, didn't show any motor symptoms at the age of 42. The index patient showed slowing

of movement and left sided stiffness in the arm and leg as well as tremor and rigidity. He also suffered from non-motor symptoms like depression and sleep disturbances. Positron emission tomography showed an altered dopamine transporter binding in the striatum. The patient responds well to L-Dopa treatment (Hering et al., 2004).

Table 2: **List of PARK7 mutations.**

This is a list of all published PARK7 mutations linked to PD including for the type of mutation, the occurance, the population in which the mutation was found, the effect of the mutation if known and the reference.

Mutation	Occurance	Population	Predicted effect	Reference
L166P	Homozygous	Italian	Protein instability	(Bonifati, 2003)
14-kb deletion	Homozygous	Dutch	Loss of protein	(Bonifati, 2003)
M26I	Homozygous	Ashkenazi Jewish	Protein instability	(Abou-Sleiman et al., 2003)
D149A	Heterozygous	Afro Caribbean	Unknown	(Abou-Sleiman et al., 2003)
IVS6-1 G-C	Heterozygous	Hispanic	Altered transcript	(Hague et al., 2003)
c.56delC	Heterozygous	Hispanic	Frameshift	(Hague et al., 2003)
g.168_185del	Both	Global	Unrelated Polymorphism	(Hague et al., 2003)
R98Q	Heterozygous	Global	No effect/polymorphism	(Hague et al., 2003)
A104T	Heterozygous	Latino	Polymorphism	(Hague et al., 2003)
Ex5-7del	Heterozygous	Northern Italian	Altered transcript	(Hedrich et al., 2004)
IVS5+2-12del	Heterozygous	Russian	Altered transcript	(Hedrich et al., 2004)
E64D	Homozygous	Turkish	Unknown	(Hering et al., 2004)
E163K	Homozygous	Italian	Altered activity	(Annesi et al., 2005)
g.168_185dup	Homozygous	Italian	Unknown	(Annesi et al., 2005)
L10P	Homozygous	Chinese	Decreased protein stability	(Guo et al., 2008)
P158del	Homozygous	Dutch	Decreased protein stability	(Macedo et al., 2009)
A179T	Heterozygous	Dutch	Unknown	(Macedo et al., 2009)
Ex1–5dup	Heterozygous	Dutch	Altered transcript	(Macedo et al., 2009)
A107P	Homozygous	Iranian	Unknown	(Ghazavi et al., 2011)
c.91-2AG	Homozygous	Iranian	Splicing	(Ghazavi et al., 2011)
c.317_322del: p.106_108del	Homozygous	Kurdish	Unknown	(Jose M. Bras et al., 2014)

1.2.4 DJ-1 animal models are sensitive to mitochondrial toxins and oxidative stress

As DJ-1 is an evolutionarily ancient protein. Homologues are found in many evolutionary distant organisms. This allows the study of DJ-1 function in these different organisms.

E.coli:

In *E.coli* there are two DJ-1-related proteins called *YaiL* (formerly known as *ThiJ*) and *YhbO* which is stress inducible. Interestingly, *YhbO* reacts in a C104-dependant manner upon environmental stress caused by hydrogen peroxide (H_2O_2), very similar to mammalian DJ-1 (corresponding to the C106 residue in human DJ-1) (Abdallah et al., 2007, Wilson et al., 2005). These two bacterial proteins however showed no protease or chaperone

activity unlike mammalian DJ-1, suggesting DJ-1 having rather a cytoprotective responsibility by sensing ROS (Abdallah et al., 2007, Fioravanti et al., 2008).

Ceanorhabditis elegans:

Knocking down the DJ-1 homologue B0432.2 in *Ceanorhabditis elegans* lines resulted in an increase in vulnerability to mitochondrial complex I inhibitors like rotenone. This substantiates the role of DJ-1 as a protector of mitochondrial function against oxidative stress (Ved et al., 2005).

Zebrafish (*Danio rerio*):

Danio rerio are also used to study the function of DJ-1. The zebrafish orthologue of DJ-1 (zDJ-1) is present in the adult brain of the fishes (Bai et al., 2006). Also in this organism an increased sensitivity to oxidative stress was seen after knockdown of zDJ-1 (Bretaud et al., 2007).

Drosophila melanogaster (*D. melanogaster*):

The fruit fly *D. melanogaster* has two DJ-1 homologous: DJ-1a and DJ-1b, with DJ-1b being ubiquitously expressed like human DJ-1. As described for other animal models *D. melanogaster* DJ-1 null mutants are sensitive to oxidative stress and paraquat, which could be rescued by both *D. melanogaster* DJ-1b and human DJ-1 (Menzies et al., 2005, Meulener et al., 2005). Interestingly C104 DJ-1b (corresponding to the C106 residue in human DJ-1) mutants did not rescue the phenotype (Meulener et al., 2006).

Fruit flies also showed comprised mitochondrial function and reduced ATP levels, together with a shortened life span, male sterility and reduced climbing ability in an DJ-1 mutant background (Hao et al., 2010).

Mouse models:

In contrast to findings in humans the knockout of *DJ-1* homologues in *D. melanogaster (Meulener et al., 2005, Park et al., 2005)*, zebrafish (Bretaud et al., 2007) and mice (Chen et al., 2005, Pham et al., 2010, Yamaguchi and Shen, 2007) doesn't cause a degeneration of dopaminergic neurons under basal conditions with the exception of one $DJ\text{-}1^{-/-}$ mouse line which shows age dependent neurodegeneration as well as motor deficits (Rousseaux et al., 2012).

The $DJ\text{-}1^{-/-}$ null mutant mice which were used for the generation of hippocampal primary neuron cultures in this work show a decrease in dopamine-producing neurons in the ventral tegmental area (~6% reduction), but no reduction of dopaminergic neurons in the *sub-*

stantia nigra. Interestingly enough they seem to compensate for the loss of DJ-1 by up-regulating mitochondrial respiratory enzyme activities in order to protect the cells against oxidative stress (Pham et al., 2010).

1.3 Patient-derived cellular models for PD

A limitation for studies in the field of neurodegenerative disorders including PD is, that the diseased tissue is not directly accessible for studies based on well-understandable ethical reasons. Therefore affected neuronal populations are only accessible via post mortem brains, but at that stage most of the cells of interest, for PD these are the midbrain dopaminergic neurons, are already degenerated. Another issue is that even at disease onset most of the affected neurons (approximately 50 %) are already gone (Kirik et al., 2004).

Although animal models enable to study the disease in an intact organism, modelling the effect of aging and the slow progression of the loss of dopaminergic neurons characteristic for PD is difficult in these models. Also animal models fail to display the full spectrum of symptoms seen in humans (Westerlund et al., 2010).

The use of patient-derived models render the possibility of studying disease mechanisms as well as the search for biomarkers in cells from patients of known clinical disease history and genetic disease background.

1.3.1 Patient derived fibroblasts

In contrast to cancer cell lines with artificial overexpression of a certain gene of interest, patient- derived fibroblasts allow to study the effect of a certain PD mutation at an endogenous level. Furthermore, they permit to investigate the disease mechanisms in an *in vitro* system displaying the *in vivo* situation.

As described before, mitochondria are involved in PD pathogenesis. Making use of patient-derived fibroblasts, it is possible to investigate these organelles in an *in vivo* situation, making also mild defects detectable in contrast to studies where mitochondria are isolated before analysing them (Winkler-Stuck et al., 2004, Burbulla and Kruger, 2012).

Several studies using patient-derived fibroblasts provided insight into mitochondrial phenotypes relevant for PD. Primary cells obtained from two different *PINK1* PD mutation carriers showed altered mitochondrial morphology (Exner et al., 2007). In another study of control fibroblasts, it was shown that knocking down *Parkin* leads to a greater degree of mitochondrial branching in the studied fibroblasts (Mortiboys et al., 2008).

These cells are not neuronal and hence, it is not possible to study the underlying and relevant disease mechanisms of PD - the loss of dopaminergic neurons - in the respective

cell type. However, they open up the possibility to get a first insight into mechanisms relevant for the disease which can be further validated in other cellular models.

Human fibroblasts also provide a source of cells which can be used to generate induced pluripotent stem cells (iPSCs). These cells can be used to generate different patient specific disease phenotypes, important to better understand the nature of PD.

1.3.2 iPSCs and iPSC-derived neurons

As mentioned before, the absence of appropriate neuronal models of the disease represents a major drawback for PD research. The protocol to generate human iPSCs from patient-derived somatic cells described by Yamanaka and colleagues eight years ago provides a new tool in this regard (Takahashi et al., 2007). It is now possible to study a disease in their endogenous genomic background with its transcriptional feedbacks largely intact. The year before, they introduced the concept of iPSC generation through introduction of a cocktail of genes which are normally expressed during embryogenesis, namely o*ct4, s*ox2, *klf4* and *c-myc* (later named the four 'Yamanaka factors') into a differentiated/somatic cell. Thereby changing the potency state of the cell back to the pluripotent state (Takahashi and Yamanaka, 2006).

Oct4:

Oct4, also known as *POU class 5 homeobox 1* (*POU5F1*), encodes a transcription factor containing a POU homeodomain. This transcription factor activates other transcription factors (Pesce and Scholer, 2001). Furthermore, by binding to its own regulatory region, it activates itself thus leading to the transcription of endogenous *oct4*. Oct4 has been shown to be a core regulator in embryonic stem cells (ESCs), which underlines its importance for pluripotency (Boyer et al., 2005).

Sox2:

Sox2 is an intronless gene encoding another transcription factor involved in the regulation of embryonic development and in the determination of cell fate (Avilion et al., 2003). It is important for stem cell maintenance and its expression is detected during early embryonal development (Niwa et al., 2000).

Oct4 and Sox2 interact with each other by activating enhancers for both genes as well as for *nanog* and thereby maintaining the pluripotency state in ESCs (Masui et al., 2007).

Klf4:

Kruppel-like factor 4 (*Klf4*) and *c-myc* are related to cell proliferation and renewal. The proteins are found in tumours and therefore known as oncogenes (Huangfu et al., 2008).

C-myc:

C-myc is also known to increase the ability of transcription factors to bind to their target sequences (Faiola et al., 2005, Takahashi and Yamanaka, 2006). Klf4 also regulates the expression of *sox2* and *oct4* thereby also regulating nanog (Wei et al., 2009).

In the meantime, different reprogramming vector types such as protein, RNA and DNA based ones, but also different viral vectors (integrating and non-integrating) have been published. Moreover, new combinations of reprogramming factors are known [reviewed in (Rony et al., 2015).

iPSCs have the ability to form cells from all three germ layers, allowing them to differentiate into various different cell types (such as skin, blood, nerve and muscle cells). Another positive feature is that they can be frozen down and thawed again, providing the ability of long- term storage. The cells can be used to study disease mechanisms, to test the effectiveness of compounds or drugs and look for side effects. Importantly, they may also have a potential for regenerative medicine as the cells could be used as autologous transplants avoiding histocompatibility issues. Since in PD, a certain type of cells dies in the brain, cell replacement therapies are a possible leverage point for future therapies of the disease. However there are many obstacles to be overcome: current replacement strategies do not account for physiological connections, there are problems with the integration in neuronal circuits and there is no control of pluripotency, therefore tumorigenesis is an issue.

After the classical reprogramming process with the 'Yamanaka factors', the generated lines have to undergo a quality control to proof transgene silencing, to validate stem cell characteristics, such as the ability to form cells from all three germ layers and the expression of stem cell markers, but also genotyping microarray analysis and karyotype analysis have to be performed. In spite of all these quality controls, the different clones from each source line (typically people work with two to three lines per donor cell line) vary a lot (Devine et al., 2011). This phenomenon is due to the different number and sites of integration of the retroviral vectors used for the reprogramming. Around twenty integrations per clone where described by Yamanaka and colleagues in the first lines (Takahashi et al., 2007, Takahashi and Yamanaka, 2006).

The generation of iPSCs from patient-derived fibroblasts is a tool to model PD. The important step is to differentiate these iPSC lines and, if available, the isogenic pairs into the important cell types and maturate or treat them in a certain way to model the disease and aging. This concept has been termed the modelling of a 'disease in a dish' (Vogel, 2010). For PD, the loss of dopaminergic neurons of the *substantia nigra pars compacta* is characteristic; therefore to model PD, iPSCs are differentiated to midbrain dopaminergic (mDA)

neurons. The above mentioned effect of different integration sites of the reprogramming factors amongst other things leads to a variability in the efficiency of these iPSC lines to be differentiated into neurons (Sanchez-Danes et al., 2012).

iPSC-based studies on several PD genes and the respective mutations have been published, including *LRRK2*, *Parkin*, *PINK1*, but also *SNCA* (Soldner et al., 2011) as well as *GBA (Schondorf et al., 2014)*:

LRRK2:

Most of the studies in iPSC-derived neurons have been on the G2019S mutation in *LRRK2*. These studies revealed that G2019S carrying mDA neurons have more apoptotic markers like cleaved caspase 3 and they were more vulnerable to oxidative stress (Nguyen et al., 2011, Reinhardt et al., 2013b, Sanchez-Danes et al., 2012).

Parkin:

Loss of Parkin neurons showed an increase in oxidative stress, SNCA accumulation and defective mitophagy (Imaizumi et al., 2012).

PINK1:

mDA neurons carrying *PINK1* mutations also hinted to impaired mitophagy, because they had more mitochondria which were not degraded upon depolarisation of the membrane potential possibly because of the impossibility of Parkin recruitment (Seibler et al., 2011).

Some studies even include isogenic lines. These studies could support previous findings in other cell types, as they showed disruptions of autophagy and mitochondrial dysfunction. Newer approaches include the use of the cells in drug screens and tests (Lee et al., 2012a).

As stated before, mDA neurons are a great source for the study of the cause of degeneration of these neurons in the brain of PD patients, however they are still lacking some characteristics of the mDA neurons of the brain. Therefore, the protocols which are currently used to generate these cells need to be improved. Simulating aging of the cells is a big issue, also their networks are not as complex as the ones in the brain, studies with mixed populations of different neuronal subtypes as well as glia cells displaying the physiological conditions including the high energy demand of the cells should be performed (Pissadaki and Bolam, 2013).

So far, an important potential of iPSC-derived mDA neurons is seen in the field of drug screenings and dose tests for clinical trials of new compounds as this can be done for a certain genetic background *in vitro* [reviewed in (Beevers et al., 2013)].

1.3.2.1 Gene editing

Recent advances in generating isogenic lines have largely helped improve studies of diseases such as PD, which can be genetically inherited. In the meantime, different techniques have been successfully used such as zinc finger nucleases (ZFNs) [reviewed in (Collin and Lako, 2011)], transcription activator-like effector nucleases (TALENs) (Kim et al., 2013) and clustered regularly interspaced short palindromic repeat (CRISPR)/CAS9 RNA-guided nucleases (Cho et al., 2013b, Jinek et al., 2013).

By using isogenic lines, one can ensure that experiments are performed under genetically defined conditions, with the control and mutated or the mutant and corrected line carrying the same genetic background with the disease-causing mutation being the sole modified variable. It also allows to control for effects from genetic modifier loci. This is the ideal situation, however to date there is still the problem of off-target effects of all three systems, ZFNs, TALENs and CRISP/CAS9 [reviewed in (Li et al., 2014)].

1.4   Splicing and disease

Taking into consideration that splicing occurs in nearly all human genes, it is evident that the splicing process can lead to diseases through inherited mutations or errors occuring during the splicing process. Furthermore, every gene that contains an intron needs to undergo splicing and more than 90 % of all genes are alternatively spliced (Pan et al., 2008, Wang et al., 2008). Therefore, it is not surprising that approximately 10 % to 15 % of all pathogenic mutations are mutations found in splice sites (Baralle et al., 2009, Krawczak et al., 2007). An even higher amount of up to 50 % of all disease-causing mutations is reached when the number of mutations are counted that affect splicing in some way (Lopez-Bigas et al., 2005). Mutations leading to missplicing are found in various common diseases such as Duchenne muscular dystrophy, familial dysautonomia (FD), cystic fibrosis, spinal muscular atrophy, retinitis pigmentosa, but also breast cancer predisposition and blood disorders like thalassaemias and anaemias [reviewed in (Baralle et al., 2009)].

Splicing mutations can have different consequences for the splicing process. Most of them cause the skipping of one or more exons, second most common is the activation of aberrant 5'donor splice sites or 3'acceptor splice sites or full intron retention (Baralle and Baralle, 2005, Cooper, 1993, Nakai and Sakamoto, 1994). Another possibility is the activation of a cryptic splice site meaning a new splice site is created in an exon or intron (Roca et al., 2003).

For future therapeutic approaches of diseases caused by missplicing of the mRNA, it is important to know whether the splicing defect is the direct cause of the disease. If this is

the case and the underlying mechanism is clear, the disease-causing mutation is a potential target for therapy where the missplicing is corrected to a physiological state [reviewed in (Rahman et al., 2015)]. Such potential therapeutic strategies could be: small molecules, antisense oligonucleotides, bifunctional oligonucleotides, spliceosome-mediated RNA *trans*-splicing and modified U1 snRNPs [reviewed in (Baralle et al., 2009)].

1.4.1 Basic precursor mRNA splicing process

Before a protein-coding gene can be translated into a protein, several post-transcriptional modifications need to take place before the final mRNA can be translated. The initial mRNA transcript therefore is called precursor mRNA (pre-mRNA). The modifications include 5'capping, polyadenylation and the actual splicing process: the removal of the introns and ligation of the exons. This last step is referred to as pre-mRNA splicing.

The performance of correct splicing is a complicated process where the coding sequences, the exons, need to be selected from the non-coding sequences, the introns, which are much more frequent. The exons need to get ligated together afterwards. As described above, mutations in the exonic as well as in the intronic region can lead to aberrant splicing and could potentially be disease causing.

The splicing reaction takes place in the spliceosome and includes hundreds of interactions between proteins, small nuclear RNAs (snRNAs) as well as interactions between the two and leads to a precise excision and ligation of the respective exons (Madhani and Guthrie, 1994, Nilsen, 1994).

The two catalytic steps of pre-mRNA splicing are shown (Figure 3B and C). Conserved motifs that are essential for splicing are the 5' splice site, the 3' splice site, the branche point as well as the polypyrimidin tract (Figure 3A). They are mainly in the intron and are called 5' splice site and 3' splice site (Shapiro and Senapathy, 1987).

The 5' splice site, also called splice donor, is a short sequence of bases, with the first two bases of the intron (gu) being conserved in mammals. The surrounding sequence (partially in the exon) (MAGguragu) is important too, but not conserved (Aebi et al., 1987).

The 3' splice site consists of three elements which can lie up to one hundred base pairs in the intron: the branch point (yncurac), the polypyrimidin tract (y_n) and the splice acceptor with the canonical sequence of (nyag). Looking at the sequences of the 3' splice site and the 5' splice site, it is surprising how few bases are responsible for the recognition of the splice site. Therefore, it seems obvious that there need to be more than just these few necessary bases or elements. Intriguingly, a study where the authors did an *in silico* analysis to find possible splice sites of the human *hprt* gene found the eight correct 5' splice

sites, but also 100 other possible 5' splice sites and 683 additional possible 3' splice sites (Sun and Chasin, 2000). The question how the "real" splice site amongst these many possible splice sites, also called pseudo-splice sites is found cannot be answered to date.
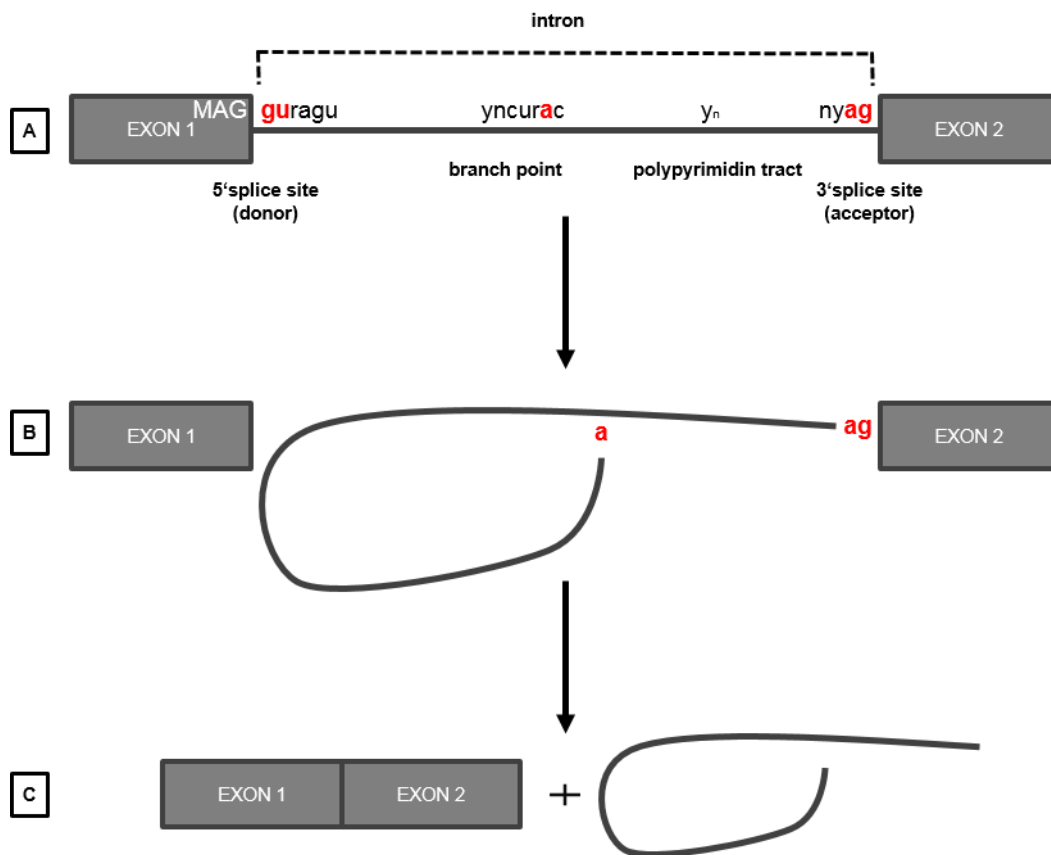
Figure 3: **The basic pre-mRNA splicing process.**

Exons are shown as grey boxes and the intron as line. **A)** shows the conserved motifs essential for splicing. The splice donor includes the invariant (gu) at the 5' splice site and the splice acceptor the invariant (ag) at the 3' splice site. The branch point lies within one hundred bases after the 3' end of the intron. The polypyrimidin tract (y_n) lies nearby the branch point (yncurac). **B)** shows the first catalytic step of the splicing reaction where exon 1 is seperated from exon 2 with the intron as lariat at the branch point. **C)** shows the end products of the pre-mRNA splicing: exon 1 and exon 2 spliced together and the intron lariat. These two products are created by a second trans-esterification step caused by exon 1 attacking the 3' splice site.

The 5' splice site and the 3' splice site are the sites where the two catalytic trans-esterifications take place (Aebi et al., 1987, Lamond, 1993). The first trans-esterification step is shown (Figure 3B). Here, the adenosine residue in the branch point carries out a nucleophilic attack on the 5' splice site. This results in a free exon 1 and an exon 2 with a lariat intron. The next trans-esterification happens when the free exon 1 attacks the 3' splice site. This results in two splicing products, the ligated exons and the intron lariat (Figure 3C) (Lamond, 1993).

1.4.2   Spliceosome assembly on the pre-mRNA

As described before, the pre-mRNA splicing takes place in the spliceosome. This macro-molecular complex consists of five different uridine-rich small nuclear ribonucleoproteins (U snRNPs) and over more than one hundred other splicing factors. The U snRNPs consist of one uridine-rich small nuclear RNA plus multiple proteins.

The assembly of the spliceosome starts with the binding of U1 snRNP to the 5' splice site (Figure 4A1), at the same time SF1/mBBP recognising the branch point and U2AF, which is a heterodimer consisting of U2AF35 and U2AF65, binding to the 3' splice site and the polypyrimidin tract (Figure 4A2). The formation of this complex, called E complex, is ATP-independent and has the purpose of bringing the splice sites together by bridging the introns. In the next step the so-called A complex is built, here SF1/mBBP is replaced by the U2 snRNP at the branch point, this is ATP-dependant (Figure 4B). Subsequently the tri-snRNP complex consisting of U4/U5-U6 snRNP binds to the precatalytic B complex (Figure 4C). This step is followed by the activation of the B complex now called active B* complex. Here, the U1 snRNP and U4 snRNP destabilise while the Prp19/CDC5L complex associates with the B complex. This comes along with remodelling and conformation changes of the complex. Once U1 snRNP and U4 snRNP dissociated, the complex is termed C complex. The C complex is now able to catalyse splicing.

In addition to the sequences important for the spliceosome to bind, there are other sequences that affect splicing. These sequences can be intronic or exonic elements depending on whether they lie in the intron or exon, respectively and they are much more variable than the above mentioned splice site sequences. Also these sequences can enhance the recognition of a splice site, in that case they are called enhancers, or decrease the recognition of a splice site in that case they are called silencers. Enhancers and silencers can have and influence on each other by antagonising the activity of each other and their function can overlap. Figure 4 shows an exonic splice enhancer (ESE) and an exonic splice silencer (ESS) on the left and an intronic splice enhancer (ISE) as well as an intronic splice silencer (ISS) on the right. The ESE, ESS, ISE and ISS together with the other splicing sequences are called *cis*-acting sequence elements. All *cis*-acting sequence elements are possible targets for pathogenic mutations. The *cis*-acting sequence elements act by the binding of so called *trans*-acting factors to these sequences or by forming secondary structures. The *trans*-acting factors are regulated as well. Their expression can be tissue- and developmental stage- specific or depend on phosphorylation and posttranslational modification [the spliceosome assembly has been recently reviewed in (De Conti et al., 2013, Baralle and Baralle, 2005, Mohammad Alinoor Rahman, 2015)].
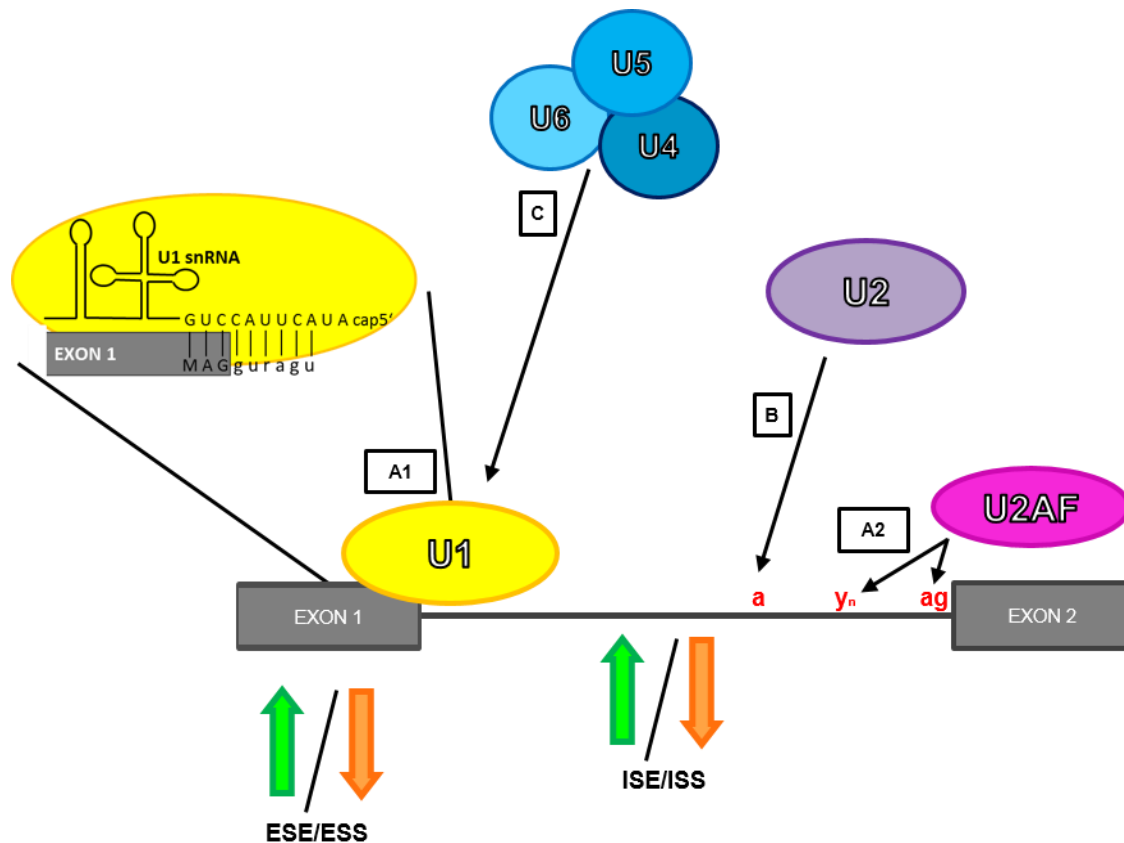
Figure 4: **The steps of the spliceosome assembly.**

Exons are shown as boxes, introns as line, the *cis*-acting sequences are indicated by arrows and U snRNPs are depicted as circles. The assembly of the spliceosome happens in a stepwise and coordinated manner. **A1)** The assembly is initiated by the U1 snRNP binding to the 5' splice site. **A2)** At the same time one part of U2AF heterodimer binds to the polypyrimidin tract and the other part to the 3' splice site. The thus formed complex is called E complex. **B)** Next, the U2 snRNP binds to the branch point thereby replacing SF1/mBBP. Now the complex is called A complex. **C)** Binding of the U4/U5-U6 tri-snRNP leads to the formation of the so called B complex. The disassociation of U1 snRNP and U4 snRNP from the B complex includes remodelling and conformational changes of the B complex. The result is the catalytically active C complex which catalyses splicing. So called *cis*-acting sequences influence the splicing process as well. They can lie in the exon or in the intron. These elements can either have a positive, in that case they are called enhancers (shown in green), or a negative, in that case they are called silencers (shown in orange), influence on the splicing process. Their full name combines their location and their function: exonic splice enhancer (ESE) and exonic splice silencer (ESS), as well as intronic splice enhancer (ISE) and intronic splice silencer (ISS).

The vast majority of mutations in *cis*-acting sequences lead to the skipping of an exon (Krawczak et al., 2007). This can be the exon carrying the mutation or a neighbouring exon (Baralle et al., 2006).

ESE sequence elements are mainly bound by serine/arginine-rich (SR) proteins (Graveley, 2000, Lin and Fu, 2007). Upon binding through their RNA binding domains, SR proteins

influence splicing by recruiting splicing components and interacting with them through protein-protein and protein-RNA interaction through the SR site (Shen and Green, 2004, Shen et al., 2004).

ESS and ISS are mainly bound by *trans*-acting factors belonging to the group of heterogeneous nuclear ribonucleoproteins (hnRNPs), these factors act through protein-protein interaction (Krecic and Swanson, 1999, Martinez-Contreras et al., 2007).

The ISE *cis*-acting sequences are less studied. Different hnRNPs might be candidates as well as GT repeats could be involved (Gabellini, 2001, Mauger et al., 2008, Ule et al., 2006, Wang et al., 2012a, Yeo et al., 2009).

Another factor that comes into focus is that also the secondary structure of the RNA influences the splicing process (Buratti and Baralle, 2004).

Looking at the complex interaction of factors and sequence elements described in this chapter, it becomes clear that any silent mutation or any other sequence variation lying in one of the *cis*-acting sequences might interfere with the splicing process and thus be disease causing. This aspect should therefore not be underestimated.

2 Material and Methods

2.1 Tables of equipment, reagents and software

2.1.1 Table of equipment

Table 3: **List of equipment used.** Table shows equipment and manufacturer.

Equipment	Manufacturer
Agarose gel chamber	Peqlab (Erlangen, Germany)
Amaxa nucleofector I	Lonza Group Ltd (Basel, CH)
Autoclave (VX-150)	Systec (Wettenberg, Germany)
AxioImager microscope with ApoTome Imaging system	Carl Zeiss Microimaging GmbH (Jena, Germany)
Bacterial incubator	Binder (Multimed) (Tuttlingen, Germany)
BD LSRFortessa	Becton,Dickinson and Company.© (Erembodegem, Belgium)
Biofuge pico and fresco	Thermo Fisher Hereaus, (Hamburg, Germany)
Cell incubator (Heracell 240)	Thermo Fisher Hereaus (Hamburg, Germany)
Centrifuge (Evolution Rc)	Thermo Fisher Sorvall, (Hamburg, GERMANY)
Centrifuge (Micro 22R)	Hettich (Tuttlingen, Germany)
Centrifuge 5810R	Eppendorf (Hamburg, Germany)
Chirurgical tools	Carl Roth GmbH (Karslruhe, Germany)
CyAn ADP Analyzer	Beckman Coulter (California, USA)
Developer	Fujifilm (Düsseldorf, Germany)
Electroporation cuvettes	Bio-Rad laboratories GmbH (Munich, Germany)
Electroporation device (MicroPulser)	Bio-Rad laboratories GmbH (Munich, Germany)
Amersham film cassettes	GE Healthcare (Freiburg, Germany)
iBlot® system	Invitrogen GmbH (Karslruhe, Germany)
Light cycler 480 II	Roche Applied Science (Mannheim, Germany)
Live Cell MicroscopeAxiovert 2000 plus Zeiss incubator XL with ApoTome, CO_2 humidifier, plan-aprochromat objectives and AxioCam MRc	Carl Zeiss Microimaging GmbH (Jena, Germany)
Micro wave oven	Panasonic (Hamburg, Germany)
Microtiter plate reader	Bio-Rad laboratories GmbH (Munich, Germany)
Milli-Q Synthesis	Millipore Corporation (Darmstadt , Germany)
Mithras LB 940	BERTHOLD Technologies GmbH & Co. KG (Bad Wildbad, Germany)
Mulitfuge3 S-R	Thermo Fisher Hereaus, (Hamburg, Germany)
NanoDrop (ND1000)	Peqlab (Erlangen, Germany)
Pipetboy Integra	Bioscience (Fernwald, Germany)
Power supply	Bio-Rad laboratories GmbH (Munich, Germany)
Epson Perfection V700 Photo	EPSON Deutschland GmbH (Meerbusch, Germany)
ABI 3100 Genetic Analyzer	Applied Biosystems/Ambio (Austin, Tx, USA)
Spectrophotometer (Ultrospec 2100 Pro)	Amersham Biosciences GmbH (Munich, Germany)
Stereo microscope MZ7	Leica (Solms, Germany)
Sterile bench (Herasafe)	Thermo Fisher Heraeus (Hanau, Germany)
Stirer (RH basic)	IKA (Staufen, Germany)
Synergy™ Mx Microplate Reader	BioTek Instruments, Inc. (Bad Friedrichshall, Germany)
Thermocycler (2720)	Applied Biosystems (Darmstadt, Germany)

Equipment	Manufacturer
Thermomixer (Comfort)	Eppendorf (Hamburg, Germany)
UV-table Vilber Lourmant	Vilber Lourmant (Eberhardzell, DE)

2.1.2   Table of chemicals

Table 4: **List of chemicals used.** Table shows chemical and manufacturer.

Chemical	Manufacturer
1,4-Dithiothreitol (DTT)	Carl Roth GmbH (Karslruhe, Germany)
2-propanol	Merck KGaA (Darmstadt, Germany)
40% Acrylamide/Bis solution 19:1	Bio-Rad laboratories GmbH (Munich, Germany)
4xLDS sample buffer	Expedeon Ltd (Cambridgeshire, UK)
Accutase solution	Merck KGaA (Darmstadt, Germany)
Acetic acid (glacial) 100%	Merck KGaA (Darmstadt, Germany)
Agar	Fluka Analytical (Munich, Germany)
Agarose	Biozym Scientific (Hessisch Oldendorf, Germany)
Amaxa® Human Dermal Fibroblast Nucleofector® Kit	Lonza Group Ltd (Basel, CH)
Amersham ECL Western Blotting Detection Reagent	GE Healthcare (Freiburg, Germany)
Ammonium persulfate (APS)	Sigma Aldrich Chemie GmbH (Munich, Germany)
Ampicillin (sodium salt)	Sigma Aldrich Chemie GmbH (Munich, Germany)
Amplify™	GE Healthcare (Freiburg, Germany)
Ascorbic acid	Sigma Aldrich Chemie GmbH (Munich, Germany)
Bafilomycin A1	Enzo Life Sciences BVBA (Antwerpen, Belgium)
BDNF	PeproTech Worldwide (New Jersey, USA)
BigDye Terminator v3.1	Applied Biosystems (Darmstadt, Germany)
Boric acid	Sigma Aldrich Chemie GmbH (Munich, Germany)
Bovine Serum Albumin (BSA)	Carl Roth GmbH (Karslruhe, Germany)
Bradford reagent	Thermo Fisher Scientific (Braunschweig, Germany)
Bromphenol blue (sodium salt)	Merck KGaA (Darmstadt, Germany)
Calcium chloride	Merck KGaA (Darmstadt, Germany)
CF-1 Mouse Embryonic Fibroblasts (MEF) feeder cells, irradiated	GlobalStem (Maryland, USA)
CHIR 99021	Axon Medchem BV (Groningen, Netherlands)
Chloramphenicol sulfate	Sigma Aldrich Chemie GmbH (Munich, Germany)
cOmplete protease inhibitor	Roche Applied Science (Mannheim, Germany)
Coomassie Brilliant Blue G-250	Carl Roth GmbH (Karslruhe, Germany)
DAPI (4',6-Diamidino-2-Phenylindole, Dihydrochloride)	Thermo Fisher Scientific (Braunschweig, Germany)
dbcAMP	Sigma Aldrich Chemie GmbH (Munich, Germany)
Dimethyl sulfoxide (DMSO)	Sigma Aldrich Chemie GmbH (Munich, Germany)
DirectPCR Lysis Reagent (Mouse Tail) Kit	Viagen Biotech, Inc. (Los Angeles, USA)
Dispase (1 U/mL)	Stemcell Technologies, Inc. (Grenoble, France)
DNA 1 kb ladder	Fermentas GmbH (St Leon-Rot, Germany)
DNA loading dye (6x)	Thermo Fisher Scientific (Braunschweig, Germany)
DNA T4 ligase (1U/µl)	New England Biolabs GmbH (Frankfurt, Germany)
dNTPs	Merck KGaA (Darmstadt, Germany)
Dorsomorphin	R&D Systems, Inc. (Oxfordshire, UK)
Dulbecco's minimal essential medium (DMEM) -high glucose	Biochrom AG (Berlin, Germany)

Chemical	Manufacturer
Ethanol	Merck KGaA (Darmstadt, Germany)
Ethidium bromide (1% in water)	Merck KGaA (Darmstadt, Germany)
Ethylenediaminetetraaceticacid (EDTA sodium salt)	Sigma Aldrich Chemie GmbH (Munich, Germany)
Fetal bovine serum (FCS)	PAA Laboratories GmbH (Pasching, Austria)
FuGENE 6 / X-tremeGENE 9	Roche Applied Science (Mannheim, Germany)
GDNF	PeproTech Worldwide (New Jersey, USA)
Gelatin solution (Type B, 2% in H_2O)	Sigma Aldrich Chemie GmbH (Munich, Germany)
GeneRulerTM 100 bp Plus DNA ladder	Thermo Fisher Scientific (Braunschweig, Germany)
GeneRulerTM 1 kp Plus DNA ladder	Thermo Fisher Scientific (Braunschweig, Germany)
Geneticin® Selective Antibiotic (G418 Sulfate) (50 mg/mL)	Thermo Fisher Scientific (Braunschweig, Germany)
Gentamycin	Invitrogen GmbH (Karslruhe, Germany)
Glycerin	VWR International (Pennsylvania, USA)
Glycerol	AppliChem GmbH (Darmstadt, Germany)
Glycine	Carl Roth GmbH (Karslruhe, Germany)
GoTaq Polymerase Kit	Promega (Mannheim, Germany)
HBSS	Thermo Fisher Scientific (Braunschweig, Germany)
HEPES	Sigma Aldrich Chemie GmbH (Munich, Germany)
High pure RNA isolation Kit	Roche Applied Science (Mannheim, Germany)
Hoechst 33342, Trihydrochloride, Trihydrate	Thermo Fisher Scientific (Braunschweig, Germany)
human FGF8	PeproTech Worldwide (New Jersey, USA)
Hydrochloric acid (HCl)	Merck KGaA (Darmstadt, Germany)
Hydrogen peroxide solution 30 %	Sigma Aldrich Chemie GmbH (Munich, Germany)
iBlot® 2 NC Regular Stacks	Thermo Fisher Scientific (Braunschweig, Germany)
Kanamycinsulfate	Sigma Aldrich Chemie GmbH (Munich, Germany)
KOD Hot Start DNA Polymerase	Merck KGaA (Darmstadt, Germany)
Lipofectamine® 2000 Transfection Reagent	Thermo Fisher Scientific (Braunschweig, Germany)
Magnesium chloride (MgCl2)	Carl Roth GmbH (Karslruhe, Germany)
Matrigel	Corning Incorporated (New York, USA)
Methanol	Merck KGaA (Darmstadt, Germany)
Midori Green Advance DNA Stain	Biozym Scientific (Hessisch Oldendorf Germany)
MitoSOX™ Red Mitochondrial Superoxide Indicator	Thermo Fisher Scientific (Braunschweig, Germany)
MitoTracker® Green FM	Thermo Fisher Scientific (Braunschweig, Germany)
Mowiol/DABCO	Carl Roth GmbH (Karslruhe, Germany)
N,N,N',N'-Tetramethylethyldiamine (TEMED)	Merck KGaA (Darmstadt, Germany)
Non-fat milk powder	Sucofin, (Zeven, Germany)
Normal Goat serum	Sigma Aldrich Chemie GmbH (Munich, Germany)
NP40	VWR International (Pennsylvania, USA)
Nuclease-Free Water	Qiagen GmbH (Hilden, Germany)
One Shot® TOP10 Chemically Competent E. coli	Thermo Fisher Scientific (Braunschweig, Germany)
OptiMEM	Invitrogen GmbH (Karslruhe, Germany)
PageRuler Plus Prestained Protein Ladder	Thermo Fisher Scientific (Braunschweig, Germany)
Paraformaldehyde	Sigma Aldrich Chemie GmbH (Munich, Germany)
PenicillinG/Streptomycin sulfate 100x	Biochrom AG (Berlin, Germany)
pLenti-III-SV40	Applied Biological Materials – abm Biotechnology Company (Richmond, Canada)
Polybrene®	Thermo Fisher Scientific (Braunschweig, Germany)
Poly-DL-ornithine hydrobromide (PORN)	Sigma Aldrich Chemie GmbH (Munich, Germany)

Chemical	Manufacturer
Poly-L-lysine solution	Sigma Aldrich Chemie GmbH (Munich, Germany)
polyethylene glycol	Sigma Aldrich Chemie GmbH (Munich, Germany)
Potassium Chloride (KCl)	Merck KGaA (Darmstadt, Germany)
Potassium hydroxide	Carl Roth GmbH (Karslruhe, Germany)
Purmorphamine	Sigma Aldrich Chemie GmbH (Munich, Germany)
QIA blood and tissue DNA kit	Qiagen GmbH (Hilden, Germany)
Qiagen Plasmid Midi/Maxi Kit/Endotoxin free Maxi Kit	Qiagen GmbH (Hilden, Germany)
QIAprep spin MiniPrep Kit	Qiagen GmbH (Hilden, Germany)
QIAquick Gel Extraction Kit	Qiagen GmbH (Hilden, Germany)
QIAquick PCR Purification Kit	Qiagen GmbH (Hilden, Germany)
QuikChange® Site-Directed Mutagenesis Kit	Agilent Technologies (Santa Clara, USA)
Recombinant Human FGF basic	R&D Systems, Inc. (Oxfordshire, UK)
Restriction Enzymes and Buffer	Fermentas GmbH (St Leon-Rot, Germany), New England Biolabs GmbH (Frankfurt, Germany)
ROCK inhibitor Y-27632	Merck KGaA (Darmstadt, Germany)
Rotenone	Sigma Aldrich Chemie GmbH (Munich, Germany)
SB432542	Sigma Aldrich Chemie GmbH (Munich, Germany)
Shrimp alkaline phosphatase (SAP)	Promega (Mannheim, Germany)
Skim Milk Powder	Sigma Aldrich Chemie GmbH (Munich, Germany)
Sodium chloride (NaCl)	Merck KGaA (Darmstadt, Germany)
Sodium dodecyl sulfate (SDS)	Sigma Aldrich Chemie GmbH (Munich, Germany)
Sodium hydroxide (NaOH)	Merck KGaA (Darmstadt, Germany)
SYBR Green I mini kit	Roche Applied Science (Mannheim, Germany)
Tetramethylrhodamine, methyl ester (TMRE)	Thermo Fisher Scientific (Braunschweig, Germany)
TGF-β3	PeproTech Worldwide (New Jersey, USA)
Thiazolyl blue tetrazolium bromide	Sigma Aldrich Chemie GmbH (Munich, Germany)
TOPO® TA Cloning® Kit for Subcloning	Thermo Fisher Scientific (Braunschweig, Germany)
Transcriptor High Fidelity cDNA Synthesis kit	Roche Applied Science (Mannheim, Germany)
Tris base	Carl Roth GmbH (Karslruhe, Germany)
Triton X-100	AppliChem GmbH (Darmstadt, Germany)
Trizma hydrochloride	Sigma Aldrich Chemie GmbH (Munich, Germany)
Trypsin-EDTA (0.05%), phenol red	Thermo Fisher Scientific (Braunschweig, Germany)
Tween 20	Merck KGaA (Darmstadt, Germany)
ViraPower™ Lentiviral Packaging Mix	Thermo Fisher Scientific (Braunschweig, Germany)
Zeocin	Invivogen (La Jolla, CA, USA)
Z-Leu-Leu-Leu-al (MG-132)	Sigma Aldrich Chemie GmbH (Munich, Germany)
β-Mercaptoethanol	Carl Roth GmbH (Karslruhe, Germany)

2.1.3 Compounds for treatment of eukaryotic cells

For compound treatment of eukaryotic cells, cells were washed twice with PBS. Subsequently, medium containing compound was added. For concentration and length of treatment see Table 5. Cells were kept under standard conditions until pellets were collected and processed.

Table 5: **List of compounds used for treatment of eukaryotic cells.** Table includes compound, treatment conditions and manufacturer.

Compound	Treatment Conditions	Manufacturer
2iP	10, 25 µM, 24h	Sigma Aldrich Chemie GmbH (Munich, Germany)
Aclarubicin	10, 25 µM, 24h	Santa Cruz Biotechnology Inc (California, USA)
Benzyladenine	10, 25, 50, 100, 500 µM, 1mM, 24h	Sigma Aldrich Chemie GmbH (Munich, Germany)
Cucurmin	10, 25 µM, 24h	Sigma Aldrich Chemie GmbH (Munich, Germany)
Dexamethasone	10, 25 µM, 24h	Sigma Aldrich Chemie GmbH (Munich, Germany)
Kinetin	10, 25 µM, 24h	Sigma Aldrich Chemie GmbH (Munich, Germany)
Resveratrol	10, 25 µM, 24h	Sigma Aldrich Chemie GmbH (Munich, Germany)
Sodium butyrate	10, 25 µM, 24h	Sigma Aldrich Chemie GmbH (Munich, Germany)
Valproic acid	10, 25 µM, 24h	R&D Systems, Inc.(Oxfordshire, UK)
Zeatin	10, 25 µM, 24h	Sigma Aldrich Chemie GmbH (Munich, Germany)

2.1.4   Table of software

Table 6: **List of software used.** Table shows software, application software was used for and company or reference.

Software	Application	Company/Reference
AxioVision	Microscope	Carl Zeiss AG
Chimera	Drawing of molecular model	freeware (www.cgl.ucsf.edu/chimera)
EndNote X7	Reference Manager	EndNote
ESEfinder (2001-2006, Cold Spring Harbor Laboratory)	Prediction of ESE	freeware
Flowjo software	Flow cytometry	Flowjo LLC (Oregon, USA)
Graph Pad Prism 5	Statistical analysis, graphs	GraphPad Software Inc.
HaploPainter1.043	Pedigree drawing	freeware
ImageJ	Image quantification	Wayne Rasband, NIH
Light Cycler 480 1.5 Software	qRT-PCR analysis	Idaho Technology Inc.
Microsoft Excel 2010	Data analysis	Microsoft Corp.
MutationTaster	Evaluate pathogenic mutation	(Schwarz et al., 2010)
Primer3Plus	Designing primers	freeware
Staden package	Sequencing analysis	freeware
Summit 4.3.02b2451	Flow cytometry	Beckman Coulter (California, USA)

2.1.5   Table of consumables

Table 7: **List of consumables used.** Table shows consumable and manufacturer.

Consumables	Manufacturer
Amersham Hyperfilm ECL High performance chemiluminescence	GE Healthcare (Freiburg, Germany)
Cell culture consumables	BD Biosciences (Heidelberg, Germany), Corning (Kaiserslautern, Germany), Greiner Bio-One GmbH (Frickenhausen, Germany), Thermo Fisher Scientific (Braunschweig, Germany)
Coverslips	Carl Roth GmbH (Karslruhe, Germany)
Disposable pipettes	Corning (Kaiserslautern, Germany)
Glass slides	Langenbrinck (Emmendingen, Germany)
Light Cycler 384 well plates	Roche Applied Science (Mannheim, Germany)

Consumables	Manufacturer
Microtiter plates	Greiner Bio-One GmbH (Frickenhausen, Germany)
Nitrocellulose membrane	GE Healthcare (Freiburg, Germany)
Nunc™ Lab-Tek™ Chamber Slide	Thermo Fisher Scientific (Braunschweig, Germany)
PCR reaction tubes	PeqLab (Erlangen, Germany)
Pipette tips	Sarstedt AG & Co (Nürnbrecht, Germany) Biozym Scientific (Hessisch Oldendorf, Germany)
Reaction tubes	Greiner Bio-One GmbH (Frickenhausen, Germany), Eppendorf AG (Hamburg, Germany)
Scalpels, dissecting set	Braun (Melsungen, Germany), Fine Science Tools GmbH (Heidelberg, Germany)
Syringe filters (0.45 µm)	Thermo Fisher Scientific (Hamburg, Germany)
Whatman paper	Schleicher und Scheull (Dassel, Germany)

2.2 Deoxyribonucleic acid (DNA) analysis

2.2.1 Quantification of deoxyribonucleic acid samples

All quantifications of DNA were performed using NanoDrop (ND1000) (Peqlab Erlangen, Germany).

2.2.2 Isolation of DNA from eukaryotic cells

DNA isolation from eukaryotic cultured cells was performed using QIA blood and tissue DNA kit (Qiagen GmbH, Hilden, Germany) according to manufacturers' instructions.

2.2.3 Next generation sequencing (NGS)

NGS of *PARK7* locus of the homozygous c.192G>C *DJ-1* mutation carrier was performed at the Institute for Ophthalmic Research (Tübingen, Germany) by the Molecular Genetics Laboratory of Prof. Bernd Wissinger using pooled long distance polymerase chain reaction (LD-PCR) fragments of genomic DNA.

2.2.4 Sequencing of plasmid and genomic DNA

Sequencing was performed using the sanger sequencing method (Sanger et al., 1977).

Sequencing was done using BigDye Terminator v3.1 Kit (Applied Biosystems, Darmstadt, Germany) following manufacturers' instructions on the ABI 3100 Genetic Analyzer (Applied Biosystems/Ambio, Austin, USA). Run module used is shown in Table 8. Primers and PCR programme used for sequencing are shown in Table 9 and Table 10.

Table 8: **ABI 3100 Genetic Analyzer run module.** Table shows settings of the run module.

Name	Value	Range
oven_temperatuer	60	18...65 Deg. C
Poly_Fill_Vol	6500	6500...38000steps
Current_Stability	5.0	0...2000 uAmps
PreRun_Time	15.0	0...15 KVolts
PreRun_Voltage	180	1...1000 sec.
Injection_Voltage	1.2	1...15 KVolts
Injection_Time	18	1...600 sec.
Voltage_Number_Of_Steps	30	1...100 nk
Voltage_Step_Interval	15	1...60 sec.
Data_Delay_Time	120	1...3600 sec.
Run_Voltage	8.5	0...15KVolts
Run_Time	2780	300...14000 sec.

Table 9: **Primers used for sequencing.** These primers were used to verify correct and mutation free integration of an insert into a vector. Table shows label, type of sequencing primers were used for, sequences of primers and the company primers were ordered from.

Label	Product	Sequence	Company
IRES rev	plasmid	5'- tatagacaaacgcacaccg -3'	Metabion international AG (Steinkirchen, Germany)
M13 for	plasmid	5'- tgtaaaacgacggccag -3'	
T7 for	plasmid	5'- taatacgactcactatagg -3'	
U6 for	plasmid	5'- gggcaggaagagggcctat -3'	
CAG forw	plasmid	5'- catgccttcttctttttcc -3'	Eurogentec (Liège, Belgium)
DJ1_gen_seq_Exon3_fw	genomic	5'- acagtgttactctgaatttatgtttca -3'	Metabion international AG (Steinkirchen, Germany)
DJ1_gen_seq_Exon3_rev	genomic	5'- tgctaacaacactcttaagacatttca -3'	

Table 10: **Thermocycler programme used for sequencing PCR.**

cycles		1		29		1
	temp.	time	temp.	time	temp.	time
	94 °C	1 min	94 °C	10 s		
			60 °C	4 min	12 °C	hold

All Lenti-viral constructs were sent to Seqlab - Sequence Laboratories Göttingen GmbH (Göttingen, Germany) for sequencing.

All sequencing results were analysed using Staden package (freeware) software tool to exclude that mutations were introduced during the cloning procedure and to confirm the correct orientation and position of inserts or the correct genotype.

2.2.5   Mitochondrial DNA (mtDNA) damage and mtDNA copy number

DNA was extracted from cell pellets using the QIA blood and tissue DNA kit (Qiagen GmbH, Hilden, Germany) following the manufacturers instructions. Elution step was performed twice per column using 30 µl of Elution buffer. For analysis samples had to have a concentration of at least 10 ng/µl. Pellets were kept at – 20°C until analysis was performed.

Measurement of mtDNA damage and mtDNA copy number was performed by the DNA Damage & Repair Service Unit Tübingen (Tübingen, Germany). DNA lesion rates were performed using LORD-Q real-time PCR (qPCR) method (Lehle et al., 2014).

2.2.6   *In vitro* mutagenesis

In vitro mutagenesis was performed to insert a C>G mutation in U1 snRNA cloned into the pGEM3 vector (Promega, Mannheim, Germany). Mutagenesis was performed using Quik-Change® Site-Directed Mutagenesis Kit (Agilent Technologies, Santa Clara, USA) according to manual instructions. Primers used to insert the mutation are shown in Table 11. Site of mutation is highlighted in red.

Table 11: *In vitro* **mutagenesis primers used for introducing the C>G mutation in the U1snRNA.** Table shows label, PCR product of forward and reverse primer, sequence of primers and the company primers were ordered from.

Label	Product	Sequence	Company
c402g	U1snRNA	5'- gcccaagatctcatacttac**g**tggcaggggagat -3'	Metabion international AG (Steinkirchen, Germany)
c402g_antisense	U1snRNA	5'- atctcccctgcca**c**gtaagtatgagatcttgggc -3'	

2.3   Ribonucleic acid (RNA) analysis

2.3.1   Isolation and quantification of RNA from eukaryotic cells

RNA was isolated from iPSCs for characterisation of generated stem cell lines. Expression level of stem cell markers and silencing of reprogramming factors was determined using qPCR.

RNA was isolated from different eukaryotic cell types (fibroblasts, immortalised fibroblasts, iPSCs, iPSC derived mDA neurons and small molecule neural precursor cells (smNPCs)) to measure gene expression of *DJ-1* semi-quantitatively by reverse transcription PCR (rtPCR) and quantitatively by qPCR.

2.3.1.1   *RNA isolation*

Eukaryotic cells were grown under standard conditions. Cells were collected by enzymatic detachment and washed twice with PBS. Dry pellets were stored at – 80°C until RNA was

isolated using High pure RNA isolation Kit (Roche Applied Science, Mannheim, Germany). Isolation was performed following instructions of the manufacturer. Elution was carried out with 30 µl of RNAse-free water. RNA samples were stored at – 80°C until they were processed further.

2.3.1.2 Quantification of ribonucleic acid samples

All quantifications of RNA were performed using NanoDrop (ND1000) (Peqlab Erlangen, Germany).

2.3.1.3 Reverse transcription

Reverse transcription of RNA was carried out using Transcriptor High Fidelity complimentary deoxyribonucleic acid (cDNA) Synthesis kit (Roche Applied Science, Mannheim, Germany). 50 ng – 200 ng of RNA were used for the reaction. The reaction was performed using anchored-oligo(dT) primers. A negative control was included where transcription was performed without reverse transcriptase. cDNA samples were stored at – 20°C until they were processed further.

2.4 Polymerase chain reactions (PCRs)

2.4.1 PCR amplification

The PCR reaction was performed in order to amplify DNA for subsequent reactions. Amplification of DNA that was foreseen for cloning was amplified using KOD Hot Start DNA Polymerase Kit (Merck KGaA, Darmstadt, Germany) according to instruction manual. All other amplifications were performed using the amplification protocol shown in Table 13. Annealing temperature and primers used are shown in Table 12. All primers were designed using Primer3Plus (freeware) software tool. The reaction mixture for PCR was composed of 0.5 µM forward and 0.5 µM reverse primer (Metabion international AG, Steinkirchen, Germany), 0.5 mM dNTP mix (Merck KGaA, Darmstadt, Germany), 0.02 U/µl GoTaq polymerase (Promega, Mannheim, Germany), 5 x GoTaq Reaction Buffer (Promega, Mannheim, Germany) (final concentration 1 x), and approximately 100 ng DNA in Nuclease-Free Water (Qiagen GmbH, Hilden, Germany).

PCR products were run in a 1.5-2 % agarose gel (Biozym Scientific, Hessisch Oldendorf Germany) containing 7 µl/100 ml Midori Green Advance DNA Stain (Biozym Scientific, Hessisch Oldendorf Germany). The percentage of agarose depended on the size of amplification products. A DNA ladder was used to evaluate the size of bands (GeneRuler™ 100 bp Plus DNA ladder or GeneRuler™ 1 kb Plus DNA ladder, Thermo Fisher Scientific, Hamburg, Germany).

Table 12: **PCR primers used.** Table shows label, PCR product of forward and reverse primer, sequence of primers, annealing temperature (Temp.) used and the company primers were ordered from.

Label	Product	Sequence	Annealing Temp.	Company
pCMV-EcoRI-DJ1-for2	*DJ-1*	5'- acgaattcgaatggcttccaaaagagctctggt -3'	54 °C	Metabion international AG (Steinkirchen, Germany)
pCMV-STOP-Not-rev		5'- agcggccgcctagtctttaagaacaagtggagcc -3'		
DJ1_cDNA_NotI_fwd	*DJ-1 cDNA*	5'- atatagcggccgcatggcttccaaaagagc-3'	58 °C	Eurogentec (Liège, Belgium)
DJ1_cDNA_XhoI_rev		5'- cccccctcgagctagtctttaagaacaag -3'		
DJ1_cDNA_BamHI_fwd	*DJ-1 cDNA*	5'- ctcggatccatggcttccaaaagagctctggtcatc -3'	58 °C	Metabion international AG (Steinkirchen, Germany)
DJ1_cDNA_EcoRI_rev		5'- gcagaattcctagtctttaagaacaagtggagccttc-3'		
U1 in Lenti wt fwd	*U1 snRNA*	5'- cccccggatccatacttacctggcagggg -3'	62 °C	Eurogentec (Liège, Belgium)
U1 in Lenti mut fwd		5'- cccccggatccatacttacgtggcagggg -3'		
U1 in Lenti rev		5'- cccccctcgagcttagcgtacagtctac -3'		

Table 13: **Basic cycler programme.** Annealing temperature depends on the G-C content of the primers used and is shown in Table 12 for each primer pair respectivly.

cycles	1		29		1	
	temp.	time	temp.	time	temp.	time
denaturation	95 °C	2 min	95 °C	30 s		
annealing			X °C	30 s		
elongation			72 °C	approx. 1 min/1kb	72 °C	6 min

2.4.2 Semi-quantitative measurement of cDNA

Semi-quantitative measurement of *DJ-1* gene expression was performed by rtPCR. Primers and cycler programme used are shown in Table 14 and Table 15, respectively. Results were visualised by agarose gel electrophoresis (see 2.4.1).

Table 14: **Primers used for the detection of *DJ-1* in semi-quantitative rtPCR.** Table shows label, PCR product of forward and reverse primer and the company primers were ordered from.

Label	Product	Sequence	Company
pCMV-EcoRI-DJ1-for2	*DJ-1*	5'- acgaattcgaatggcttccaaaagagctctggt -3'	Metabion international AG (Steinkirchen, Germany)
pCMV-STOP-Not-rev	*DJ-1*	5'- agcggccgcctagtctttaagaacaagtggagcc -3'	

Table 15: **Cycler programme used for detection of *DJ-1* in the semi-quantitative rtPCR.**

cycles	1		29		1	
	temp.	time	temp.	time	temp.	time
denaturation	94 °C	2 min	95 °C	30 s		
annealing			54 °C	30 s		
elongation			72 °C	90 s	72 °C	6 min

2.4.3 Quantitative measurement of cDNA

Quantification of cDNA was performed using qPCR. cDNA samples and primers were diluted 1:10 in sterile water. Standards were prepared as mixtures of all control cDNAs in

concentrations of 0.1, 0.02, 0.04, 0.008 and 0.0016 µg/µl. Master mixture for qPCR was composed of 5 µl SYBR Green (Roche Applied Science, Mannheim, Germany), 1 µl primer mixture, and 1.5 µl water. Master mixture was distributed into 384-well plates and 2.5 µl of cDNA were added, respectively. RT- and water control were also included as controls at the same concentrations as the cDNA. qPCR was performed with the Light cycler 480 II (Roche Applied Science, Mannheim, Germany). Exemplary amplification curve and standard curve are shown in (Figure 5A). Relative expression was calculated with Light Cycler 480 1.5 Software (Idaho Technology Inc.) using housekeeping gene levels and the second derivative maximum method (Rasmussen R., 2001). Cycler programme is shown in Table 16.

Relative expression of stem cell markers and silencing of reprogramming factors was calculated using housekeeping gene level of *HMBS* and the second derivative maximum method. Primers used are shown in Table 18.

Relative expression of *DJ-1* was calculated using housekeeping gene levels of *TBP* and *β-actin* and the second derivative maximum method. Primers used are shown in Table 17.

Specificity of amplification products was verified by analysing the melting curve (example Figure 5B) and also by randomly doing an agarose gel electrophoresis of the qPCR products. Samples with two peaks in the melting curve were excluded from the analysis.

Table 16: **Light Cycler programme used for detection of *DJ-1* in qPCR.**

	target temp. (°C)	acquisition mode	time	ramp rate (°C/s)	cycles
pre incubation	95	none	9 min	4.8	1
amplification	95	none	15 s	4.8	55
	58	none	30 s	2.5	
	72	single	20 s	4.8	
melting curve	95	none	5 s	4.8	1
	65	none	1 min	2.5	
	97	continuous		0.11	
cooling	40	none	15 s	2.5	1

Table 17: **Primers used for detection of *DJ-1* in qPCR.**

Label	Product	Sequence	Company
RTPCR DJ1 fwd	*DJ-1*	5'- ggttctaccaggaggtaatctgg -3'	Metabion international AG (Steinkirchen, Germany)
RTPCR DJ1 rev	*DJ-1*	5'- atttcatgagccaacagagc -3'	
RTPCR Ex3 fwd	*DJ-1 with exon 3*	5'- cgagctgggattaaggtcac -3'	
RTPCR Ex3 rev	*DJ-1 with exon 3*	5'- atcttcaaggctggcatcag -3'	
RTPCR TBP fwd	*TBP*	5'- gaagttgggtttttccagctaa -3'	
RTPCR TBP rev	*TBP*	5'- ggagaacaattctgggtttga -3'	
RT_ACTb_fwd	*β-actin*	5'- ctggaacggtgaaggtgaca -3'	Eurogentec (Liège, Belgium)
RT_ACTb_rev	*β-actin*	5'- aagggacttcctgtaacaatgca -3'	

Table 18: **Primers used for detection of stem cells markers and silencing of reprogramming factors in iPSCs by qPCR.**

Label	Product	Purpose	Sequence	Company
endo_Klf4 fwd	endogenous klf4	stem cell marker expression	5'- acagtctgttatgcactgtggtttca -3'	Metabion international AG (Steinkirchen, Germany)
endo_Klf4 rev			5'- catttgttctgcttaaggcatacttgg -3'	
endo_cMyc fwd	endogenous cmyc	stem cell marker expression	5'- ccagcagcgactctgagga -3'	
endo_cMyc rev			5'- gagcctgcctcttttccacag -3'	
REX1 fwd	rex1	stem cell marker expression	5'- gcacactaggcaaacccacc -3'	
REX1 rev			5'- catttgtttcagctcagcgatg -3'	
endo_OCT4 fwd	endogenous oct4	stem cell marker expression	5'- ggaaggaattgggaacacaaagg -3'	
endo_OCT4 rev			5'- aacttcaccttccctccaacca -3'	
endo_SOX2 fwd	endogenous sox2	stem cell marker expression	5'- tggcgaaccatctctgtggt -3'	
endo_SOX2 rev			5'- ccaacggtgtcaacctgcat -3'	
NANOG fwd	nanog	stem cell marker expression	5'- cctgtatttgtgggcctg -3'	
NANOG rev			5'- gacagtctccgtgtgaggcat -3'	
TDGF1 fwd	TDGF1	stem cell marker expression	5'- ctgctgcctgaatgggggaacctgc -3'	
TDGF1 rev			5'- gccacgaggtgctcatccatcacaagg -3'	
UPF1 fwd	UPF1	stem cell marker expression	5'- ccgtcgctgaacaccgccctgctg -3'	
UPF1 rev			5'- cgcgctgcccagaatgaagcccac -3'	
DNMT3B fwd	DNMT3B	stem cell marker expression	5'- gctcacagggcccgatactt -3'	
DNMT3B rev			5'- gcagtcctgcagctcgagttta -3'	
OCT4 viral fwd	viral oct4	silencing of reprogramming factors	5'- ggctctcccatgcattcaaac -3'	
OCT4 viral rev			5'- catggcctgcccggttatta -3'	
SOX2 viral fwd	viral sox2	silencing of reprogramming factors	5'- gcacactgcccctctcacac -3'	
SOX2 viral rev			5'- caccagaccaactggtaatggtagc -3'	
KLF4 viral fwd	viral klf4	silencing of reprogramming factors	5'- cctcgccttacacatgaagagaca -3'	
KLF4 viral rev			5'- caccagaccaactggtaatggtagc -3'	
c-MYC viral fwd	viral cmyc	silencing of reprogramming factors	5'- gctacggaactcttgtgcgtga -3'	
c-MYC viral rev			5'- caccagaccaactggtaatggtagc -3'	
HMBS fwd	HMBS	housekeeping level	5'- atgccctggagaagaatgaagt -3'	
HMBS rev			5'- ttgggtgaaagacaacagcatc -3'	

A)

B)
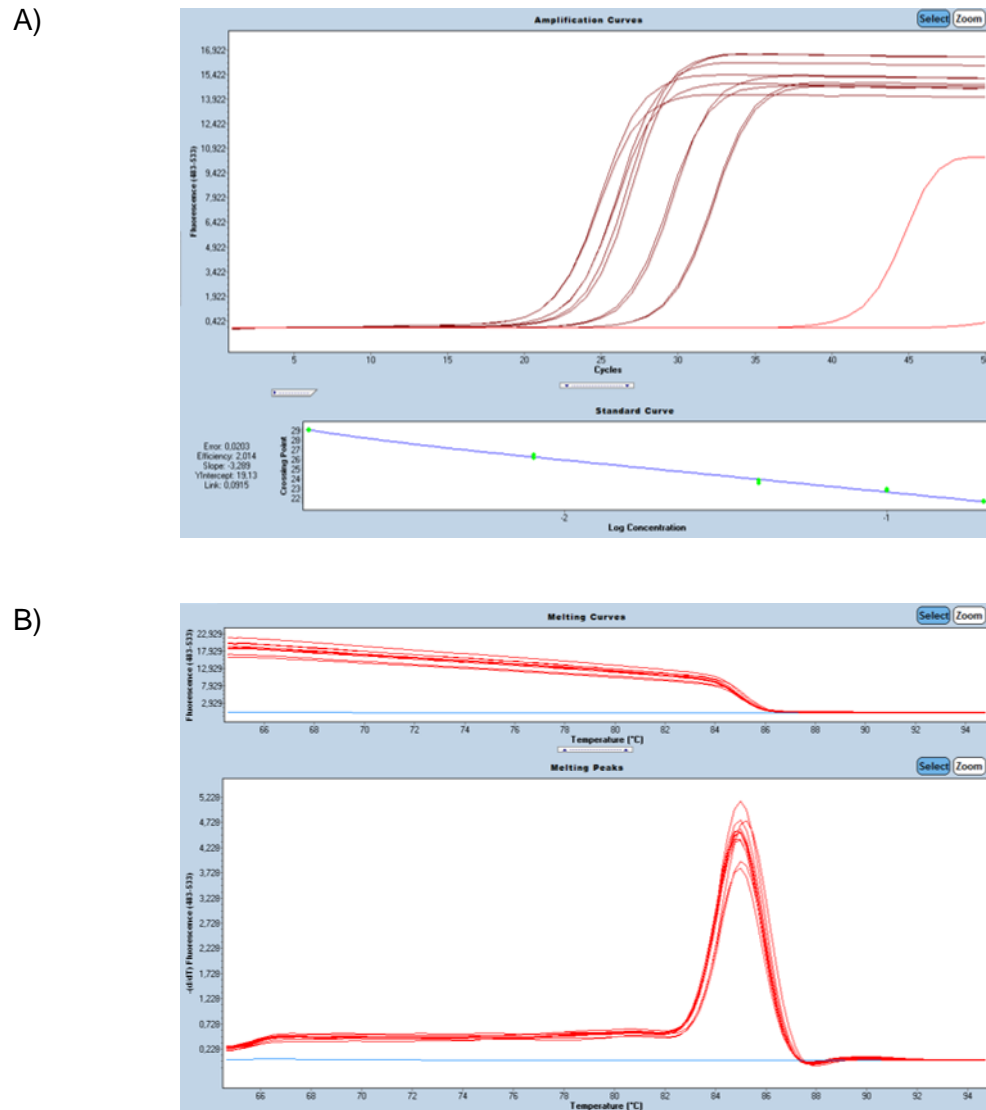
Figure 5: **Exemplary amplification curve, standard curve, melting curve and melting preaks of LC 480 II run.**

A) shows amplifiaction curve of standards of mixtures of control cDNAs in concentrations of 0.1, 0.02, 0.04, 0.008 and 0.0016 µg/µl as well as standard curve with an error of 0.0203 and an efficiency of 2.014. Brown lines represent the standard samples in duplicates and red lines represent RT- and water control. **B)** shows melting curve and corresponding peaks. Blue line represents water control.

2.5 Cloning

2.5.1 Plasmid purification

Plasmid-bearing bacteria were kept at -80°C as glycerol stocks containing 850 µl of bacterial suspension mixed with 150 µl of sterilized glycerin (VWR International, Pennsylvania, USA) (100 %). To grow plasmids, a small amount of frozen stock was scraped off and put into autoclaved LB media with appropriate antibiotic stock solution. Plasmids were then purified by manufacturer's protocol with QIAprep spin MiniPrep Kit if small amounts of DNA

were needed and Qiagen Plasmid Midi/Maxi Kit if larger amounts of DNA were needed or Endotoxin free Maxi Kit (Qiagen GmbH, Hilden, Germany) if DNA was subsequently used for transfection of eukaryotic cells.

Plasmids were eluted in appropriate volume of elution buffer and concentration was measured using NanoDrop (ND1000) (Peqlab Erlangen, Germany). Prepared plasmids were stored at -20 °C.

2.5.2 Transformation of bacteria

Transformation of DNA into One Shot® TOP10 Chemically Competent *E. coli* (Thermo Fisher Scientific, Braunschweig, Germany) was performed following manual instructions.

2.5.3 Cloning procedure

wt U1 sn RNA and mutated U1 sn RNA were cloned into pRNAT-U6.2/Lenti (GenScript USA Inc., New Jersey, USA).

For cloning of other DNA sequences of interest into different expression vectors template DNAs were amplified using primers with a spacer (approximately 5 bp) sequence followed by a short restriction site sequence on the 5' end of PCR primer. Restriction site sequences used were chosen according to multiple cloning site of expression vector. PCR products were purified using 1-2 % agarose gels and QIAquick Gel Extraction Kit (Qiagen GmbH, Hilden, Germany). PCR products and expression vectors were incubated with respective restriction enzymes. Restriction reaction is shown in Table 19 and was performed for 1.5 h at 37 °C. After digestion vector was treated with 1 µl of shrimp alkaline phosphatase (SAP) for DNA amounts up to 1 µg in 1 x MULTI-CORE™ buffer (Promega, Mannheim, Germany) for 15 min at 37 °C followed by heat-inactivation of SAP for 15 min at 74 °C. Reaction was stopped by adding 10 µl of 6 x DNA loading dye (Thermo Fisher Scientific, Braunschweig, Germany). Samples were purified as in previous step. PCR products were ligated for 2 h with vector using DNA T4 ligase (New England Biolabs GmbH, Frankfurt, Germany) at room temperature. Ratio of vector to insert was calculated based on equation (1). For inserts, which have been difficult to transfect the calculated amount of insert was increased up to 5 x.

$$\frac{x \; bp \; insert \; \times \; 50 \; ng \; vector}{y \; bp \; vector} = x \; ng \; insert \qquad (1)$$

One Shot® TOP10 Chemically Competent *E. coli* (Thermo Fisher Scientific, Braunschweig, Germany) were transformed with ligated products following manual instructions. Bacterial colonies were screened by colony PCR for correct transformation with ligated plasmid or grown in LB medium containing appropriate antibiotics to perform DNA isolation QIAprep spin MiniPrep Kit (Qiagen GmbH, Hilden, Germany) and test digest of ligated plasmid. Before using the generated constructs sequencing (see 2.2.4) was performed to validate the cloning procedure.

Table 19: **Composition of restriction digest reaction.**

	Amount	Chemical	Supplier
restriction digest reaction	10 Units/µg DNA	restriction enzyme	New England Biolabs GmbH (Frankfurt, Germany)
	up to 1 µg	DNA	
	1 x	CutSmart™	New England Biolabs GmbH (Frankfurt, Germany)
	add 50 µl	Nuclease-Free Water	Qiagen GmbH (Hilden, Germany)

To clone expression vectors for wt *DJ-1* and *DJ-1* lacking exon 3 the TOPO® TA Cloning® Kit for Subcloning (Thermo Fisher Scientific, Braunschweig, Germany) was used according to manual instructions.

2.6   Transfection of eukaryotic cells

Cells were transfected with various plasmids, which were purified from bacterial cultures. Before plating for transfection, cells were grown under standard conditions. Total cell number for plating was calculated by counting the cells on the Neubauer-chamber before seeding and an appropriate number of cells for the different well formats was distributed into cell culture plates.

2.6.1   Lipofection

For lipofection, cells were transfected using Lipofectamine® 2000 Transfection Reagent (Thermo Fisher Scientific, Braunschweig, Germany) according to manual instructions.

2.6.2   Calcium phosphate precipitation of HEK-293ft cells

For Lentiviral vector production, human embryonic kidney (HEK)-293ft cells were transfected using calcium phosphate precipitation. Cells were transfected in 10 cm culture dishes at a confluency of 50 %. 1-3 h before transfection, HEKft medium (Table 24) was replaced by 7 ml HEKft medium without antibiotics (Penicillin-Streptomycin, Geneticin® Selective Antibiotic). Transfection mixture was prepared: 12 µg DNA (see 2.7) per 10 cm dish was mixed with 50 µl 2,5 M $CaCl_2$ and filled up with sterile water to 500 µl. Same volume of 2 x HBSS (Table 20) was added dropwise to this mix while vortexing. Final

mixture was subsequently added dropwise to cells and dishes were subsequently shaken forward and backward and side-to-side before placing them in the incubator. After 1 h, a sand-like precipitate was visible under the microscope.

Table 20: **Composition of 2 x HBSS.**

Medium	Amount	Chemical	Supplier
2 x HBSS	3.2 g	NaCl	Merck KGaA (Darmstadt, Germany)
	0.14 g	KCl	
	0.08 g	Na2HPO4-7H2O	Sigma Aldrich Chemie GmbH (Munich, Germany)
	0.54 g	Dextrose	
	2.0 g	HEPES (free acid)	

pH to 7.12 with NaOH (Merck KGaA, Darmstadt, Germany) and bring up to 200 ml.

2.6.3   Electroporation

To yield higher transfection efficiencies of difficult to transfect immortalised fibroblasts, the Amaxa nucleofector I (Lonza Group Ltd, Basel, CH) was used.

Cells were detached using trypsin and appropriate cell number was calculated by counting cells on Neubauer-chamber before nucleofection and an appropriate number of cells was used. Immortalised fibroblasts were nucleofected using the Amaxa® Human Dermal Fibroblast Nucleofector® Kit (Lonza Group Ltd, Basel, CH) according to manual instructions.

2.7   Viral vector production

Lentiviral vectors were produced to yield higher transfection efficiencies and to be able to transduce difficult-to-transfect cells.

For Lentiviral vector production, HEK-293ft cells were used. For vector production, cells were grown in HEKft medium without antibiotics (Table 24). Cells were plated on Poly-L-lysine-coated (2.8.1.3) plates and transfected using calcium phosphate precipitation (2.6.2) with ViraPower™ Lentiviral Packaging Mix (Thermo Fisher Scientific, Braunschweig, Germany) (VSV-G, pLP1, pLP2 (3 µg each per 10 cm culture dish)) together with 3 µg per 10 cm culture dish of the respective plasmid DNA at a density of 40 %. ViraPower™ Lentiviral Packaging Mix was kindly provided by the Metabolomics group, Luxembourg Centre for Systems Biomedicine, Université du Luxembourg. After 16 h, medium was changed. After 40 h, supernatant was collected and transferred to a 50 ml tube and fresh medium was added to plates. After 64 h, supernatant was collected again cooled to 4 °C, mixed with supernatant from previous step. To remove cell debris, supernatant was centrifuged for 10 min, 3,000 rcf, 4 °C. Subsequently, supernatant was filtered (0.45 µm filter). Viral vectors were concentrated using polyethylene glycol (PEG)-concentration 24 h later 1/5 volume 40 % sterile PEG was added and mixed by inverting the tube and left at

4 °C over night. 24 h later, virus concentration was finished by centrifugation at 1.500 rcf, 4 °C for 30 min followed by aspiration and second centrifugation at 1.500 rcf, 4 °C for 5 min. Supernatant was removed completely. Virus pellet was resuspended in appropriate amount of PBS (Thermo Fisher Scientific, Braunschweig, Germany) and stored at -80 °C until it was used.

In parallel, MOCK-controls were produced using only packaging plasmids for viral vector production. MOCK-controls served as negative control for all experiments.

2.8   Cell culture

All cells were grown in cell culture approved flasks and plates (BD Biosciences, Heidelberg, Germany, Corning, Kaiserslautern, Germany, Greiner Bio-One GmbH, Frickenhausen, Germany, Thermo Fisher Scientific, Braunschweig, Germany) at 37 °C and 5 % CO_2. Other cell culture consumables were ordered from BD Biosciences, Heidelberg Germany; Corning, Kaiserslautern, Germany; Greiner Bio-One GmbH, Frickenhausen, Germany; and Thermo Fisher Scientific, Braunschweig, Germany.

Cells were stored at -150 °C or liquid nitrogen in freezing medium (Table 21). Freezing medium for iPSCs was supplemented with with ROCK inhibitor Y-27632, 10 µM (Merck KGaA, Darmstadt, Germany). Cells were thawed in 10 ml of medium and centrifuged for 5 min, 300 g to remove DMSO (Sigma Aldrich Chemie GmbH, Munich, Germany) and plated into appropriate cell culture flasks.

Table 21: **Composition of freezing medium.**

Medium	Amount	Chemical
Freezing medium	50 %	culture medium
	40 %	FBS
	10 %	DMSO

Informed consent was obtained from all patients included in this study prior to skin biopsy collection and generation of iPSCs. The Ethics Committee of the Medical faculty and the University Hospital Tübingen approved the consent form.

2.8.1   Coatings of cell culture plates

Different types of cell lines or cells require different biological coatings or extracellular matrices to promote optimal cell attachment on surfaces.

2.8.1.1   Matrigel coating

iPSCs for karyotyping, mDA neurons and smNPCs were grown on matrigel coated plates.

Matrigel coating was performed by adding matrigel (Corning Incorporated, New York, USA) 1:100 in DMEM/F12 (1:1) (1x) - L-Glutamine (Thermo Fisher Scientific, Braunschweig, Germany) for 1 h at 37 °C and 5 % CO_2. Afterwards matrigel was removed and coated plates were used immediately.

2.8.1.2 Gelatin coating

MEF cells which were used as feeder cells for iPSCs were plated on gelatin-coated plates.

Gelatin solution (Type B, 2% in H_2O) (Sigma Aldrich Chemie GmbH, Munich, Germany) was diluted in water to obtain a 0.1 % solution. Plates were coated for 15 min at room temperature. Afterwards solution was aspirated and plates were used immediately.

2.8.1.3 Poly-L-lysine coating

HEKft cells for viral vector production were grown on Poly-L-lysine-coated plates.

Sufficient amount of 0.01 % poly-L-lysine ready-to-use solution was added to cover the bottom of a culture dish. The solution was then collected again and used to coat the next culture dish. This procedure can be repeated up to 10 x.

2.8.1.4 Poly-DL-ornithine hydrobromide (PORN) coating

Murine primary neuron cultures were plated on PORN-coated plates.

500 mg PORN (Sigma Aldrich Chemie GmbH, Munich, Germany) were dissolved in 10 ml 0.15 M boric acid (Sigma Aldrich Chemie GmbH, Munich, Germany) in H_2O (pH 8.35) and sterile filtered with a 0.22 μm filter. These 100 x stocks were stored at -20 °C. Before use, 1 x PORN was prepared by adding 0.15 M boric acid in H_2O (pH 8.35). 1 x PORN was added on coverslips and incubated at 4 °C over night. PORN was removed and coverslips were washed 3 x with HBSS (Thermo Fisher Scientific, Braunschweig, Germany) before use.

2.8.2 Taking skin biopsy in culture

Skin biopsy was collected in a sterile 50 ml falcon tube with 15 ml DMEM +/+ medium (Table 22) (room temperature). Fresh biopsies were processed immediately. Skin biopsy was washed 3x with PBS (Thermo Fisher Scientific, Braunschweig, Germany). Blood, hair and fatty tissue was removed. Biopsy was cut into approximately 8-12 pieces. PBS was removed and 3 pieces were put in a T25 cell culture flask with 1.5 ml DMEM +/+ medium (Table 22). Skin pieces were distributed evenly in flask; not to close to edges. Flasks were kept at 37 °C and 5 % CO_2 for around one week without moving them. After one week, half of medium was replaced with fresh medium. Then, medium was changed twice per week. After flask with skin pieces was confluent, cells were detached by trypsinising and

frozen down or passaged on new culture flask. Flask with skin pieces was kept and pro-
cedure was repeated at least 3 times.

2.8.3 Maintenance of primary fibroblasts, immortalised fibroblasts and HEK293 cells

Primary fibroblasts, immortalised fibroblasts and HEK293 cells were grown in
DMEM +/+ medium shown in Table 22. For splitting, cells were washed once with PBS
and Trypsin-EDTA (0.05%), phenol red (Thermo Fisher Scientific, Braunschweig, Ger-
many) was added for 10 min, 37 °C, 5 % CO_2. After cells detached, medium was added to
inactivate Trypsin-EDTA. Suspension was collected, afterwards required cell numbers
were seeded in new cell culture dishes.

Table 22: **Composition of DMEM +/+ medium.**

Medium	Amount	Chemical	Supplier
DMEM +/+ medium	89 %	DMEM (1x) + 4.5 g/l D-Glucose + L-Glutamine - Pyruvate	Thermo Fisher Scientific (Braunschweig, Germany)
	10 %	FBS	
	1 %	Penicillin-Streptomycin	

2.8.3.1 List of fibroblasts of healthy controls used

Fibroblasts from healthy controls used in this study are shown in Table 23.

Table 23: **Fibroblasts** from healthy controls. Table shows name, internal ID, gender and date of birth.

Name	Internal ID	Gender	Year of birth
Female A	18156	female	1954
Female B	18075	female	1939
Female C	BJ	female	1958
Female D	17956	female	1964
Male a	18220	male	1943
Male b	15243	male	1956
Male c	17556	male	1969

2.8.4 Maintenance of HEK-293ft cells

HEK-293ft cells were used for Lentiviral vector production.

HEK-293ft cells were grown in HEKft medium shown in Table 18. For splitting, cells were
washed once with PBS and Trypsin-EDTA (0.05%), phenol red (Thermo Fisher Scientific,
Braunschweig, Germany) was added for 10 min, 37 °C, 5 % CO_2. Detached cells were
collected, triturated and required cell numbers were seeded in new cell culture dishes.

Table 24: **Composition of HEKft medium.**

Medium	Amount	Chemical	Supplier
HEKft medium	87 %	DMEM (1x) + 4.5 g/l D-Glucose + L-Glutamine - Pyruvate	Thermo Fisher Scientific (Braunschweig, Germany)
	10 %	FBS	
	1 %	Penicillin-Streptomycin	
	1 %	MEM NEAA (100x)	
	1 %	Geneticin® Selective Antibiotic (G418 Sulfate) (50 mg/mL)	

For Lentiviral vector production cells were cultivated in HEKft medium without antibiotics.

2.8.5 Immortalisation of human dermal fibroblasts

Human dermal fibroblasts were immortalised to be able to use them at higher passages for experiments and to have lines available as an unlimited source.

For immortalisation, a lentiviral vector expressing SV40 was used: pLenti-III-SV40 (Applied Biological Materials – abm Biotechnology Company, Richmond, Canada). Lentiviral vector stocks were produced (2.7) and stored at -80 °C. Human dermal fibroblasts were transduced with lentiviral vector in the presence of polycation Polybrene® (Thermo Fisher Scientific, Braunschweig, Germany). Subsequently, cells were incubated for 14 h at 37 °C, 5 % CO_2. Medium was changed and DMEM +/+ medium (Table 22) was added. Each 6-well was splitted onto a 10 cm dish 2 days after transduction. Immortalised fibroblasts were separated from non-immortalised fibroblasts based on morphology by serial passaging of 1:10 until only immortalised fibroblasts were left. Cells were propagated further and stocks were frozen down (2.8).

2.8.6 Maintenance of feeder cells for iPSCs

As feeder cells, irradiated mouse embryonic fibroblasts (MEF) cells were used (GlobalStem, Maryland, USA). MEF cells were thawed and plated on Gelatin-coated plates (2.8.1.2) and fed with DMEM +/+ medium (Table 22). Approximately 4400 MEF cells were plated per cm^2. The next day, iPSCs were plated on MEF cells. After one week, iPSCs were splitted onto fresh feeder cells.

2.8.7 Reprogramming of human fibroblasts to iPSCs

Human dermal fibroblast obtained from skin biopsies of patients with PD were reprogrammed using an adapted protocol from (Takahashi et al., 2007). Fibroblasts were transduced with a mix of retroviral vectors encoding o*ct4*, s*ox2*, k*lf4* and *c-myc*. Five days after

transduction, cells were split onto 10 cm dishes with irradiated MEF cells (GlobalStem, Maryland, USA) (2.8.6). Seven days after transduction medium was changed to hES medium (Table 25). Once colonies were visible they were picked, propagated, stocks were frozen down (2.8) and clones were characterised. At least two clones per patient line were used for all experiments.

2.8.8 Maintenance of iPSCs

iPSCs were grown in hES medium (Table 25). For splitting, cells were washed once with PBS and 5 U/ml dispase (Stemcell Technologies, Inc., Grenoble, France) were added for 5 min, 37 °C, 5 % CO_2. Afterwards colonies were detached by pipetting and washed 3x with hES medium. Required colony numbers were seeded on new cell culture dishes with irradiated MEF cells (GlobalStem, Maryland, USA) (2.8.6).

Table 25: **Composition of hES medium.**

Medium	Amount	Chemical	Supplier
hES medium	77 %	KnockOut™DMEM (1x) + 4.5 g/l D-Glucose - L-Glutamine + Sodium pyruvate	Thermo Fisher Scientific (Braunschweig, Germany)
	20 %	Knockout serum replacement	
	1 %	MEM NEAA (100x)	
	1 %	GlutaMAX (100x)	
	1 %	Penicillin-Streptomycin	
	50 µM	β-mercaptoethanol	Carl Roth GmbH (Karslruhe, Germany)
	10 ng/µl	Recombinant Human FGF basic	R&D Systems, Inc. (Oxfordshire, UK)

2.8.9 Germ layer characterisation of iPSCs

Germ layer characterisation of iPSCs is done by a cooperation partner at the Northwestern Universtiy (Chicago, IL, USA) at the Department of Neurology of Dimitri Kranic, MD, PhD.

2.8.10 Genomic characterisation of iPSCs

After correct reprogramming of fibroblasts with retroviral vectors generated iPSCs underwent a genomic characterisation. Genomic aberrations were excluded by performing karyotyping and a genotyping microarray.

2.8.10.1 Karyotyping

Karyotyping of newly reprogrammed iPSC lines is necessary to exclude major chromosomal aberrations and show maintenance of an euploid karyotype over several passages *in vitro.*

iPSCs were grown under standard conditions. Cells were detached using dispase (Stemcell Technologies, Inc., Grenoble, France). 10 medium sized colonies were harvested and single cells were obtained by adding accutase solution (Merck KGaA, Darmstadt, Germany) for 5 min at 37 °C. Cells were triturated and accutase solution was inactivated using serum containing medium. Cells were plated on a matrigel-coated (2.8.1.1) Nunc™ Lab-Tek™ Chamber Slide (Thermo Fisher Scientific, Braunschweig, Germany) with hES medium (Table 25).

G-banding of iPSCs was performed at the Cytogenetics Research Group at the Institute for Medical Genetics and Applied Genomics of the University Hospital Tübingen.

2.8.10.2 Genotyping microarray

A genotyping microarray analysis of newly reprogrammed iPSCs was performed to exclude mutations caused by/during the reprogramming process, e.g. by the retroviral vectors.

iPSCs were grown under standard conditions. Cells were detached using dispase (Stemcell Technologies, Inc., Grenoble, France). DNA was isolated using QIA blood and tissue DNA kit (Qiagen GmbH, Hilden, Germany) according to manufacturers' instructions. Isolated and nanodropped DNA was sent for genotyping.

The genotyping was performed at the Microarray Genome Chip Facility at the Institute for Medical Genetics and Applied Genomics of the University Hospital Tübingen. The Illumina HumanCytoSNP-12 was used. Row data were analysed using the 'cytogenetics report' we received from the Microarray Genome Chip Facility.

2.8.11 Differentiation of iPSCs to mDA neurons and maintenance of mDA neurons

For differentiation an appropriate number of iPSC colonies was dissociated using accutase solution (Merck KGaA, Darmstadt, Germany) and seeded in hES medium (Table 25) without Recombinant Human FGF basic with ROCK inhibitor Y-27632, 10 µM (Merck KGaA, Darmstadt, Germany) at a density of 3×10^5 cells per matrigel-coated (2.8.1.1) 6-well. A modified floor plate-based mDA neuron induction protocol (Kriks et al., 2011, Chambers et al., 2009, Nguyen et al., 2011, Reinhardt et al., 2013b) was followed for differentiation (Figure 6):

Cells were kept in hES medium (Table 25) without Recombinant Human FGF basic from day 1-3. Then N2 medium (Table 26) was added sequentially (25 %, 50 %, 75 %) from day 3-6. Cells were kept in N2 medium from day 6-18 and splitted on new matrigel-coated plates on day 13. On day 18, a mixture of 50 % N2 and 50 % Maturation medium (Table 27) was added. From day 19 onwards, they were kept in maturation medium until they

were analysed. Cells were splitted again on fresh matrigel-coated plates on day 21 and 38. Differentiation was based on exposure to Purmorphamine (0.5 µM) (Sigma Aldrich Chemie GmbH, Munich, Germany), from day 0-19 and SB432542 (20 µM) (Sigma Aldrich Chemie GmbH, Munich, Germany) and Dorsomorphin (1 µM) (R&D Systems, Inc., Oxfordshire, UK) from day 0-6. From day 10-12 medium was supplemented with human FGF8 (PeproTech Worldwide, New Jersey, USA). Ascorbic acid (AA) (Sigma Aldrich Chemie GmbH, Munich, Germany) and BDNF (PeproTech Worldwide, New Jersey, USA) were added from day 10 onwards and GDNF (PeproTech Worldwide, New Jersey, USA), TGF-β3 (PeproTech Worldwide, New Jersey, USA) and dbcAMP (Sigma Aldrich Chemie GmbH, Munich, Germany) from day 12 onwards.

Cells were kept in maturation medium with supplements (AA, BDNF, GDNF, TGF-β3 and dbcAMP) until they were processed further for measurements.
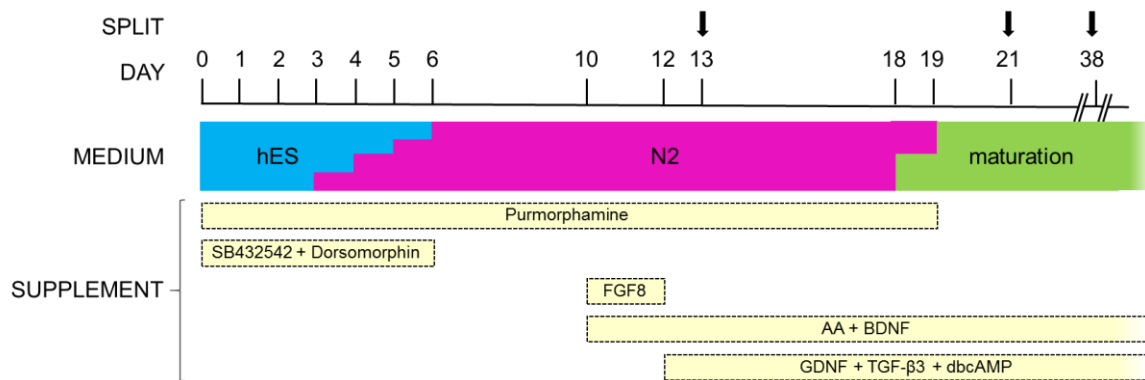
Figure 6: **Floor plate-based mDA neuron induction protocol.**

mDA neurons were differentiated from iPSCs using an adapted floor plate-based protocol from (Kriks et al., 2011, Chambers et al., 2009, Nguyen et al., 2011, Reinhardt et al., 2013b). iPSCs were differentiated on matrigel-coated 6-well plates. Differentiation was started by supplementing hES medium with Purmorphamine (0.5 µM), SB432543 (20 µM) and Dorsomorphin (1 µM). By changing medium to N2 medium supplemented with Purmorphamine (0.5 µM), human FGF8 (100 ng/µl), AA (20 µM) and BDNF (20 ng/ml) mDA patterning was performed. Maturation was induced by supplementing N2 medium with AA (20 µM), BDNF (20 ng/ml), GDNF (10 ng/ml), TGF-β3 (1 ng/ml) and dbcAMP (500 µM) and medium was changed to maturation medium on day 19. On day 13, 21 and 38 cells were replated as single cells on fresh matrigel-coated culture plates.

Table 26: **Composition of N2 medium.**

Medium	Amount	Chemical	Supplier
N2 medium		DMEM/F12 (1:1) (1x) - L-Glutamine	Thermo Fisher Scientific (Braunschweig, Germany)
	1:200	N-2 supplment (100x)	
	500 µl	Penicillin-Streptomycin	

Table 27: **Composition of Maturation medium.**

Medium	Amount	Chemical	Supplier
maturation medium	49 %	Neurobasal® medium (1x)	Thermo Fisher Scientific (Braunschweig, Germany)
	49 %	DMEM/F12 (1:1) (1x) - L-Glutamine	
	1 %	Penicillin-Streptomycin	
	1 %	GlutaMAX (100x)	
	1:100	B-27® Supplement (50X)	
	1:200	N-2 supplment (100x)	

2.8.12 Electrophysiology of mDA neurons

Electrophysiology of mDA neurons is done by a cooperation partner at the Northwestern Universtiy (Chicago, IL, USA) at the Department of Neurology of Dimitri Kranic, MD, PhD.

2.8.13 Generation and Maintenance of small molecule neural precursor cells (smNPCs)

smNPCs were generated following a smNPC derivation protocol (Reinhardt et al., 2013a). smNPCs were grown in Maturation medium (Table 27) supplemented with CHIR 99021, 3 µM (Axon Medchem BV, Groningen, Netherlands), Purmorphamine, 0.5 µM (Sigma Aldrich Chemie GmbH, Munich, Germany) and AA, 150 µM (Sigma Aldrich Chemie GmbH, Munich, Germany). For splitting, cells were washed once with PBS and accutase solution (Merck KGaA, Darmstadt, Germany) was added for 15 min, 37 °C, 5 % CO_2. Afterwards cells were washed once with DMEM/F12 (1:1) (1x) - L-Glutamine (Thermo Fisher Scientific, Braunschweig, Germany). Required cell numbers were seeded on new matrigel-coated (2.8.1.1) cell culture dishes.

2.9 Murine primary neuron cultures

Mice were kept under standard conditions with free access to food and water in a cycle of 12 h of light and 12 h of dark. The local animal welfare and ethics committee of the country commission Tübingen approved all experiments and procedures. Number of animals used and their suffering was kept to a minimum. DJ-1 -/- mice with a C57BL6/J background were compared to C57BL6/J wildtype (wt) mice.

Table 28: **Mouse lines used for the generation of primary neuron cultures and sequences of genotyping primers.**

Mouseline	Information	Genotyping Primers	Reference
C57BL6/J	wt mouseline with black fur for breeding and backcrossing	DJ-1ko-rv: 5'-CGGTACCAGACTCTCCCATC-3' DJ-1wt-fwd: 5'-AGGCAGTGGAGAAGTCCATC-3' DJ-1wt-rv: 5'-AACATACAGACCCGGGATGA-3'	Charles River Laboratories International, Inc., Wilmington, US
DJ-1 -/-	Transgene: DJ-1, Vector: pGT1Lxf		(Pham et al., 2010)

Genotype of mice was determined from a tip of the tail which was taken after mice were sacrificed. Whole genome DNA was isolated from tail biopsy using DirectPCR Lysis Reagent (Mouse Tail) kit (Viagen Biotech, Inc., Los Angeles, USA). Genotyping was performed by PCR using primers shown in Table 28. For experiments only new born (P0) mice were used.

The day before preparation, coverslips were coated with Poly-DL-ornithine hydrobromide (PORN) (2.8.1.4). Newborn pups were decapitated, and whole brains were removed. Brain from each pup was handled separately. Hippocampi were dissected in 6 cm dishes with HBSS (Thermo Fisher Scientific, Braunschweig, Germany). Both Hippocampi were put in a 1.5 ml reaction tube with 400 µl HBSS. HBSS was removed afterwards and 200 µl trypsin was added and incubated for 14 min at 37 °C. To remove trypsin completely, cultivation medium (composition Table 29) was added and all the liquid was aspirated afterwards. This was followed by 3 washing steps with cultivation medium, during the last step the tissue was triturated carefully by pipetting 8 x with a 100 µl pipet tip. Finally, cells were plated on the coverslips. After 4-6 h cultivation medium was replaced by plating medium (composition Table 30). Cells were used for measurements after 5-10 days.

Table 29: **Composition of cultivation medium.**

Medium	Amount	Chemical
cultivation medium	500 ml	Neurobasal®-A Medium Minus Phenol Red
	5 ml	Glutamax I

Table 30: **Composition of plating medium.**

Medium	Amount	Chemical
plating medium	24,5 ml	cultivation medium
	0,5 ml	B27® Supplement GIBCO®
	5 ng/ml	bFGF

2.10 Microscopic imaging

Microscopic imaging analysis was performed with fixed cells (2.10.1) and live cells (2.10.2).

2.10.1 Immunofluorescence of cells

After correct reprogramming of fibroblasts with retroviral vectors expressing the 'Yamanaka factors', pluripotency marker expression was assessed using immunocytochemistry (ICC).

After differentiation of iPSCs to mDA neurons, neurons were tested for expression of different neuronal markers as well using ICC.

iPSCs or mDA neurons, respectively were grown on coverslips pre-coated with matrigel (2.8.1.1) under standard conditions. For fixation, medium was removed and 4 % formaldehyde (FA) in PBS was added for 20 min at room temperature. FA was aspirated and ice-cold 100 % methanol was added for 5 min at -20 °C to permeabilise cells. Methanol was aspirated and cells were washed 2 x using PBS. Samples were blocked using 10 % FCS in PBS for 30 min at room temperature. Cells were incubated with primary antibody (Table 35) for 1-2 h at 37 °C or at 4 °C over night. Cover slips were washed 3 x with PBS before secondary antibody (Table 35) was added in 10 % FCS in PBS for 1 h at room temperature in the dark. Cover slips were washed 3 x with PBS and then stained with 10 µl of DAPI (4',6-Diamidino-2-Phenylindole, Dihydrochloride) (Thermo Fisher Scientific, Braunschweig, Germany) in 500 µl of PBS and incubated for 10 min at room temperature. Afterwards, they were washed 2 x with PBS and mounted on glass slides using Mowiol/DABCO (Carl Roth GmbH, Karslruhe, Germany).

2.10.2 Live cell imaging

Cells (fibroblasts, mDA neurons or murine primary neuron cultures, respectively) were grown under standard conditions and plated into Nunc™ Lab-Tek™ Chamber Slides (Thermo Fisher Scientific, Braunschweig, Germany) for measurement. Live cell imaging experiments were performed using the Live Cell Microscope Axiovert 2000 (Carl Zeiss Microimaging GmbH, Jena, Germany). Measurements were performed in a humidified 5 % CO_2 atmosphere at 37 °C.

2.10.2.1 MitoTracker green staining

To perform staining of mitochondria MitoTracker® Green FM (Thermo Fisher Scientific, Braunschweig, Germany) was used. This green fluorescent dye stains mitochondria regardless of the mitochondrial membrane potential (MMP).

Cells were stained with 0.1 nM MitoTracker® Green FM and 2 µg/ml Hoechst 33342, Trihydrochloride, Trihydrate (Thermo Fisher Scientific, Braunschweig, Germany) in PBS for 20 min at 37 °C and 5 % CO_2.

2.10.2.2 TMRE staining

TMRE is sequestered by active mitochondria. The MMP was measured via the red fluorescent intensity of the cell-permeant, cationic dye.

To measure MMP, cells were stained using Tetramethylrhodamine, methyl ester (TMRE) (Thermo Fisher Scientific, Braunschweig, Germany) per manufacturer's instructions. Cells were stained with 100nM TMRE and 2 µg/ml Hoechst 33342, Trihydrochloride, Trihydrate (Thermo Fisher Scientific, Braunschweig, Germany) in PBS for 20 min at 37 °C and 5 % CO_2.

2.10.2.3 Neurite outgrowth

Neurite outgrowth of mature mDA neurons (between 80 and 100 days of differentiation) was measured. Neurons were splitted onto matrigel-coated (2.8.1.1) Nunc™ Lab-Tek™ Chamber Slides (Thermo Fisher Scientific, Braunschweig, Germany) and outgrowth was measured using the Live Cell Microscope Axiovert 2000 (Carl Zeiss Microimaging GmbH, Jena, Germany). Pictures were taken using the Carl Zeiss Plan-Apochromat 63x/1.40 oil objective every 5 min for 30 min. Images were analysed using AxioVision (Carl Zeiss AG) and ImageJ (Wayne Rasband, NIH) software with MTrackJ plugin.

2.11 Flow cytometry

Flow cytometry allows the analysis of cells using a laser-based detection method. Size and granularity as well as fluorescent dies can be detected at the same time allowing the characterisation of the cells.

Flow cytometry measurements were performed using the BD LSRFortessa (Becton,Dickinson and Company.© Erembodegem, Belgium) or the CyAn ADP Analyzer (Beckman Coulter, California, USA). Analysis of flow cytometry was performed using Flowjo software (Flowjo LLC, Oregon, USA) or Summit 4.3.02b2451 software (Beckman Coulter, California, USA), respectively.

2.11.1 MitoSOX staining

To measure mitochondrial ROS, cells were stained using MitoSOX™ Red Mitochondrial Superoxide Indicator (Thermo Fisher Scientific, Braunschweig, Germany).

MitoSOX™ Red reagent is a fluorogenic dye which gets oxidised by superoxide resulting in red fluorescence. MitoSOX™ Red selectively targets mitochondria in living cells.

Cells were grown under standard conditions. Before staining, they were washed twice with HBSS (Thermo Fisher Scientific, Braunschweig, Germany). 2 µM MitoSOX™ Red-solution was added to cells and incubated for 20 min at 37 °C in a no-CO_2 incubator. A negative control to determine autofluorescence and a positive control using MitoSOX™ Red-solution and 10 µM rotenone (Sigma Aldrich Chemie GmbH, Munich, Germany) were included. Afterwards, cells were washed once with HBSS and detached using accutase solution

(Merck KGaA, Darmstadt, Germany) for 15 min at 37 °C. Cells were centrifuged for 5 min with 200 g and medium was removed afterwards and cells were resuspended in 200 µl HBSS with 1 % BSA. Cells were measured using 582 nm filter. At least 30000 events in required area were measured.

2.12 Protein biochemistry

2.12.1 Western blot analysis

Western blot analysis was done to measure the levels of DJ-1 in different eukaryotic cell types.

Cells were collected and pelleted. Samples were stored at -80 °C until they were processed. Pellets were lysed in Lysis buffer containing protease inhibitor (Roche Applied Science, Mannheim, Germany). Protein concentration was measured by Bradford assay (see chapter 2.12.1.1) and adjusted to required protein concentration using lysis buffer (Table 31). A 10 % SDS gel with a 4 % stacking gel was prepared and run in running buffer (Table 33). Samples were mixed with 5 x Laemmli buffer (Table 32) plus 100 µl of 1 M DTT per 2 ml Laemmli buffer. Denaturing of sample lysates was done by incubating at 96 °C for 5 min, afterwards samples were snap cooled on ice, quickly centrifuged and directly loaded on the gel. As a size standard PageRuler Plus Prestained Protein Ladder (Thermo Fisher Scientific, Braunschweig, Germany) was loaded as well. Samples were resolved with a one-dimensional discontinuous sodium dodecyl sulfate polyacrylamide gel electrophoresis (SDS-PAGE). While samples were running through the stacking gel, voltage was set to 80 V, when samples entered the running gel, voltage increased to 120 V to 150 V. Blotting of gel onto a nitrocellulose membrane (Thermo Fisher Scientific, Braunschweig, Germany) was done for 7 min, 20 V using the iBlot® device (Invitrogen GmbH, Karslruhe, Germany). Subsequently, membrane was blocked using 5 % skim milk powder (Sigma Aldrich Chemie GmbH, Munich, Germany) in TBS-T buffer (Table 34) for 1 h at room temperature. Primary antibody (Table 35) was added at 4 °C over night under agitating conditions. Membranes were washed 6x for 5 min in TBS-T buffer and incubated with secondary antibody (Table 35) for 1 h in 5 % milk powder in TBS-T at room temperature. Blots were washed 6 x for 5 min with TBS-T buffer and labelled proteins were detected after incubation with a 1:1 Amersham ECL Western Blotting Detection Reagent (GE Healthcare, Freiburg, Germany) mixture. X-ray films were exposed to blots and developed using an X-ray developer (Fujifilm, Düsseldorf, Germany).

Table 31: **Composition of Lysis buffer.**

Buffer	Amount	Chemical	Supplier
Lysis buffer pH 7.4	10 mM	HEPES	Sigma Aldrich Chemie GmbH (Munich, Germany)
	1.5 mM	$MgCl_2$	Carl Roth GmbH (Karslruhe, Germany)
	10 mM	KCl	Merck KGaA (Darmstadt, Germany)
	0.5 mM	DTT	Carl Roth GmbH (Karslruhe, Germany)
	0.05 %	NP40	VWR International (Pennsylvania, USA)
	add fresh 1 %	Triton X 100	AppliChem GmbH (Darmstadt, Germany)

Table 32: **Composition of Laemmli buffer.**

Buffer	Amount	Chemical	Supplier
5 x Laemmli buffer	62.5 mM, pH 6.8	Trizma hydrochloride	Sigma Aldrich Chemie GmbH (Munich, Germany)
	5 %	β-mercaptoethanol	Carl Roth GmbH (Karslruhe, Germany)
	10 %	Glycerin	VWR International (Pennsylvania, USA)
	2 %	SDS	Sigma Aldrich Chemie GmbH (Munich, Germany)
	1 spatula tip	Bromphenol blue	Merck KGaA (Darmstadt, Germany)

Table 33: **Composition of 5 x running buffer.**

Buffer	Amount	Chemical	Supplier
5 x running buffer	45 g	Tris	Carl Roth GmbH (Karslruhe, Germany)
	216 g	Glycine	Carl Roth GmbH (Karslruhe, Germany)
	150 ml, 10 %	SDS	Sigma Aldrich Chemie GmbH (Munich, Germany)
	add to 3 l	VE water	

Table 34: **Composition of 10 x TBS and TBS-T.**

Buffer	Amount	Chemical	Supplier
10 x TBS pH 7.5	50 mM	Tris	Carl Roth GmbH (Karslruhe, Germany)
	150 mM	NaCl	Merck KGaA (Darmstadt, Germany)

For TBS-T buffer add 1 % Tween 20 to 1 x TBS in VE water.

Table 35: **List of antibodies used including species, company, dilution and use.**

Antibody	Protein/Name	Species	Company	Dilution	Use
Primary	DJ-1 (D29E5) XP® mAB	rabbit	Cell Signaling Technology (Cambridge, UK)	1:2000	WB
Primary	Anti-PARK7/DJ1 ab169520	rabbit	Abcam (Cambridge, UK)	1:1000	WB
Primary	Mous anti-DJ-1 (37-8800) mAB	mouse	Invitrogen GmbH (Karslruhe, Germany)	1:20	WB
Primary	Anti-Glyceraldehyde-3-Phosphate Dehydrogenase Antibody MAB374	mouse	Merck KGaA (Darmstadt, Germany)	1:5000	WB
Primary	GAPDH antibody GTX100118	rabbit	GeneTex International Corporation (Hsinchu City, Taiwan)	1:80000	WB
Primary	Monoclonal Anti-β-Actin antibody A5441	mouse	Sigma Aldrich Chemie GmbH (Munich, Germany)	1:3000	WB

Primary	Anti-Nanog antibody ab80892	rabbit	Abcam (Cambridge, UK)	1:1000	ICC
Primary	Anti-Oct4 antibody ab19857	rabbit	Abcam (Cambridge, UK)	1:300	ICC
Primary	Anti-Stage-Specific Embryonic Antigen-4 Antibody MAB4304	mouse	Merck KGaA (Darmstadt, Germany)	1:100	ICC
Primary	Anti-TRA-1-81 Antibody MAB4381	mouse	Merck KGaA (Darmstadt, Germany)	1:50	ICC
Primary	Monoclonal Mouse anti-TUBB3 antibody #MMS-435P	mouse	Covance Research Products Inc (Pennsylvania, USA)	1:500	ICC
Primary	Anit-Tyrosine Hydroxilase Antibody P40101-150	rabbit	Pel Freez Biologicals (Arkansas, USA)		
Primary	HNF-3β Antibody (B-2) sc-271103	mouse	Santa Cruz Biotechnology, Inc (California, USA)	1:100	ICC
Primary	Lmx1A	rabbit	Merck KGaA (Darmstadt, Germany)	1:1000	ICC
Secondary	Amersham ECL Mouse IgG, HRP-linked whole Ab NA931-1ML	mouse	GE Healthcare (Freiburg, Germany)	1:5000	WB
Secondary	Amersham ECL Rabbit IgG, HRP-linked whole Ab NA934-1ML	rabbit	GE Healthcare (Freiburg, Germany)	1:5000	WB
Secondary	Goat anti-Mouse IgG (H+L) Secondary Antibody, Alexa Fluor® 488 conjugate	mouse	Invitrogen GmbH (Karslruhe, Germany)	1:1000	ICC
Secondary	Goat anti-Rabbit IgG (H+L) Secondary Antibody, Alexa Fluor® 568 conjugate	rabbit	Invitrogen GmbH (Karslruhe, Germany)	1:1000	ICC

2.12.1.1 Bradford Assay

Bradford assay was used to measure and normalise total protein concentration for all Western blot samples. Protein concentrations were calculated using a standard protein ladder done for each independent experiment using 0, 1, 2, 4, 6, 8, 10 µg BSA (Carl Roth GmbH, Karslruhe, Germany) as standard. 1 µl of sample diluted with 49 µl of water and 150 µl of Bradford reagent (Thermo Fisher Scientific, Braunschweig, Germany) were mixed. Absorbance was measured at 595 nm using plate reader: Mithras LB 940 (BERTHOLD Technologies GmbH & Co. KG, Bad Wildbad, Germany) or the Synergy™ Mx Microplate Reader (BioTek Instruments, Inc., Bad Friedrichshall, Germany).

2.12.1.2 Blocking of proteasomal and lysosomal degradation

To block proteasomal degradation smNPCS were grown under standard conditions. Cells were treated with Z-Leu-Leu-Leu-al (MG-132) (Sigma Aldrich Chemie GmbH, Munich, Germany) for 24 h with different concentrations of: 0.5 µM, 1 µM, 5 µM, 10 µM, 25 µM, 50 µM. DMSO treatment was included as control.

To block lysosomal degradation smNPCS were grown under standard conditions. Cells were treated with Bafilomycin A1 (Enzo Life Sciences BVBA, Antwerpen, Belgium) for 24 h

with different concentrations: 25 nM, 50 nM, 100 nM, 150 nM, 200 nM. DMSO treatment was included as control.

24 h after treatment cells were harvested and Western blot analysis (2.12.1) was performed.

2.13 Assessment of metabolic activity using Thiazolyl blue tetrazolium bromide (MTT) reduction assay

MTT reduction assay was performed to determine metabolic activity of cells after treatment with compounds.

Cells take up MTT substrate. It gets reduced by mitochondrial and endoplasmatic reticulum dehydrogenase enzymes. Depending on cell integrity the reduced MTT purple formazan accumulates (Cookson et al., 1995).

Cells were seeded in a 96-well plate and grown to 80 % confluence in empty medium or medium supplemented with compound at concentration of interest (Table 5). Highest used solvent concentration was used as control. Medium was removed and 0.5 mg/ml MTT stock solution (Sigma Aldrich Chemie GmbH, Munich, Germany) in PBS (Thermo Fisher Scientific, Braunschweig, Germany) was added and incubated for 30 min at 37 °C, 5 % CO_2. Afterwards medium was removed and 100 µl DMSO (Sigma Aldrich Chemie GmbH, Munich, Germany) was added to solubilise the crystals. Absorbance at 595 nm was measured using the Mithras LB 940 (BERTHOLD Technologies GmbH & Co. KG, Bad Wildbad, Germany) or the Synergy™ Mx Microplate Reader (BioTek Instruments, Inc., Bad Friedrichshall, Germany) plate reader.

2.14 Splicing assay

Splicing analysis was performed to ascertain differential splicing of the c.192G>C *DJ-1* mutation.

2.14.1 Minigene assay

Minigene assay is used to analyse splicing of an exon of interest by cloning it into a vector (pSPL3) between two given exons (Exon A and Exon B) and subsequent analysis of the cDNA by rtPCR and sequencing (Figure 7).
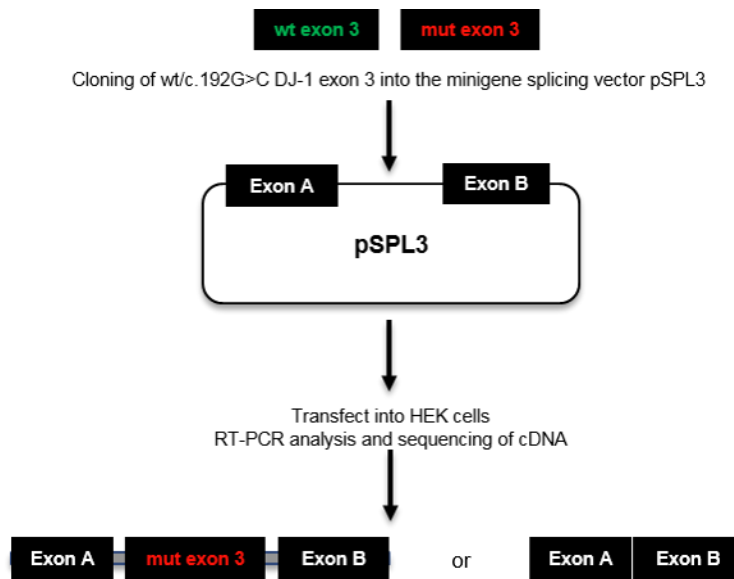
Figure 7: **Schematic overview of Minigene assay.**

wt *DJ-1* exon 3 or mutant *DJ-1* exon 3 carrying the c.192G>C *DJ-1* mutation respectively including flanking intronic sequences were cloned in a vector (pSPL3) (Invitrogen GmbH, Karslruhe, Germany) between two given exons (A and B). After transfection of the final plasmids splicing of wt or mutant exon 3 was analysed by rtPCR and subsequent sequencing of cDNA. It was analysed wether the c.192G>C *DJ-1* mutation leads to physiological splicing or missplicing with skipping of exon 3.

2.14.1.1 U1 cotransfection in minigene assay

To assess the effect of U1 on c.192G>C *DJ-1* splicing, U1 was cotransfected together with the minigene constructs to HEK293 cells.

HEK293 cells (2.8.3) were transfected at 80 – 90 % confluence using Lipofectamine® 2000 Transfection Reagent (Thermo Fisher Scientific, Braunschweig, Germany) according to manufacturers' instructions. Cells were transfected with 4 µg minigene plasmid and 4 µg U1snRNA. RNA isolation, cDNA synthesis and Sanger sequencing were performed as described by (Weisschuh et al., 2012). Subcloning of rtPCR products into the pCR2.1 vector (Invitrogen GmbH, Karslruhe, Germany) was performed according to the manufacturer´s instructions.

2.14.2 MutationTaster

To perform an *in silico* analysis to evaluate the effect of the c.192G>C *DJ-1* mutation MutationTaster (Schwarz et al., 2010) software was used.

2.15 Statistical analyses

Statistical analyses were performed using Graph Pad Prism 5 Software (GraphPad Software Inc.).

2.16 Pedigree drawing

The pedigree of the E64D family was drawn using the HaploPainter1.043 (access free software).

3 Results

3.1 Clinical phenotype of the c.192G>C *DJ-1* family

The samples analysed in this study are derived from family members of the c.192G>C *DJ-1* family pedigree (Figure 8). Individual III.13 represents the index patient, a homozygous c.192G>C *DJ-1* mutation carrier. Individual III.11 represents the sister of the index patient, who is also a homozygous carrier of the c.192G>C *DJ-1* mutation. The two heterozygous family members included in this study are represented by individual III.7 (male) and individual IV.9 (female). A pedigree with information to all individuals including individual II.1, II.2 (born 1934), III.3 (born 1955), III.6 (born 1956), III.7 (born 1958), III.11 (born 1961) and III.13 (born 1962) was previously published (Hering et al., 2004).

The heterozygous brothers of the index patient, which were published in the above-mentioned study, did not show any symptoms at that time. Similarily, the mother of the index patient also did not display any PD symptoms at the age of 63.

The homozygous mutation-carrying sister who was published in the same study did not have extrapyramidal symptoms at the time the samples were collected. In a follow-up examination in 2010 she still had no extrapyramidal signs, but meanwhile she has been suffering from a severe depression even under medication.

The index patient developed first PD symptoms, namely slowing of movements and akinetic-rigidic-sydrome of the left arm and leg, at the age of 34. Later he developed speech difficulties and depression. The index patient responds well to levodopa therapy and receives anti-depressive treatment. More detailed information on the clinical features of the patients can be found in the original study (Hering et al., 2004). In the follow-up examination in 2010 he showed further excellent response to levodopa therapy, the depression was well controlled under antidepressant medication, no autonomous dysregulation was seen as well as no relevant motor fluctuations.
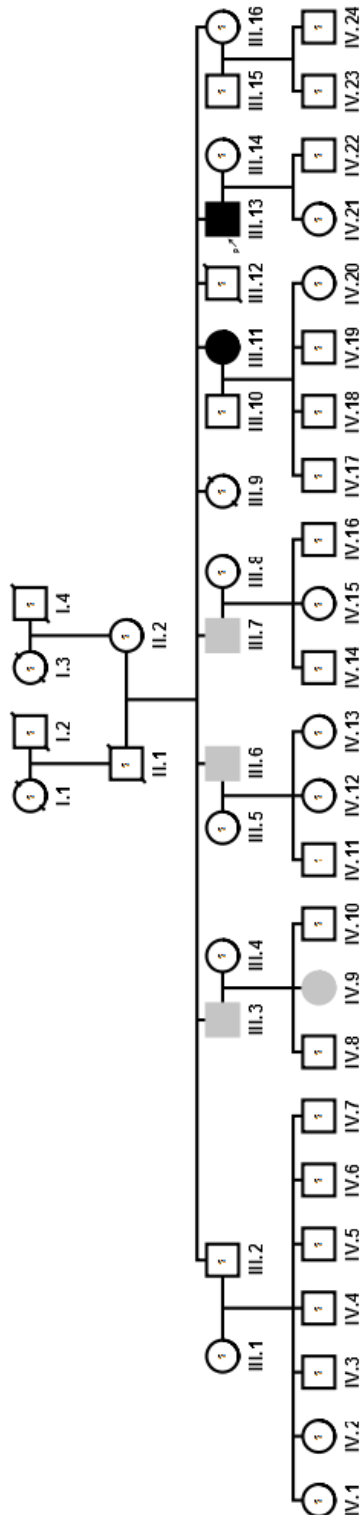
Figure 8: **Pedigree structure of the family with the c.192G>C *DJ-1* mutation.**

Black symbols denote homozygous mutation carriers of the c.192G>C *DJ-1* mutation. Grey symbols denote heterozygous c.192G>C *DJ-1* mutation carriers. The arrow points to individual III.13 representing the index patient.

3.2 Mitochondrial phenotypes in carriers of the c.192G>C *DJ-1* mutation

To investigate the effect of the c.192G>C *DJ-1* mutation on mitochondrial function, assays were performed in cells derived from the human mutation carriers and healthy controls. Analyses were performed in human dermal fibroblasts, iPSCs generated from the fibroblasts, mDA neurons differentiated from these iPSCs as well as smNPCs also generated from these iPSCs.

3.2.1 The c.192G>C *DJ-1* mutation leads to changes in mitochondrial morphology

To detect the effect of the c.192G>C *DJ-1* mutation on mitochondrial morphology, measurements were performed using MitoTracker® Green FM to stain mitochondria in live human dermal fibroblasts from family members of the c.192G>C *DJ-1* family carrying the c.192G>C *DJ-1* mutation and an unrelated healthy control. Analysis of single mitochondria revealed significant changes in morphology in terms of length and branching of mitochondria in carriers of the c.192G>C *DJ-1* mutation (Figure 9). A significant reduction in the aspect ratio, indicating the length of a mitochondrion was seen in both homozygous c.192G>C *DJ-1* mutation carriers when compared to an unrelated healthy control and to the brother who is a heterozygous carrier of the same mutation (Figure 9B). Analysis of form factor, measuring the degree of branching of mitochondria revealed a significant reduction in both homozygous c.192G>C *DJ-1* mutation carriers in comparison to the heterozygous mutation carrying brother. The comparsion to the unrelated healthy control showed a significant reduction in the degree of branching of the premotor diseased homozygous c.192G>C *DJ-1* mutation carrier and a significant increase in branching in the heterozygous c.192G>C *DJ-1* mutation carrier (Figure 9C).
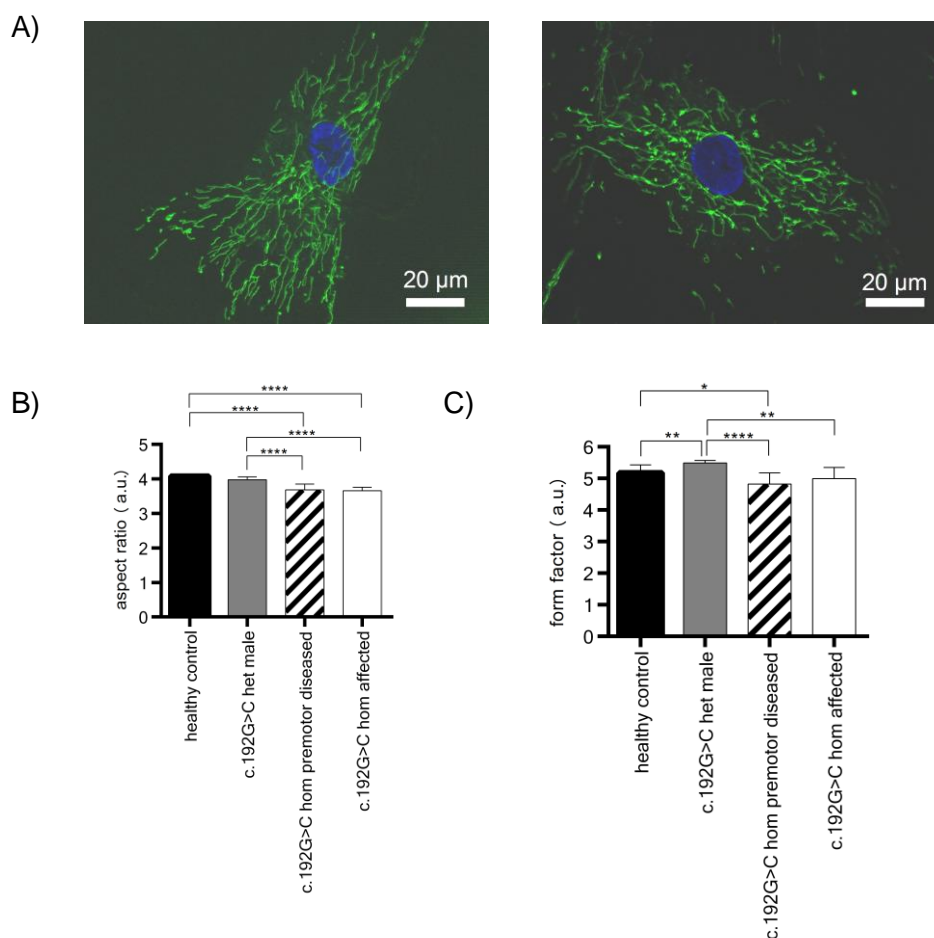
Figure 9: **Effect of the c.192G>C *DJ-1* mutation on mitochondrial morphology.**

Mitochondrial morphology in human dermal fibroblasts from carriers of the c.192G>C *DJ-1* mutation and a healthy control were analysed by live cell imaging microscopy using ApoTome optical slices with 0.35-0.4 z-stacks. Mitochondrial morphology measurements were performed using MitoTracker® Green FM to stain mitochondria. Nuclei were stained with Hoechst 33342. **A)** Representative microscopy image of a human dermal fibroblast of the control (left) and the index pateint (right) with mitochondria stained in green and nucleus in blue. (Scale bars, 20 µm) **B)** Aspect ratio indicates the length of a single mitochondrion. Aspect ratio is calculated as ratio between the major and the minor axes of the ellipse equivalent to the object. Aspect ratio was significantly reduced in fibroblasts from both homozygous c.192G>C *DJ-1* mutation carriers when compared to fibroblasts from a healthy control. Aspect ratio was not reduced when compairing the heterozygous c.192G>C *DJ-1* mutation carrier to the healthy control. Comparison within the c.192G>C *DJ-1* family members showed significant reduction in mitochondrial length of both homozygous c.192G>C *DJ-1* mutation carriers when compared to the heterozygous mutation carrier. **C)** Form factor indicates mitochondrial branching. Form factor is calculated as: $perimeter^2/4\pi*area$. Form factor was significantly reduced in fibroblasts from the heterozygous and the premotor diseased homozygous c.192G>C *DJ-1* mutation carrier when compared to fibroblasts from a healthy control. A reduced degree of branching was observed of both homozygous c.192G>C *DJ-1* mutation carriers when compairing them with the heterozygous mutation carrier of the same family. **B) + C)** Images from 36 individual cells of each proband were analysed by an investigator blinded to the experimental design. * $p \leq 0.05$, ** $p \leq 0.01$, *** $p \leq 0.001$, **** $p \leq 0.0001$ by two-way ANOVA followed by Tukey's multiple comparisons test. Values show mean + SEM. N=3.

3.2.2 The c.192G>C *DJ-1* mutation causes a reduction of MMP in patient derived dermal fibroblasts

Next, we investigated mitochondrial function by measuring MMP through TMRE fluorescence intensity in live human dermal fibroblasts from family members of the c.192G>C *DJ-1* family carrying the c.192G>C *DJ-1* mutation and an unrelated healthy control. Analysis of c.192G>C *DJ-1* mutation carriers revealed a reduction of the MMP of both homozygous mutation carriers when compared to the healthy control which could be resued by reintroducing physiological wt DJ-1 in the fibroblasts of the index patient (Figure 10). These results in human carriers of DJ-1 mutations are in line with previous findings in MEFs from DJ-1 knockout mice, which had a reduced MMP when compared to wt controls (Krebiehl et al., 2010). Together, these results indicate once more the importance of DJ-1 loss of function for maintaining MMP and thus indicate the relevance of DJ-1 for mitochondrial function in general.
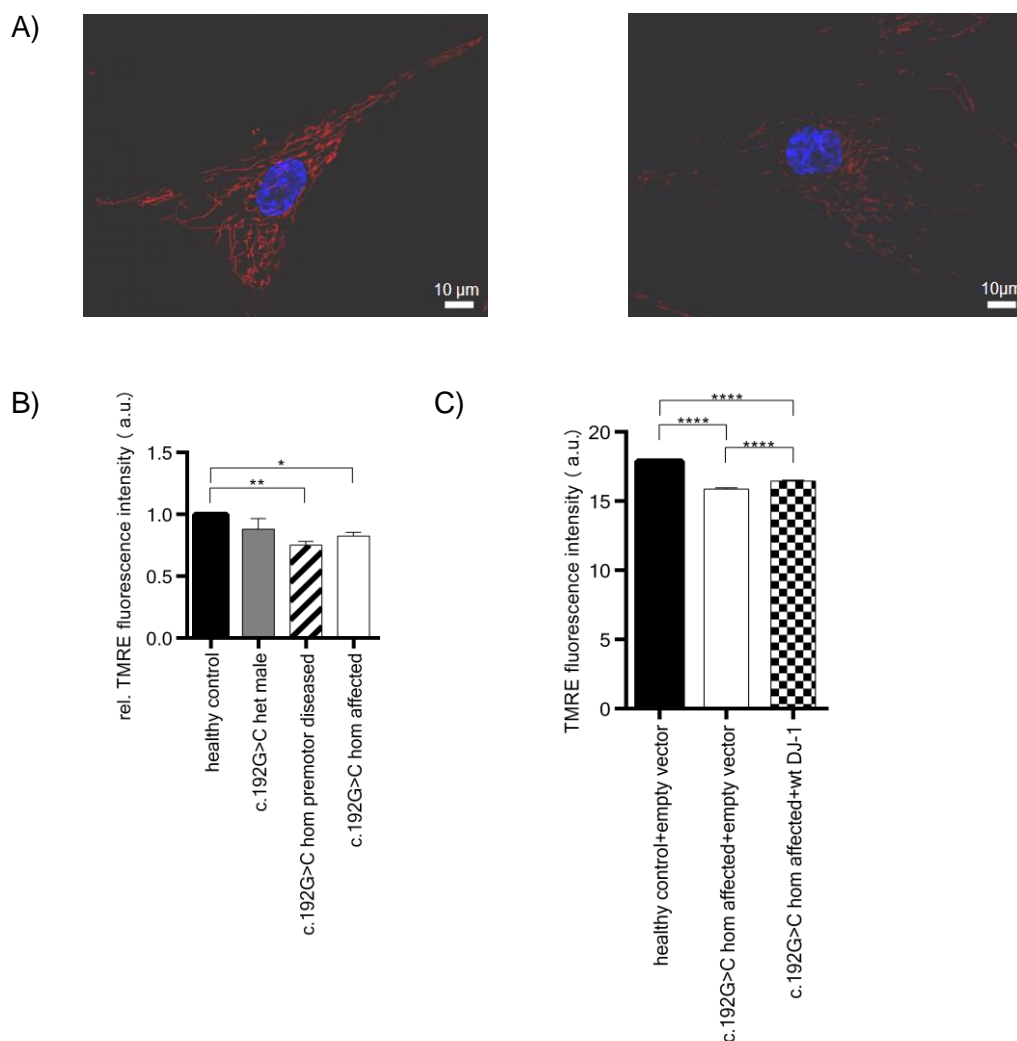
Figure 10: **Effect of the c.192G>C *DJ-1* mutation on MMP.**

MMP in human dermal fibroblasts from carriers of the c.192G>C *DJ-1* mutation and a healthy control were analysed by live cell imaging microscopy. MMP measurements were performed by staining cells with the membrane potential-sensitive dyeTMRE to measure active mitochondria. Nuclei were stained with Hoechst 33342. Cells were measured using a live cell microscope with 63x magnification and ApoTome technique to define single layers of cells. Exposure time was set to 200-300 ms. Pictures were analysed using Image J software by applying the "despeckle" function and the "Lookup Tables–Fire" condition, followed by "analyze particles" option. **A)** Exemplary microscopy image of a human dermal fibroblast of a healthy control (left) and the homozygous c.192G>C *DJ-1* mutation carrier (right) with mitochondria in red and nucleus in blue. (Scale bars, 10 µm) **B)** TMRE fluorescence intensity depends on the activity of mitochondria. Both homozygous c.192G>C *DJ-1* mutation carriers showed a decreased MMP when compared to an unrelated healthy control. Images from 36 individual cells of each proband were analysed by an investigator blinded to the experimental design. * $p \leq 0.05$, ** $p \leq 0.01$ by two-way ANOVA followed by Dunnett's multiple comparisons test. **C)** As shown in B) MMP is significantly reduced in the index patient when compared to an unrelated healthy control. MMP increases significantly when reintroducing wt DJ-1 in the c.192G>C *DJ-1* mutation carrier. Images from 36 individual cells of each proband were analysed by an investigator blinded to the experimental design. Values show mean + SEM. N=3. **** $p \leq 0.0001$ by one-way ANOVA followed by Tukey's multiple comparisons test.

3.3 Mitochondrial analysis of murine primary hippocampal neuronal cultures

To be able to screen for neuron-specific mitochondrial phenotypes we investigated the influence of loss of DJ-1 protein on mitochondrial transport by looking at mitochondria using live cell imaging of murine primary hippocampal neuronal cultures. These experiments have been performed before human iPSC derived neuronal cultures were available.

3.3.1 Velocity of mitochondrial transport

An exemplary image of a movie of the primary neuronal cultures with mitochondria stained with MitoTracker® Green FM is shown (Figure 11).
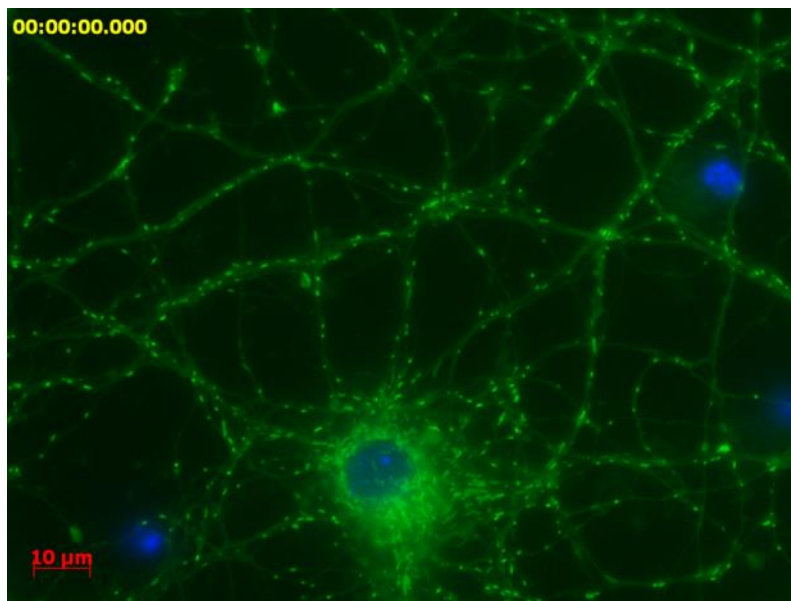
Figure 11: **Exemplary image of mitochondria of a primary neuronal culture.**

Mitochondrial analysis in murine primary hippocampal neuronal cultures from wt and DJ-1 -/- mice were analysed by live cell imaging microscopy. Mitochondrial measurements were performed using MitoTracker® Green FM to stain mitochondria. Nuclei were stained with Hoechst 33342. Representative microscopy image of a movie with mitochondria stained in green and nucleus in blue. (Scale bar, 10 µm)

When analysing the velocity of mitochondrial transport of wt mice in comparison to DJ-1 -/- mice we measured an equal velocity of about 0.025 µm/s (Figure 12A). The maximum velocity of mitochondria from wt mice and DJ-1 -/- mice was about 0.1 µm/s and slightly higher for mitochondria from wt mice (Figure 12B).
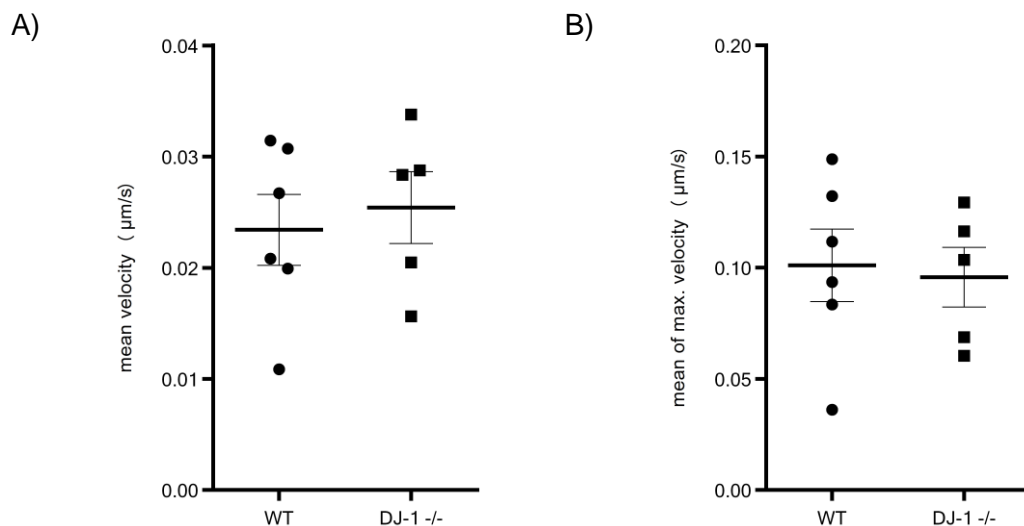
Figure 12: **Velocity of mitochondrial transport.**

Mitochondrial analsysis was performed using live cell imaging for 3 min, 5 s per time and analysed with ImageJ using the plugin "*TrackMate*" in *Fiji*. Two to three movies per mouse were taken from 6 wt and 5 DJ-1 -/- mice. Each dot/square represent mean of mitochondria of individual mouse. Error bars indicate +/- SEM. **A)** shows velocity of mitochondria. **B)** shows maxium (max.) velocity of mitochondria.

3.3.2   Number of moving mitochondria

We investigated the difference of mitochondria which move between wt and DJ-1 -/- mice. The mean of the percentage of moving mitochondria per mouse was higher in DJ-1 -/- mice both when analysing overall displacement as well as when analysing the displacement only when it was further than 1 μm (Figure 13).

A)

B)
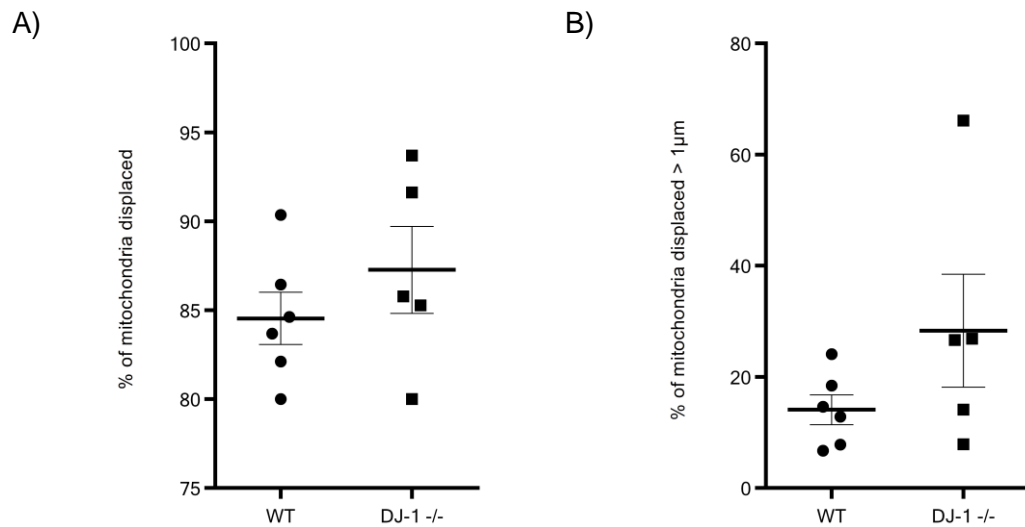
Figure 13: **Percentage of moving mitochondria.**

Mitochondrial analsysis was performed using live cell imaging for 3 min, 5 s per time and analysed with ImageJ using the plugin "*TrackMate*" in *Fiji*. Two to three movies per mouse were taken from 6 wt and 5 DJ-1 -/- mice. Each dot/square represent mean of mitochondria of individual mouse. Error bars indicate +/- SEM. **A)** shows percentage of moving mitochondria. **B)** shows percentage of mitochondria moving further than 1 μm.

3.3.3   Displacement of mitochondria

Next, we investiged whether in DJ-1 -/- mice where more mitochondria moved, their displacement was greater as well. When looking at the mean of the overall displacement of the mice indeed the mitochondria of the DJ-1 -/- mice moved a greater distance (Figure 14A). When looking only at mitochondria with a displacement >1 μm however the mitochondria of the wt mice had a higer mean displacement (Figure 14B).

A)

B)

ure

Mi-

to-

Fig-

14:
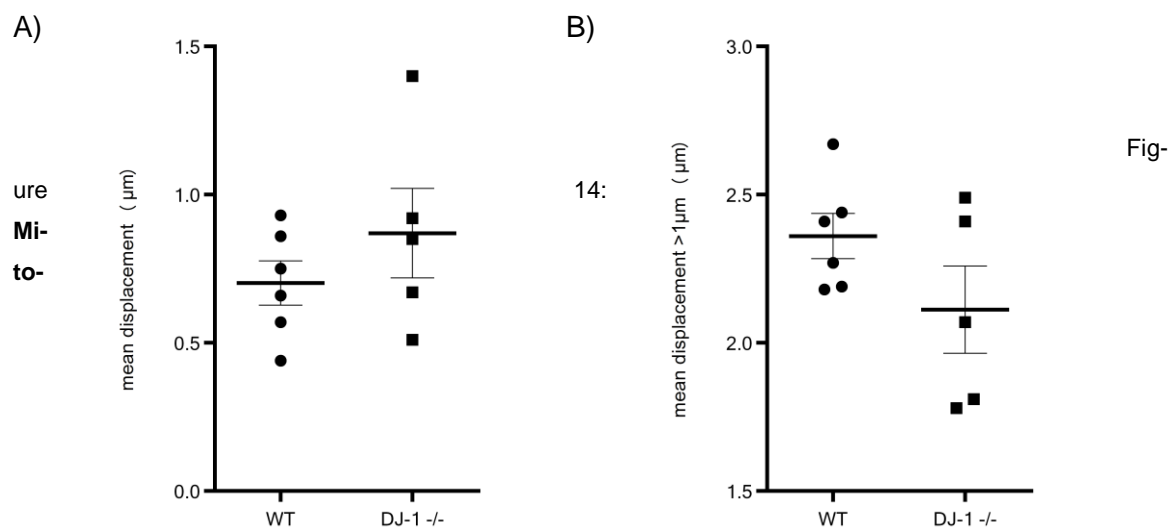
chondrial displacement.

Mitochondrial analsysis was performed using live cell imaging for 3 min, 5 s per time and analysed with ImageJ using the plugin "*TrackMate*" in *Fiji*. Two to three movies per mouse were taken from 6 wt and 5 DJ-1 -/- mice. Each dot/square represent mean of mitochondria of individual mouse. Error bars indicate +/- SEM. **A)** shows mean displacement of mitochondria. **B)** shows mean displacement of mitochondria moving further than 1 µm.

3.4   Establishment of an iPSC model from patient derived fibroblasts

Being able to generate pluripotent stem cells from somatic cells was a milestone for many fields of research including neurodegeneration. It opens up the possibility to analyse disease specific phenotypes in the respective affected types of cells. Making use of the opportunity to study disease mechanisms in neurons and to control for tissue-specific effects, iPSCs were generated from the indicated patient derived dermal fibroblasts of the c.192G>C *DJ-1* family.

Reprogramming of both homozygous c.192G>C *DJ-1* mutation carriers and the heterozygous c.192G>C *DJ-1* mutation carrier (individual III.7) was performed using retroviral vectors expressing the classical four 'Yamanaka factors'. A minimum of 20 clones per individual was picked, passaged and stocks were frozen down for subsequent characterisation of the clones. Characterisation included tests about pluripotency and stem cell characteristics of the clones. Therefore, qPCR was performed to ensure silencing of the four exogenous viral factors and endogenous expression of pluripotency markers, ICC was used to show the expression of stem cell markers. Furthermore, the picked clones were tested for major chromosomal abberations and mutations via G-banding and a genotyping microarray analysis. Additionally, the mutation carrying exon 3 of *DJ-1* was sequenced in all clones to verify the correct genotype. Likewise, the ability of the clones to differentiate in cell types of all three germ layers was tested by ICC after differentiating the clones. At least two

different clones per one individual were correctly characterised and a sufficient number of stocks was frozen down.

Table 36 shows a list of all generated iPSC clones from the respective fibroblasts of the c.192G>C *DJ-1* family members.

Table 36: **List of reprogrammed human iPSC lines used in this study.** Table shows number of individual of the c.192G>C *DJ-1* family (Figure 8), diagnosis and genotype of the individual as well as iPSC clone ID and name used in this study.

Individual	Diagnosis	Genotype	iPSC clone ID/Name in this study
III.13	PD	homozygous c.192G>C *DJ-1* mutation	c.192G>C hom affected c1
			c.192G>C hom affected c4
			c.192G>C hom affected c5
III.11	PD	homozygous c.192G>C *DJ-1* mutation	c.192G>C hom premotor diseased c1
			c.192G>C hom premotor diseased c4
III.7	healthy	heterozygous c.192G>C *DJ-1* mutation	c.192G>C het c1
			c.192G>C het c3

Both control iPSC lines included in this study were a kind gift from Christine Klein, MD of the Institute of Neurogenetics at the University of Lübeck (Germany). These lines were fully characterised already. Names of the control lines used in this study are 'healthy control c2' and 'healthy control c5'. Heahlty control c5 has been published as L2135 (Cooper et al., 2012).

3.4.1 Sucessful characterisation of reprogrammed iPSCs

In a first step, silencing of retroviral transgenes of the newly reprogrammed iPSC clones was analysed by qPCR. Relative expression of exogenous *oct4*, *sox2*, *klf4* and *c-myc* was calculated using housekeeping gene level of *HMBS* and normalised to fibroblasts 4 days post infection with the same retroviral vectors (Figure 15).

Retroviral transgenes used for reprogramming are correctly silenced in established iPSC clones.
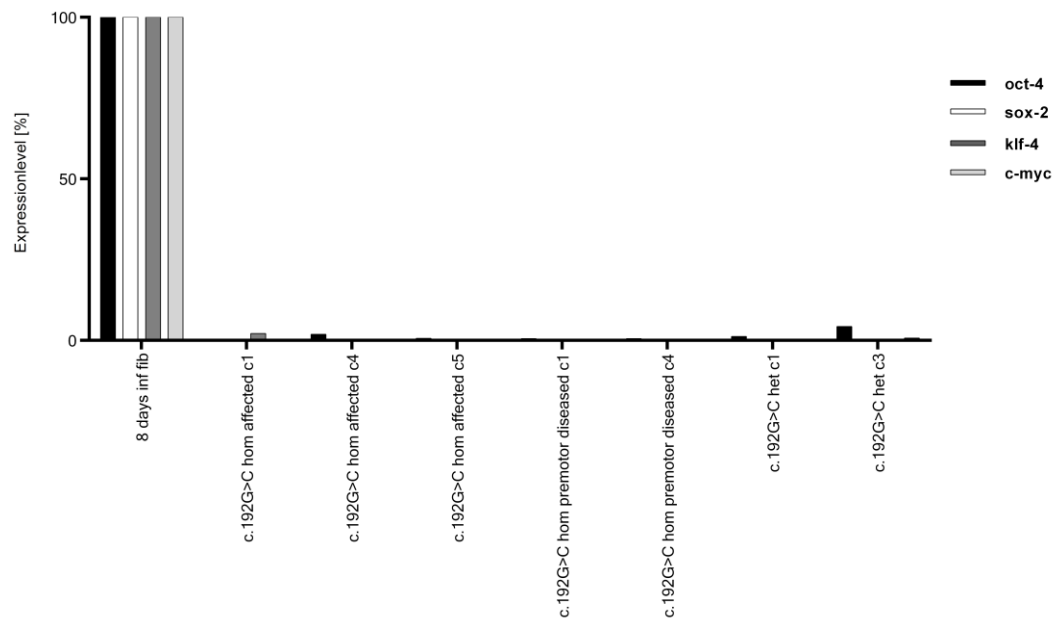
Figure 15: **Silencing of retroviral transgenes (*oct4*, *sox2*, *klf4* and *c-myc*) in established iPSC lines.** Expression is normalised to fibroblasts 4 days post-infection and calculated using houskeeping gene levels of *HMBS*. N=1.

Next, a qPCR was performed in order to show the expression of endogenous *oct4*, *sox2*, *klf4* and *c-myc* as markers of pluripotency. In the same experiment, the expression of other pluripotency markers for the indicated genes were tested. A fibroblast sample (called fibroblasts in Figure 16) served as a negative control and a published iPSC sample (iPSC control) as positive control. qPCR shows induction of endogenous transcripts of *oct4*, *sox2*, *klf4* and *c-myc* and the expression of the other pluripotency markers (Figure 16).
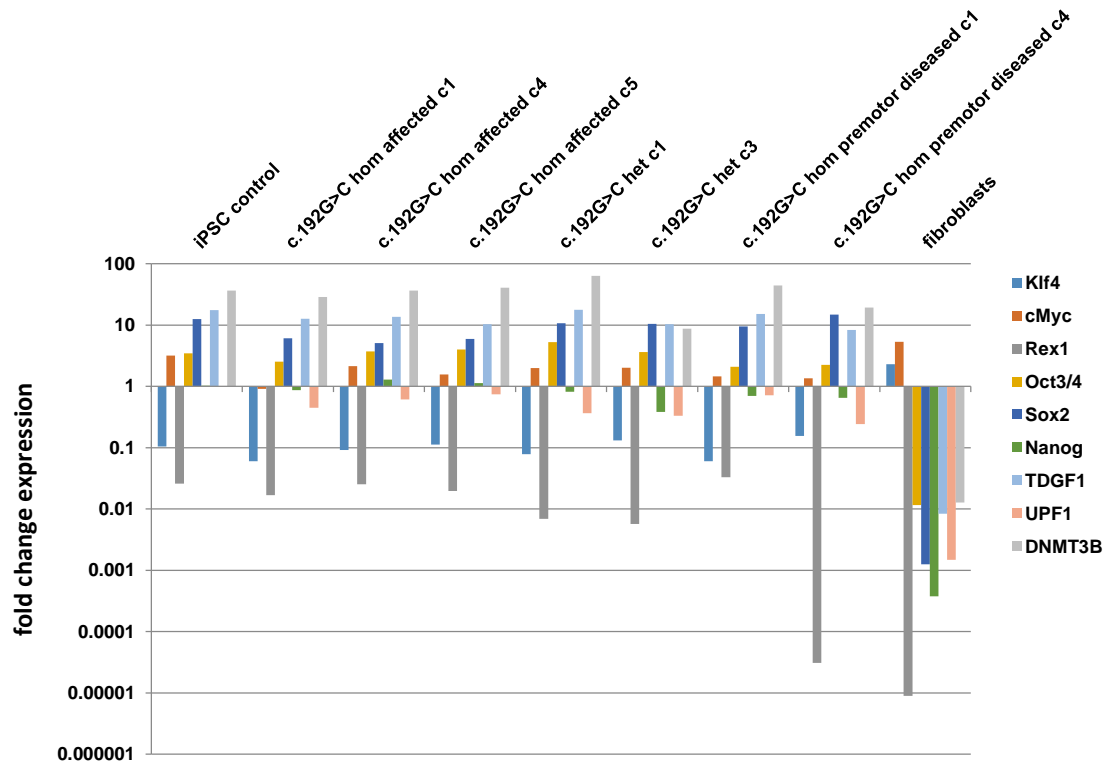
Figure 16: **Pluripotency marker gene expression of established iPSC lines.**

qPCR shows expression of endogenous reprogramming markers *oct4*, *sox2*, *klf4* and *c-myc* compared to a published iSPC control (Reinhardt et al., 2013b). Also other pluripotency markers (namely *rex1*, *nanog*, *TDGF1*, *UPF1* and *DNMT3B*) are expressed. Expression is calculated using houskeeping gene levels of *HMBS*. N=1.

In addition to the qPCR, the expression of stem cell markers of the established iPSC clones was tested by ICC. iPSC clones were stained for *nanog*, *oct-4*, *SSEA4* and *Tra-1-81* along with nuclear counterstaining using DAPI. All clones show expression of the stained stem cell markers (Figure 17).
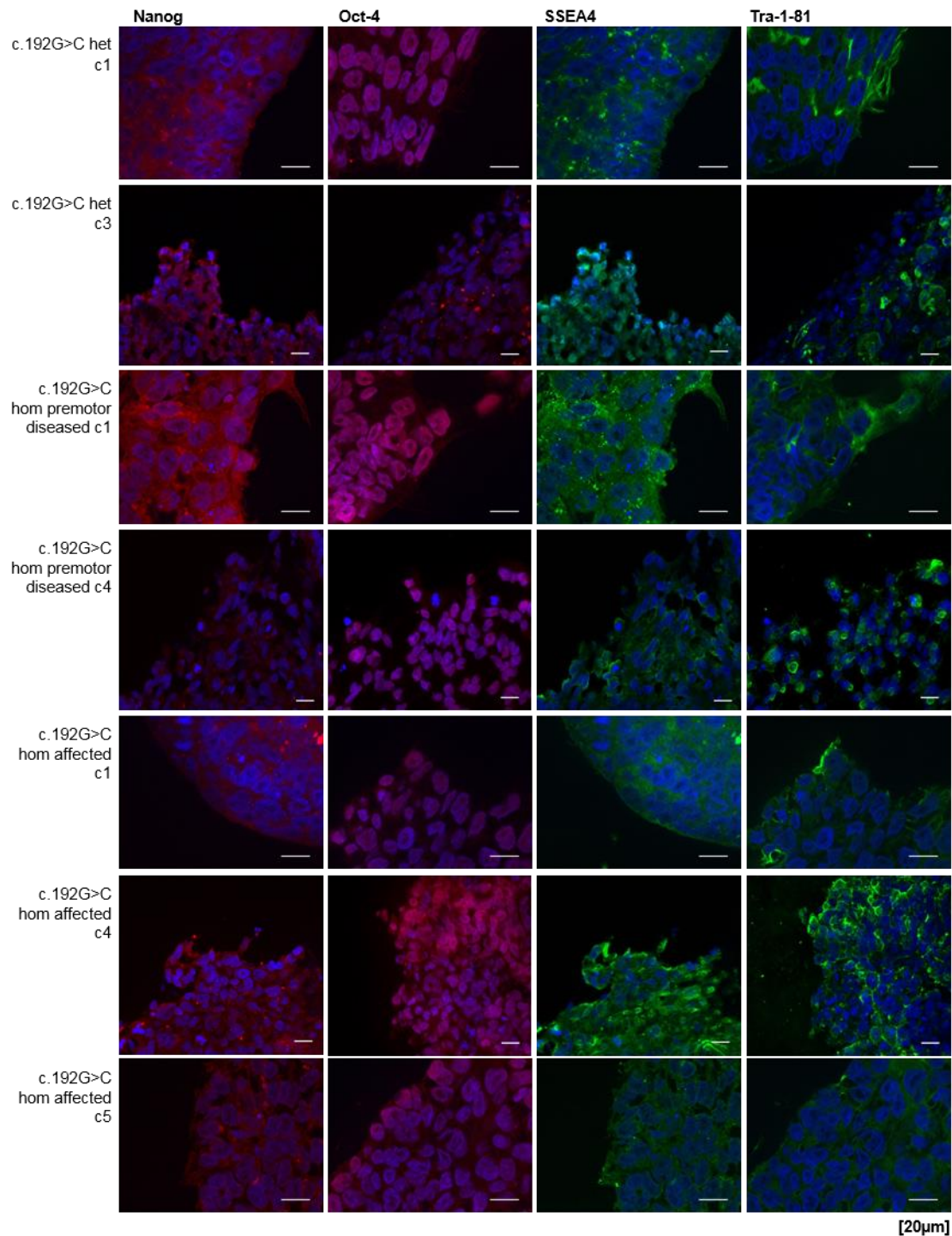
Figure 17: **Stem cell marker expression of established iPSC clones.**

ICC of stem cell markers *nanog*, *oct-4* (both shown in red) and *SSEA4* and *Tra-1-81* (both shown in green) counterstained with DAPI for nuclear staining (shown in blue) of iPSC clones. All established clones express indicated stem cell markers. (Scale bars, 20 µm).

Another important characteristation step is to test for genomic aberrations. Major chromosomal aberrations selected during reprogramming were excluded in the established iPSC clones by karyotyping using G-banding (Figure 18).

c.192G>C het c3
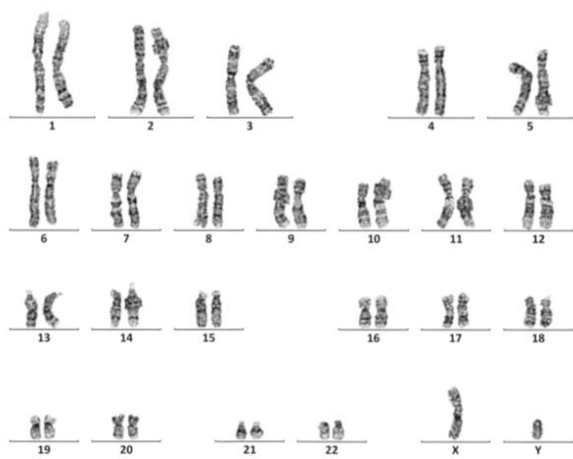
c.192G>C hom premotor diseased c4
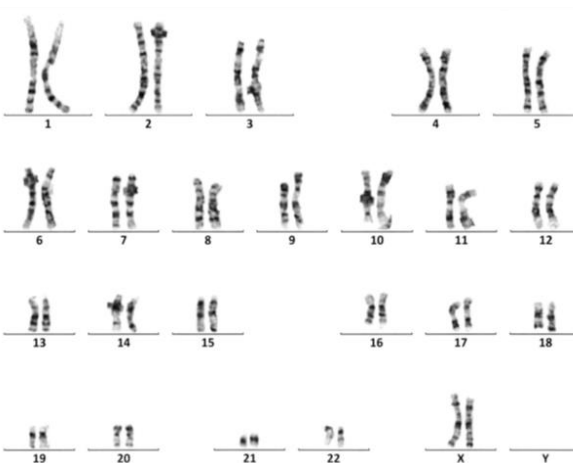
c.192G>C hom affected c4
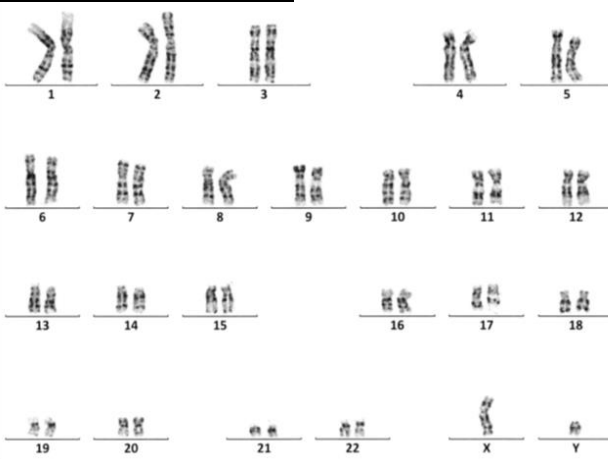
Figure 18: **G-banding of established iPSC clones.**

Exemplary G-banding of one clone per reprogrammed individual. Data shown kindly provided by the Cytogenetics Research Group at the Institute for Medical Genetics and Applied Genomics of the University Hospital Tübingen (Germany). All clones show normal karyotypes.

Genotyping microarray analysis of all iPSC clones was performed to exclude mutations caused by or during the reprogramming process. An Illumina HumanCytoSNP-12 analysis showed no mutations (except for the investigated c.192G>C *DJ-1* mutation) in all established iPSC clones. The genotyping was performed at the Microarray Genome Chip Facility at the Institute for Medical Genetics and Applied Genomics of the University Hospital Tübingen (Germany). CHIP data were analysed by ourselfes. Exemplary results of Illumina HumanCytoSNP-12 analysis of c.192G>C hom affected c4 are shown (Figure 19). As expected, because the index patient is male, the CHIP data show a loss for the X-chromosome (G/L loss) (exemplary region, Figure 19A). Interestingly, for chromosome 1, 2, 3, 4, 6, 8, 12, 16, 22 and X a loss of heterozygousity (value 2) was detected in the CHIP analysis (example for chromosome 3, Figure 19B). The loss of heterozygousity of several loci was not only detected for the iPSC clones of the index patient, but also for both clones of the pre-motor diseased homozygous c.192G>C *DJ-1* mutation carrier (c.192G>C hom premotor diseased c1 and c.192G>C hom premotor diseased c4), as well as for both clones of the heterozygous mutation carrier (c.192G>C het c1 and c.192G>C het c3). The c.192G>C *DJ-1* mutation which we investigate in this study could also be detected in the CHIP analysis as expected (shown on CHIP results as Micordeletion 1p36) (Figure 19C).

To control the established iPSC clones for the correct genotype in terms of the inheritance c.192G>C *DJ-1* mutation, sequencing of *DJ-1* exon 3 was performed in all clones (Figure 20). The black line in all sequencing segments marking homozygous cysteine are sequencing results from three iPSC clones from the index patient and two iPSC clones from the homozygous c.192G>C *DJ-1* mutation carrying sister. The two sequencing segments showing heterozygousity of cysteine and guanine marked by the black line belong to the two clones from the heterozygous c.192G>C *DJ-1* mutation carrier. The sequencing results show correct genotypes of all generated iPSC clones.

A)

Known Regions						
X-linked agammaglobulinemia	CytoGen227	X	98200000 : 102500000	Len	4300000
Pelizaeus-Merzbacher	CytoGen228	X	102500000 : 103600000	Len	1100000
FG5	CytoGen229	X	103600000 : 110500000	Len	6900000
X-linked lissencephaly	CytoGen230	X	110500000 : 116800000	Len	6300000
X-linked mental retardation30	CytoGen231	X	110500000 : 116800000	Len	6300000
Lowe	CytoGen232	X	120700000 : 129800000	Len	9100000
X-linked lymphoproliferative syndrome (XLP)	CytoGen233	X	120700000 : 129800000	Len	9100000
X-linked heterotaxy	CytoGen234	X	133500000 : 137800000	Len	4300000

B)

C)

Known Regions						
1p36 Microdeletion	CytoGen1	1	0 : 27800000	Len	27800000

Figure 19: **Exemplary results of Illumina HumanCytoSNP-12 analysis of c.192G>C hom affected c4.**

A) CHIP results show a male person by loss of loci of the X-chromosome. Indicated by G/L loss. **B)** CHIP detects loss of heterozygosity as here shown for chromosome 3 indicated by a value of 2 determining loss of heterozygousity (LOH). **C)** The c.192G>C DJ-1 mutation is detected by the CHIP assay (1p36 Microdeletion).
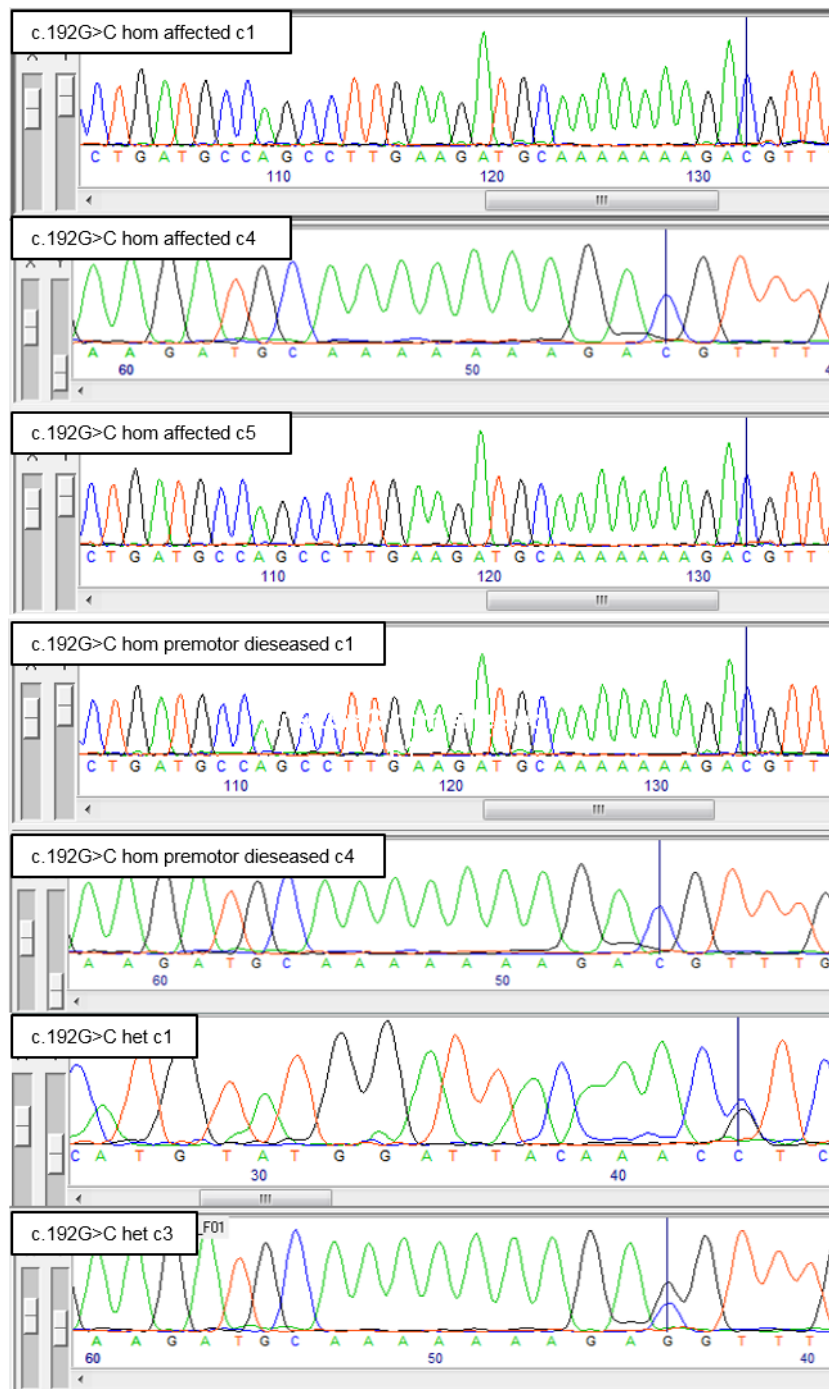
Figure 20: **Sequences of *DJ-1* exon 3 of all established iPSC clones.**

Sequencing of DNA of all established iPSC clones was performed. Clones were grown in feeder-free conditions before cells were pelleted. DNA was isolated and sequencing reaction was performed using *DJ-1* exon 3 specific sequencing primers. Black line in each sequencing result marks the position of the c.192G>C *DJ-1* mutation. Clones from both homozygous c.192G>C *DJ-1* mutation carriers show homozygous results and clones from heterozygous c.192G>C *DJ-1* mutation carrier show heterozygous sequencing results.

3.5 Differentiation of iPSCs to mDA neurons

Once the required number of iPSC clones from homozygous and heterozygous carriers of the c.192G>C *DJ-1* mutation as well as iPSC clones from healthy controls were generated and enough stocks of these cells were frozen down a protocol was established in the lab to differentiate these iPSCs to mDA neurons. Differentiation to mDA neurons opens up the possibility to study PD related mechanisms in the affected cell type.

3.5.1 Differentiated iPSCs express mDA neuronal markers

Successful differentiation of iPSCs to mDA neurons was verified by ICC of a neuron-specific class III β-tubulin marker (Beta-III-Tubulin), a dopaminergic neuron-specific marker (TH), a midbrain marker (FoxA2) and counterstaining of nuclei with Hoechst 33342 or DAPI. Differentiated iPSCs include cells expressing Beta-III-Tubulin, TH and FoxA2 (Figure 21).
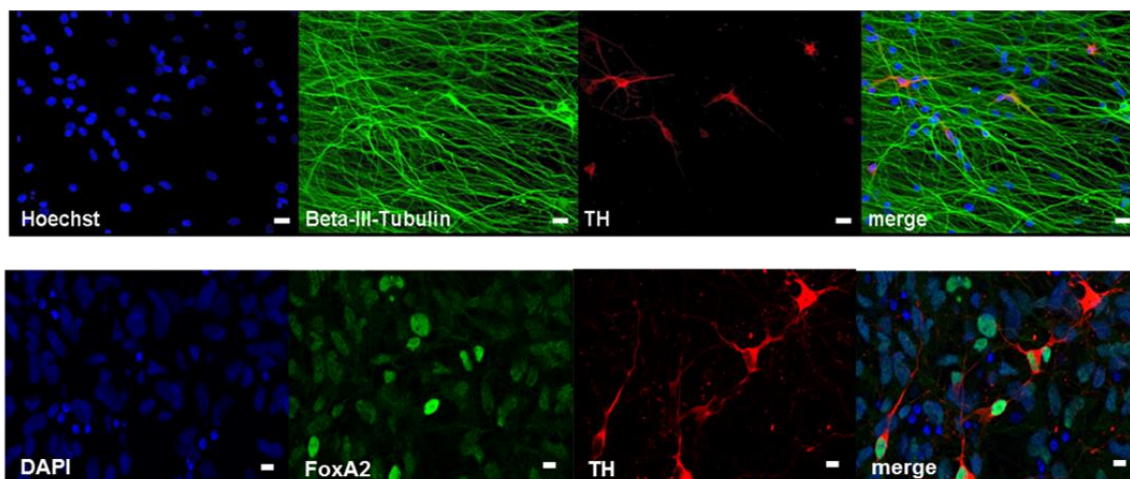
Figure 21: **mDA neuronal marker expression of differentiated iPSCs.**

Exemplary immunocytochemical analysis of neurons after 80 days of differentiation of iPSCs of homozygous c.192G>C *DJ-1* mutation carrier c4 to mDA neurons. Cells were stained for Beta-III-Tubulin, a neuron-specific class III β-tubulin marker, shown in green and TH, a dopaminergic neuron-specific marker, shown in red and nuclei counterstained with Hoechst 33342 shown in blue (upper pictures) or FoxA2, a midbrain marker, shown in green and TH shown in red and nuclei counterstained with DAPI shown in blue (lower pictures). (Scale bars, 20 μm).

3.5.2 mDA neurons derived from affected patient show increased mtDNA damage after oxidative stress, but no compensatory increase in copy number

As DJ-1 plays a role in mitochondrial function, the effect of the c.192G>C *DJ-1* mutation on mtDNA copy number and damage was of particular interest. mtDNA copy number and

mtDNA damage cohere in terms that damaged (for example lesioned) mtDNA degrades depending on the damage and undamaged mtDNA gets replicated.

To see the effect of the c.192G>C *DJ-1* mutation in the cell type affected in PD, mtDNA copy number and damage, measured as detected lesions, where further analysed in neurons differentiated applying the adapted floor plate-based protocol from iPSCs of the c.192G>C *DJ-1* mutation carriers and unrelated healthy controls. Relative mtDNA copy number of mDA neurons of the index patient was reduced when compared to unrelated control c2 under basal conditions (Figure 22).
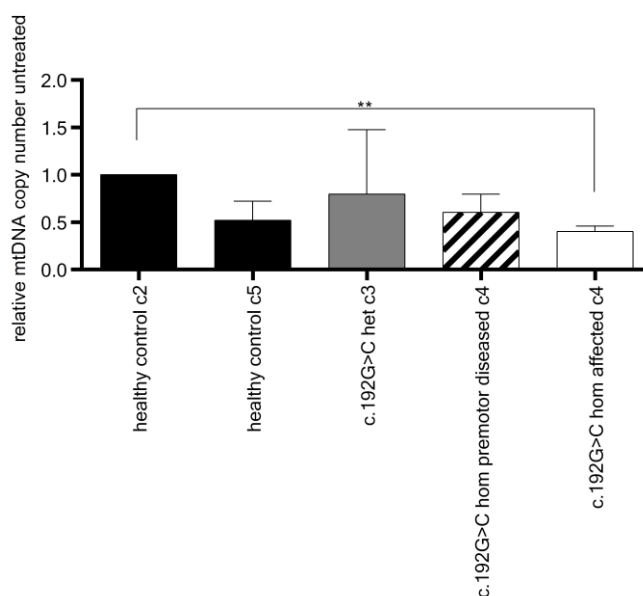
Figure 22: **Relative mtDNA copy number of mDA neurons of healthy controls and c.192G>C *DJ-1* mutation carriers.**

48 h before isolation of pellets, cells were grown in low glucose (1 g/l) maturation medium. Pellets were isolated from cells without treatment. Subsequently, DNA was isolated and stored at -20 °C until measurement was performed. Relative mtDNA copy number measurements were performed by the DNA Damage & Repair Service Unit Tübingen (Germany). mtDNA copy number is calculated in relation to nuclear DNA. Figure shows relative mtDNA copy numbers of mDA neurons differentiated from iPSCs from patients from the c.192G>C *DJ-1* family in comparison to healthy controls. Relative mtDNA copy number is significantly reduced in mDA neurons from the index patient when compared to healthy control c2. Relative mtDNA copy number is not significantly altered between mDA neurons from other individuals. Relative mtDNA copy number expression is normalised to healthy control c2. Values show mean + SD. ** $p \leq 0.01$ by one-way ANOVA followed by Tukey's multiple comparisons test. N=3.

Mitochondria produce ROS as a natural by-product of the electron transport chain activity. DJ-1 is a sensor for oxidative stress and translocates to mitochondria to quench ROS (Taira et al., 2004b). We wanted to investigate the effect of the c.192G>C *DJ-1* mutation

on relative mtDNA copy number after treating mDA neurons with the mitochondrial complex I inhibitor rotenone or by treating the cells directly with reactive oxygen species (H_2O_2), or both. An increase in relative mtDNA copy number was seen after treatment with rotenone or H_2O_2. It is significant in all indicated mDA neurons after treating cells with both compounds together except for mDA neurons from the index patient (Figure 23).
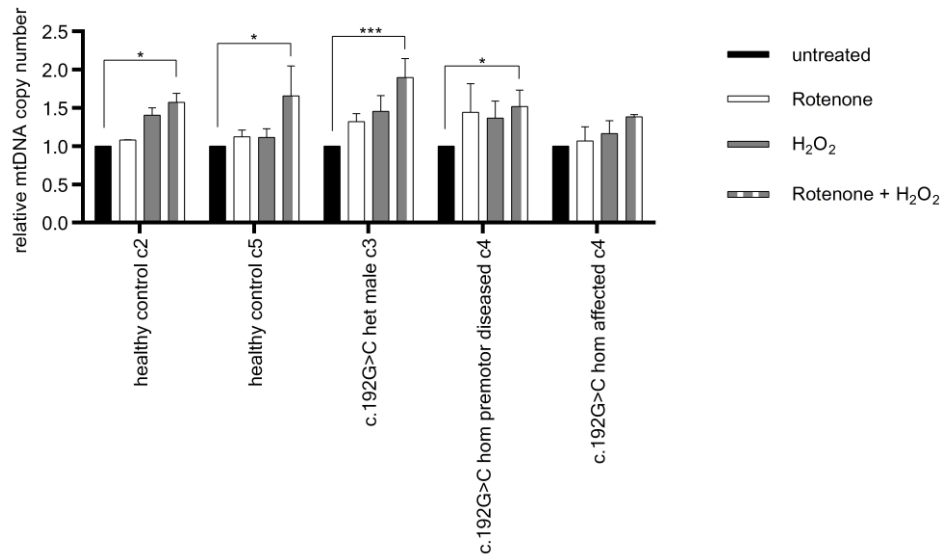
Figure 23: **Relative mtDNAcopy number of mDA neurons after treatment with rotenone or H_2O_2 or both.**

48 h before isolation of pellets, cells were grown in low glucose (1 g/l) maturation medium. Pellets were isolated from cells without treatment, with rotenone or H_2O_2 treatment or both treatments together. Rotenone: 24 h before pellets were isolated, cells were treated with rotenone (10 µM). H_2O_2: H_2O_2 (5 mM, 5 min, 37 °C) treatment was applied directly before pellets were isolated. Subsequently, DNA was isolated and stored at -20 °C until measurement was performed. Relative mtDNA copy number measurements were performed by the DNA Damage & Repair Service Unit Tübingen (Germany). mtDNA copy number is calculated in relation to nuclear DNA. A significant increase of relative mtDNA copy number was only seen after rotenone and subsequent H_2O_2 treatment in all individuals shown except for the homozygous c.192G>C *DJ-1* mutation carrier. Generally, relative mtDNA copy number increases after treatment with rotenone or H_2O_2 or both in all individuals. Relative mtDNA copy number expression normalised to untreated condition of each indicated individual. Values show mean + SEM. * $p \leq 0.05$, *** $p \leq 0.001$ by two-way ANOVA. N=3.

Using the same samples we also tested the effect of rotenone and H_2O_2 treatment or treatment with both compounds on mtDNA damage in mDA neurons. Relative mtDNA copy number was increased in mtDNA damage indicated by detected lesions/10 kb after treatment with rotenone or H_2O_2 or treatment with both compounds. A significant increase however was seen in mDA neurons from healthy control c2 and mDA neurons from the affected homozygous c.192G>C *DJ-1* mutation carrier c4. No significant difference was seen when looking at basline mtDNA damage of mDA neurons from indicated individuals (Figure 24).
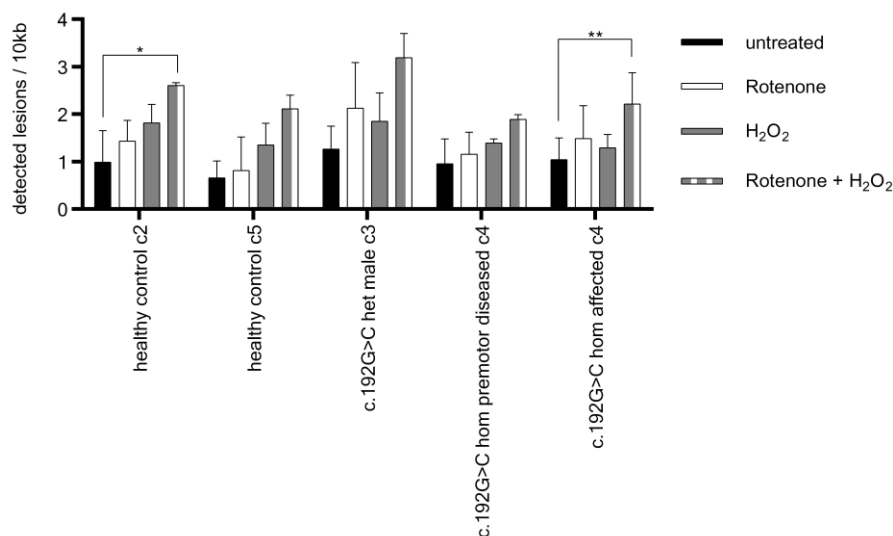
Figure 24: **mtDNA damage of mDA neurons after treatment with rotenone or H_2O_2 or both.**

48 h before isolation of pellets, cells were grown in low glucose (1 g/l) maturation medium. Pellets were isolated from cells without treatment, with rotenone or H_2O_2 treatment or both treatments together. Rotenone: 24 h before pellets were isolated, cells were treated with rotenone (10 µM). H_2O_2: H_2O_2 (5 mM, 5 min, 37 °C) treatment was applied directly before pellets were isolated. Subsequently, DNA was isolated and stored at -20 °C until measurement was performed. mtDNA damage measurements were performed by the DNA Damage & Repair Service Unit Tübingen (Germany). mtDNA damage in mDA neurons is shown as detected lesions/10 kb. For relative mtDNA copy number mtDNA damage increases after treatment of the cells with rotenone or H_2O_2 or both. A significant increase in detected lesion/10 kb was only seen in mDA neurons from healthy control c2 and mDA neurons from affected homozygous c.192G>C *DJ-1* mutation carrier after treatment of the cells with rotenone and H_2O_2 together. There was no significant difference in baseline level of detected lesion/10 kb in mDA neurons from indicated individuals. Values show mean + SEM. * $p \leq 0.05$, ** $p \leq 0.01$ by two-way ANOVA followed by Tukey's multiple comparisons test. N=3.

3.5.3 No changes in mitochondrial ROS level in mDA neurons of c.192G>C *DJ-1* mutation carriers

Next, we measured mitochondrial ROS levels in mDA neurons from c.192G>C *DJ-1* mutation carriers and healthy controls to investigate if the c.192G>C *DJ-1* mutation leads to changes in mitochondrial ROS levels in mDA neurons. Mitochondrial ROS production was measured by flow cytometry using MitoSOX™ Red (Thermo Fisher Scientific, Braunschweig, Germany). This dye is targeted to mitochondria and oxidised by superoxide. Mitochondrial ROS measurement was performed under high (4.5 g/l) (Figure 25A) and low (1 g/l) glucose conditions (Figure 25B). Neither of the conditions led to significant changes in mitochondrial ROS levels in neurons of c.192G>C *DJ-1* mutation carriers.
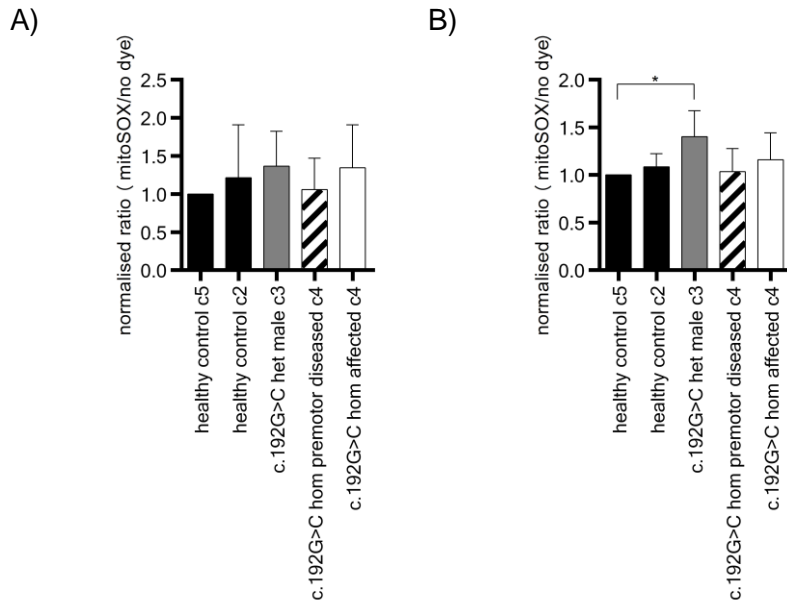
Figure 25: **Mitochondrial ROS levels in neuorns of healthy controls and c.192G>C *DJ-1* mutation carriers.**

Neurons differentiated from iPSCs of healthy controls and c.192G>C *DJ-1* mutation carriers were stained with 2 µM MitoSOX™ Red-solution (Thermo Fisher Scientific, Braunschweig, Germany) for 20 min at 37 °C in a no-CO_2 incubator. **A)** 48 h before staining, cells were kept in maturation medium. No significant changes in mitochondrial ROS were detected between neurons from healthy controls and neurons from c.192G>C *DJ-1* mutation carriers. **B)** 48 h before staining maturation medium was replaced by maturation medium with low (1 g/l) glucose. No significant changes in mitochondrial ROS were detected between neurons from healthy controls and neurons from homozygous c.192G>C *DJ-1* mutation carriers. An increase in mitochondrial ROS was found in the heterozygous c.192G>C *DJ-1* mutation carrier when compared to one of the healthy controls (c5). Ratios were normalised to healthy control c5. Values show mean + SEM. * p ≤ 0.05, by two-way ANOVA followed by Dunnett's multiple comparisons test.

3.5.4 Increased neurite outgrowth in mDA neurons of premotor diseased homozygous c.192G>C *DJ-1* mutation carrier

We sought to determine whether neurite outgrowth was altered in mDA neurons of c.192G>C *DJ-1* mutation carriers. Outgrowth distance was measured using live cell imaging by taking pictures every 5 min for 30 min. Outgrowth distance was increased in c.192G>C *DJ-1* mutation carriers. Significantly longer distance was measured between healthy control and premotor diseased homozygous c.192G>C *DJ-1* mutation carrier. Outgrowth distance of these mDA neurons was also significantly longer when compared to mDA neurons from index patient (Figure 26).
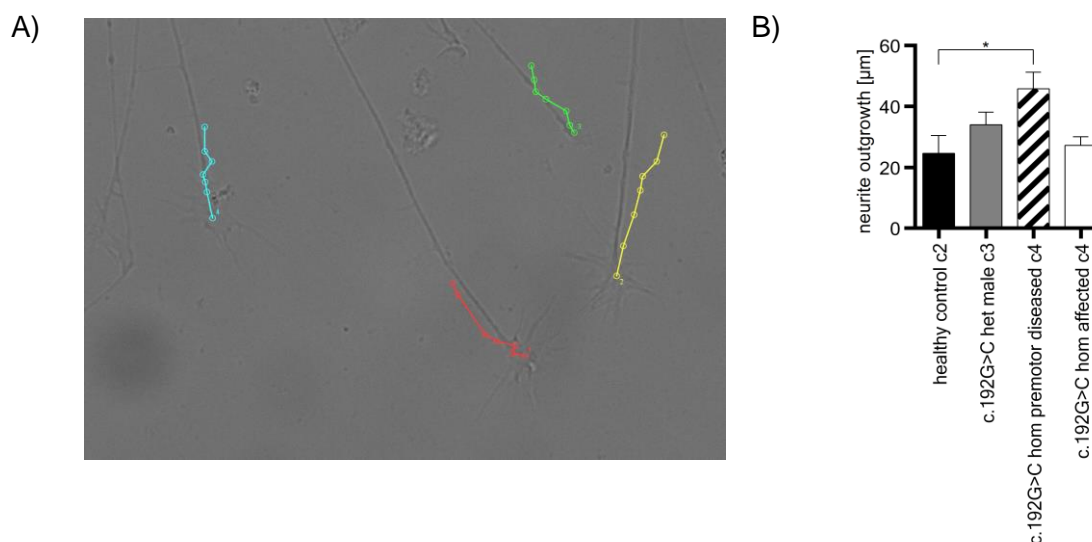
Figure 26: **Increased neurite outgrowth in premotor diseased homozygous c.192G>C** *DJ-1* **mutation carrier.**

Neurite outgrowth assays were performed using live cell imaging. 3-5 neuronal clusters were mechanically detached after differentiation and transfered on matrigel-coated chamber slides and incubated over night. Neurite outgrowth velocity was measured after 24 h. Pictures were taken every 5 min for 30 minutes and analysed with ImageJ plug-in MTrackJ. **A)** Sample picture from a neurite outgrowth experiment of mDA neurons differentiated from premotor diseased c.192G>C *DJ-1* mutation carrier c4. Colourful lines indicate outgrowth-length. Dots resemble different time points when picture was taken. **B)** Outgrowth distance of mDA neurons of c.192G>C *DJ-1* mutation carriers is longer when compared with outgrowth distance of healthy control c2. Significant distance was calculated between healthy control c2 and premotor diseased c.192G>C *DJ-1* mutation carrier and between this individual and affected c.192G>C *DJ-1* mutation carrier, with latter one growing out less. Values show mean + SEM. * $p \leq 0.05$, ** $p \leq 0.01$ by two-way ANOVA followed by Tukey's multiple comparisons test. N=3.

3.6 Analysis of the c.192G>C *DJ-1* mutation

The main part of this study was to analyse the effect of the c.192G>C *DJ-1* mutation, previously reported as p.E64D mutation in *DJ-1* in early onset PD (Hering et al., 2004).

3.6.1 DJ-1 protein level varies between different human control fibroblasts and c.192G>C *DJ-1* mutation carriers do not express DJ-1 protein

Loss of DJ-1 function is a rare cause of familial PD. To calculate the steady state DJ-1 protein levels in different healthy individuals in comparison to the c.192G>C *DJ-1* mutation carriers, samples from the respective individulas were analysed on a low percentage SDS-PAGE gel (4 % acrylamide). We took cell lysates from three different female human control individuals and from two different male human control individuals. Lysates

from fibroblasts of family members of the c.192G>C *DJ-1* family were taken as well. Lysates were taken from individual IV.9 who is a female heterozygous c.192G>C *DJ-1* mutation carrier, from individual III.7, who is a male heterozygous c.192G>C *DJ-1* mutation carrier and from individual III.11 and III.13 who are both homozygous c.192G>C *DJ-1* mutation carriers; III.11 being female and premotor diseased and III.13 being the male index patient with motor symptoms (pedigree, Figure 8).

DJ-1 proteins were examined by immunoblotting using a DJ-1 specific antibody (Figure 27). Whereas DJ-1 protein levels vary between control fibroblasts and heterozygous c.192G>C *DJ-1* mutation carriers, DJ-1 protein is not detectable in both homozygous c.192G>C *DJ-1* mutation carriers.

A)
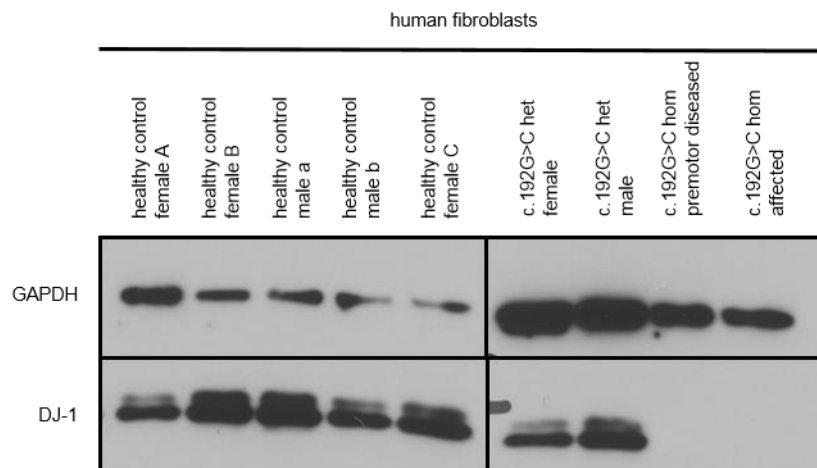
B)
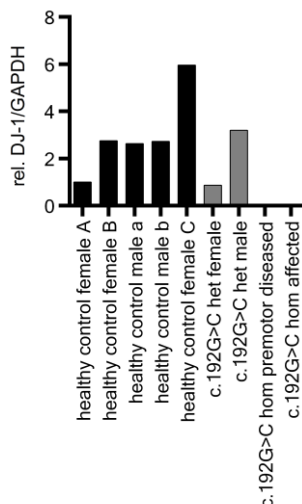
Figure 27: **A) Western blot and B) densitometry of Western blot of cell lysates prepared from human control fibroblasts and c.192G>C *DJ-1* mutation carriers.**

Samples are separated in a 4 % acrylamide SDS-PAGE gel. Result shows a variation of DJ-1 level in controls and heterozygous c.192G>C *DJ-1* mutation carriers and results show the undetectability of DJ-1 protein in homozygous c.192G>C *DJ-1* mutation carriers. N=1.

After having seen different DJ-1 protein levels between different control fibroblasts we tested for inter-individual variations of DJ-1 protein. Therefore we took lysates from two male and three female human control fibroblasts, as well as lysates from the female heterozygous c.192G>C *DJ-1* mutation carrier and the index patient at two timepoints. Subsequently, samples were analysed on a low percentage SDS-PAGE gel (4 % acrylamide). The second lysate from the same fibroblasts was isolated after 8 hours. This Western blot again shows variations of DJ-1 protein level between different healthy individuals, but also variations can be seen between the two samples taken from the same individual, but after eight hours. DJ-1 protein level is lower in the heterozygous c.192G>C *DJ-1* mutation carrier in comparison to most controls (except healthy control female D) and DJ-1 protein level of the index patient is under the detection level (Figure 28).

Expression of DJ-1 protein was determined in different human cell types to exclude tissue specific effects and show that loss of protein occurred across all available cell types. DJ-1 protein expression in human dermal fibroblasts of a control person and three E64D family members is shown (Figure 29). DJ-1 proteins were examined by immunoblotting using a DJ-1 specific antibody. Compared to the DJ-1 protein level of the healthy control the heterozygous c.192G>C *DJ-1* mutation carrier shows approximately 80 % less expression in this case. DJ-1 protein is not detectable in both homozygous c.192G>C *DJ-1* mutation carriers.

A)

B)
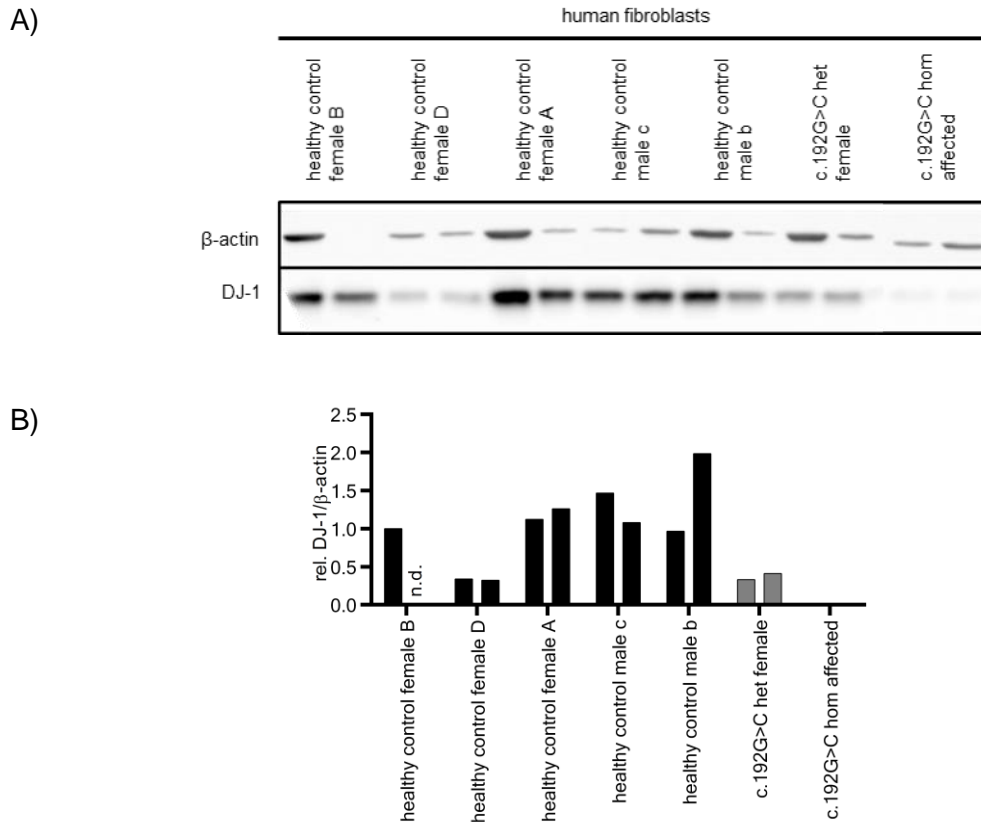
Figure 28: **A) Western blot and B) densitometry of Western blot of cell lysates prepared from human control fibroblasts and one heterozygous and one homozygous c.192G>C *DJ-1* mutation carrier.**

Samples are separated in a 4 % acrylamide SDS-PAGE gel. Result shows a fluctuation of DJ-1 level in controls and heterozygous c.192G>C *DJ-1* mutation carrier when comparing the different individuals, but also interindividual fluctuations in DJ-1 protein levels. DJ-1 protein in indicated homozygous c.192G>C *DJ-1* mutation carrier is not detectable. (n.d. = not determined). N=1.

Cell lysates were prepared from control fibroblasts and c.192G>C *DJ-1* mutation carriers, in a 4 % acrylamide SDS-PAGE gel and detected with a DJ-1 specific antibody. Result shows a reduced level (approx. 20 %) of DJ-1 protein in a heterozygous c.192G>C *DJ-1* mutation carrier (individual III.7) and DJ-1 protein is not detectable homozygous c.192G>C *DJ-1* mutation carriers (individual III.11 and III.13). Ratios were normalised to healthy control. N=1.
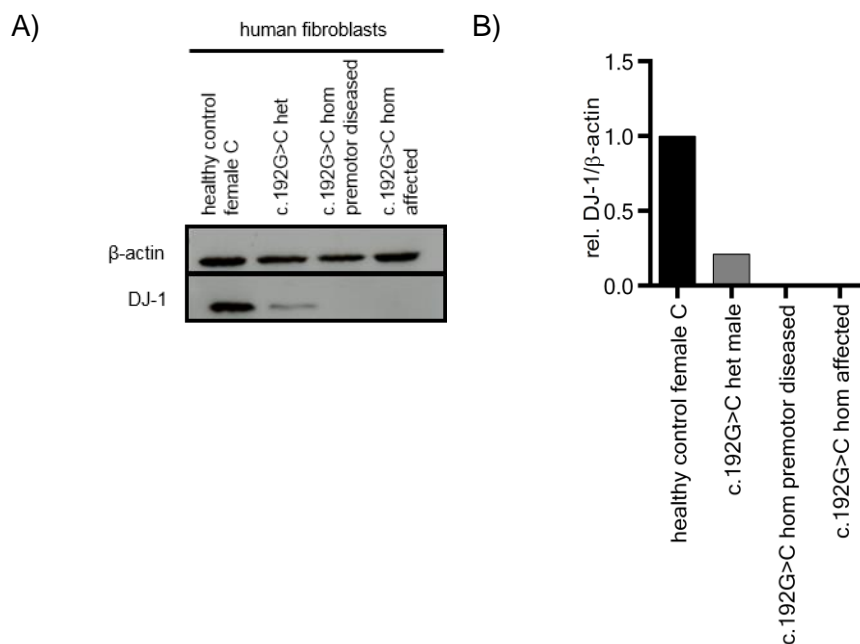
Figure 29: **A) Western blot and B) densitometry of Western blot of DJ-1 protein level in human fibro-blasts.**

Primary fibroblasts from patients are a useful tool but at the same time they only grow very slow and particularly from older people they become senescent after a certain times of passaging. To not loose the ability to work with fibroblasts from the c.192G>C *DJ-1* family we immortalised fibroblasts using a lentiviral vector expressing SV40. This opened the opportunity to work with cells from patients that grow faster and can be used at higher passages.

To test if the immortalisation had an effect on DJ-1 protein level and to see if the c.192G>C *DJ-1* mutation still results in undetectable DJ-1 protein in immortal cells we repeated the Western blot for DJ-1 in this cell type which has a higher metabolic rate. Indeed DJ-1 protein could not be detected in both homozygous c.192G>C *DJ-1* mutation carriers. The DJ-1 protein level of the heterozygous c.192G>C *DJ-1* mutation carrier was reduced to about 20 % of the amount seen in the healthy control (Figure 30).
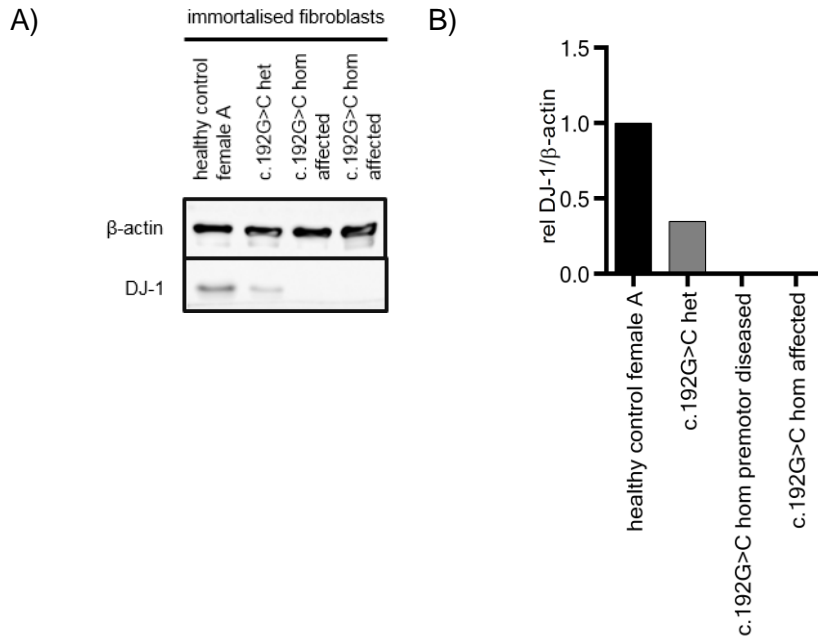
Figure 30: **A) Western blot and B) densitometry of Western blot of DJ-1 protein level in immortalised fibroblasts.**

Cell lysates prepared from immortalised fibroblasts of a healthy control and indicated c.192G>C *DJ-1* mutation carriers were prepared and separated in a 4 % acrylamide SDS-PAGE gel and detected with a DJ-1 specific antibody. Result shows an appoximatly 65 % reduced level of DJ-1 protein in the heterozygous c.192G>C *DJ-1* mutation carrier and DJ-1 protein is not detectable homozygous c.192G>C *DJ-1* mutation carriers. Ratios were normalised to healthy control female A. N=1.

The generation of iPSCs from fibroblasts of the c.192G>C *DJ-1* mutation carriers allowed us to also determine DJ-1 protein expression in pluripotent cells as well as cells differentiated from the iPSCs, to give insight into whether loss of DJ-1 protein in mutation carriers is tissue specific or not. DJ-1 protein level in iPSCs was measured by Western blot similar to the Western blots performed before with a DJ-1 specific antibody. As seen in the fibroblasts both homozygous c.192G>C *DJ-1* mutation carriers do not express DJ-1 protein. DJ-1 protein level is reduced in the heterozygous c.192G>C *DJ-1* mutation carrier in comparison to DJ-1 protein levels in both healthy controls (Figure 31).
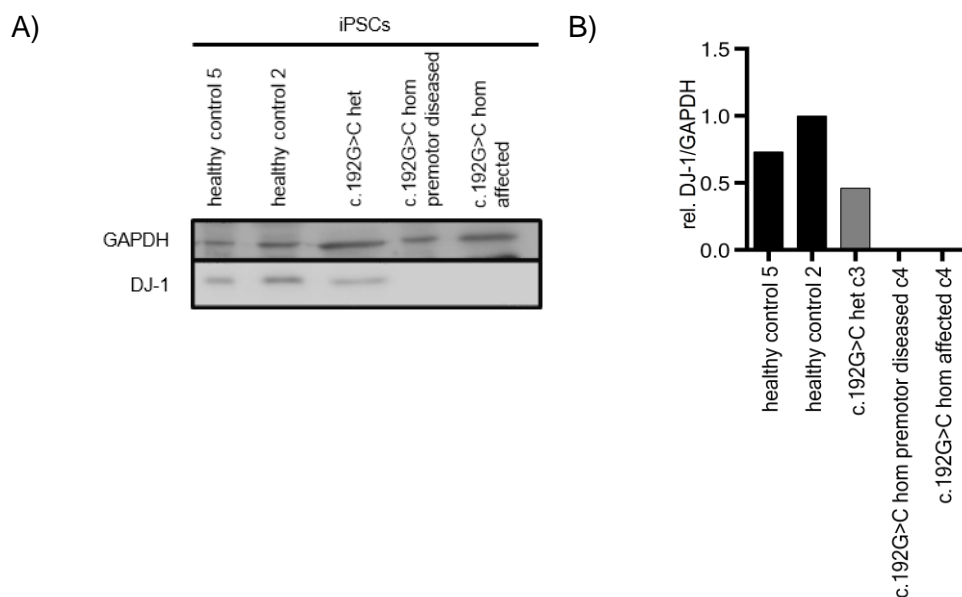
Figure 31: **A) Western blot and B) densitometry of Western blot of DJ-1 protein level in iPSCs from c.192G>C *DJ-1* mutation carriers and healthy controls.**

Cell lysates prepared from iPSCs of a healthy control and indicated c.192G>C *DJ-1* mutation carriers were prepared and separated in a 4 % acrylamide SDS-PAGE gel and detected with a DJ-1 specific antibody. DJ-1 protein expression is reduced in heterozygous c.192G>C *DJ-1* mutation carrier when compared to healthy controls. DJ-1 protein is not detectable in both homozygous c.192G>C *DJ-1* mutation carriers. Ratios were normalised to healthy control 2. N=1.

Next, we were interested in determining DJ-1 protein level in mDA neurons, the cells that die in PD patients. Therefore, DJ-1 protein level in mDA neurons differentiated from iPSCs were assessed as previously shown (Figure 32).

Once more DJ-1 protein level was not detectable in both indicated homozygous c.192G>C *DJ-1* mutation carriers. DJ-1 protein level was slightly reduced in heterozygous c.192G>C *DJ-1* mutation carrier when compared to healthy control (Figure 32).
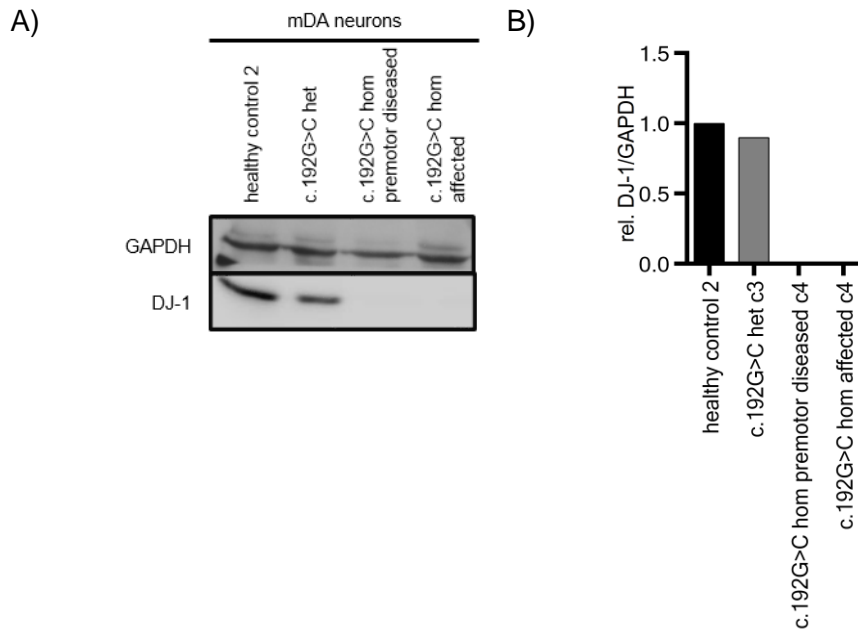
Figure 32: A) Western blot and B) densitometry of Western blot of DJ-1 protein level in mDA neurons from c.192G>C *DJ-1* mutation carriers and healthy controls.

Cell lysates prepared from mDA neurons of a healthy control and indicated c.192G>C *DJ-1* mutation carriers were prepared and separated in a 4 % acrylamide SDS-PAGE gel and detected with a DJ-1 specific antibody. DJ-1 protein expression is approximately 10 % reduced in heterozygous c.192G>C *DJ-1* mutation carrier when compared to healthy controls. DJ-1 protein is not detectable in both homozygous c.192G>C *DJ-1* mutation carriers. Ratios were normalised to healthy control 2. N=1.

iPSC clones were also used to generate smNPCs. Indicated clones of smNPCs were tested for DJ-1 protein levels as well. DJ-1 level varies between healthy controls and heterozygous c.192G>C *DJ-1* mutation carrier with one control clone showing higher DJ-1 protein levels compared to the other two. DJ-1 protein level is under the detection level in smNPCs generated from both iPSC clones of the index patient (Figure 33).
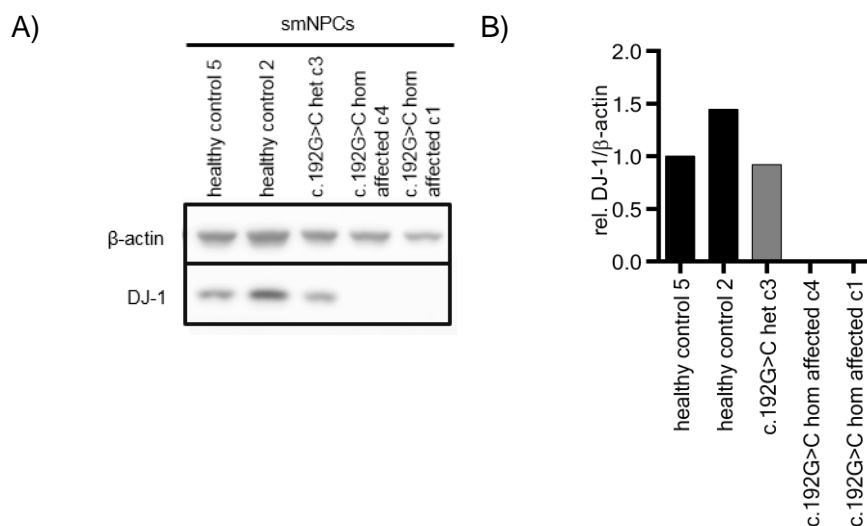
Figure 33: **A) Western blot and B) densitometry of Western blot of DJ-1 protein level in smNPCs from c.192G>C *DJ-1* mutation carriers and healthy controls.**

Cell lysates prepared from smNPCs of indicated healthy controls and indicated clones from c.192G>C *DJ-1* mutation carriers were prepared and separated in a 4 % acrylamide SDS-PAGE gel and detected with a DJ-1 specific antibody. DJ-1 protein expression varies between the two different controls. DJ-1 level of heterozygous c.192G>C *DJ-1* mutation carrier is approximately the same as healthy control 5. DJ-1 protein is not detectable in both homozygous c.192G>C *DJ-1* mutation carriers. Ratios were normalised to healthy control 5. N=1.

3.6.2 The c.192G>C *DJ-1* mutation causes skipping of *DJ-1* exon 3

The findings on DJ-1 protein level in c.192G>C *DJ-1* mutation carriers raised interest in the underlying effect of the mutation. As a first quick step, the *in silico* software MutationTaster (Schwarz et al., 2010) was used in order to evaluate the disease causing potential of the c.192G>C *DJ-1* mutation. The predicted effect of the analysed mutation was amino acid sequence changed, protein feature (might be) affected and interestingly splice site changes (Figure 34). The latter one being the most interesting one for us, as we do not see DJ-1 protein expression in any of the analysed cell types carrying the c.192G>C *DJ-1* mutation homozygously.

Figure 34: ***In silico* evaluation of the disease causing potential of c.192G>C *DJ-1* mutation using MutationTaster software.**

DJ-1 ensembl transcript ENST00000493678 was used to evaltuate disease causing potential of the c.192G>C *DJ-1* mutation via MutationTaster software (Schwarz et al., 2010). Software predicted: aminoacid sequence changed, known disease mutation, protein features (might be) affected and splice site changes.

To determine the reason for the absence of DJ-1 protein in homozygous c.192G>C *DJ-1* mutation carriers and to test for predicted splice site changes, the RNA in c.192G>C *DJ-1* mutation carriers was in the focus. In a first experiment, RNA from patient derived fibroblasts was isolated, transcribed into cDNA and amplified *DJ-1* by PCR. Agarose gel revealed a reduced length of c.192G>C *DJ-1* carrying cDNA and a normal size band as well as the short band in the heterozygous c.192G>C carrying cDNA. cDNA from a healthy control served as positive control for correct length (Figure 35).

Figure 35: ***DJ-1* amplification of cDNA of indicated patient derived fibroblasts of c.192G>C *DJ-1* mutation carriers and healthy control.**

Fibroblasts were pelleted, RNA was extracted from the cell pellet and cDNA was transcribed. *DJ-1* was amplified by PCR and subsequently run on an agarose gel. DNA gel analysis showed reduced mRNA length in both homozygous c.192G>C *DJ-1* mutation carriers. Bands corresponding to both reduced and normal length mRNA were visible in the heterozygous c.192G>C *DJ-1* mutation carrier.

Subsequently, these results led us to sequence the amplified cDNA to find out which sequence segment was missing in the cDNA of c.192G>C *DJ-1* mutation carriers. Sequencing result shows that the end of *DJ-1* exon 2 is directly followed by the beginning of exon 4. Complete sequence of *DJ-1* exon 3 was missing or skipped (Figure 36).
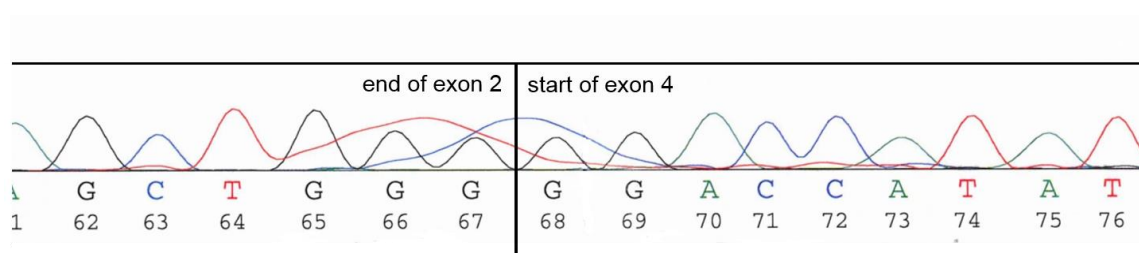
Figure 36: **Sequencing result of cDNA from homozygous c.192G>C *DJ-1* mutation carrier after *DJ-1* amplification.**

Fibroblasts were pelleted, RNA was extracted from the cell pellet and cDNA was transcribed. *DJ-1* was amplified by PCR. Subsequently, sanger sequencing was performed. Results show absence of complete *DJ-1* exon 3 in cDNA from affected homozygous c.192G>C *DJ-1* mutation carrier.

After obtaining these results, we wanted to validate the finding of skipping of *DJ-1* exon 3 in c.192G>C *DJ-1* mutation carrying cells. Therefore, DNA of the index patient and a healthy control was given to the Molecular Genetics Laboratory of Prof. Bernd Wissinger of the Institute for Ophthalmic Research (Tübingen, Germany). They designed and performed a minigene assay to assess the effect of *DJ-1* exon 3 on splicing:

In the minigene assay we tested wt exon 3 of the control and mutant exon 3 (carrying the c.192G>C *DJ-1* mutation) from the index patient. At the same time minigene constructs were tested where the wt exon 3 was mutated to carry the c.192G>C mutation and the

corrected exon from the index patient now carrying the wt allel. Agarose gel electrophoresis (Figure 37) revealed that cultures transfected with pSPL3 constructs with the mutant c.192 C-allele yielded rtPCR products that were clearly smaller than products from cultures transfected with the wildtype c.192 G-allele, indicating abnormal splicing/skipping of the mutant minigene construct. Subsequent sequencing showed that rtPCR products derived from the transfection with the mutant c.192 C-allele lacked exon 3 of the DJ1 gene.
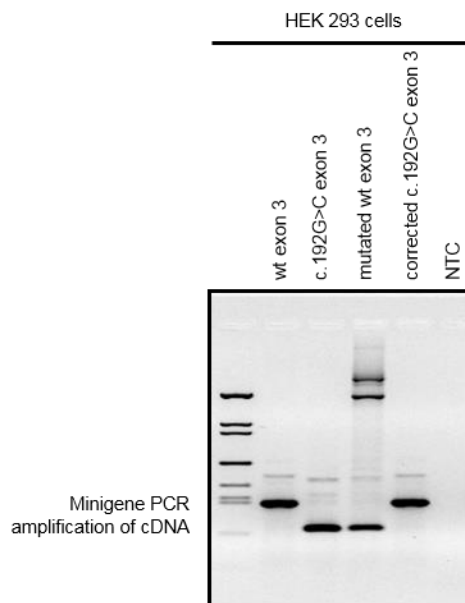
Figure 37: **rtPCR result of minigene assay of wt and c.192G>C *DJ-1* mutation carrying exon.**

Minigene transient transfection assay showing the effect of wt exon 3 and mutant DJ-1 exon 3 carrying the c.192G>C mutation. Two prominent products are seen on agarose gel, with the shorter band representing a PCR product lacking *DJ-1* exon 3 (lane 3 and 4) and the longer band a product including *DJ-1* exon 3 (lane 2 and 5). No template control (NTC). Size standard: 100 bp ladder (Invitrogen GmbH, Karslruhe, Germany).

The c.192G>C *DJ-1* mutation in exon 3 which does not lead to a premature stop codon and which does not cause a frameshift in the RNA caused the skipping of exon 3 in the minigene assay. In addition to the correction of the mutation in the patient exon 3 and the mutating of exon 3 to carry the c.192G>C *DJ-1* mutation from a healthy control in the minigene, sequencing of the entire *DJ-1* locus of the patient's DNA was performed. This was done in order to have a second confirmation that the c.192G>C *DJ-1* mutation suffices to cause skipping of exon 3 in c.192G>C *DJ-1* mutation carriers and other sequence variants can be excluded. The NGS of pooled long distance PCR products and gap closure at two GC-rich regions by Sanger sequencing was performed by the Molecular Genetics Laboratory of Prof. Bernd Wissinger of the Institute for Ophthalmic Research (Tübingen, Germany). All exons and introns plus additional upstream and downstream sequences of *DJ-1* from all individuals were sequenced with 99.8 % of the target region being covered >50 fold. Apart from the c.192G>C DJ-1 mutation which was called in the sample of the

index patient just three additional rare variants were found. None of these variants overlap with other known non-coding transcripts or putative regulatory sequences.

The minigene assay showed, in an artificial system, that the c.192G>C *DJ-1* mutation which lies at the end of exon 3 leads to skipping of the respective exon. Skipping of this exon does not lead to a frameshift (Figure 38) or a premature stop codon.

<div style="border:1px solid black; padding:10px;">

Sequence of *DJ-1* exon 3:

GCTGGG/ATTAAGGTCACCGTTGCAGGCCTGGCTGGAAAAGACCCAGTACAGTGTAGC
CGTGATGTGGTCATTTGTCCTGATGCCAGCCTTGAAGATGCAAAAAAAGAG/GGACCA

</div>
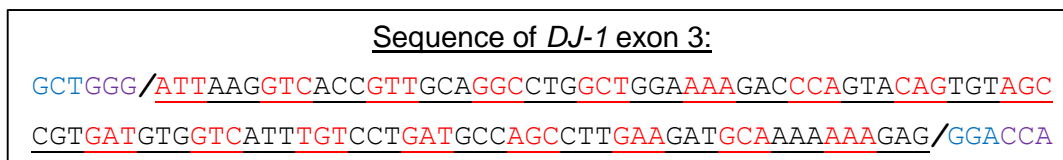
Figure 38: **Sequence of *DJ-1* exon 3.**

End of sequence of exon 2 (blue and purple), followed sequence of *DJ-1* exon 3 (red and black), followed by beginning of sequence of exon 4 (blue and purple). Triplets are highlighted in different colours to show that skipping of this exon does not cause a frameshift.

To make sure that DJ-1 protein was not detectable in the patient dereived cells because it was absent and not because the antibody used binds to an aminoacid encoded in exon 3 we tested another DJ-1 specific antibody. Exemplary Western blot experiment of immortalised fibroblasts where we used the two different DJ-1 antibodies (Figure 39). Scheme shows binding sites of the two different antibodies used showing that their binding sites are not in exon 3 (Figure 57).
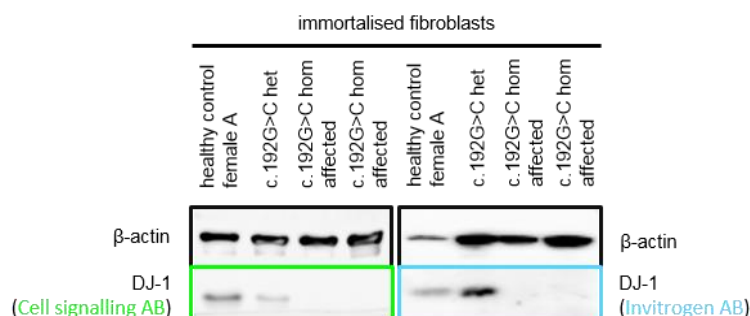
Figure 39: **Western blot to test two different AB to detect DJ-1 protein in homozygous c.192G>C *DJ-1* mutation carriers.**

Cell lysates prepared from immortalised fibroblasts of a healthy control and indicated c.192G>C *DJ-1* mutation carriers were prepared and separated in a 4 % acrylamide SDS-PAGE gel and detected with two different DJ-1 specific antibodies. Left side shows blot probed with DJ-1 (D29E5) XP® mAB (Cell Signaling Technology, Cambridge, UK) outlined in green. Right side shows blot probed with Mous anti-DJ-1 (37-8800) mAB (Invitrogen GmbH, Karslruhe, Germany) outlined in blue.

Next, we wanted to verify our minigene assay results in the different cell types available from the c.192G>C *DJ-1* mutation carriers. Therefore, cells were grown under standard conditions, harvested, RNA was extracted and transcribed into cDNA. Quantitative qPCR was performed using cDNA and two different pairs of primers for amplification. One primer

pair to detect correctly spliced DJ-1 as well as cDNA lacking exon 3 and another primerpair where one primer is complementary with exon 2 and exon 3, leading to only correctly spliced (with exon 3) *DJ-1* cDNA detected by qPCR. qPCR was performed with cDNA from immortalised fibroblasts (Figure 40), iPSCs, mDA neurons and smNPCs.

qPCR results generated with primers that detect normal and misspliced *DJ-1* cDNA show a reduction which is not significant of *DJ-1* RNA expression in all c.192G>C *DJ-1* mutation carriers (Figure 40A). Reduction is even higher when looking at normal spliced RNA where we see a significant reduction of *DJ-1* RNA expression between the healthy control and the heterozygous c.192G>C *DJ-1* mutation carrier. Even lower levels in both indicated homozygous c.192G>C *DJ-1* mutation carriers were seen. RNA expression of *DJ-1* is significantly reduced in both homozygous c.192G>C *DJ-1* mutation carriers when compared to healthy control or heterozygous carrier of the same mutation (Figure 40B).
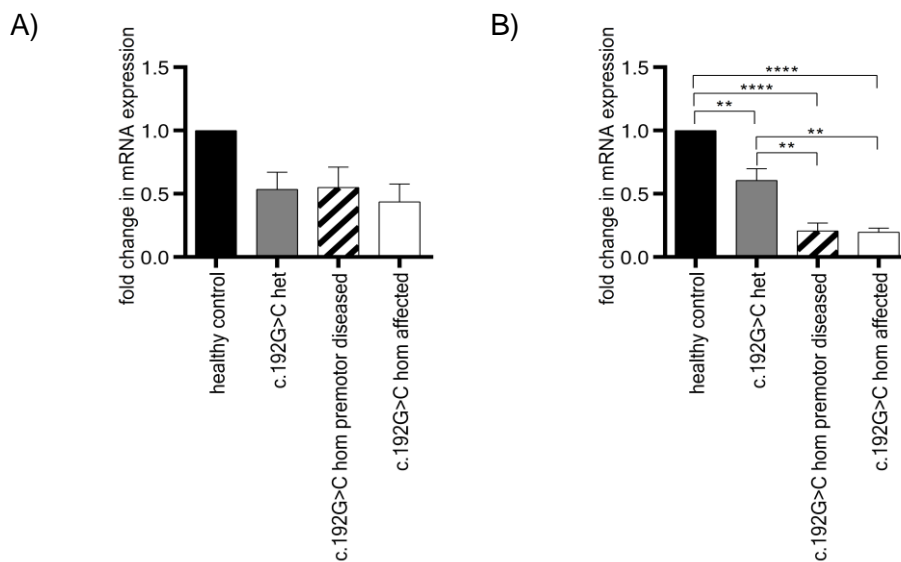
Figure 40: **qPCR of *DJ-1* RNA expression level with and without exon 3 in immortalised fibroblasts.**

Cell pellets were collected, RNA was isolated and transcribed into cDNA. cDNA was amplified by qPCR using one primerpair that amplifies *DJ-1* cDNA with and without exon 3 (A) and one primerpair amplifying *DJ-1* cDNA only in the presence of exon 3 (B). **A)** DJ-1 RNA expression is about 40 % reduced in c.192G>C *DJ-1* mutation carriers. **B)** Correctly spliced full length *DJ-1* mRNA is around 30 % reduced in heterozygous c.192G>C *DJ-1* mutation carrier and about 80 % in homozygous c.192G>C *DJ-1* mutation carriers. Ratios were normalised to healthy control. Values show mean + SEM. ** $p \leq 0.01$, **** $p \leq 0.0001$ by one-way ANOVA followed by Tukey's multiple comparisons test. N=3.

When looking at the qPCR results in iPSCs derived from these fibroblasts one sees a reduction in RNA expression of *DJ-1* with and without skipping of exon 3 of the c.192G>C

DJ-1 mutation carriers. With two clones (homozygous premotor diseased c4 and homozygous affected c4) being particularly low (Figure 41A). The results generated with primers that only detect *DJ-1* cDNA when exon 3 is present all cDNAs from homozygous carriers are practically not detectable. The two indicated heterozygous clones vary with one showing the same RNA expression level as the healthy control and the other one showing a 50 % decrease in correctly spliced *DJ-1* RNA (Figure 41B).
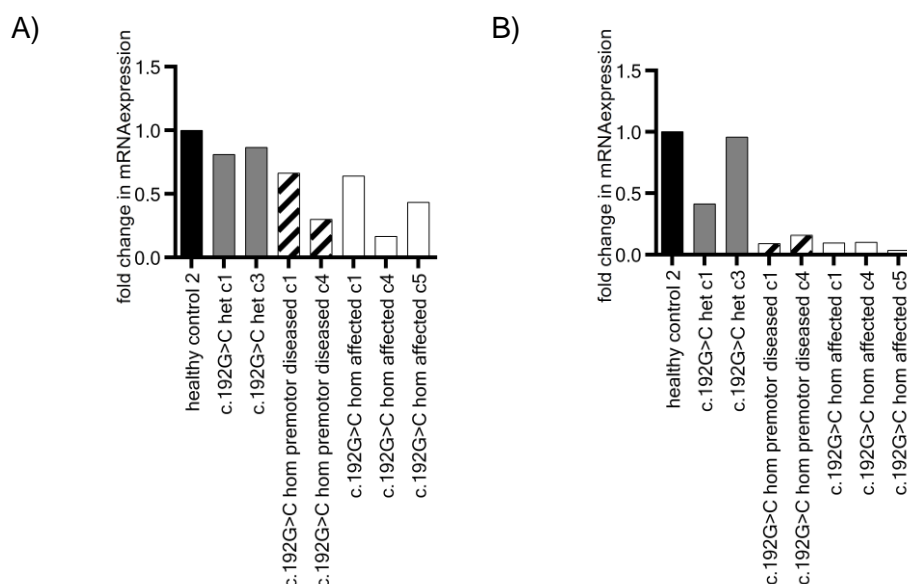
Figure 41: **qPCR of *DJ-1* RNA expression level with and without exon 3 in iPSCs.**

Cell pellets of indicated iPSC clones were collected, RNA was isolated and transcribed into cDNA. cDNA was amplified by qPCR using one primerpair that amplifies *DJ-1* cDNA with and without exon 3 (A) and one primerpair amplifying *DJ-1* cDNA only in the presence of exon 3 (B). **A)** *DJ-1* RNA expression is reduced in two indicated homozygous c.192G>C *DJ-1* mutation carrying clones from affected and premotor diseased individuals. **B)** Correctly spliced full length *DJ-1* gene expression is reduced to 50 % in one heterozygous c.192G>C *DJ-1* mutation carrying clone in comparison to healthy control and strongly reduced in all homozygous c.192G>C *DJ-1* mutation carriers. Ratios were normalised to healthy control 2. N=1

The qPCR results of *DJ-1* RNA expression of mDA neurons in terms of skipping of exon 3 were of particular interest as mDA neurons are most vulnerable to degeneration in PD.

Looking at the *DJ-1* RNA expression results of qPCR done with pellets from mDA neurons of healthy control and indicated c.192G>C *DJ-1* mutation carriers using primers that detect *DJ-1* cDNA with and without exon 3 shows no differences between analysed individuals. Results of qPCR using primers that only detect *DJ-1* RNA expression when exon 3 is present show a significant reduction of *DJ-1* RNA expression in all c.192G>C *DJ-1* mutation carriers in comparison to healthy control. RNA is also significantly reduced in both homozygous mutation carriers when compared to expression in heterozygous c.192G>C *DJ-1* mutation carrier (Figure 42).

A)

B)
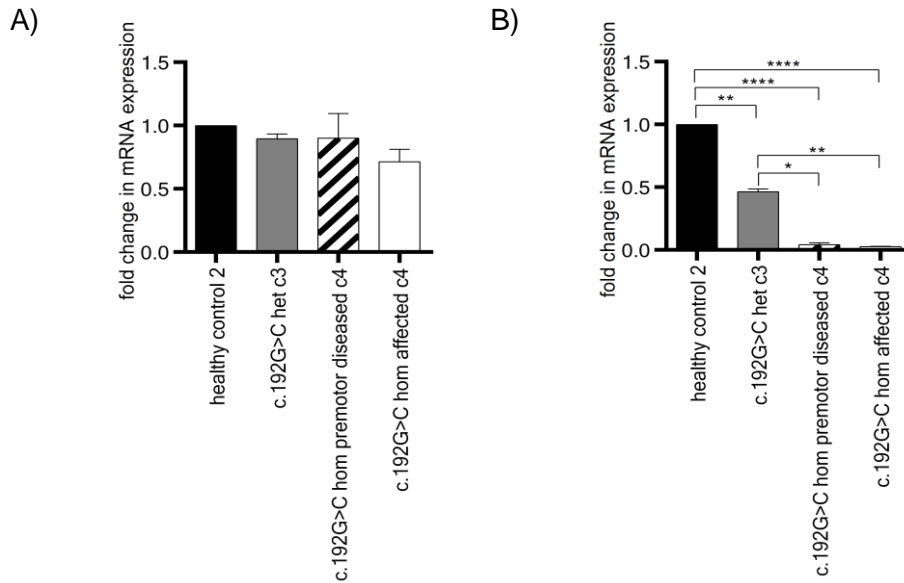
Figure 42: **qPCR of *DJ-1* RNA expression level with and without exon 3 in mDA neurons.**

Cell pellets of indicated mDA neurons differentiated from indicated iPSC clones were collected, RNA was isolated and transcribed into cDNA. cDNA was amplified by qPCR using one primer pair that amplifies *DJ-1* cDNA with and without exon 3 (A) and one primer pair amplifying *DJ-1* cDNA only in the presence of exon 3 (B). **A)** No significant changes in total *DJ-1* gene expression of correctly and misspliced *DJ-1* RNA. **B)** gene expression of *DJ-1* mRNA with exon 3 is nearly absent in heterozygous c.192G>C *DJ-1* mutation carries to about 45 % in comparison to indicated healthy control. *DJ-1* gene expression of both indicated homozygous c.192G>C *DJ-1* mutation carriers is significantly reduced to healthy control as well as to heterozygous c.192G>C *DJ-1* mutation carrier as well and virtually not detectable. Ratios were normalised to healthy control 2. Values show mean + SEM. * $p \leq 0.05$, ** $p \leq 0.01$, **** $p \leq 0.0001$ by one-way ANOVA followed by Tukey's multiple comparisons test. N=3.

Next, we calculated the RNA expression of smNPCs generated from the iPSC clones to have a second neuronal model to detect c.192G>C *DJ-1* RNA expression. When looking at the results of the qPCR where a primer pair was used that detects *DJ-1* cDNA with and without exon 3, levels in all indicated smNPCs was the same except for healthy control 2 where we saw a reduced RNA expression (Figure 43A). When primers were used that only detect *DJ-1* cDNA when exon 3 is integrated a reduction is shown in both clones from the index patient as well as in healthy control 2. smNPCs from the heterozygous c.192G>C *DJ-1* mutation carrier showed a reduction of approximately 70 % when compared to healthy control 5 (Figure 43B).
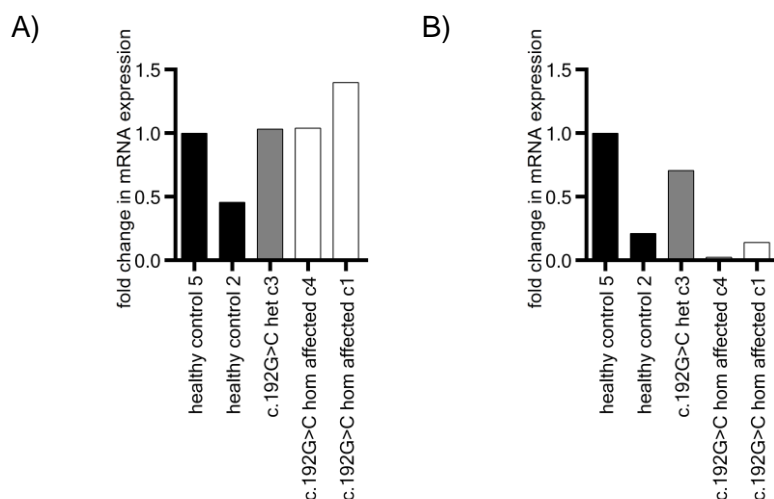
Figure 43: **qPCR of *DJ-1* RNA level with and without exon 3 in smNPCs.**

Cell pellets of indicated smNPCs generated from indicated iPSC clones were collected, RNA was isolated and transcribed into cDNA. cDNA was amplified by qPCR using one primer pair that amplifies *DJ-1* cDNA with and without exon 3 (A) and one primer pair amplifying *DJ-1* cDNA only in the presence of exon 3 (B). **A)** gene expression is about the same in all indicated smNPCs except for healthy control 2 where *DJ-1* gene expression is reduced in comparison to other indicated lines. **B)** gene expression of *DJ-1* with exon 3 is reduced in smNPCs from both homozygous c.192G>C *DJ-1* mutation carrying clones as well as in healthy control 2 when compared to healthy control 5 and heterozygous c.192G>C *DJ-1* mutation carrier. Ratios were normalised to healthy control 5. N=1.

The expression analysis by qPCR showed that expression of correctly spliced *DJ-1* RNA was reduced or even absent in analysed cell types of c.192G>C *DJ-1* mutation carriers when compared to controls. Missplicing occurs in the allel carrying the c.192G>C *DJ-1* mutation. Missplicing leads to complete exclusion of *DJ-1* exon 3 and shorter mRNA. Western blot analysis showed absence of DJ-1 protein in homozygous c.192G>C *DJ-1* mutation carriers.

3.6.3 Genetically modified U1 rescues skipping of exon 3

Further experiments aimed at analysing why the c.192G>C base exchange leads to mis-splicing of *DJ-1* pre-mRNA and skipping of exon 3 during the splicing process. Hypothesised mechanism of splicing of pre-mRNA carrying the c.192G>C *DJ-1* mutation is shown (Figure 44). The c.192G>C *DJ-1* mutation lies at the end of exon 3 and hence in the splice donor recognition site. If the splice donor sequence does not get recognised as such due to the mutation, the splice acceptor site will also not be recognised. During the splicing process, U1 snRNP and U2 snRNP will recognise the splice donor sequence of exon 2 and the splice acceptor sequence of exon 4 respectively, surrounding exon 3, but not exon 3 itself. This will finally lead to skipping of *DJ-1* exon 3 and a shortened *DJ-1* mRNA (Figure 44).
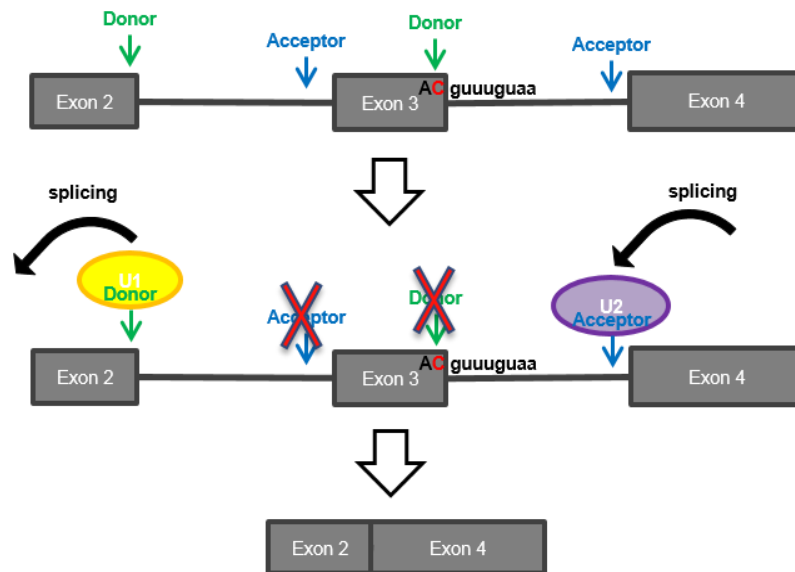
Figure 44: **Scheme of splicing of c.192G>C *DJ-1* mutation carrying pre-mRNA.**

Upper lane shows *DJ-1* exon 3 carrying the c.192G>C mutation, which is the last base of exon 3 (red) and therefore lies in the splice donor site. During the splicing process of the pre-mRNA, exon 3 does not get recognised as exon as the c.192G>C *DJ-1* mutation changes the splice donor site which, no longer gets recognised as such. Due to that, the splice acceptor does not get recognised either. Finally, this leads to skipping of exon 3.

This hypothesis was strengthened by findings from Carmel and colleagues (2004) (Carmel et al., 2004) showing the frequency and conservation of human splice sites by analysing nearly 50,000 sequences. Frequencies of bases in splice donor sites were analysed in that study. A modified figure from that study and shows the frequencies of the individual bases in the situation when the first two bases of the intron are 'GT' (Figure 45). The size of the letter indicates the frequency of the respective base. The bigger the letter the more frequent. A vertical bar also shows a highly frequent base in the respective position and a colon less common ones. According to this figure the last base of the analysed exons is a guanine, whereas cytosine is found least often. For the c>192G>C *DJ-1* mutation that means that in the wt situation, *DJ-1* exon 3 ends by the most common base: guanine, whereas in mutation carriers the exon ends with the most unusual base: cytosine.

As the c.192G>C *DJ-1* mutation lies in the splice donor site normally it would get recognised by the U1 snRNP which is initiating the formation of the spliceosome. U1 snRNP recognises the 5' splice site through base pairing at the 5' end. Of note, a hundred percent match is not necessary. In case of *DJ-1* exon 3 in the wt situation there are already four mismatches between U1 snRNA and the splice donor site (Figure 46A). The presence of the c.192G>C *DJ-1* mutation leads to five mismatches between U1 and the splice donor site (Figure 46B). The aim of this part of the project was to test whether this additional

mismatch causes U1 snRNP to not recognise the splice donor site hence leading to skipping of exon 3 (Figure 44).
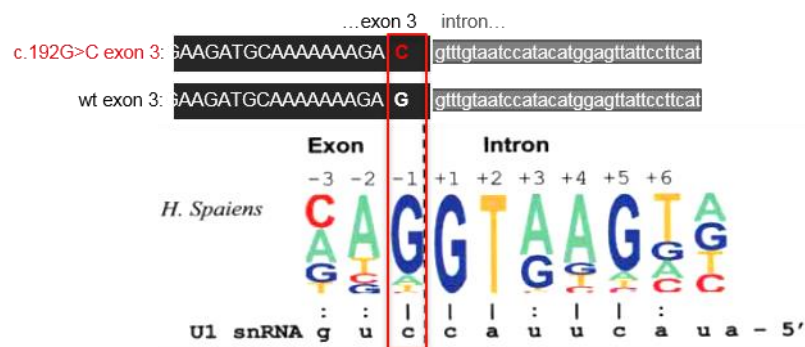
Figure 45: **Frequencies of potential basepairs of U1 snRNA in human.**

Potential base pairs of U1 snRNA and 5' splice site in human. In the study they used 49,778 human U2-dependent 5' sequences, which were used with the canonical 'GT' nucleotides as first bases of the intron. Potential base pairs with the appropriate nucleotide of U1 snRNA are marked either by a vertical bar for highly frequent basepairs (>0.7) or by a colon for less common ones (<0.7). Size of the letters indicates frequencies. Guanine as last base of an exon therefore is very frequent whereas cytosine is the least often one. Wt *DJ-1* exon 3 ends with a guanine, in carriers of the c.192G>C mutation *DJ-1* exon 3 ends with a cytosine.

Figure modified from (Carmel et al., 2004).

A)   B)
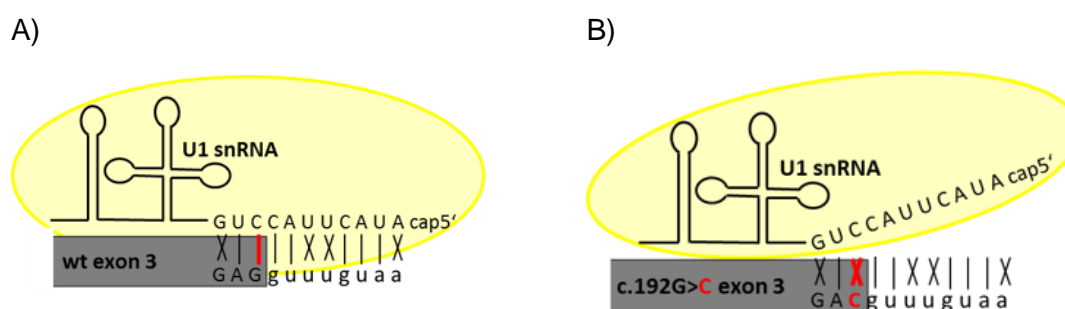
Figure 46: **Binding of U1 snRNP to wt *DJ-1* exon 3 and c.192G>C mutant *DJ-1* exon 3.**

U1 snRNP binds to the pre-mRNA by base pairing to initiate the formation of the spliceosome. **A)** Binding of U1 snRNP to wt *DJ-1* exon 3. Binding takes place in the presence of 4 mismatches. **B)** Not binding of U1 snRNP to c.192G>C mutant *DJ-1* exon 3. The c.192G>C *DJ-1* mutation leads to the fifth mismatch between U1 snRNA and the pre-mRNA therefore U1 snRNP does not bind to c.192G>C mutant *DJ-1* exon 3.

To test this hypothesis, one base of the U1 snRNA was modified in the sense that it matches the c.192G>C mutation in *DJ-1* exon 3, namely C>G were exchanged as indicated in cyan (Figure 47). A vector containing the U1 snRNA was a kind gift from Prof. Francisco E. Baralle and Marco Baralle, PhD of the International Centre for Genetic Engineering and Biotechnology (ICGEB) in Trieste, Italy.
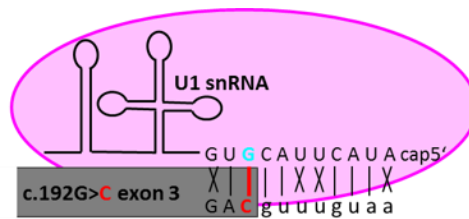
Figure 47: **Binding of C>G mutant U1 snRNP to c.192G>C mutant *DJ-1* exon 3.**

By mutagenesis, a C>G base exchange (indicated in cyan) was introduced in the U1 snRNA so that it matches the c.192G>C *DJ-1* mutation and hence binds to c.192G>C mutant *DJ-1* exon 3.

In a splicing reaction where C>G mutant U1 snRNP is present and recognises the splice donor sequence of c.192G>C mutant *DJ-1* exon 3 skipping of this exon does not take place.
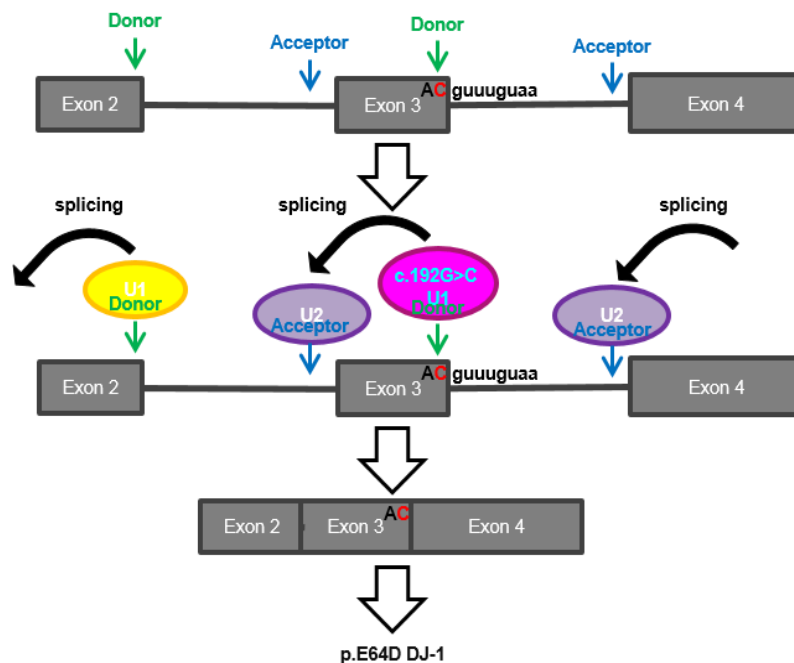
Figure 48: **Scheme of splicing of c.192G>C *DJ-1* mutation carrying *DJ-1* exon 3 pre-mRNA in the presence of c.192G>C U1 snRNP.**

Upper lane shows *DJ-1* exon 3 carrying the c.192G>C mutation indicated in red as last base of *DJ-1* exon 3 in the splice donor sequence. In a splicing reaction where c.192G>C U1 snRNP is present, shown in pink in the second lane, c.192G>C mutant *DJ-1* exon 3 gets recognised. U1 snRNP binds to the splice donor sequence and U2 snRNP (purple) to the splice acceptor sequence surrounding c.192G>C mutant *DJ-1* exon 3. Consequently, splicing leads to the inclusion of c.192G>C mutation carrying *DJ-1* exon 3 (third lane). mRNA will presumably be translated to c.192G>C DJ-1 protein (fourth lane).

In order to test the hypothesis, the previously performed minigene experiment was repeated and a plasmid expressing c.192G>C U1 snRNA was contransfected. This experiment was carried out by the Molecular Genetics Laboratory of Prof. Bernd Wissinger of the Institute for Ophthalmic Research (Tübingen, Germany).

The minigene construct expressing wt exon 3 resulted in the inclusion of the exon 3 when the minigene assay was performed with the minigene construct alone, when wt U1 snRNP was cotransfected and when c.192G>C U1 snRNA was cotransfected, this is shown by the long prominent bands on the agarose gel picture in Figure 49 lane 2 – 4. When the experiment was performed with a minigene construct with the c.192G>C mutation carrying *DJ-1* exon 3 alone or cotransfected with wt U1 snRNA, a short prominent band can be seen on lane 5 and 6 of the agarose gel as rtPCR result. This means that in these cases mutant exon 3 was skipped. When this minigene construct was cotransfected together with c.192G>C U1 snRNA in the minigene assay, however, two products were amplified by rtPCR, displayed by the short band, indicating skipping of exon 3, and the long band indicating the presence of exon 3. This is shown in lane 7 on the agarose gel picture in (Figure 49).
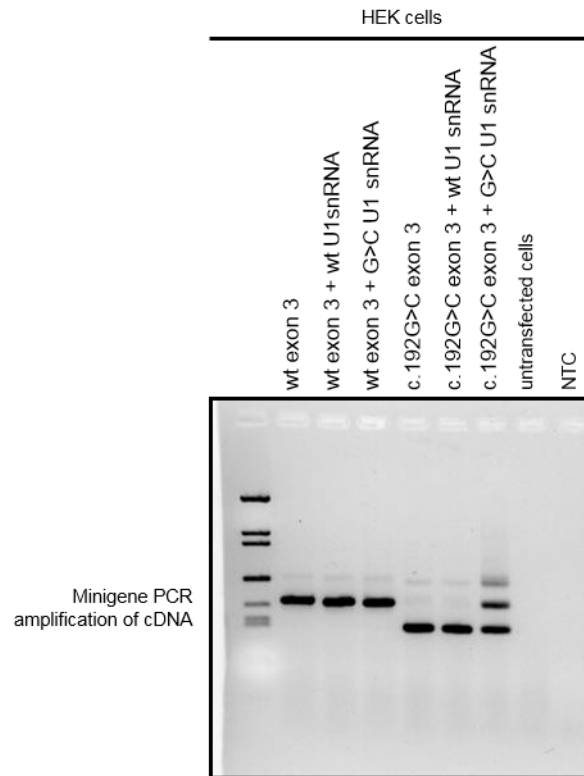
Figure 49: **rtPCR result of minigene assay of wt and c.192G>C *DJ-1* mutation carrying exon cotransfected with wt U1 snRNA or c.192G>C U1 snRNA.**

Minigene transient transfection assay showing the effect of wt exon 3 and mutant *DJ-1* exon 3 carrying the c.192G>C mutation cotransfected with wt U1 snRNA or c.192G>C U1 snRNA. Wt exon 3 in all three indicated and tested conditions leads to the inclusion of exon 3, resulting in a long band in the rtPCR (lane 2, 3 and 4). rtPCR results of c.192G>C mutation carrying exon 3 mingene without cotransfection and after cotransfection with wt U1 snRNA lead to a short band, representing skipping of exon 3 (lane 5 and 6). Two prominent products, the short and the long band, are seen on agarose gel, when c.192G>C exon 3 minigene was cotransfected with c.192G>C U1 snRNA (lane 7). No template control (NTC). Size standard: 100 bp ladder (Invitrogen GmbH, Karslruhe, Germany).

As c.192G>C U1 snRNA was able to rescue skipping of c.192G>C *DJ-1* mutation carrying exon 3 in the minigene assay in HEK cells, the next step was to test the effect of c.192G>C U1 snRNA in patient-derived cells.

Immortalised fibroblasts of the index patient carrying the c.192G>C *DJ-1* mutation were electroporated with empty vector, wt U1 snRNA or c.192G>C U1 snRNA, respectively. Electroporation with wt U1 snRNA caused a significant increase in *DJ-1* RNA expression of normal RNA and RNA lacking *DJ-1* exon 3 in comparision to electroporation with empty vector or c.192G>C U1 snRNA. c.192G>C U1 snRNA also caused higher RNA levels in comparison to empty vector (Figure 50A). When only looking at correctly spliced *DJ-1* RNA (including exon 3), more RNA expression was seen after electroporation with wt U1 snRNA

and even more expression after electroporation with c.192G>C U1 snRNA, compared to electroporation with empty vector (Figure 50B).

A)

B)

C)
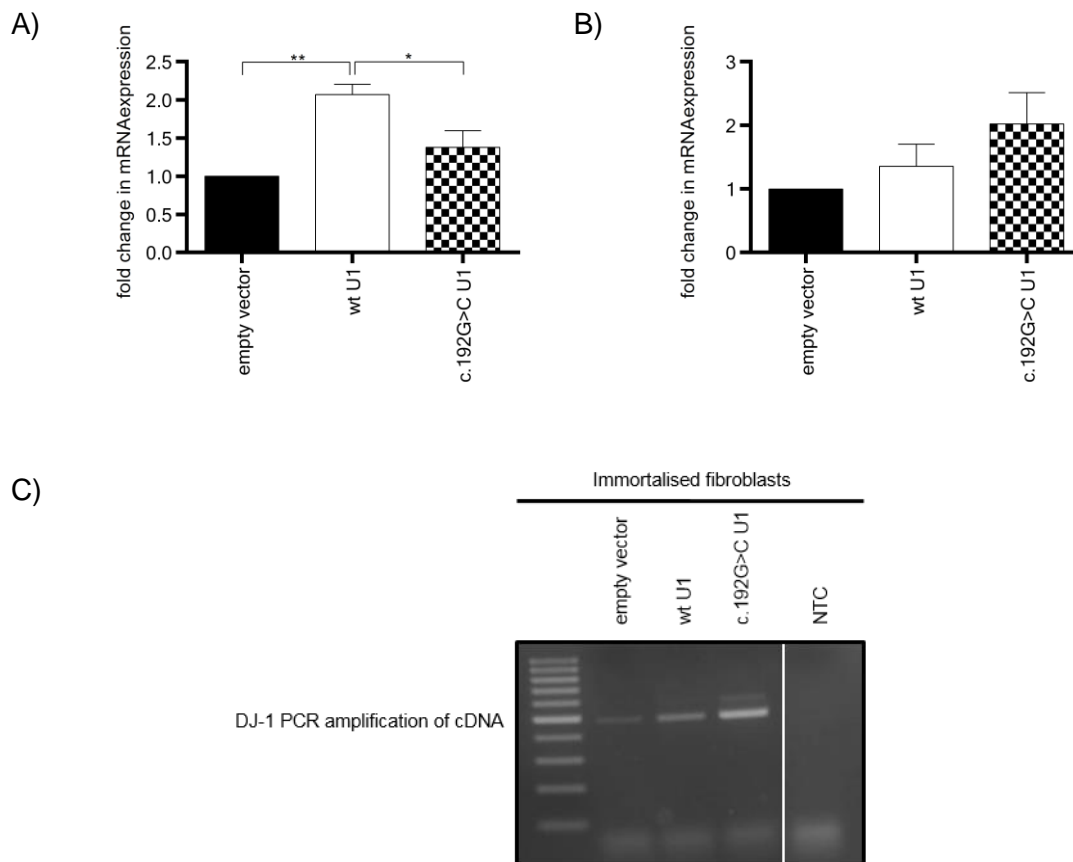
Figure 50: **Transient transfection of wt and c.192G>C U1 snRNA in immortalised fibroblasts of the index patient.**

6 µg of empty vector, wt U1 snRNA or c.192G>C U1 snRNA respectively were electroporated into immortalised fibroblasts of the index patient carrying the c.192G>C *DJ-1* mutation using the Amaxa nucleofector I (Lonza Group Ltd, Basel, CH). 24 h after electroporation cell pellets were collected, RNA was isolated and transcribed into cDNA. cDNA was amplified by qPCR using one primer pair that amplifies *DJ-1* cDNA with and without exon 3 (A) and one primer pair amplifying *DJ-1* cDNA only in the presence of exon 3 (B). **A)** A significantly higher RNA expression was measured after electroporation of wt U1 snRNA. Expression was significantly higher in comparison to RNA expression after electroporation with empty vector and c.192G>C U1 snRNA. **B)** An increase in RNA expression of *DJ-1* RNA including exon 3 was measured after electroporation with wt U1 snRNA in comparsion to electroporation with empty vector. The increase was even higher after electroporation with c.192G>C U1 snRNA. Ratios were normalised to empty vector treatment. Values show mean + SEM. * $p \leq 0.05$, ** $p \leq 0.01$ by one-way ANOVA followed by Tukey's multiple comparisons test. N=3. **C)** DJ-1 was amplified by rtPCR from cDNA from homozygous c.192G>C *DJ-1* mutation carrier after transient electroporation with empty vector control (lane 2), wt U1 snRNA (lane 3) or c.192G>C U1 snRNA (lane 4). Lane 1 shows marker and lane 5 NTC. Rescue of splicing of DJ-1 exon 3 indicated by longer band can only be seen after electroporation with c.192G>C U1 snRNA.

3.6.3.1 The c.192G>C DJ-1 mutation leads to a change in predicted SR protein binding

The strength of a splice site also depends on splicing enhancers and silencers. To assess if the c.192G>C *DJ-1* mutation leads to a change of these *cis*-acting elements we used an *in silico* approach to predict ESE with the ESEfinder (2001-2006, Cold Spring Harbor Laboratory) (Cartegni et al., 2003, Smith et al., 2006).

Another program that looks for splicing enhancers is the RESCUE-ESE Web Serve (http://genes.mit.edu/burgelab/rescue-ese/) which however resulted in nothing in the area of the splice site.

ESEfinder prediction showed an increase of the SRSF1 and a loss of SRSF2 binding with the mutation (Figure 51).
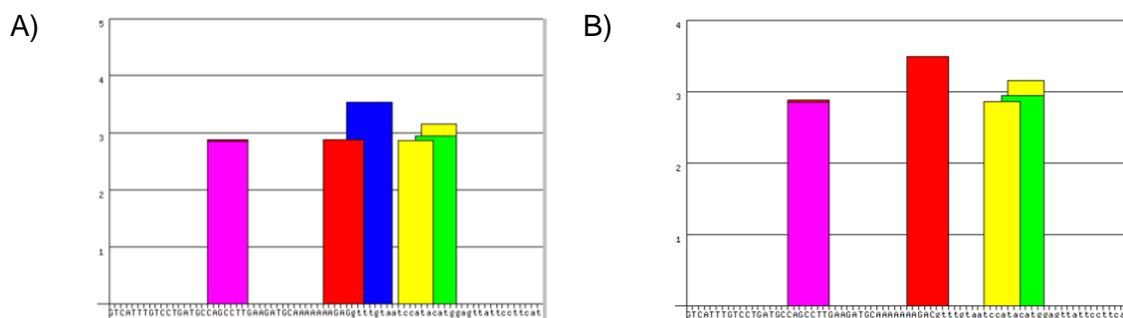
Figure 51: **ESE sequence prediction for binding of SR proteins.**

ESE sequence prediction was performed using the wt or the c.192G>C mutant sequence of DJ-1 and the software ESEfinder (2001-2006, Cold Spring Harbor Laboratory) (Cartegni et al., 2003, Smith et al., 2006). Binding to SRSF1 (SF2/ASF) is shown in red, to SRSF1 (IgM-BRCA1) in pink, to SRSF2 in blue, to SRSF5 in green and to SRSF6 in yellow. **A)** Shows predicted binding of SR proteins to the wt seqeunce and **B)** predicted binding of SR proteins to the c.192G>C mutant sequence.

3.6.4 Pharmacological rescue of skipping of c.192G>C mutant *DJ-1* exon 3

After having identified the effect of the c.192G>C *DJ-1* mutation and being able to genetically correct skipping of *DJ-1* exon 3 by introducing c.192G>C U1 snRNP, the main aim is to find a pharmacological substance that is able to correct splicing of c.192G>C mutant *DJ-1* pre-mRNA. Two individuals of the c.192G>C DJ-1 family are carrying the c.192G>C *DJ-1* mutation. The index patient suffers from PD and his sister did not display motor symptoms at the last examination. Hence a major aim is to find a substance that could be given to homozygous c.192G>C *DJ-1* mutation carriers as a treatment.

A similar effect of exon skipping is described for FD where a homozygous mutation in intron 20 leads to skipping of exon 20. The mutation in intron 20 lies in the splice donor site analogically to the c.192G>C *DJ-1* mutation. Studies about this IVS20+6T>C mutation

in the *IKBKAP* gene in FD showed that a compound called kinetin improved splicing and wt *IKBKAP* gene expression in patients with this mutation (Axelrod et al., 2011). The chemical name of kinetin is 6-furfurylaminopurin, it is a plant cytokinin.

To test whether kinetin was able to improve splicing of the c.192G>C *DJ-1* mutation, a compound treatment in immortalised fibroblasts and smNPCs of the index patient carrying the c.192G>C *DJ-1* mutation was performed. Cells were treated with 100 µM kinetin for 24 h. As it has been shown that for splicing correction of the IKAPKB that after 1 h correct splicing was seen, it was maximal after 8 h and maintained for at least 72 h without kinetin replenishment. To be in that range and at the maximum we choose 24 h for our experiments. In the same study they showed the highest splicing correction at 200 µM kinetin (Slaugenhaupt et al., 2004). As results from the MTT reduction assay as an indicator for toxicity showed a decrease in the MTT reduction ability at 200 µM we decided to test our cells using 100 µM kinetin.

Subsequently, cells were harvested and RNA was isolated. Afterwards, cDNA was transcribed and qPCR perfomed with a primer pair that detects *DJ-1* cDNA with and without exon 3 and a primer pair which only detects *DJ-1* cDNA in the presence of exon 3.

To determine the metabolic activity of cells after treatment with compounds a MTT reduction assay was performed using different concentrations of kinetin as an indirect evidence for potential toxicity. As an example the results of a reduction assay was performed with immortalised fibroblasts (Figure 52). Using this data we choose a treatment with kinetin of 100 µM for 24 h for the immortalised fibroblasts.

Treatment with kinetin did not lead to changes in RNA expression of *DJ-1* mRNA with and without exon 3. RNA expression was reduced in c.192G>C mutation carrier in comparison to the healthy control (Figure 53A). Also RNA expression of correctly spliced *DJ-1* RNA did not increase upon kinetin treatment both in the healthy control and in the index patient. Again, RNA expression was strongly reduced in cells from the c.192G>C *DJ-1* mutation carrier (Figure 53B).

A)

Kinetin - 24h

B)

Kinetin - 48h
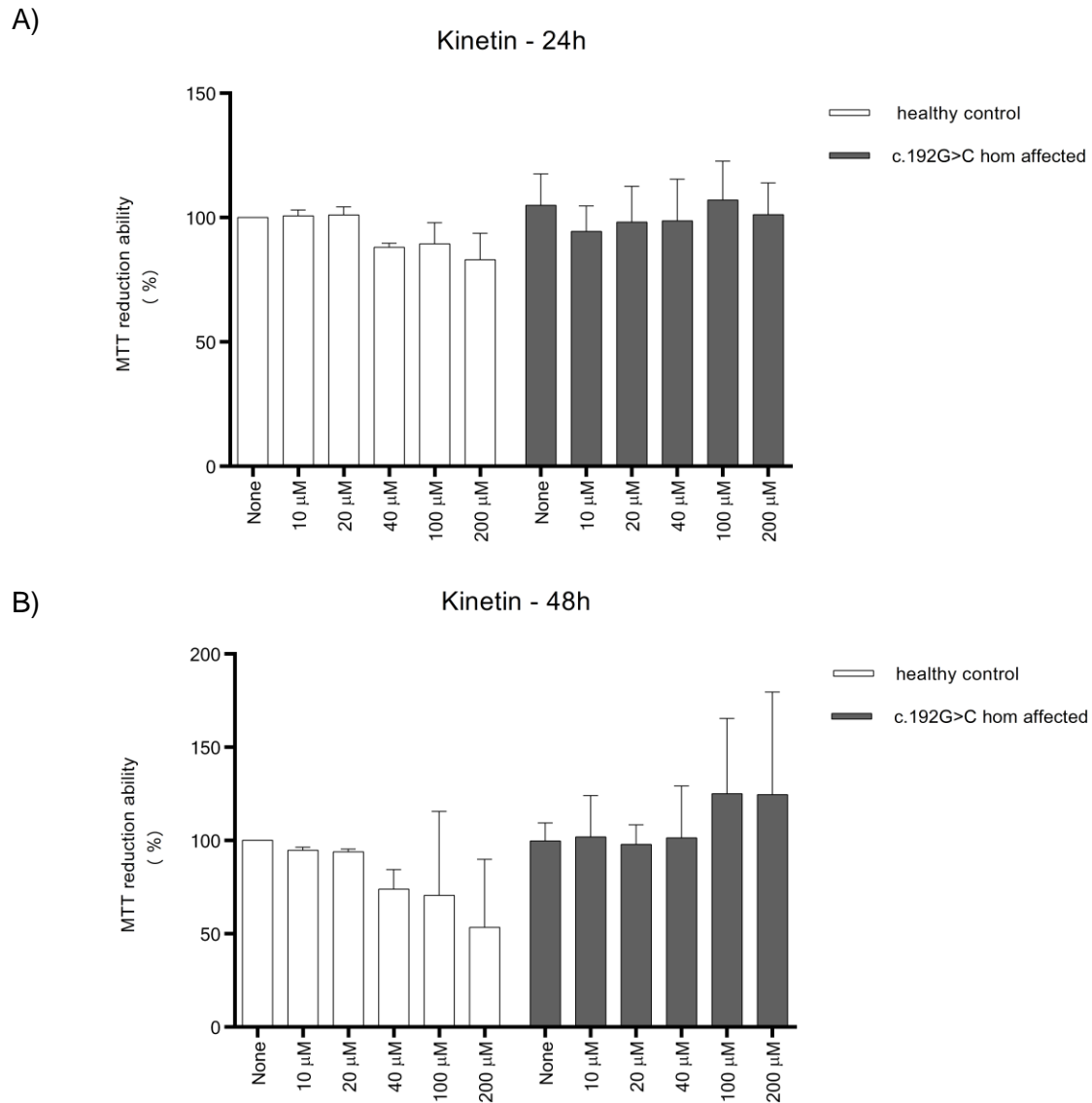
Figure 52: **MTT reduction ability after treatment with different concentrations of kinetin.**

MTT reduction ability was measured using absorbance after treatment with indicated concentrations of kinetin. Test was performed for immortalised fibroblasts of healthy control and homozygous c.192G>C *DJ-1* mutation carrying index patient. Absorbance was measured after **A)** 24 h of treatment with kinetin and after **B)** 48 h of compound treatment.

A)

B)
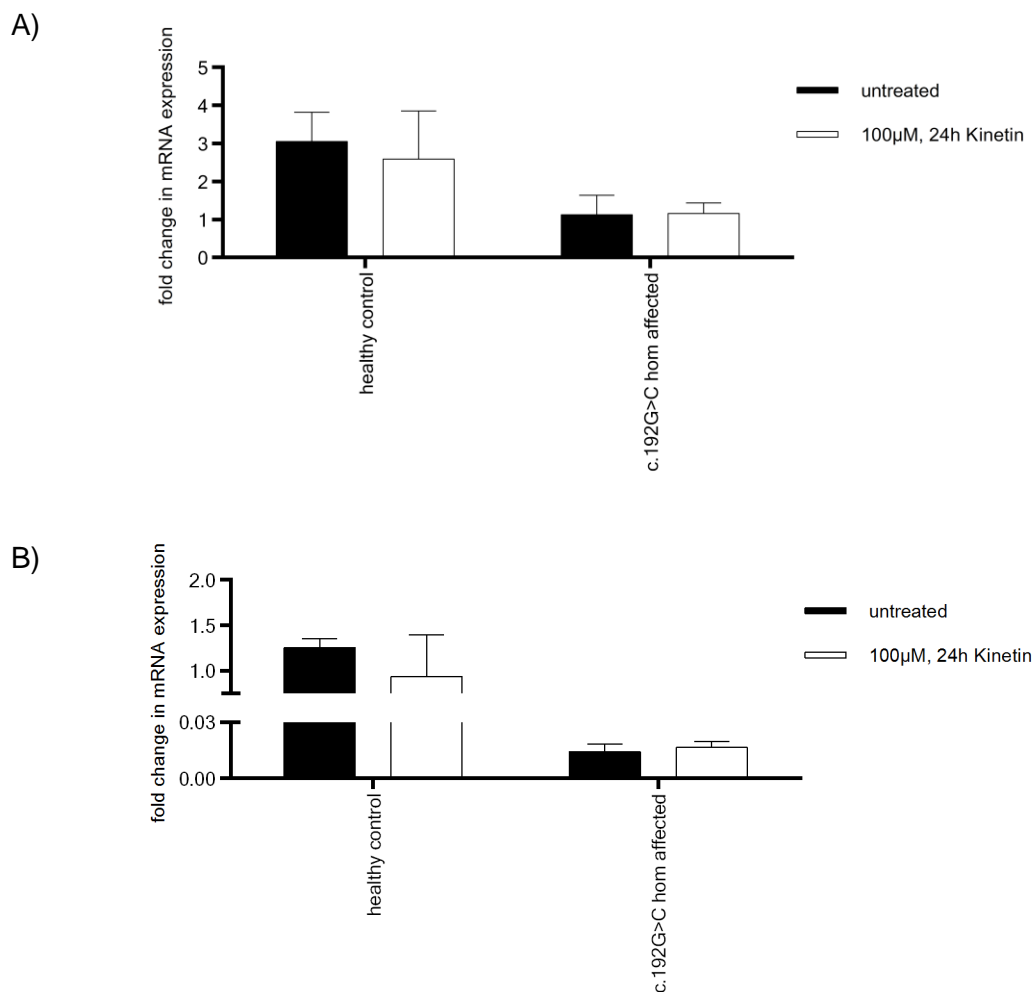
Figure 53: **Kinetin treatment in immortalised fibroblasts.**

Cells were kept under standard conditions. Medium was aspirated and fresh medium was added which was supplemented with 100 µM kinetin. After 24 h cells were collected and RNA was isolated and transcribed into cDNA. cDNA was amplified by qPCR using one primer pair that amplifies *DJ-1* cDNA with and without exon 3 (A) and one primer pair amplifying *DJ-1* cDNA only in the presence of exon 3 (B). **A)** No significant changes in the amount of gene expression after kinetin treatment were seen. Gene expression is lower in c.192G>C *DJ-1* mutation carrier when compared to healthy control. **B)** No significant changes in the amount of gene expression after kinetin treatment were seen. Gene expression is much lower in c.192G>C *DJ-1* mutation carrier when compared to healthy control. Values show mean + SEM. N=3.

Gene expression in smNPCs of *DJ-1* mRNA with and without exon 3 did not increase after 24 h of kinetin treatment. In healthy control 2, gene expression declined upon kinetin treatment (Figure 54A). When looking at gene expression of *DJ-1* mRNA which is correctly spliced and carries exon 3, gene expression was reduced in both indicated healthy controls and increased in smNPCs of the homozygous c.192G>C *DJ-1* mutation carrier. Both, increase and decrease were, however, not significant (Figure 54B).

A)

B)
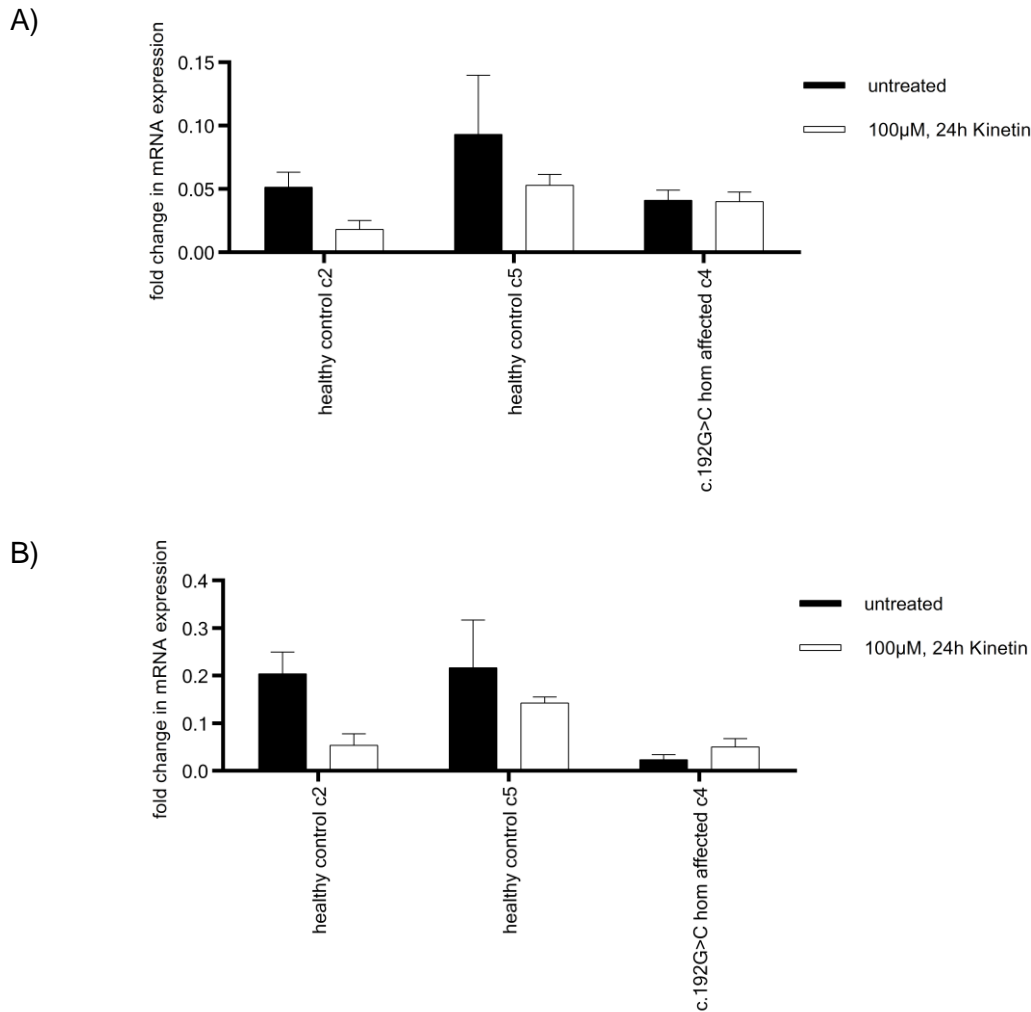
Figure 54: **Kinetin treatment in smNPCs.**

Cells were kept under standard conditions. Medium was aspirated and fresh medium was added which was supplemented with 100 µM kinetin. After 24 h cells were collected and RNA was isolated and transcribed into cDNA. cDNA was amplified by qPCR using one primer pair that amplifies *DJ-1* cDNA with and without exon 3 (A) and one primer pair amplifying *DJ-1* cDNA only in the presence of exon 3 (B). **A)** No significant changes in the amount of gene expression after kinetin treatment were seen. Gene expression of *DJ-1* is reduced in healthy control 2 upon kinetin treatment. **B)** No significant changes in the amount of gene expression after kinetin treatment were seen. Gene expression is reduced in c.192G>C *DJ-1* mutation carrier when compared to indicated healthy controls. A reduction of gene expression is seen after kinetin treatment in healthy control 2. Values show mean + SEM. N=3.

In contrast to IVS20+6T>C *IKBKAP* mutation carriers, kinetin treatment in cells from c.192G>C *DJ-1* mutation carriers did not increase correct splicing without skipping of an exon and therefore, other compounds that were in any way involved with splicing were tested. Compounds together with references are listed in Table 37.

Table 37: **List of compounds used for exon skipping rescue.** Table includes compound, gene tested, diesease and reference where it was applied.

Compound	Gene tested	Disease	Reference
2iP	*IKBKAP*	FD	(Slaugenhaupt et al., 2004)
Aclarubicin	*SMN2* *NF1*	Spinal muscular atropy Neurofibromatosis type 1	(Andreassi et al., 2001) (Pros et al., 2010)
Benzyladenine	*IKBKAP*	FD	(Slaugenhaupt et al., 2004)
Cucurmin	*SMN2*	Spinal muscular atropy	(Sakla and Lorson, 2008)
Dexamethasone	*ATM*	Ataxia telangiectasia	(Menotta et al., 2012)
Kinetin	*IKBKAP* *NF1*	FD Neurofibromatosis type 1	(Slaugenhaupt et al., 2004) (Pros et al., 2010)
Resveratrol	*GAA*	Glycogen storage disease type II	(Dardis et al., 2014)
Sodium butyrate	*SMN2* *NF1*	Spinal muscular atropy Neurofibromatosis type 1	(Chang et al., 2001) (Pros et al., 2010)
Valproic acid	*SMN2* *NF1*	Spinal muscular atropy Neurofibromatosis type 1	(Sumner et al., 2003) (Pros et al., 2010)
Zeatin	*IKBKAP*	FD	(Slaugenhaupt et al., 2004)

Compounds tested at two different concentrations (10 µM and 25 µM) (Figure 55). qPCR results of gene expression of DJ-1 including and excluding exon 3 are shown (Figure 55A). Gene expression increased upon treatment with the solvent of the compounds, DMSO. Treatment with both concentrations of aclarubicin increased gene expression further. *DJ-1* gene expression in immortalised fibroblasts of the healthy control was in the same range as indicated. When looking at gene expression of correctly spliced DJ-1 pre-mRNA, meaning mRNA including exon 3, DMSO treatment did not increase mRNA expression. Gene expression of indicated baseline and treated cells of homozygous c.192G>C DJ-1 mutation carrier was reduced when compared to gene expression in healthy control. 25 µM benzyladenine treatment more than doubled the expression of the gene including *DJ-1* exon 3. All other indicated compounds did not alter gene expression (Figure 55B).

A)

B)
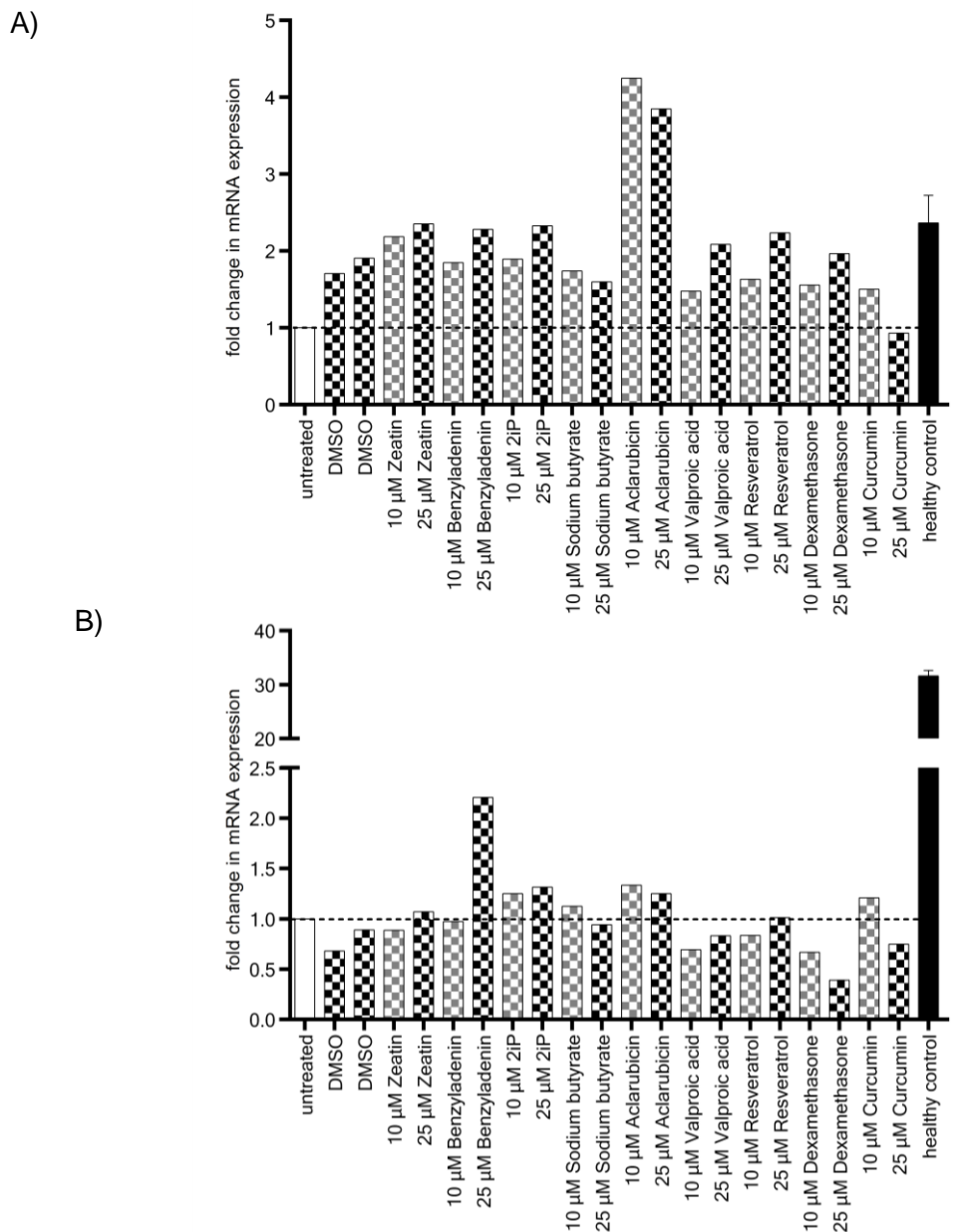
Figure 55: **Compound treatment in immortalised fibroblasts.**

Cells were kept under standard conditions. Medium was aspirated and fresh medium was added which was supplemented with 10 µM of the indicated compound or 25 µM of the indicated compound. DMSO treatment was used to control for the effect of the solvent. After 24 h cells were collected and RNA was isolated and transcribed into cDNA. cDNA was amplified by qPCR using one primer pair that amplifies *DJ-1* cDNA with and without exon 3 (A) and one primer pair amplifying *DJ-1* cDNA only in the presence of exon 3 (B). **A)** *DJ-1* gene expression increases slightly upon DMSO treatment. Treatment with aclarubicin leads to 4-fold increase in gene expression of *DJ-1* gene with and without exon 3. Gene expression level is in the range of gene expression of cells treated with indicated compounds. **B)** *DJ-1* gene expression of mRNA including exon 3 does not vary after DMSO treatment. mRNA level is much lower in cells from homozygous c.192G>C *DJ-1* mutation carrier with and without indicated treatments when compared to healthy control. mRNA more than doubles though upon treatment with 25 µM benzyladenine.

4   Discussion and Perspectives

PD is a chronic, degenerative neurological disorder of the *substantia nigra pars compacta* in the CNS. The definite cause of PD is unknown, although it is assumed that a combination of genetic and environmental factors cause PD. The single only yet established risk factor for the disease is advancing age and as people get older thanks to medical advances, the overall worldwide prevalence of PD is increasing (Reeve et al., 2014). Currently, there is no cure for PD and the underlying pathological mechanism by which neurons die is not known. Familial PD cases open up the opportunity to identify genes involved in neurodegeneration. Studying these genes allows to shed light on pathways leading to dysfunction and subsequent cell death of nigrostriatal neurons which thereby enables to identify or develop novel neuroprotective therapeutic approaches. Here, iPSCs allow for the first time to study the in the living patients affected cell type *in vitro*. Furthermore, iPSCs have the potential to support the development of patient-based disease-modifying treatments for PD as they can serve as progressive, predictive models of PD for drug screens. Moreover iPSCs can help to study the underlying biological mechanisms associated with PD directly in the affected cell type. We made use of patient derived cells of family members of the c.192G>C DJ-1 family to further investigate the role of the *DJ-1* gene (*PARK7*) for PD. Homozygous loss-of-function mutations in *DJ-1* are a rare cause of familial early-onset PD. Also DJ-1 provides a mechanistic link between PD and mitochondrial dysfunction as mechanisms involved in neurodegeneration include oxidative stress, dysfunctional mitochondria and impaired autophagy and they all depend on proper DJ-1 function or have been shown to be altered by dysfunction or absence of DJ-1 protein (Abbott et al., 2003, Blackinton et al., 2009, Krebiehl et al., 2010, Meulener et al., 2006).

4.1   Generation of iPSCs from c.192G>C *DJ-1* mutation carrying fibroblasts and successful differentiation to neurons

The work of Yamanka and colleagues (Takahashi and Yamanaka, 2006) on the generation of iPSCs that was awarded with the Nobel Prize in 2012, allowed a new type of biomedical research of human diseases with patient derived cells. It allows to generate an unlimited source of patient- and at the same time disease-specific pluripotent cells to study a human disease, but is also a promising new tool for replacement therapy. Since their publication on how human somatic cells can be reprogrammed into iPSCs using retroviruses (Takahashi et al., 2007), this method has been applied successfully by many different labs to model diseases in the disease relevant cell types. Some of the first ones are named here (Dimos et al., 2008, Ebert et al., 2009, Park et al., 2008, Soldner et al., 2009). To study neurological disorders protocols have been established and applied to differentiate

the respective types of neurons as effectively as possible. Amongst these first studies are also some of the above-mentioned ones. The studies were on amyotrophic lateral sclerosis (Dimos et al., 2008) spinal muscular atropy (Ebert et al., 2009) and FD (Lee et al., 2009) with the latter ones showing first neuronal phenotypes. The first study on PD was from (Soldner et al., 2009) where mDA neurons were generated from iPSCs of sporadic PD patients. No phenotypes, however, were found in this study. The first genetic forms of PD were studied in iPSCs generated from fibroblasts of *PINK1, LRRK2* and *SNCA* mutation carriers which were subsequently differentiated to mDA neurons (Seibler et al., 2011, Devine et al., 2011, Nguyen et al., 2011). In these studies, the phenotypes were compared to normal subjects.

In the present study, we measured mitochondrial ROS levels in mDA neurons of the c.192G>C *DJ-1* mutation carriers. Unlike our findings in MEF cells of DJ-1 knockout mice, where we saw a significant increase in mitochondrial ROS formation (Krebiehl et al., 2010), mitochondrial ROS formation was not altered in iPSC derived mDA neurons. This might be due to subtle effects that we do not see an increase. One crucial limitation for research of especially late onset human diseases is to detect subtle phenotypes. This issue, however, can be solved using iPSCs as well. Studies can be performed under genetically defined conditions using isogenic pairs. Different approaches have already been published making use of different strategies to perform gene corrections and generate isogenic pairs of iPSCs for PD research. These include ZFNs for *SNCA* and *LRRK2* (Reinhardt et al., 2013b, Soldner et al., 2011) or TALEN established by (Boch et al., 2009, Moscou and Bogdanove, 2009) and used in iPSCs by (Hockemeyer et al., 2011). The most recent approch is to use the CRISPR/CAS9 system to correct disease-causing mutations (Ding et al., 2013, Mali et al., 2013).

In the present study, we were successful in generating iPSCs from the index patient, the premotor diseased sister of the index patient, who is also a carrier of the c.192G>C *DJ-1* mutation and a brother of the two who is a heterozygous carrier of the same mutation. Generated lines are shown in Table 36. Reprogramming was performed using the four 'Yamanaka factors' with a retroviral delivery system. Using this system leads to an integration of the reprogramming factors which can be a disadvantgage for projects that are aimed at cellular replacement therapy. In the meantime systems have been established effectively to overcome the integration by excising integrated reprogramming factors with loxP sites that serve as substrates for Cre-mediated excision or by using non-integrating reprogramming strategies such as episomal vectors, Sendai virus, adenovirus or miRNA for example [reviewed in (Rao and Malik, 2012)]. For the present study, however, a system without integration is not mandatory. All genertated iPSC clones from skin fibroblasts of

the three c.192G>C *DJ-1* mutation carriers were characterised to assess their pluripotent status and to make sure that the harsh reprogramming procedure using retroviral vectors did not lead to chromosomal aberrations or mutations.

Silencing of all four reprogramming factors indicating that the generated iPSCs are efficiently reprogrammed and do not depend on the continuous expression of the transgenes for self-renewal was analysed (Figure 15). The change from dermal fibroblasts to iPSCs having upregulated 'stemness' genes was tested by RNA expression of undifferentiated ESC markers (Figure 16) as well as the actual expression of the stem cell markers *nanog*, *oct-4*, *SSEA4* and *Tra-1-81* on protein level (Figure 17). To make sure that chromosomal integrity was retained and not altered by the retroviral vectors G-banding was performed. iPSCs showed a normal karyotype of 46XY or 46XX (Figure 18). Smaller mutations that are under the detection level of G-banding could be excluded by genotyping with the Illumina HumanCytoSNP-12 (example, Figure 19). Interestingly, for all generated lines of individuals of the same family a loss of heterozygousity was detected in the CHIP analysis on several different chormosomes. These results could be tied back to the consanguinuity of the family.

To double-check the generated clones in terms of the c.192G>C *DJ-1* mutation to be investigated in the present study DNA sequencing of the respective region was performed. All clones show the respective homozygous or heterozygous genotype at position c.192 of the *DJ-1* gene (Figure 20).

Germ layer differentiation is done in collaboration with the Northwestern University (Chicago, IL, USA) at the Department of Neurology of Dimitri Kranic, MD, PhD.

iPSC are pluripotent and that allows to differentiate them into any cell type of interest. To study PD, the cell type of interest are neurons, in particular mDA neurons. To investigate the effect of the c.192G>C *DJ-1* mutation we applied two different protocols to differentiate neurons:

1) mDA neurons were differentiated using an adapted floor plate-based protocol from (Kriks et al., 2011, Chambers et al., 2009, Nguyen et al., 2011, Reinhardt et al., 2013b)
2) smNPCs were differentiated following the smNPC derivation protocol (Reinhardt et al., 2013a).

Both protocols have their advantages and disadvantages depending on the issue to be addressed one can be more useful or the other.

To address and analyse the functional effects of loss of DJ-1 protein in different patient-derived cells carrying the c.192G>C *DJ-1* mutation, we applied the floor plate-based protocol. The floor plate-based strategy to differentiate human mDA neurons from iPSCs is a robust and well established protocol to model neuronal phenotypes in PD, showed for example for the *LRRK2* G2019S mutation in (Reinhardt et al., 2013b). It gives rise to functionally active neurons with a high efficiency to engraft *in vivo* (Kriks et al., 2011). However, applying this protocol is time intensive as it starts with the differentiation to neurons followed by subsequent maturation, also involves intense hands-on time for frequent splitting events. Moreover, it is rather costly due to the big amount of recombinant growth factors that are needed. Finally, for this protocol it is very important to stick to a precise timing and keep the same concentrations of supplements in each differentiation to have efficient and comparable, reproducible differentiations and less variability between different rounds of differentiations.

Because of the previously mentioned downsides of the floor plate-based protocol, for continuing the compound screen in a patient-derived *ex vivo* neuronal model future studies will be performed applying a newer protocol by (Reinhardt et al., 2013a) which describes the generation of neural progenitor cells using only small molecules. smNPCs are immortal and therefore can be expanded easily and further differentiated into all of the neuronal subtypes. It is a faster and less expensive (e.g. fewer amounts of expensive growth factors needed) protocol and can be very useful for example for high throughput screens where large amounts of cells are needed. On the contrary, these cells are less established and the efficiency to derive mDA from these precursors needs still to be determined.

For this study, we applied the first strategy of the adapted floor plate-based protocol, to determine effects in mDA neurons, but also the second one using small molecules to ascertain effects of the c.192G>C *DJ-1* mutation in smNPCs.

To characterise the cell population after applying the adapted floor plate-based protocol differentiated cells were stained by ICC using a Beta-III-Tubulin antibody, which is a neuron-specific class III β-tubulin marker, a TH antibody, which is a dopaminergic neuron-specific marker and a FoxA2 antibody, which is a midbrain marker (Figure 21). The combination of these markers showed approximately 20 % mDA neurons after differentiation and at least 20 days of maturation.

4.2 The c.192G>C *DJ-1* mutation leads to mitochondrial phenotypes in patient derived cells

4.2.1 Reduced mitochondrial branching and length in fibroblasts of the homozygous c.192G>C *DJ-1* mutation carriers

In the first study showing data of fibroblasts of the index patient and a heterozygous c.192G>C *DJ-1* mutation carrier mitochondrial morphology was analysed and reduced form factor and aspect ratio were found in the mutation carriers (Krebiehl et al., 2010). In the present study, we did the same analysis, but looking at the sister of the index patient who is a homozygous c.192G>C *DJ-1* mutation carrier as well. The only symptom apparent in the sister is depression, but so far, she has not been suffering from motor symptoms. This analysis helps to obtain additional information about the prodromal stage of PD. Including primary fibroblasts from the sister may aid to define, whether mitochondrial morphology may serve as an early biomarker - even before symptoms occur, to identify individuals at risk.

We could confirm the previous results. We saw a reduced length of mitochondria indicated by a reduced aspect ratio as well as less branching of mitochondria, indicated by a reduction of the form factor in both homozygous *DJ-1* mutation carriers (Figure 9B and C). Seeing the same effect in a second homozygous c.192G>C *DJ-1* mutation carrier and taken together with our findings that we saw a loss of DJ-1 protein in both homozygous c.192G>C *DJ-1* mutation carriers we suggest that DJ-1 plays a role in fission and fusion events. Particularily, the significant morphological changes within the c.192G>C *DJ-1* family between the heterozygous and both homozygous c.192G>C *DJ-1* mutation carriers imply the requirement of a certain level of wt DJ-1 protein for proper mitochondrial morphology.

As an abnormal function of the mitochondria can result in an imbalance of mitochondrial fission and fusion processes we furthermore investigated mitochondrial function by measuring MMP which is an important parameter for mitochondrial function. These results could help to futher decipher the more precise effect of the c.192G>C *DJ-1* mutation and DJ-1 itself on disease specific mitochondrial phenotypes.

4.2.2 The c.192G>C *DJ-1* mutation leads to a reduced MMP in fibroblasts of the homozygous mutation carrier

To better understand the morphological findings of mitochondria in the patient derived cells we had a look at mitochondrial function as well. In the above-mentioned study by (Krebiehl

et al., 2010). MEF cells from DJ-1 knockout mice revealed a reduced MMP when compared to wt littermates. In the present study, we measured the MMP through reduced TMRE fluorescence intensity by live microscopy of the patient derived fibroblasts. In line with the findings in MEFs from knockout mice, we found a reduced MMP in both homozygous c.192G>C *DJ-1* mutation carriers when compared to a healthy control (Figure 10). Although, we did not achieve the fluorescence intensity of the healthy control, which can be explained by a reduced efficiency of the transfection, the reduction could be restored significantly when reintroducing wt DJ-1 protein in the patient's fibroblasts by transfection in comparison to untransfected patient derived fibroblasts even though the transfection efficiency is reduced in fibroblasts (30 %). This allows the assumption that indeed the lack of wt DJ-1 was causative for the decreased MMP (Figure 10B and C). Under normal conditions, DJ-1 protects cells against oxidative stress-related death by translocating to the mitochondria and maintaining mitochondrial complex I activity (Bonifati, 2003, Hayashi et al., 2009, Yokota et al., 2003, Zhang et al., 2005). We suggest that in our cells mitochondrial function is impaired due to the loss of the oxidative stress sensor DJ-1 and therefore the MMP is reduced. Over time, this could have an impact on the viability of the cells and lead to death of nigral dopaminergic neurons in PD, because these cells have a high load of ROS due to dopamine itself and its metabolism and therefore are more prone to suffer from oxidative stress in the situation of lacking a sensor for this type of stress (Dias et al., 2013, Lotharius and Brundin, 2002, Sayre et al., 2008). Moreover, dopaminergic neurons of the *substantia nigra* may be particularly susceptible as in mice they were shown to have a reduced mitochondrial mass (Liang et al., 2007).

To understand the exact influence of DJ-1 on these mechanisms and functions, however, needs further investigation. Our patient derived cells including the iPSCs that we generated together with the established protocols for different neuronal cultures constitute excellent knockout model systems to further dissect the role of DJ-1 function through reintroducing DJ-1 and even offer the opportunity to perform isogenic control experiments.

4.2.3 Consequences of oxidative stress in mDA neurons derived from affected c.192G>C *DJ-1* mutation carriers

We used the adapted floor plate-based protocol to differentiate iPSCs and further analyse the effect of the c.192G>C *DJ-1* mutation on mtDNA damage and copy number as well as mitochondrial ROS levels.

We also aimed to address mtDNA changes in neurons of c.192G>C *DJ-1* mutation carriers. Mitochondria bare high concentrations of ROS because of the oxidative phosphorylation. Therefore, mtDNA is exposed to high levels of ROS which can lead to alterations of

mtDNA (Wei, 1998). The fact that mtDNA is less condensed than nuclear DNA makes mtDNA more vulnerable (Valko et al., 2004, Yakes and Van Houten, 1997). mtDNA damage can be causative for mitochondrial dysfunction as reviewed for PD by (Schapira, 2008). Also the copy number of mtDNA was shown to compensate for increases in energy demand or reduced mitochondrial function, therefore we also had a look at the copy number (Sahin and Depinho, 2010).

It has previously been described that after the progress of reprogramming of hiPSCs the mitochondria display hESC-like features (Prigione and Cortopassi, 2007). During the reprogramming process the metabolism of the cells changes from somatic oxidative phosphorylation to glycolysis. This happens at one time with the upregulation of glycolytic genes and downregulation of mitochondrial respiratory chain complexes, consequently leading to a reduced mtDNA copy number (Facucho-Oliveira et al., 2007, Folmes et al., 2011, Prigione et al., 2010, Suhr et al., 2010, Varum et al., 2011). After differentiation to mDA neurons, we expected higher mtDNA copy numbers, due to the above-mentioned effect that neurons should change to more mitochondrial respiration again, thus leading to higher mtDNA copy numbers. Previous findings also show that high levels of mtDNA deletions are found in cells with high energy demands like the brain (Corral-Debrinski et al., 1992, Cortopassi and Arnheim, 1992, Cortopassi and Wong, 1999).

To analyse differences between mutation carriers and controls, we performed experiments with iPSC, which were differentiated to mDA neurons following the floor plate-based protocol. To increase mitochondrial stress to challenge mild phenotypes, we measured the mtDNA under basal conditions, after rotenone treatment, after H_2O_2 treatment and after treatment with both stressors. The LORD-Q method we applied, uses a rapid high-fidelity DNA polymerase and a second-generation fluorescent DNA dye, therefore it is a sensitive method to detect DNA-damage and to quantify DNA lesions in mitochondrial and nuclear probes of up to 4-kb length.

We saw a significantly reduced mtDNA copy number in the index patient when compared to one of the indicated healthy controls even under baseline conditions (Figure 22). Furthermore, when looking at the effect of different mitochondrial stressors in the analysed individuals we saw a significant increase of mtDNA copy number in all individuals except for the index patient after treatment with the stressors (Figure 23). Interestingly, the index patient showed the biggest increase in detected mtDNA lesions after applying both stressors (rotenone and H_2O_2) (Figure 24). This is in line with findings in human post mortem brains of idiopathic PD patients (and aged individuals) where an increased number of mtDNA deletions has been observed in dopaminergic neurons of the *substatia nigra pars compacta* (Bender et al., 2006). Taken together, these results suggest that, as described

before in mutant mice carrying mtDNA deletions, human neurons compensate for the high levels of mtDNA deletions by increasing their mtDNA copy number (Perier et al., 2013). The same has been shown for *PINK1* mutant cells, where unlike in the DJ-1-cells of the index patient, the neurons react to the mitochondrial dysfunction by compensating through increasing the mtDNA copy number (Seibler et al., 2011). Healthy individuals as well as the homozygous c.192G>C *DJ-1* mutation carrier without motor symptoms apply the previously discussed compensation mechanism whereas the neurons of the index patient do not show a significant increase of mtDNA copies.

As mentioned before, one reason for mtDNA damage are mitochondrial ROS this fact and previous findings by our group that in MEF cells of DJ-1 knockout mice mitochondrial ROS formation is significantly increased (Krebiehl et al., 2010) led us to the idea that mitochondrial ROS could be increased in patient-derived neurons. To test if this holds true in human iPSCs after floor plate-based neuronal differentiation from c.192G>C *DJ-1* mutation carriers, we stained the differentiated cells with MitoSOX™ Red-solution and subsequently measured them by flow cytometry. We kept the cells under basal conditions with normal high glucose medium when we measured mitochondrial ROS for the first time, as changes in mitochondrial ROS have been seen under basal conditions in mice before. As the results in mice could not be confirmed, we decided to challenge the neurons and grow them under low glucose conditions. The low glucose condition should force cells to produce ATP more through mitochondrial respiration and as mitochondrial respiration (mainly complex I and III) is the major source of mitochondrial ROS (Sugioka et al., 1988, Turrens and Boveris, 1980), we expected to be able to have better conditions to detect subtle changes in mitochondrial ROS levels in the cells carrying the c.192G>C *DJ-1* mutation. It has to be mentioned, however, that in general the main metabolism of neurons to produce ATP, due to the high energy demand of the brain, is respiration, because mitochondrial respiration produces much more ATP than glycolysis (Sokoloff et al., 1977). Higher glucose levels make the glycolysis more possible than lower glucose levels. Generally speaking, the more respiration, the more mitochondrial ROS are produced and this makes cells more prone to cell death in conditions of lack of compensatory mechanisms.

We did not see significant changes in mitochondrial ROS levels when comparing homozygous c.192G>C *DJ-1* mutation carrying cells to healthy individuals either under high or low glucose conditions. Under low glucose conditions the heterozygous c.192G>C *DJ-1* mutation carrying cells showed an increase in mitochondrial ROS in comparison to one of the healthy controls (Figure 25). The measurement could be repeated applying even harsher treatment to further challenge the cells. Another aspect could be that even though neurons were maturated until day 100, the age of the neurons was not advanced enough,

there one could apply artificial ageing e.g. using progerin to see age-related phenotypes as described by (Miller et al., 2013). Measurements were performed with around 100 days old differentiations and therefore neuronal cultures were already sticky and clumpy and we observed differences between independent differentiations. Therefore, flow cytometry should be repeated with more uniform cultures. For this reason, mitochondrial ROS measurement using the same technique in smNPCs is currently underway. Our current findings, however, did not show any alterations in mitochondrial ROS levels in homozygous c.192G>C *DJ-1* mutation carriers when compared to controls. This is unexpected due to the fact that DJ-1 is a sensor for oxidative stress and plays a crucial role in this regard (Canet-Aviles et al., 2004). To exclude inter-individuel variation experiments can be performed making use isogenic lines, which are currently being produced.

4.2.4 Increased outgrowth in mDA neurons derived from premotor diseased female c.192G>C *DJ-1* mutation carrier

We saw a significant increase of outgrowth velocity in the neurons derived from the premotor diseased homozygous c.192G>C *DJ-1* mutation carrier when compared to the indicated healthy control. Neurons from the index patient, however, showed no changes in the outgrowth properties (Figure 26).

The *LRRK2* G2019S mutation is associated with neurite shortening (MacLeod et al., 2006, Reinhardt et al., 2013b, Sanchez-Danes et al., 2012) and also in DJ-1-deficient mice a declined dendritic complexity has been observed (Sheng et al., 2013). Therefore, we analysed neurite outgrowth in neurons from c.192G>C *DJ-1* mutation carriers differentiated with the adapted floor plate-based protocol. However, our results were opposed to the observed phenotypes of declined dendritic complexity in DJ-1-deficient mice.

To be able to see the real DJ-1-dependent effect, the experiment has to be repeated with isogenic pairs, thereby excluding possible inter-individual differences and looking at the c.192G>C *DJ-1* mutation as a sole modifying genetic factor.

4.3 Analysis of mitochondrial transport in primary hippocampal neuronal cultures of DJ-1 -/- mice

The *DJ-1 -/-* null mutant mice (Pham et al., 2010) which were used for the generation of hippocampal primary neuron cultures in this work show a decrease in dopamine-producing neurons in the ventral tegmental area (~6% reduction), but no reduction of dopaminergic neurons in the *substantia nigra*. DJ-1 -/- mice do not show an age-related neuropathology like it is seen in humans, suggesting a compensatory or protective mechanism in these animals (Andres-Mateos et al., 2007, Chandran et al., 2008, Goldberg et al., 2005, Kim et

al., 2005b, Pham et al., 2010). Interestingly enough, they seem to compensate for the loss of DJ-1 by upregulating mitochondrial respiratory enzyme activities in order to protect the cells against oxidative stress (Pham et al., 2010). Under basal conditions, DJ-1 is required for cytoprotection, it localises to mitochondria under oxidative stress conditions thereby maintaining complex I activity (Hayashi et al., 2009, Blackinton et al., 2009, Canet-Aviles et al., 2004, Junn et al., 2009, Kim et al., 2005b, Lev et al., 2008, Mullett and Hinkle, 2011).

We were interested in seeing whether there is an effect of loss of DJ-1 on mitochondrial transport, which we analysed in DJ-1 -/- mice (Pham et al., 2010) in comparison to wt controls, to further shed light on the relation between mitochondrial dynamics and synaptic function and transport and also to mitophagy.

We found that in DJ-1 -/- mice, more mitochondria displaced compared to mitochondria in neurons of the wt mice. Interestingly, when analysing the number of mitochondria that displaced over distances over 1 µm (to exclude stationary flickering of mitochondria in the calcultation of the displacement), the mitochondria of the wt mice displaced further distaces.

Loss of DJ-1 did not lead to changes of mitochondrial transport velocity in the DJ-1 -/- mice.

Defective mitochondrial transport has been shown for PD, including rodent models (Kim-Han et al., 2011, Sterky et al., 2011). Another PD gene, *PINK1*, is associated with correct axonal tansport of mitochondria. As in rat primary hippocampal neuronal cultures the lateral movement of mitochondria was inhibited by *PINK1* overexpression (Yu et al., 2011).

We suggest for our results that upon loss of DJ-1 function, the individual mitochondrial transport could be less efficient in terms of distances that mitochondria are transported along an axon. Neurons could try to compensate this by displacing more mitochondria.

Another option is that the mitochondria of the DJ-1 -/- mice are dysfunctional and therefore undergo local mitophagy instead of being transported to the soma by retrograde transport. This has been shown for ROS-induced depolarisation of neuronal mitochondria, with the suggestion that this effect prevents from further spreading oxidative damage (Ashrafi et al., 2014, Wang et al., 2012b).

However, one limitation of our analysis is that the direction of mitochondrial movement is not analysed. By distinguishing anterograde and retrograde transport one can obtain functional information on mitochodnria.

4.4 Splicing defect leads to loss of DJ-1 protein in patient derived cells

4.4.1 No DJ-1 protein in different cell types derived from c.192G>C *DJ-1* mutation carrying patients

The major result of this study was the elucidation of the underlying mechanism of the single base exchange of G to C at chromosomal position 192 in the *DJ-1* gene (*PARK7*). The effect of this PD associated mutation has not been known until today. Other PD causing mutations in *DJ-1* lead to protein instability, loss of protein, frameshift, splicing defect, altered activity or an altered transcript (Table 2). The c.192G>C *DJ-1* mutation has as yet been described to cause a p.E64D amino acid exchange in the DJ-1 protein and that this might cause an impairment of binding of DJ-1 to other proteins (Hering et al., 2004). The analysis of two mutant fibroblasts of carriers of this mutation allowed us to show a loss of DJ-1 protein in different cell types generated from the patient derived fibroblasts. The first observation of loss of DJ-1 protein was made in fibroblasts of both homozygous c.192G>C *DJ-1* mutation carriers, interestingly, cells from the heterozygous brother showed a reduction of the DJ-1 protein level when compared to a not related control (Figure 29). As expected, immortalisation of these patient derived fibroblasts did not change the absence of DJ-1 protein in the homozygous c.192G>C *DJ-1* mutation carriers and the reduced level of protein in the cells of the heterozygous carrier of this mutation (Figure 30). Tissue-specific differences of protein expression of mutant c.192G>C *DJ-1* were excluded by detecting the protein level in iPSCs generated from the patient derived fibroblasts (Figure 31). Again, a reduction of DJ-1 protein is seen in iPSCs of the heterozygous c.192G>C *DJ-1* mutation carrier when compared to two different control lines. DJ-1 protein levels were also analysed in the in PD affected cell type. Like before, in neuronal precursor cells as well as neurons differentiated with the adapted floor plate-based protocol no DJ-1 protein could be detected in both homozygous c.192G>C *DJ-1* mutation carriers (Figure 32 and Figure 33).

To find out the minimal amount of DJ-1 protein needed for healthy functioning, we analysed DJ-1 protein level of fibroblast controls of our biobank. We addressed the question whether levels of heterozygous mutation carriers are the same as the ones in controls to see how much protein is sufficient to not be affected. At the same time, we got a better understanding of average DJ-1 levels in different individuals by analysing inter- and intra-individual variations of DJ-1 protein expression of fibroblasts from healthy controls stored in our biobank. When compared to control subjects, both heterozygous c.192G>C *DJ-1* mutation carriers showed DJ-1 protein levels in the range of levels seen in healthy controls

(Figure 27). This led us to the hypothesis that interventions leading to incomplete restoration of DJ-1 levels (compared to high expressing controls) could be sufficient in the homozygous c.192G>C *DJ-1* mutation carriers to have a detectable phenotypic improvement. Except for one control, no intra-individual variation was observed militating for different protein levels in different individuals, but rather constant levels of single individuals when looking at a time frame of eight hours (Figure 28).

4.4.2   The c.192G>C *DJ-1* mutation causes skipping of exon 3

Next, we sought to determine the reason for the absence of protein in homozygous c.192G>C *DJ-1* mutation carriers. An *in silico* analysis using the MutationTaster software predicted splice site changes caused by the c.192G>C *DJ-1* mutation (Figure 34). Following on, in the course of literature mining we found a publication where another *in silico* tool was used to predict mutations causing missplicing. Two PD mutations, including the c.192G>C *DJ-1* mutation, were predicted to cause exon skipping by the software. Furthermore, through literature mining we found a publication looking at frequencies of potential bases in human genomes at the exon-intron boarder (Carmel et al., 2004). This study reports that guanine, which is the base present at the end of exon 3 in wt *DJ-1*, is the most common base at the end of an exon with a frequency of over 70 %. Whereas cytosine, which is the base in case of the c.192G>C *DJ-1* mutation, is the least frequent one of all four bases at the end of an exon (Figure 45).

Therefore, we decided to repeat the minigene assay, using patient DNA for the generation of the minigene constructs. Furthermore, we generated isogenic pairs for the minigene assay to be sure that it is the c.192G>C *DJ-1* mutation that causes the exon skipping and not any other unknown variant in the patients DNA. Therefore, the c.192G>C *DJ-1* mutation in the exon 3 from the patient was corrected by IVM and the c.192G>C *DJ-1* mutation was introduced in the *DJ-1* exon 3 of a healthy control by the same method. We could show that in both cases where exon 3 carried the c.192G>C *DJ-1* mutation the complete mutation carrying exon was skipped in the minigene (Figure 37). Based on this we could confirm the previous results from (Sahashi et al., 2007).

Indeed, a literature mining revealed an *in silico* study suggesting a missplicing due to the c.192G>C *DJ-1* mutation (Sahashi et al., 2007). However, the analysis in this study was performed with a mutated exon of a healthy individual and not with patient derived material.

To double check that the index patient does not carry another variant that could affect splicing in any way, we applied NGS of the entire sequence of the *PARK7* locus. No putative functional/disease relevant variants were found.

Sequencing *DJ-1* of the cDNA from the index patient approved in *in vivo* material, the results of the artificial minigene assay, which was performed in HEK cells, that the c.192G>C *DJ-1* mutation causes skipping of complete exon 3. The respective sequencing segment showing the transition of exon 2 to exon 4 is shown (Figure 36). Subsequently, we examined whether the skipping of exon 3 leads to a frameshift or even a premature stop codon, which is not the case. Exon 2 ends with a triplet, similarly to exon 3, which also ends with a triplet (Figure 38) therefore, the c.192G>C *DJ-1* mutation does not lead to a frameshift nor to a premature stop codon.

The agarose gel, where *DJ-1* was amplified from cDNA from fibroblasts of both indicated homozygous and the heterozygous c.192G>C *DJ-1* mutation carrier shows the skipping of exon 3 in the presence of the c.192G>C *DJ-1* mutation (Figure 35).

By qPCR, using primers binding in exon 2 and exon 3, we could show that the c.192G>C *DJ-1* mutation leads to skipping of exon 3 in all analysed patient derived cell types: immortalised fibroblasts (Figure 40), iPSCs (Figure 41), mDA neurons (Figure 42) and smNPCs (Figure 43).

When measuring gene expression by qPCR small amounts of full length *DJ-1* mRNA were detected in homozygous c.192G>C *DJ-1* mutation carriers. A possible explanation for this finding is that the U1 snRNP in very rare cases binds to the c.192G>C mutation carrying exon 3. This is possible because wt and mutant exon 3 only differ in the last base of the exon.

A summarising scheme of the splicing pattern of wt *DJ-1* mRNA, as well as of homozygous c.192G>C *DJ-1* mutation carrying mRNA and heterozygous c.192G>C *DJ-1* mutation carrying mRNA is shown in (Figure 56).
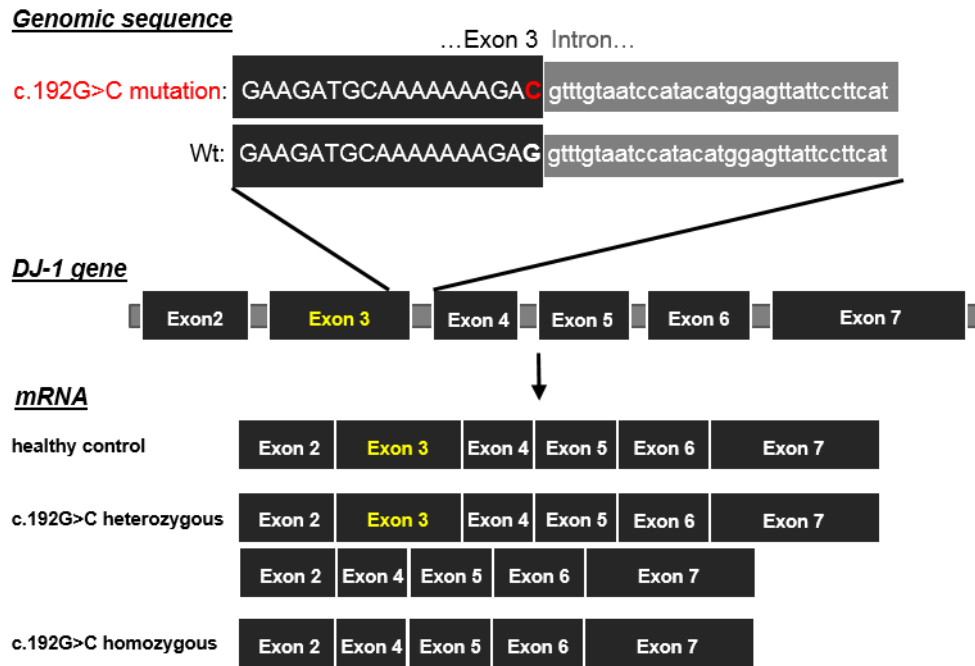
Figure 56: **Schematic overview of c.192G>C *DJ-1* mutation and its effect on splicing.**

The c.192G>C *DJ-1* mutation lies at the end of *DJ-1* exon 3. Splicing of pre-mRNA of the heterozygous *DJ-1* mutation leads to a correctly spliced mRNA transcript and a transcript lacking exon 3. Homozygous carriers of this mutation express misspliced mRNA without exon 3.

4.4.3   Specific U1 snRNP (SpeU1) rescues skipping of exon 3

It has been published that approximately 10 % of all human disease causing splicing defects are due to genetic mutations (Stenson et al., 2003). Furthermore, skipping of a complete exon is also known to be causative for other diseases, such as the skipping of exon 20 causing FD in c.2204+6T>C mutation carriers (Anderson et al., 2001, Slaugenhaupt et al., 2001), or skipping of exon 7 in the *SMN2* gene leading to spinal muscular atrophy (Lorson et al., 1999, Monani et al., 1999), or skipping of exon 3 by an exon 3+5 G>C mutation in neurofibromatosis type 1 (Baralle et al., 2003), as well as skipping of exon 9 in the *CFTR* gene causing cystic fibrosis (Pagani et al., 2000). The skipping of an exon happens during the splicing process. Each exon is defined by a splice donor (5' end of the intron) and a splice acceptor (3' end of the intron) site. The c.192G>C *DJ-1* mutation changes one base of the splice donor site, particularly the last base of the exon. We could show that this single base exchange is the reason for the skipping of exon 3, because it leads to an additional mismatch between the pre-mRNA and the U1 snRNA which prevents U1 snRNP from binding to the mutated exon. In the case of the presence of the mutation, the potential number of mismatching base pairs between U1 snRNA and the 5'splice site is increased from four to five (Figure 46). This number of mismatches is only present in less than 5 % of normal 5'splice sites (Carmel et al., 2004).

We show that through generating a specific U1 snRNP (SpeU1) by mutating the U1 snRNA at the respective base only, exon skipping was rescued (Figure 47). Making use of the SpeU1, correct splicing of c.192G>C mutant *DJ-1* exon 3 was achieved in the artificial minigene assay (Figure 49) as well as in an *in vivo* experiment with immortalised fibroblasts (Figure 50).

4.4.4 Potential reasons for the absence of DJ-1 protein in the presence of mRNA lacking exon 3

4.4.4.1 *Not being able to detect short DJ-1 protein with the antibody we use is not the case*

Knowing that the c.192G>C *DJ-1* mutation causes skipping of complete exon 3 lead us to immediately look at the binding site of the DJ-1 antibody we used for our Western blot experiments. To make sure that we have not been able to detect DJ-1 protein in the patient-derived cells because it was not there and not because the antibody used binds to an amino acid encoded in exon 3, we had a look at the binding site of the DJ-1 antibody used in the respective experiments: Binding site of the DJ-1 (D29E5) XP® mAB (Cell Signaling Technology, Cambridge, UK) is shown in green. Amino acids encoded by exon 3 are highlighted in yellow. Further, we tested whether we would be able to detect DJ-1 in homozygous c.192G>C *D-1* mutation carrying cells with another antibody which recognises the N-terminal region of DJ-1 (shown in blue) (Figure 57). Independently from our own experiments two collaboration partners who used different DJ-1 antibodies also could not detect DJ-1 protein in homozygous mutation carriers of the c.192G>C *DJ-1* mutation: The group of Dr. Daniela Vogt-Weissenhorn at the Institute of Developmental Genetics of the Helmholtz Zentrum München used the Human Park7/DJ-1 Affinity Purified Polyclonal Ab (AF3995) from R&D Systems, Inc. (Oxfordshire, UK). The group of Dimitri Kranic, MD, PhD of the Department of Neurology at the Northwestern Universtiy (Chicago, IL, USA) used the Anti-PARK7/DJ1 antibody [malphaDJ-1/E2.19] from Abcam (Cambridge, UK).
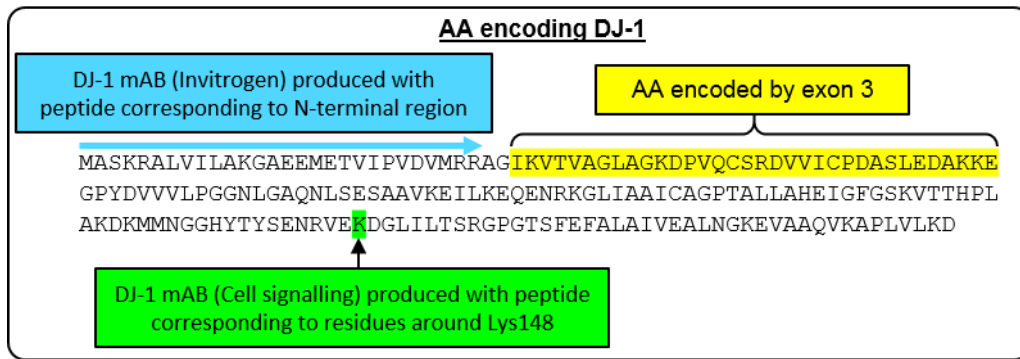
Figure 57: **Binding site of DJ-1 antibodies used.**

Figure shows amino acid (AA) sequence of DJ-1 with AA encoded by exon 3 in yellow. DJ-1 (D29E5) XP® mAB (Cell Signaling Technology, Cambridge, UK) monoclonal antibody (mAB) is produced against a peptide corresponding to residues surrounding Lys148 (K) highlighted in green. Mouse anti-DJ-1 (37-8800) mAB (Invitrogen GmbH, Karslruhe, Germany) is produced against the N-terminal region of recombinant human DJ-1.

4.4.4.2 Enhanced proteasomal or lysosomal degradation is not the cause for reduced DJ-1 protein levels in c.192G>C DJ-1 mutation carriers

To test whether similar to the L166P mutation, the c.192G>C mutation enhances DJ-1 degradation by the 20S/26S proteasome (Moore et al., 2003), we blocked proteasomal degradation in smNPCs from homozygous c.192G>C *DJ-1* mutation carriers. Furthermore, as this was not the cause for the absence of DJ-1 protein in c.192G>C *DJ-1* mutation carriers we blocked lysosomal degradation to determine if this might be the cause of the absence of the protein. Again, Western blot results showed that c.192G>C mutant DJ-1 does not get degraded by the proteasomal nor by the lysosomal pathway.

4.4.4.3 Mislocalisation of RNA

Through defining the subcellular location of the mRNA, it can be tested whether the mRNA is only in the nucleus, due for example to conformational changes and therefore no translation can occur, because there is no mRNA in the cytosol. This would open up further therapeutic strategies, which could be the improvement of the translocation of the mRNA to the cytosol.

Defining the subcellular localisation of the mRNA will be performed by Northern blot analysis.

4.4.4.4 Splicing defects can lead to mRNA instability or decay

By using our Light cycler approach were we are able to detect full length *DJ-1* mRNA as well as mRNA without *DJ-1* exon 3 we show that in the homozygous c.192G>C *DJ-1* mutation carriers mRNA lacking exon 3 is present, in some cases the level is even higher

than the healthy control (Figure 43). Therefore, we assume that the mRNA is neither degraded by a decay mechanism nor instable due to the missplicing.

4.4.5 Pharmacological rescue of the c.192G>C *DJ-1* mutation

Mutations causing partial exon skipping through a mutation in the splice donor site impairing U1 snRNP binding could already be successfully corrected. One example is the above-mentioned c.2204+6T>C in the *IKBKAP* gene accounting for more than 99.5 % of all familial dystonia cases (Slaugenhaupt et al., 2004). In a first study it was demonstrated that the plant cytokinin kinetin (6-furfurylaminopurine) rescued splicing in a minigene experiment (Slaugenhaupt et al., 2004). In the meantime, it could be shown that kinetin improved normal splicing of *IKBKAP* pre-mRNA *in vivo* in FD patients (Axelrod et al., 2011). Kinetin is a small cytokinin that is able to cross the BBB (Sitek study No. 0849-M208; SITEK Research Laboratories, Rockville, MD, 2005). The effect on how kinetin improves correct splicing in this case is, however, not known. Due to its anti-ageing effect and anti-oxidant ability, it is an ingredient for skin treatments (Olsen et al., 1999, Rattan and Clark, 1994, Sharma et al., 1995). In a first attempt to address potential pharmacological agents that can correct splicing of mutant exon 3 in patient cells carrying the c.192G>C *DJ-1* mutation, we treated patient derived immortalised fibroblasts as well as smNPCs with kinetin due to its promising features (crosses BBB, can be applied in patients, rescues splicing in similar conditions). A slight increase in correctly spliced mRNA was seen after treatment however it was not as high as the effects seen for exon 20 inclusion in FD (Figure 53 and Figure 54). To achieve a splicing correction effect that could be sufficient for a potential therapeutic effect *in vivo* in patients or has a more promising correction effect we tested other compounds known to alter splicing for example as well in FD or in spinal muscular atrophy (Table 37). Benzyladenine which was also found to alter splicing in the c.2204+6T>C in the *IKBKAP* gene in FD had a positive effect (more than 100 % increase of correctly spliced mRNA) on splicing of the c.192G>C *DJ-1* mutation. The other tested compounds, however, did not increase correctly spliced exon 3 after 24 h of treatment. The experiment could only be carried out once so far and has to be repeated. Also different conditions will be applied in case of hit compounds to be able to test whether more promising results can be achieved.

4.5 Perspectives

Different aspects of this project are still ongoing and will be continued beyond the scope of this thesis.

4.5.1   Mechanism of the c.192G>C *DJ-1* mutation leading to loss of DJ-1 protein

One focus will be on further understanding how the skipping of mutant exon 3 leads to the absence of DJ-1 protein in homozygous c.192G>C *DJ-1* mutation carriers.

A Northern blot of a nuclear and a cytosolic fraction can help to understand two aspects in this context:

1) It will confirm with another method besides qPCR whether there is mRNA in the cells and

2) It will show where the mRNA is located.

If the Northern blot, like the qPCR result, shows mRNA, the qPCR experiments can be confirmed by another methodology that the mRNA is not degraded or unstable because of the mutation.

If no mRNA can be seen on the Northern blot, further experiments will focus on nonsense mediated decay pathways that might degrade the mutant mRNA.

Apart from that, computational tools allow to model and predict changes in mRNA folding and to predict possible secondary structures caused by the skipping of complete exon 3.

Furthermore, we try to express *DJ-1* mRNA lacking exon 3 and if it can be expressed, it will be tested if a short DJ-1 protein lacking the amino acids encoded by exon 3 will be able to rescue the phenotypes we already saw in our knockout models. For this purpose, we already cloned lentiviral expression plasmids expressing either full-length DJ-1 or DJ-1 lacking exon 3. These constructs will be used to transduce the knockout cell models we have available and subsequently test if DJ-1 protein can be expressed and to which amount using the construct expressing DJ-1 lacking exon 3. If it can be expressed, these constructs can be used to further assess the function of this short DJ-1 protein in case we find a compound, which leads to the presence of short DJ-1 protein in patient derived cells. We will first try to rescue phenotypes we saw in our knockout model systems.

4.5.2   Knockout model systems to further dissect the role of *DJ-1* in neurodegeneration in PD

As stated before, having generated iPSCs from the patient derived fibroblasts of c.192G>C *DJ-1* mutation carriers opens up the opportunity to further analyse the role of DJ-1 function in the neurodegeneration process of PD.

The iPSCs and the cell types that can be differentiated from them provide a valuable source and tool to perform further analyses. The establishment of the protocol for classical neuronal differentiation and smNPC generation allow to carry out further measurements

to validate existing data in these cell types as well as to assess neuron specific disease related phenotypes.

Experiments validating the morphological and functional mitochondrial data in smNPC derived neurons we described in the patient derived fibroblasts in this study are currently ongoing. Also neurons will be used in near future to look at mitochondrial transport to compare these data with the ones we generated with the murine primary knockout cultures.

These human DJ-1 knockout models also offer an opportunity to generate isogenic control experiments with restituted endogenous DJ-1 background which is currently underway for the iPSCs of the index patient as well as a control line which will be mutated homozygously for the c.192G>C *DJ-1* mutation. A heterozygous gene correction in the immortalised fibroblasts of the index patient has already successfully been generated by our collaboration partners in the group of Dr. Daniela Vogt-Weissenhorn at the Institute of Developmental Genetics of the Helmholtz Zentrum München and can already be used for comparative experiments under a defined genetic background. In this isogenic fibroblast line of the index patient, now with a heterozygous c.192G>C *DJ-1* mutation, DJ-1 protein was detected by Western blot analysis. The genetic correction of the mutation successfully restored DJ-1 protein expression.

Furthermore, to be able to even detect subtle PD related phenotypes of this late-onset disorders, which are age-dependent and therefore might not be detectable in iPSCs due to their identity back to an embryonic age, challenges by artificial ageing can be applied to induce ageing-related features (Miller et al., 2013).

Another aspect that can be addressed using isogenic controls is why the homozygous c.192G>C *DJ-1* mutation carrying sister has not displayed any motor symptoms so far, although in the meantime she is older than the index patient was at disease onset when he displayed first motor symptoms. Studies in these regards could reveal modifiers that attenuate loss of DJ-1 function in the pre-motor diseased sister.

During this work we generated:

- patient derived <u>fibroblasts</u> of c.192G>C *DJ-1* mutation carriers
- which we successfully <u>immortalised</u>
- and reprogrammed into <u>iPSCs</u>
- which can be differentiated to <u>mDA neurons</u> following the classical floor plate-based protocol, which was already successfully applied
- also, we provide <u>smNPCs</u>, as neuronal precursor cells which can be expanded fast and efficiently and can be differentiated further into neuronal subtypes.

- But also <u>hippocampal primary neuron cultures</u> from DJ-1 knockout mice were successfully generated for experiments.

4.5.3 Opportunity of discovering potential therapeutic agents for PD patients

Having deciphered the mechanism of the c.192G>C *DJ-1* mutation opens up the opportunity to screen for pharmacological intervention as already initiated in this study. To test for correct splicing, as done in this study, provides a reliable and straight forward readout to test for rescuing the effect of the c.192G>C *DJ-1* mutation. Identifying compounds that lead to an increase of correct splicing of *DJ-1* exon 3 in homozygous c.192G>C mutation carriers could yield novel therapies for these patients.

Furthermore, potential drug candidates identified with our model have a high potential to also have a positive effect in other diseases caused by a mutation with the same genetic mechanism.

Not only does this study provide the underlying mechanism of the mutation, which can be used to screen for compounds that tackle the disease-causing mechanism at its starting point, but also with the models generated we provide excellent tools for large-scale drug discovery screenings.

We generated iPSCs from patient derived fibroblasts and differentiated smNPCs from these cells. Both models provide a source of cells allowing to test for large sets of candidate drugs.

Small sets of compounds have been tested, making use of various disease specific patient-derived iPSCs which were further differentiated into the relevant cell types of interest for the screen. Amongst the first ones were screens for the treatment of diseases like FD (Lee et al., 2009), spinal muscular atrophy (Ebert et al., 2009), Rett syndrome (Marchetto et al., 2010), long-QT syndrome (Itzhaki et al., 2011, Moretti et al., 2010), schizophrenia (Brennand et al., 2011), Timothy syndrome (Yazawa et al., 2011) and Alzheimers Disease (Yahata et al., 2011). (Lee et al., 2012a) showed that a large compound screen in a 384-well format could be performed and suggest further studies of that kind to come closer to the era of personalised medicine. Screening for compounds in the cell type they are supposed to work in, particularly if it is a neuronal cell type assures the specificity and ameliorates further specificity tests for their clinical efficacy, as shown for glioblastoma tumors (Cho et al., 2013a). Also, using these cells for screens allows to ascertain neurotoxicity of the compounds at the same time, as shown in a big compound screen unsing neural stem cells (Malik et al., 2014).

Mitochondrial phenotypes caused by stressors in iPSC-derived neuronal cells could be improved using drugs in a study by (Cooper et al., 2012). This is particularly interesting in this context as we saw different mitochondrial phenotypes in our patient derived cells.

Another aspect could be to block splice silencer sequences or enhance splice enhancer sequences surrounding the mutant exon to increase the inclusion of exon 3 using compounds or even by using antisense oligonucleotides. A first bioinformatical analysis predicted an increase of the splicing factor SRSF1 together with a loss of SRSF2 binding with the mutation (Figure 51). It needs further investigation on whether the aberrant splicing occurs because aside the weakening of the splice site from consensus also eliminating a SR protein binding influences 5' splice site recognition. An example for a mutation that abolishes a binding site for an SR protein and at the same time creates an ESS is the c.840C>T transition at position +6 in exon 7 of *SMN2 (Cartegni et al., 2006, Kashima et al., 2007)*.

Discovering a drug to rescue skipping of *DJ-1* exon 3 in c.192G>C mutation carriers could be the first causative treatment for PD patients as until today only symptomatic treatment of the disease exists.

5   References

ABBOTT, R. D., ROSS, G. W., WHITE, L. R., SANDERSON, W. T., BURCHFIEL, C. M., KASHON, M., SHARP, D. S., MASAKI, K. H., CURB, J. D. & PETROVITCH, H. 2003. Environmental, life-style, and physical precursors of clinical Parkinson's disease: recent findings from the Honolulu-Asia Aging Study. *J Neurol,* 250 Suppl 3**,** III30-9.

ABDALLAH, J., CALDAS, T., KTHIRI, F., KERN, R. & RICHARME, G. 2007. YhbO protects cells against multiple stresses. *J Bacteriol,* 189**,** 9140-4.

ABOU-SLEIMAN, P. M., HEALY, D. G., QUINN, N., LEES, A. J. & WOOD, N. W. 2003. The role of pathogenic DJ-1 mutations in Parkinson's disease. *Ann Neurol,* 54**,** 283-6.

AEBI, M., HORNIG, H. & WEISSMANN, C. 1987. 5' cleavage site in eukaryotic pre-mRNA splicing is determined by the overall 5' splice region, not by the conserved 5' GU. *Cell,* 50**,** 237-46.

ALAM, Z. I., JENNER, A., DANIEL, S. E., LEES, A. J., CAIRNS, N., MARSDEN, C. D., JENNER, P. & HALLIWELL, B. 1997. Oxidative DNA damage in the parkinsonian brain: an apparent selective increase in 8-hydroxyguanine levels in substantia nigra. *J Neurochem,* 69**,** 1196-203.

ANDERSON, S. L., COLI, R., DALY, I. W., KICHULA, E. A., RORK, M. J., VOLPI, S. A., EKSTEIN, J. & RUBIN, B. Y. 2001. Familial dysautonomia is caused by mutations of the IKAP gene. *Am J Hum Genet,* 68**,** 753-8.

ANDREASSI, C., JARECKI, J., ZHOU, J., COOVERT, D. D., MONANI, U. R., CHEN, X., WHITNEY, M., POLLOK, B., ZHANG, M., ANDROPHY, E. & BURGHES, A. H. 2001. Aclarubicin treatment restores SMN levels to cells derived from type I spinal muscular atrophy patients. *Hum Mol Genet,* 10**,** 2841-9.

ANDRES-MATEOS, E., PERIER, C., ZHANG, L., BLANCHARD-FILLION, B., GRECO, T. M., THOMAS, B., KO, H. S., SASAKI, M., ISCHIROPOULOS, H., PRZEDBORSKI, S., DAWSON, T. M. & DAWSON, V. L. 2007. DJ-1 gene deletion reveals that DJ-1 is an atypical peroxiredoxin-like peroxidase. *Proc Natl Acad Sci U S A,* 104**,** 14807-12.

ANNESI, G., SAVETTIERI, G., PUGLIESE, P., D'AMELIO, M., TARANTINO, P., RAGONESE, P., LA BELLA, V., PICCOLI, T., CIVITELLI, D., ANNESI, F., FIERRO, B., PICCOLI, F., ARABIA, G., CARACCIOLO, M., CIRO CANDIANO, I. C. & QUATTRONE, A. 2005. DJ-1 mutations and parkinsonism-dementia-amyotrophic lateral sclerosis complex. *Ann Neurol,* 58**,** 803-7.

ANTONY, P. M., DIEDERICH, N. J., KRUGER, R. & BALLING, R. 2013. The hallmarks of Parkinson's disease. *FEBS J,* 280**,** 5981-93.

ASHRAFI, G., SCHLEHE, J. S., LAVOIE, M. J. & SCHWARZ, T. L. 2014. Mitophagy of damaged mitochondria occurs locally in distal neuronal axons and requires PINK1 and Parkin. *J Cell Biol,* 206**,** 655-70.

AVILION, A. A., NICOLIS, S. K., PEVNY, L. H., PEREZ, L., VIVIAN, N. & LOVELL-BADGE, R. 2003. Multipotent cell lineages in early mouse development depend on SOX2 function. *Genes Dev,* 17**,** 126-40.

AXELROD, F. B., LIEBES, L., GOLD-VON SIMSON, G., MENDOZA, S., MULL, J., LEYNE, M., NORCLIFFE-KAUFMANN, L., KAUFMANN, H. & SLAUGENHAUPT, S. A. 2011. Kinetin improves IKBKAP mRNA splicing in patients with familial dysautonomia. *Pediatr Res,* 70**,** 480-3.

BAI, Q., MULLETT, S. J., GARVER, J. A., HINKLE, D. A. & BURTON, E. A. 2006. Zebrafish DJ-1 is evolutionarily conserved and expressed in dopaminergic neurons. *Brain Res,* 1113**,** 33-44.

BANDOPADHYAY, R., KINGSBURY, A. E., COOKSON, M. R., REID, A. R., EVANS, I. M., HOPE, A. D., PITTMAN, A. M., LASHLEY, T., CANET-AVILES, R., MILLER, D. W., MCLENDON, C., STRAND, C., LEONARD, A. J., ABOU-SLEIMAN, P. M.,

HEALY, D. G., ARIGA, H., WOOD, N. W., DE SILVA, R., REVESZ, T., HARDY, J. A. & LEES, A. J. 2004. The expression of DJ-1 (PARK7) in normal human CNS and idiopathic Parkinson's disease. *Brain,* 127**,** 420-30.

BANDYOPADHYAY, S. & COOKSON, M. R. 2004. Evolutionary and functional relationships within the DJ1 superfamily. *BMC Evol Biol,* 4**,** 6.

BARALLE, D. & BARALLE, M. 2005. Splicing in action: assessing disease causing sequence changes. *J Med Genet,* 42**,** 737-48.

BARALLE, D., LUCASSEN, A. & BURATTI, E. 2009. Missed threads. The impact of pre-mRNA splicing defects on clinical practice. *EMBO Rep,* 10**,** 810-6.

BARALLE, M., BARALLE, D., DE CONTI, L., MATTOCKS, C., WHITTAKER, J., KNEZEVICH, A., FFRENCH-CONSTANT, C. & BARALLE, F. E. 2003. Identification of a mutation that perturbs NF1 agene splicing using genomic DNA samples and a minigene assay. *J Med Genet,* 40**,** 220-2.

BARALLE, M., SKOKO, N., KNEZEVICH, A., DE CONTI, L., MOTTI, D., BHUVANAGIRI, M., BARALLE, D., BURATTI, E. & BARALLE, F. E. 2006. NF1 mRNA biogenesis: effect of the genomic milieu in splicing regulation of the NF1 exon 37 region. *FEBS Lett,* 580**,** 4449-56.

BEEVERS, J. E., CAFFREY, T. M. & WADE-MARTINS, R. 2013. Induced pluripotent stem cell (iPSC)-derived dopaminergic models of Parkinson's disease. *Biochem Soc Trans,* 41**,** 1503-8.

BEILINA, A., VAN DER BRUG, M., AHMAD, R., KESAVAPANY, S., MILLER, D. W., PETSKO, G. A. & COOKSON, M. R. 2005. Mutations in PTEN-induced putative kinase 1 associated with recessive parkinsonism have differential effects on protein stability. *Proc Natl Acad Sci U S A,* 102**,** 5703-8.

BENDER, A., KRISHNAN, K. J., MORRIS, C. M., TAYLOR, G. A., REEVE, A. K., PERRY, R. H., JAROS, E., HERSHESON, J. S., BETTS, J., KLOPSTOCK, T., TAYLOR, R. W. & TURNBULL, D. M. 2006. High levels of mitochondrial DNA deletions in substantia nigra neurons in aging and Parkinson disease. *Nat Genet,* 38**,** 515-7.

BERECZKI, D. 2010. The description of all four cardinal signs of Parkinson's disease in a Hungarian medical text published in 1690. *Parkinsonism Relat Disord,* 16**,** 290-3.

BIRKMAYER, W. & HORNYKIEWICZ, O. 1961. [The L-3, 4-dioxyphenylalanine (DOPA)-effect in Parkinson-akinesia]. *Wien. Klin. Wochenschr.,* 73**,** 787-788.

BISAGLIA, M., TESSARI, I., PINATO, L., BELLANDA, M., GIRAUDO, S., FASANO, M., BERGANTINO, E., BUBACCO, L. & MAMMI, S. 2005. A topological model of the interaction between alpha-synuclein and sodium dodecyl sulfate micelles. *Biochemistry,* 44**,** 329-39.

BISKUP, S. & WEST, A. B. 2009. Zeroing in on LRRK2-linked pathogenic mechanisms in Parkinson's disease. *Biochim Biophys Acta,* 1792**,** 625-33.

BJORKBLOM, B., ADILBAYEVA, A., MAPLE-GRODEM, J., PISTON, D., OKVIST, M., XU, X. M., BREDE, C., LARSEN, J. P. & MOLLER, S. G. 2013. Parkinson disease protein DJ-1 binds metals and protects against metal-induced cytotoxicity. *J Biol Chem,* 288**,** 22809-20.

BLACKINTON, J., LAKSHMINARASIMHAN, M., THOMAS, K. J., AHMAD, R., GREGGIO, E., RAZA, A. S., COOKSON, M. R. & WILSON, M. A. 2009. Formation of a stabilized cysteine sulfinic acid is critical for the mitochondrial function of the parkinsonism protein DJ-1. *J Biol Chem,* 284**,** 6476-85.

BOCH, J., SCHOLZE, H., SCHORNACK, S., LANDGRAF, A., HAHN, S., KAY, S., LAHAYE, T., NICKSTADT, A. & BONAS, U. 2009. Breaking the code of DNA binding specificity of TAL-type III effectors. *Science,* 326**,** 1509-12.

BONIFATI, V. 2003. Mutations in the DJ-1 gene associated with autosomal recessive early-onset parkinsonism. *Science,* 299**,** 256-259.

BONIFATI, V. 2007. LRRK2 low-penetrance mutations (Gly2019Ser) and risk alleles (Gly2385Arg)-linking familial and sporadic Parkinson's disease. *Neurochem Res,* 32**,** 1700-8.

5 References

BONIFATI, V., BREEDVELD, G. J., SQUITIERI, F., VANACORE, N., BRUSTENGHI, P., HARHANGI, B. S., MONTAGNA, P., CANNELLA, M., FABBRINI, G., RIZZU, P., VAN DUIJN, C. M., OOSTRA, B. A., MECO, G. & HEUTINK, P. 2002. Localization of autosomal recessive early-onset parkinsonism to chromosome 1p36 (PARK7) in an independent dataset. *Ann Neurol,* 51**,** 253-6.

BONIFATI, V., RIZZU, P., VAN BAREN, M. J., SCHAAP, O., BREEDVELD, G. J., KRIEGER, E., DEKKER, M. C., SQUITIERI, F., IBANEZ, P., JOOSSE, M., VAN DONGEN, J. W., VANACORE, N., VAN SWIETEN, J. C., BRICE, A., MECO, G., VAN DUIJN, C. M., OOSTRA, B. A. & HEUTINK, P. 2003. Mutations in the DJ-1 gene associated with autosomal recessive early-onset parkinsonism. *Science,* 299**,** 256-9.

BONIFATI, V., ROHE, C. F., BREEDVELD, G. J., FABRIZIO, E., DE MARI, M., TASSORELLI, C., TAVELLA, A., MARCONI, R., NICHOLL, D. J., CHIEN, H. F., FINCATI, E., ABBRUZZESE, G., MARINI, P., DE GAETANO, A., HORSTINK, M. W., MAAT-KIEVIT, J. A., SAMPAIO, C., ANTONINI, A., STOCCHI, F., MONTAGNA, P., TONI, V., GUIDI, M., DALLA LIBERA, A., TINAZZI, M., DE PANDIS, F., FABBRINI, G., GOLDWURM, S., DE KLEIN, A., BARBOSA, E., LOPIANO, L., MARTIGNONI, E., LAMBERTI, P., VANACORE, N., MECO, G., OOSTRA, B. A. & ITALIAN PARKINSON GENETICS, N. 2005. Early-onset parkinsonism associated with PINK1 mutations: frequency, genotypes, and phenotypes. *Neurology,* 65**,** 87-95.

BOYER, L. A., LEE, T. I., COLE, M. F., JOHNSTONE, S. E., LEVINE, S. S., ZUCKER, J. P., GUENTHER, M. G., KUMAR, R. M., MURRAY, H. L., JENNER, R. G., GIFFORD, D. K., MELTON, D. A., JAENISCH, R. & YOUNG, R. A. 2005. Core transcriptional regulatory circuitry in human embryonic stem cells. *Cell,* 122**,** 947-56.

BREEN, K. C. & DRUTYTE, G. 2013. Non-motor symptoms of Parkinson's disease: the patient's perspective. *J Neural Transm,* 120**,** 531-5.

BRENNAND, K. J., SIMONE, A., JOU, J., GELBOIN-BURKHART, C., TRAN, N., SANGAR, S., LI, Y., MU, Y., CHEN, G., YU, D., MCCARTHY, S., SEBAT, J. & GAGE, F. H. 2011. Modelling schizophrenia using human induced pluripotent stem cells. *Nature,* 473**,** 221-5.

BRETAUD, S., ALLEN, C., INGHAM, P. W. & BANDMANN, O. 2007. p53-dependent neuronal cell death in a DJ-1-deficient zebrafish model of Parkinson's disease. *J Neurochem,* 100**,** 1626-35.

BURATTI, E. & BARALLE, F. E. 2004. Influence of RNA secondary structure on the pre-mRNA splicing process. *Mol Cell Biol,* 24**,** 10505-14.

BURBULLA, L. F., KREBIEHL, G. & KRUGER, R. 2010. Balance is the challenge--the impact of mitochondrial dynamics in Parkinson's disease. *Eur J Clin Invest,* 40**,** 1048-60.

BURBULLA, L. F. & KRUGER, R. 2012. The use of primary human fibroblasts for monitoring mitochondrial phenotypes in the field of Parkinson's disease. *J Vis Exp.*

CALNE, D. B., DUBINI, A. & STERN, G. 1989. Did Leonardo describe Parkinson's disease? *N Engl J Med,* 320**,** 594.

CANET-AVILES, R. M., WILSON, M. A., MILLER, D. W., AHMAD, R., MCLENDON, C., BANDYOPADHYAY, S., BAPTISTA, M. J., RINGE, D., PETSKO, G. A. & COOKSON, M. R. 2004. The Parkinson's disease protein DJ-1 is neuroprotective due to cysteine-sulfinic acid-driven mitochondrial localization. *Proc Natl Acad Sci U S A,* 101**,** 9103-8.

CARLSSON, A., LINDQVIST, M. & MAGNUSSON, T. 1957. 3,4-Dihydroxyphenylalanine and 5-hydroxytryptophan as reserpine antagonists. *Nature,* 180**,** 1200.

CARLSSON, A., LINDQVIST, M., MAGNUSSON, T. & WALDECK, B. 1958. On the presence of 3-hydroxytyramine in brain. *Science,* 127**,** 471.

CARMEL, I., TAL, S., VIG, I. & AST, G. 2004. Comparative analysis detects dependencies among the 5' splice-site positions. *RNA,* 10**,** 828-40.

CARTEGNI, L., HASTINGS, M. L., CALARCO, J. A., DE STANCHINA, E. & KRAINER, A. R. 2006. Determinants of exon 7 splicing in the spinal muscular atrophy genes, SMN1 and SMN2. *Am J Hum Genet,* 78**,** 63-77.

CARTEGNI, L., WANG, J., ZHU, Z., ZHANG, M. Q. & KRAINER, A. R. 2003. ESEfinder: A web resource to identify exonic splicing enhancers. *Nucleic Acids Res,* 31**,** 3568-71.

CHAMBERS, S. M., FASANO, C. A., PAPAPETROU, E. P., TOMISHIMA, M., SADELAIN, M. & STUDER, L. 2009. Highly efficient neural conversion of human ES and iPS cells by dual inhibition of SMAD signaling. *Nat Biotechnol,* 27**,** 275-80.

CHAN, C. S., GERTLER, T. S. & SURMEIER, D. J. 2009. Calcium homeostasis, selective vulnerability and Parkinson's disease. *Trends Neurosci,* 32**,** 249-56.

CHANDRAN, J. S., LIN, X., ZAPATA, A., HOKE, A., SHIMOJI, M., MOORE, S. O., GALLOWAY, M. P., LAIRD, F. M., WONG, P. C., PRICE, D. L., BAILEY, K. R., CRAWLEY, J. N., SHIPPENBERG, T. & CAI, H. 2008. Progressive behavioral deficits in DJ-1-deficient mice are associated with normal nigrostriatal function. *Neurobiol Dis,* 29**,** 505-14.

CHANG, D. T., HONICK, A. S. & REYNOLDS, I. J. 2006. Mitochondrial trafficking to synapses in cultured primary cortical neurons. *J Neurosci,* 26**,** 7035-45.

CHANG, J. G., HSIEH-LI, H. M., JONG, Y. J., WANG, N. M., TSAI, C. H. & LI, H. 2001. Treatment of spinal muscular atrophy by sodium butyrate. *Proc Natl Acad Sci U S A,* 98**,** 9808-13.

CHARCOT, J. M. 1877. Lecture V: On Paralysis Agitans. *In Lect. Dis. Nerv. Syst. Deliv. La Salpêtrière Transl. by Georg. Seigerson. The New Sydenham Society***,** 129-156.

CHARTIER-HARLIN, M. C., DACHSEL, J. C., VILARINO-GUELL, C., LINCOLN, S. J., LEPRETRE, F., HULIHAN, M. M., KACHERGUS, J., MILNERWOOD, A. J., TAPIA, L., SONG, M. S., LE RHUN, E., MUTEZ, E., LARVOR, L., DUFLOT, A., VANBESIEN-MAILLIOT, C., KREISLER, A., ROSS, O. A., NISHIOKA, K., SOTO-ORTOLAZA, A. I., COBB, S. A., MELROSE, H. L., BEHROUZ, B., KEELING, B. H., BACON, J. A., HENTATI, E., WILLIAMS, L., YANAGIYA, A., SONENBERG, N., LOCKHART, P. J., ZUBAIR, A. C., UITTI, R. J., AASLY, J. O., KRYGOWSKA-WAJS, A., OPALA, G., WSZOLEK, Z. K., FRIGERIO, R., MARAGANORE, D. M., GOSAL, D., LYNCH, T., HUTCHINSON, M., BENTIVOGLIO, A. R., VALENTE, E. M., NICHOLS, W. C., PANKRATZ, N., FOROUD, T., GIBSON, R. A., HENTATI, F., DICKSON, D. W., DESTEE, A. & FARRER, M. J. 2011. Translation initiator EIF4G1 mutations in familial Parkinson disease. *Am J Hum Genet,* 89**,** 398-406.

CHEN, H. & CHAN, D. C. 2010. Physiological functions of mitochondrial fusion. *Ann N Y Acad Sci,* 1201**,** 21-5.

CHEN, L., CAGNIARD, B., MATHEWS, T., JONES, S., KOH, H. C., DING, Y., CARVEY, P. M., LING, Z., KANG, U. J. & ZHUANG, X. 2005. Age-dependent motor deficits and dopaminergic dysfunction in DJ-1 null mice. *J Biol Chem,* 280**,** 21418-26.

CHO, D. Y., LIN, S. Z., YANG, W. K., LEE, H. C., HSU, D. M., LIN, H. L., CHEN, C. C., LIU, C. L., LEE, W. Y. & HO, L. H. 2013a. Targeting cancer stem cells for treatment of glioblastoma multiforme. *Cell Transplant,* 22**,** 731-9.

CHO, S. W., KIM, S., KIM, J. M. & KIM, J. S. 2013b. Targeted genome engineering in human cells with the Cas9 RNA-guided endonuclease. *Nat Biotechnol,* 31**,** 230-2.

CLEMENTS, C. M., MCNALLY, R. S., CONTI, B. J., MAK, T. W. & TING, J. P. 2006. DJ-1, a cancer- and Parkinson's disease-associated protein, stabilizes the antioxidant transcriptional master regulator Nrf2. *Proc Natl Acad Sci U S A,* 103**,** 15091-6.

5 References

COLLIN, J. & LAKO, M. 2011. Concise review: putting a finger on stem cell biology: zinc finger nuclease-driven targeted genetic editing in human pluripotent stem cells. *Stem Cells,* 29**,** 1021-33.

COOKSON, M. R., MEAD, C., AUSTWICK, S. M. & PENTREATH, V. W. 1995. Use of the MTT assay for estimating toxicity in primary astrocyte and C6 glioma cell cultures. *Toxicol In Vitro,* 9**,** 39-48.

COOPER, D. N. 1993. Human gene mutations affecting RNA processing and translation. *Ann Med,* 25**,** 11-7.

COOPER, O., SEO, H., ANDRABI, S., GUARDIA-LAGUARTA, C., GRAZIOTTO, J., SUNDBERG, M., MCLEAN, J. R., CARRILLO-REID, L., XIE, Z., OSBORN, T., HARGUS, G., DELEIDI, M., LAWSON, T., BOGETOFTE, H., PEREZ-TORRES, E., CLARK, L., MOSKOWITZ, C., MAZZULLI, J., CHEN, L., VOLPICELLI-DALEY, L., ROMERO, N., JIANG, H., UITTI, R. J., HUANG, Z., OPALA, G., SCARFFE, L. A., DAWSON, V. L., KLEIN, C., FENG, J., ROSS, O. A., TROJANOWSKI, J. Q., LEE, V. M., MARDER, K., SURMEIER, D. J., WSZOLEK, Z. K., PRZEDBORSKI, S., KRAINC, D., DAWSON, T. M. & ISACSON, O. 2012. Pharmacological rescue of mitochondrial deficits in iPSC-derived neural cells from patients with familial Parkinson's disease. *Sci Transl Med,* 4**,** 141ra90.

CORRAL-DEBRINSKI, M., HORTON, T., LOTT, M. T., SHOFFNER, J. M., BEAL, M. F. & WALLACE, D. C. 1992. Mitochondrial DNA deletions in human brain: regional variability and increase with advanced age. *Nat Genet,* 2**,** 324-9.

CORTI, O., LESAGE, S. & BRICE, A. 2011. What genetics tells us about the causes and mechanisms of Parkinson's disease. *Physiol Rev,* 91**,** 1161-218.

CORTOPASSI, G. A. & ARNHEIM, N. 1992. Using the polymerase chain reaction to estimate mutation frequencies and rates in human cells. *Mutat Res,* 277**,** 239-49.

CORTOPASSI, G. A. & WONG, A. 1999. Mitochondria in organismal aging and degeneration. *Biochim Biophys Acta,* 1410**,** 183-93.

COTZIAS, G. C., PAPAVASILIOU, P. S. & GELLENE, R. 1969. Modification of Parkinsonism--chronic treatment with L-dopa. *N. Engl. J. Med.,* 280**,** 337-345.

DARDIS, A., ZANIN, I., ZAMPIERI, S., STUANI, C., PIANTA, A., ROMANELLO, M., BARALLE, F. E., BEMBI, B. & BURATTI, E. 2014. Functional characterization of the common c.-32-13T>G mutation of GAA gene: identification of potential therapeutic agents. *Nucleic Acids Res,* 42**,** 1291-302.

DAUER, W. & PRZEDBORSKI, S. 2003. Parkinson's disease: mechanisms and models. *Neuron,* 39**,** 889-909.

DE CONTI, L., BARALLE, M. & BURATTI, E. 2013. Exon and intron definition in pre-mRNA splicing. *Wiley Interdiscip Rev RNA,* 4**,** 49-60.

DE LA FUENTE-FERNANDEZ, R., SCHULZER, M., KURAMOTO, L., CRAGG, J., RAMACHANDIRAN, N., AU, W. L., MAK, E., MCKENZIE, J., MCCORMICK, S., SOSSI, V., RUTH, T. J., LEE, C. S., CALNE, D. B. & STOESSL, A. J. 2011. Age-specific progression of nigrostriatal dysfunction in Parkinson's disease. *Ann Neurol,* 69**,** 803-10.

DE RIJK, M. C., LAUNER, L. J., BERGER, K., BRETELER, M. M., DARTIGUES, J. F., BALDERESCHI, M., FRATIGLIONI, L., LOBO, A., MARTINEZ-LAGE, J., TRENKWALDER, C. & HOFMAN, A. 2000. Prevalence of Parkinson's disease in Europe: A collaborative study of population-based cohorts. Neurologic Diseases in the Elderly Research Group. *Neurology,* 54**,** S21-3.

DEHAY, B., MARTINEZ-VICENTE, M., RAMIREZ, A., PERIER, C., KLEIN, C., VILA, M. & BEZARD, E. 2012. Lysosomal dysfunction in Parkinson disease: ATP13A2 gets into the groove. *Autophagy,* 8**,** 1389-91.

DETMER, S. A. & CHAN, D. C. 2007. Functions and dysfunctions of mitochondrial dynamics. *Nat Rev Mol Cell Biol,* 8**,** 870-9.

DEUSCHL, G., SCHADE-BRITTINGER, C., KRACK, P., VOLKMANN, J., SCHAFER, H., BOTZEL, K., DANIELS, C., DEUTSCHLANDER, A., DILLMANN, U., EISNER, W., GRUBER, D., HAMEL, W., HERZOG, J., HILKER, R., KLEBE, S., KLOSS,

M., KOY, J., KRAUSE, M., KUPSCH, A., LORENZ, D., LORENZL, S., MEHDORN, H. M., MORINGLANE, J. R., OERTEL, W., PINSKER, M. O., REICHMANN, H., REUSS, A., SCHNEIDER, G. H., SCHNITZLER, A., STEUDE, U., STURM, V., TIMMERMANN, L., TRONNIER, V., TROTTENBERG, T., WOJTECKI, L., WOLF, E., POEWE, W., VOGES, J. & GERMAN PARKINSON STUDY GROUP, N. S. 2006. A randomized trial of deep-brain stimulation for Parkinson's disease. *N Engl J Med,* 355**,** 896-908.

DEVINE, M. J., RYTEN, M., VODICKA, P., THOMSON, A. J., BURDON, T., HOULDEN, H., CAVALERI, F., NAGANO, M., DRUMMOND, N. J., TAANMAN, J. W., SCHAPIRA, A. H., GWINN, K., HARDY, J., LEWIS, P. A. & KUNATH, T. 2011. Parkinson's disease induced pluripotent stem cells with triplication of the alpha-synuclein locus. *Nat Commun,* 2**,** 440.

DEXTER, D. T., CARTER, C. J., WELLS, F. R., JAVOY-AGID, F., AGID, Y., LEES, A., JENNER, P. & MARSDEN, C. D. 1989. Basal lipid peroxidation in substantia nigra is increased in Parkinson's disease. *J Neurochem,* 52**,** 381-9.

DI FONZO, A., DEKKER, M. C., MONTAGNA, P., BARUZZI, A., YONOVA, E. H., CORREIA GUEDES, L., SZCZERBINSKA, A., ZHAO, T., DUBBEL-HULSMAN, L. O., WOUTERS, C. H., DE GRAAFF, E., OYEN, W. J., SIMONS, E. J., BREEDVELD, G. J., OOSTRA, B. A., HORSTINK, M. W. & BONIFATI, V. 2009. FBXO7 mutations cause autosomal recessive, early-onset parkinsonian-pyramidal syndrome. *Neurology,* 72**,** 240-5.

DIAS, V., JUNN, E. & MOURADIAN, M. M. 2013. The role of oxidative stress in Parkinson's disease. *J Parkinsons Dis,* 3**,** 461-91.

DIMOS, J. T., RODOLFA, K. T., NIAKAN, K. K., WEISENTHAL, L. M., MITSUMOTO, H., CHUNG, W., CROFT, G. F., SAPHIER, G., LEIBEL, R., GOLAND, R., WICHTERLE, H., HENDERSON, C. E. & EGGAN, K. 2008. Induced pluripotent stem cells generated from patients with ALS can be differentiated into motor neurons. *Science,* 321**,** 1218-21.

DING, H., JIANG, N., LIU, H., LIU, X., LIU, D., ZHAO, F., WEN, L., LIU, S., JI, L. L. & ZHANG, Y. 2010. Response of mitochondrial fusion and fission protein gene expression to exercise in rat skeletal muscle. *Biochim Biophys Acta,* 1800**,** 250-6.

DING, Q., REGAN, S. N., XIA, Y., OOSTROM, L. A., COWAN, C. A. & MUSUNURU, K. 2013. Enhanced efficiency of human pluripotent stem cell genome editing through replacing TALENs with CRISPRs. *Cell Stem Cell,* 12**,** 393-4.

DORSEY, E. R., CONSTANTINESCU, R., THOMPSON, J. P., BIGLAN, K. M., HOLLOWAY, R. G., KIEBURTZ, K., MARSHALL, F. J., RAVINA, B. M., SCHIFITTO, G., SIDEROWF, A. & TANNER, C. M. 2007. Projected number of people with Parkinson disease in the most populous nations, 2005 through 2030. *Neurology,* 68**,** 384-6.

DROLET, R. E., CANNON, J. R., MONTERO, L. & GREENAMYRE, J. T. 2009. Chronic rotenone exposure reproduces Parkinson's disease gastrointestinal neuropathology. *Neurobiol Dis,* 36**,** 96-102.

EBERT, A. D., YU, J., ROSE, F. F., JR., MATTIS, V. B., LORSON, C. L., THOMSON, J. A. & SVENDSEN, C. N. 2009. Induced pluripotent stem cells from a spinal muscular atrophy patient. *Nature,* 457**,** 277-80.

EBRAHIMI-FAKHARI, D., WAHLSTER, L. & MCLEAN, P. J. 2012. Protein degradation pathways in Parkinson's disease: curse or blessing. *Acta Neuropathol,* 124**,** 153-72.

EDVARDSON, S., CINNAMON, Y., TA-SHMA, A., SHAAG, A., YIM, Y. I., ZENVIRT, S., JALAS, C., LESAGE, S., BRICE, A., TARABOULOS, A., KAESTNER, K. H., GREENE, L. E. & ELPELEG, O. 2012. A deleterious mutation in DNAJC6 encoding the neuronal-specific clathrin-uncoating co-chaperone auxilin, is associated with juvenile parkinsonism. *PLoS One,* 7**,** e36458.

5 References

EHRINGER, H. & HORNYKIEWICZ, O. 1960. [Distribution of noradrenaline and dopamine (3-hydroxytyramine) in the human brain and their behavior in diseases of the extrapyramidal system]. *Klin. Wochenschr.,* 38**,** 1236-1239.

ELBAZ, A., BOWER, J. H., MARAGANORE, D. M., MCDONNELL, S. K., PETERSON, B. J., AHLSKOG, J. E., SCHAID, D. J. & ROCCA, W. A. 2002. Risk tables for parkinsonism and Parkinson's disease. *J Clin Epidemiol,* 55**,** 25-31.

EXNER, N., LUTZ, A. K., HAASS, C. & WINKLHOFER, K. F. 2012. Mitochondrial dysfunction in Parkinson's disease: molecular mechanisms and pathophysiological consequences. *EMBO J,* 31**,** 3038-62.

EXNER, N., TRESKE, B., PAQUET, D., HOLMSTROM, K., SCHIESLING, C., GISPERT, S., CARBALLO-CARBAJAL, I., BERG, D., HOEPKEN, H. H., GASSER, T., KRUGER, R., WINKLHOFER, K. F., VOGEL, F., REICHERT, A. S., AUBURGER, G., KAHLE, P. J., SCHMID, B. & HAASS, C. 2007. Loss-of-function of human PINK1 results in mitochondrial pathology and can be rescued by parkin. *J Neurosci,* 27**,** 12413-8.

FACUCHO-OLIVEIRA, J. M., ALDERSON, J., SPIKINGS, E. C., EGGINTON, S. & ST JOHN, J. C. 2007. Mitochondrial DNA replication during differentiation of murine embryonic stem cells. *J Cell Sci,* 120**,** 4025-34.

FAIOLA, F., LIU, X., LO, S., PAN, S., ZHANG, K., LYMAR, E., FARINA, A. & MARTINEZ, E. 2005. Dual regulation of c-Myc by p300 via acetylation-dependent control of Myc protein turnover and coactivation of Myc-induced transcription. *Mol Cell Biol,* 25**,** 10220-34.

FAN, J., REN, H., JIA, N., FEI, E., ZHOU, T., JIANG, P., WU, M. & WANG, G. 2008. DJ-1 decreases Bax expression through repressing p53 transcriptional activity. *J Biol Chem,* 283**,** 4022-30.

FIORAVANTI, E., DURA, M. A., LASCOUX, D., MICOSSI, E., FRANZETTI, B. & MCSWEENEY, S. 2008. Structure of the stress response protein DR1199 from Deinococcus radiodurans: a member of the DJ-1 superfamily. *Biochemistry,* 47**,** 11581-9.

FLOOR, E. & WETZEL, M. G. 1998. Increased protein oxidation in human substantia nigra pars compacta in comparison with basal ganglia and prefrontal cortex measured with an improved dinitrophenylhydrazine assay. *J Neurochem,* 70**,** 268-75.

FOLMES, C. D., NELSON, T. J., MARTINEZ-FERNANDEZ, A., ARRELL, D. K., LINDOR, J. Z., DZEJA, P. P., IKEDA, Y., PEREZ-TERZIC, C. & TERZIC, A. 2011. Somatic oxidative bioenergetics transitions into pluripotency-dependent glycolysis to facilitate nuclear reprogramming. *Cell Metab,* 14**,** 264-71.

FOMENKO, D. E., KOC, A., AGISHEVA, N., JACOBSEN, M., KAYA, A., MALINOUSKI, M., RUTHERFORD, J. C., SIU, K. L., JIN, D. Y., WINGE, D. R. & GLADYSHEV, V. N. 2011. Thiol peroxidases mediate specific genome-wide regulation of gene expression in response to hydrogen peroxide. *Proc Natl Acad Sci U S A,* 108**,** 2729-34.

FUKAYA, C. & YAMAMOTO, T. 2015. Deep Brain Stimulation for Parkinson's Disease: Recent Trends and Future Direction. *Neurol Med Chir (Tokyo).*

FUNAYAMA, M., OHE, K., AMO, T., FURUYA, N., YAMAGUCHI, J., SAIKI, S., LI, Y., OGAKI, K., ANDO, M., YOSHINO, H., TOMIYAMA, H., NISHIOKA, K., HASEGAWA, K., SAIKI, H., SATAKE, W., MOGUSHI, K., SASAKI, R., KOKUBO, Y., KUZUHARA, S., TODA, T., MIZUNO, Y., UCHIYAMA, Y., OHNO, K. & HATTORI, N. 2015. CHCHD2 mutations in autosomal dominant late-onset Parkinson's disease: a genome-wide linkage and sequencing study. *Lancet Neurol.*

GABELLINI, N. 2001. A polymorphic GT repeat from the human cardiac Na+Ca2+ exchanger intron 2 activates splicing. *Eur J Biochem,* 268**,** 1076-83.

GASSER, T. 2009. Molecular pathogenesis of Parkinson disease: insights from genetic studies. *Expert Rev Mol Med,* 11**,** e22.

GASSER, T., MULLER-MYHSOK, B., WSZOLEK, Z. K., OEHLMANN, R., CALNE, D. B., BONIFATI, V., BEREZNAI, B., FABRIZIO, E., VIEREGGE, P. & HORSTMANN, R. D. 1998. A susceptibility locus for Parkinson's disease maps to chromosome 2p13. *Nat Genet,* 18**,** 262-5.

GEISLER, S., HOLMSTROM, K. M., SKUJAT, D., FIESEL, F. C., ROTHFUSS, O. C., KAHLE, P. J. & SPRINGER, W. 2010. PINK1/Parkin-mediated mitophagy is dependent on VDAC1 and p62/SQSTM1. *Nat Cell Biol,* 12**,** 119-31.

GHAZAVI, F., FAZLALI, Z., BANIHOSSEINI, S. S., HOSSEINI, S. R., KAZEMI, M. H., SHOJAEE, S., PARSA, K., SADEGHI, H., SINA, F., ROHANI, M., SHAHIDI, G. A., GHAEMI, N., RONAGHI, M. & ELAHI, E. 2011. PRKN, DJ-1, and PINK1 screening identifies novel splice site mutation in PRKN and two novel DJ-1 mutations. *Mov Disord,* 26**,** 80-9.

GOLDBERG, M. S., PISANI, A., HABURCAK, M., VORTHERMS, T. A., KITADA, T., COSTA, C., TONG, Y., MARTELLA, G., TSCHERTER, A., MARTINS, A., BERNARDI, G., ROTH, B. L., POTHOS, E. N., CALABRESI, P. & SHEN, J. 2005. Nigrostriatal dopaminergic deficits and hypokinesia caused by inactivation of the familial Parkinsonism-linked gene DJ-1. *Neuron,* 45**,** 489-96.

GOLDWURM, S., DI FONZO, A., SIMONS, E. J., ROHE, C. F., ZINI, M., CANESI, M., TESEI, S., ZECCHINELLI, A., ANTONINI, A., MARIANI, C., MEUCCI, N., SACILOTTO, G., SIRONI, F., SALANI, G., FERREIRA, J., CHIEN, H. F., FABRIZIO, E., VANACORE, N., DALLA LIBERA, A., STOCCHI, F., DIROMA, C., LAMBERTI, P., SAMPAIO, C., MECO, G., BARBOSA, E., BERTOLI-AVELLA, A. M., BREEDVELD, G. J., OOSTRA, B. A., PEZZOLI, G. & BONIFATI, V. 2005. The G6055A (G2019S) mutation in LRRK2 is frequent in both early and late onset Parkinson's disease and originates from a common ancestor. *J Med Genet,* 42**,** e65.

GRAVELEY, B. R. 2000. Sorting out the complexity of SR protein functions. *RNA,* 6**,** 1197-211.

GREFFARD, S., VERNY, M., BONNET, A. M., BEINIS, J. Y., GALLINARI, C., MEAUME, S., PIETTE, F., HAUW, J. J. & DUYCKAERTS, C. 2006. Motor score of the Unified Parkinson Disease Rating Scale as a good predictor of Lewy body-associated neuronal loss in the substantia nigra. *Arch Neurol,* 63**,** 584-8.

GREGORY, A., KURIAN, M. A., MAHER, E. R., HOGARTH, P. & HAYFLICK, S. J. 1993. PLA2G6-Associated Neurodegeneration. *In:* PAGON, R. A., ADAM, M. P., ARDINGER, H. H., WALLACE, S. E., AMEMIYA, A., BEAN, L. J. H., BIRD, T. D., DOLAN, C. R., FONG, C. T., SMITH, R. J. H. & STEPHENS, K. (eds.) *GeneReviews(R).* Seattle (WA).

GUO, J. F., XIAO, B., LIAO, B., ZHANG, X. W., NIE, L. L., ZHANG, Y. H., SHEN, L., JIANG, H., XIA, K., PAN, Q., YAN, X. X. & TANG, B. S. 2008. Mutation analysis of Parkin, PINK1, DJ-1 and ATP13A2 genes in Chinese patients with autosomal recessive early-onset Parkinsonism. *Mov Disord,* 23**,** 2074-9.

HAAXMA, C. A., BLOEM, B. R., BORM, G. F., OYEN, W. J., LEENDERS, K. L., ESHUIS, S., BOOIJ, J., DLUZEN, D. E. & HORSTINK, M. W. 2007. Gender differences in Parkinson's disease. *J Neurol Neurosurg Psychiatry,* 78**,** 819-24.

HAGUE, S., ROGAEVA, E., HERNANDEZ, D., GULICK, C., SINGLETON, A., HANSON, M., JOHNSON, J., WEISER, R., GALLARDO, M., RAVINA, B., GWINN-HARDY, K., CRAWLEY, A., ST GEORGE-HYSLOP, P. H., LANG, A. E., HEUTINK, P., BONIFATI, V., HARDY, J. & SINGLETON, A. 2003. Early-onset Parkinson's disease caused by a compound heterozygous DJ-1 mutation. *Ann Neurol,* 54**,** 271-4.

HALLIDAY, G. M., DEL TREDICI, K. & BRAAK, H. 2006. Critical appraisal of brain pathology staging related to presymptomatic and symptomatic cases of sporadic Parkinson's disease. *J Neural Transm Suppl***,** 99-103.

5 References

HAO, L. Y., GIASSON, B. I. & BONINI, N. M. 2010. DJ-1 is critical for mitochondrial function and rescues PINK1 loss of function. *Proc Natl Acad Sci U S A,* 107**,** 9747-52.

HARDY, J., CAI, H., COOKSON, M. R., GWINN-HARDY, K. & SINGLETON, A. 2006. Genetics of Parkinson's disease and parkinsonism. *Ann Neurol,* 60**,** 389-98.

HAYASHI, T., ISHIMORI, C., TAKAHASHI-NIKI, K., TAIRA, T., KIM, Y. C., MAITA, H., MAITA, C., ARIGA, H. & IGUCHI-ARIGA, S. M. 2009. DJ-1 binds to mitochondrial complex I and maintains its activity. *Biochem Biophys Res Commun,* 390**,** 667-72.

HEDRICH, K., DJARMATI, A., SCHAFER, N., HERING, R., WELLENBROCK, C., WEISS, P. H., HILKER, R., VIEREGGE, P., OZELIUS, L. J., HEUTINK, P., BONIFATI, V., SCHWINGER, E., LANG, A. E., NOTH, J., BRESSMAN, S. B., PRAMSTALLER, P. P., RIESS, O. & KLEIN, C. 2004. DJ-1 (PARK7) mutations are less frequent than Parkin (PARK2) mutations in early-onset Parkinson disease. *Neurology,* 62**,** 389-94.

HERING, R., STRAUSS, K. M., TAO, X., BAUER, A., WOITALLA, D., MIETZ, E. M., PETROVIC, S., BAUER, P., SCHAIBLE, W., MULLER, T., SCHOLS, L., KLEIN, C., BERG, D., MEYER, P. T., SCHULZ, J. B., WOLLNIK, B., TONG, L., KRUGER, R. & RIESS, O. 2004. Novel homozygous p.E64D mutation in DJ1 in early onset Parkinson disease (PARK7). *Hum Mutat,* 24**,** 321-9.

HICKS, A. A., PETURSSON, H., JONSSON, T., STEFANSSON, H., JOHANNSDOTTIR, H. S., SAINZ, J., FRIGGE, M. L., KONG, A., GULCHER, J. R., STEFANSSON, K. & SVEINBJORNSDOTTIR, S. 2002. A susceptibility gene for late-onset idiopathic Parkinson's disease. *Ann Neurol,* 52**,** 549-55.

HO, S. C., WOO, J. & LEE, C. M. 1989. Epidemiologic study of Parkinson's disease in Hong Kong. *Neurology,* 39**,** 1314-8.

HOCKEMEYER, D., WANG, H., KIANI, S., LAI, C. S., GAO, Q., CASSADY, J. P., COST, G. J., ZHANG, L., SANTIAGO, Y., MILLER, J. C., ZEITLER, B., CHERONE, J. M., MENG, X., HINKLEY, S. J., REBAR, E. J., GREGORY, P. D., URNOV, F. D. & JAENISCH, R. 2011. Genetic engineering of human pluripotent cells using TALE nucleases. *Nat Biotechnol,* 29**,** 731-4.

HOLLENBECK, P. J. & SAXTON, W. M. 2005. The axonal transport of mitochondria. *J Cell Sci,* 118**,** 5411-9.

HONBOU, K., SUZUKI, N. N., HORIUCHI, M., NIKI, T., TAIRA, T., ARIGA, H. & INAGAKI, F. 2003. The crystal structure of DJ-1, a protein related to male fertility and Parkinson's disease. *J Biol Chem,* 278**,** 31380-4.

HUAI, Q., SUN, Y., WANG, H., CHIN, L. S., LI, L., ROBINSON, H. & KE, H. 2003. Crystal structure of DJ-1/RS and implication on familial Parkinson's disease. *FEBS Lett,* 549**,** 171-5.

HUANGFU, D., MAEHR, R., GUO, W., EIJKELENBOOM, A., SNITOW, M., CHEN, A. E. & MELTON, D. A. 2008. Induction of pluripotent stem cells by defined factors is greatly improved by small-molecule compounds. *Nat Biotechnol,* 26**,** 795-7.

HUGHES, A. J., DANIEL, S. E., KILFORD, L. & LEES, A. J. 1992. Accuracy of clinical diagnosis of idiopathic Parkinson's disease: a clinico-pathological study of 100 cases. *J Neurol Neurosurg Psychiatry,* 55**,** 181-4.

HULLEMAN, J. D., MIRZAEI, H., GUIGARD, E., TAYLOR, K. L., RAY, S. S., KAY, C. M., REGNIER, F. E. & ROCHET, J. C. 2007. Destabilization of DJ-1 by familial substitution and oxidative modifications: implications for Parkinson's disease. *Biochemistry,* 46**,** 5776-89.

IMAIZUMI, Y., OKADA, Y., AKAMATSU, W., KOIKE, M., KUZUMAKI, N., HAYAKAWA, H., NIHIRA, T., KOBAYASHI, T., OHYAMA, M., SATO, S., TAKANASHI, M., FUNAYAMA, M., HIRAYAMA, A., SOGA, T., HISHIKI, T., SUEMATSU, M., YAGI, T., ITO, D., KOSAKAI, A., HAYASHI, K., SHOUJI, M., NAKANISHI, A., SUZUKI, N., MIZUNO, Y., MIZUSHIMA, N., AMAGAI, M., UCHIYAMA, Y., MOCHIZUKI, H., HATTORI, N. & OKANO, H. 2012. Mitochondrial dysfunction associated with

increased oxidative stress and alpha-synuclein accumulation in PARK2 iPSC-derived neurons and postmortem brain tissue. *Mol Brain,* 5**,** 35.

IRRCHER, I., ALEYASIN, H., SEIFERT, E. L., HEWITT, S. J., CHHABRA, S., PHILLIPS, M., LUTZ, A. K., ROUSSEAUX, M. W., BEVILACQUA, L., JAHANI-ASL, A., CALLAGHAN, S., MACLAURIN, J. G., WINKLHOFER, K. F., RIZZU, P., RIPPSTEIN, P., KIM, R. H., CHEN, C. X., FON, E. A., SLACK, R. S., HARPER, M. E., MCBRIDE, H. M., MAK, T. W. & PARK, D. S. 2010. Loss of the Parkinson's disease-linked gene DJ-1 perturbs mitochondrial dynamics. *Hum Mol Genet,* 19**,** 3734-46.

ITZHAKI, I., MAIZELS, L., HUBER, I., ZWI-DANTSIS, L., CASPI, O., WINTERSTERN, A., FELDMAN, O., GEPSTEIN, A., ARBEL, G., HAMMERMAN, H., BOULOS, M. & GEPSTEIN, L. 2011. Modelling the long QT syndrome with induced pluripotent stem cells. *Nature,* 471**,** 225-9.

JANETZKY, B., HAUCK, S., YOUDIM, M. B., RIEDERER, P., JELLINGER, K., PANTUCEK, F., ZOCHLING, R., BOISSL, K. W. & REICHMANN, H. 1994. Unaltered aconitase activity, but decreased complex I activity in substantia nigra pars compacta of patients with Parkinson's disease. *Neurosci Lett,* 169**,** 126-8.

JELLINGER, K. A. & PAULUS, W. 1992. Clinico-pathological correlations in Parkinson's disease. *Clin Neurol Neurosurg,* 94 Suppl**,** S86-8.

JINEK, M., EAST, A., CHENG, A., LIN, S., MA, E. & DOUDNA, J. 2013. RNA-programmed genome editing in human cells. *Elife,* 2**,** e00471.

JOSE M. BRAS, P., GUERREIRO, R. J., TEO, J. T. H., DARWENT, L., VAUGHAN, J., MOLLOY, S., HARDY, J. & SCHNEIDER, S. A. 2014. Atypical Parkinsonism-Dystonia Syndrome Caused by a Novel DJ1 Mutation. *MOVEMENT DISORDERS CLINICAL PRACTICE***,** 45-49.

JUNN, E., JANG, W. H., ZHAO, X., JEONG, B. S. & MOURADIAN, M. M. 2009. Mitochondrial localization of DJ-1 leads to enhanced neuroprotection. *J Neurosci Res,* 87**,** 123-9.

JUNN, E., TANIGUCHI, H., JEONG, B. S., ZHAO, X., ICHIJO, H. & MOURADIAN, M. M. 2005. Interaction of DJ-1 with Daxx inhibits apoptosis signal-regulating kinase 1 activity and cell death. *Proc Natl Acad Sci U S A,* 102**,** 9691-6.

KALANTZI, O. I., ALCOCK, R. E., JOHNSTON, P. A., SANTILLO, D., STRINGER, R. L., THOMAS, G. O. & JONES, K. C. 2001. The global distribution of PCBs and organochlorine pesticides in butter. *Environ Sci Technol,* 35**,** 1013-8.

KASHIMA, T., RAO, N., DAVID, C. J. & MANLEY, J. L. 2007. hnRNP A1 functions with specificity in repression of SMN2 exon 7 splicing. *Hum Mol Genet,* 16**,** 3149-59.

KATO, I., MAITA, H., TAKAHASHI-NIKI, K., SAITO, Y., NOGUCHI, N., IGUCHI-ARIGA, S. M. & ARIGA, H. 2013. Oxidized DJ-1 inhibits p53 by sequestering p53 from promoters in a DNA-binding affinity-dependent manner. *Mol Cell Biol,* 33**,** 340-59.

KIM-HAN, J. S., ANTENOR-DORSEY, J. A. & O'MALLEY, K. L. 2011. The parkinsonian mimetic, MPP+, specifically impairs mitochondrial transport in dopamine axons. *J Neurosci,* 31**,** 7212-21.

KIM, R. H., PETERS, M., JANG, Y., SHI, W., PINTILIE, M., FLETCHER, G. C., DELUCA, C., LIEPA, J., ZHOU, L., SNOW, B., BINARI, R. C., MANOUKIAN, A. S., BRAY, M. R., LIU, F. F., TSAO, M. S. & MAK, T. W. 2005a. DJ-1, a novel regulator of the tumor suppressor PTEN. *Cancer Cell,* 7**,** 263-73.

KIM, R. H., SMITH, P. D., ALEYASIN, H., HAYLEY, S., MOUNT, M. P., POWNALL, S., WAKEHAM, A., YOU-TEN, A. J., KALIA, S. K., HORNE, P., WESTAWAY, D., LOZANO, A. M., ANISMAN, H., PARK, D. S. & MAK, T. W. 2005b. Hypersensitivity of DJ-1-deficient mice to 1-methyl-4-phenyl-1,2,3,6-tetrahydropyrindine (MPTP) and oxidative stress. *Proc Natl Acad Sci U S A,* 102**,** 5215-20.

KIM, Y., KWEON, J., KIM, A., CHON, J. K., YOO, J. Y., KIM, H. J., KIM, S., LEE, C., JEONG, E., CHUNG, E., KIM, D., LEE, M. S., GO, E. M., SONG, H. J., KIM, H.,

5 References

CHO, N., BANG, D., KIM, S. & KIM, J. S. 2013. A library of TAL effector nucleases spanning the human genome. *Nat Biotechnol,* 31**,** 251-8.

KIRIK, D., GEORGIEVSKA, B. & BJORKLUND, A. 2004. Localized striatal delivery of GDNF as a treatment for Parkinson disease. *Nat Neurosci, 7***,** 105-10.

KITADA, T. 1998. Mutations in the parkin gene cause autosomal recessive juvenile parkinsonism. *Nature, 392***,** 605-608.

KLEINER-FISMAN, G., FISMAN, D. N., SIME, E., SAINT-CYR, J. A., LOZANO, A. M. & LANG, A. E. 2003. Long-term follow up of bilateral deep brain stimulation of the subthalamic nucleus in patients with advanced Parkinson disease. *J Neurosurg,* 99**,** 489-95.

KNOTT, A. B. & BOSSY-WETZEL, E. 2008. Impairing the mitochondrial fission and fusion balance: a new mechanism of neurodegeneration. *Ann N Y Acad Sci,* 1147**,** 283-92.

KOIDE-YOSHIDA, S., NIKI, T., UEDA, M., HIMENO, S., TAIRA, T., IGUCHI-ARIGA, S. M., ANDO, Y. & ARIGA, H. 2007. DJ-1 degrades transthyretin and an inactive form of DJ-1 is secreted in familial amyloidotic polyneuropathy. *Int J Mol Med,* 19**,** 885-93.

KRAWCZAK, M., THOMAS, N. S., HUNDRIESER, B., MORT, M., WITTIG, M., HAMPE, J. & COOPER, D. N. 2007. Single base-pair substitutions in exon-intron junctions of human genes: nature, distribution, and consequences for mRNA splicing. *Hum Mutat,* 28**,** 150-8.

KREBIEHL, G., RUCKERBAUER, S., BURBULLA, L. F., KIEPER, N., MAURER, B., WAAK, J., WOLBURG, H., GIZATULLINA, Z., GELLERICH, F. N., WOITALLA, D., RIESS, O., KAHLE, P. J., PROIKAS-CEZANNE, T. & KRUGER, R. 2010. Reduced basal autophagy and impaired mitochondrial dynamics due to loss of Parkinson's disease-associated protein DJ-1. *PLoS One, 5***,** e9367.

KRECIC, A. M. & SWANSON, M. S. 1999. hnRNP complexes: composition, structure, and function. *Curr Opin Cell Biol, 11***,** 363-71.

KRIKS, S., SHIM, J. W., PIAO, J., GANAT, Y. M., WAKEMAN, D. R., XIE, Z., CARRILLO-REID, L., AUYEUNG, G., ANTONACCI, C., BUCH, A., YANG, L., BEAL, M. F., SURMEIER, D. J., KORDOWER, J. H., TABAR, V. & STUDER, L. 2011. Dopamine neurons derived from human ES cells efficiently engraft in animal models of Parkinson's disease. *Nature,* 480**,** 547-51.

KRUGER, R., VIEIRA-SAECKER, A. M., KUHN, W., BERG, D., MULLER, T., KUHNL, N., FUCHS, G. A., STORCH, A., HUNGS, M., WOITALLA, D., PRZUNTEK, H., EPPLEN, J. T., SCHOLS, L. & RIESS, O. 1999. Increased susceptibility to sporadic Parkinson's disease by a certain combined alpha-synuclein/apolipoprotein E genotype. *Ann Neurol,* 45**,** 611-7.

KUJOTH, G. C., HIONA, A., PUGH, T. D., SOMEYA, S., PANZER, K., WOHLGEMUTH, S. E., HOFER, T., SEO, A. Y., SULLIVAN, R., JOBLING, W. A., MORROW, J. D., VAN REMMEN, H., SEDIVY, J. M., YAMASOBA, T., TANOKURA, M., WEINDRUCH, R., LEEUWENBURGH, C. & PROLLA, T. A. 2005. Mitochondrial DNA mutations, oxidative stress, and apoptosis in mammalian aging. *Science,* 309**,** 481-4.

LAMOND, A. I. 1993. The spliceosome. *Bioessays, 15***,** 595-603.

LANGSTON, J. W., BALLARD, P., TETRUD, J. W. & IRWIN, I. 1983. Chronic Parkinsonism in humans due to a product of meperidine-analog synthesis. *Science,* 219**,** 979-980.

LARSSON, N. G. 2010. Somatic mitochondrial DNA mutations in mammalian aging. *Annu Rev Biochem, 79***,** 683-706.

LAUTIER, C., GOLDWURM, S., DURR, A., GIOVANNONE, B., TSIARAS, W. G., PEZZOLI, G., BRICE, A. & SMITH, R. J. 2008. Mutations in the GIGYF2 (TNRC15) gene at the PARK11 locus in familial Parkinson disease. *Am J Hum Genet,* 82**,** 822-33.

LEE, C. S., SAMII, A., SOSSI, V., RUTH, T. J., SCHULZER, M., HOLDEN, J. E., WUDEL, J., PAL, P. K., DE LA FUENTE-FERNANDEZ, R., CALNE, D. B. & STOESSL, A. J. 2000. In vivo positron emission tomographic evidence for compensatory changes in presynaptic dopaminergic nerve terminals in Parkinson's disease. *Ann Neurol,* 47**,** 493-503.

LEE, G., PAPAPETROU, E. P., KIM, H., CHAMBERS, S. M., TOMISHIMA, M. J., FASANO, C. A., GANAT, Y. M., MENON, J., SHIMIZU, F., VIALE, A., TABAR, V., SADELAIN, M. & STUDER, L. 2009. Modelling pathogenesis and treatment of familial dysautonomia using patient-specific iPSCs. *Nature,* 461**,** 402-6.

LEE, G., RAMIREZ, C. N., KIM, H., ZELTNER, N., LIU, B., RADU, C., BHINDER, B., KIM, Y. J., CHOI, I. Y., MUKHERJEE-CLAVIN, B., DJABALLAH, H. & STUDER, L. 2012a. Large-scale screening using familial dysautonomia induced pluripotent stem cells identifies compounds that rescue IKBKAP expression. *Nat Biotechnol,* 30**,** 1244-8.

LEE, J. Y., SONG, J., KWON, K., JANG, S., KIM, C., BAEK, K., KIM, J. & PARK, C. 2012b. Human DJ-1 and its homologs are novel glyoxalases. *Hum Mol Genet,* 21**,** 3215-25.

LEE, S. J., KIM, S. J., KIM, I. K., KO, J., JEONG, C. S., KIM, G. H., PARK, C., KANG, S. O., SUH, P. G., LEE, H. S. & CHA, S. S. 2003. Crystal structures of human DJ-1 and Escherichia coli Hsp31, which share an evolutionarily conserved domain. *J Biol Chem,* 278**,** 44552-9.

LEHLE, S., HILDEBRAND, D. G., MERZ, B., MALAK, P. N., BECKER, M. S., SCHMEZER, P., ESSMANN, F., SCHULZE-OSTHOFF, K. & ROTHFUSS, O. 2014. LORD-Q: a long-run real-time PCR-based DNA-damage quantification method for nuclear and mitochondrial genome analysis. *Nucleic Acids Res,* 42**,** e41.

LEROY, E., BOYER, R., AUBURGER, G., LEUBE, B., ULM, G., MEZEY, E., HARTA, G., BROWNSTEIN, M. J., JONNALAGADA, S., CHERNOVA, T., DEHEJIA, A., LAVEDAN, C., GASSER, T., STEINBACH, P. J., WILKINSON, K. D. & POLYMEROPOULOS, M. H. 1998. The ubiquitin pathway in Parkinson's disease. *Nature,* 395**,** 451-2.

LEV, N., ICKOWICZ, D., MELAMED, E. & OFFEN, D. 2008. Oxidative insults induce DJ-1 upregulation and redistribution: implications for neuroprotection. *Neurotoxicology,* 29**,** 397-405.

LEWY, F. H. 1912. Handbuch der Neurologie.

LI, M., SUZUKI, K., KIM, N. Y., LIU, G. H. & IZPISUA BELMONTE, J. C. 2014. A cut above the rest: targeted genome editing technologies in human pluripotent stem cells. *J Biol Chem,* 289**,** 4594-9.

LI, Y., TOMIYAMA, H., SATO, K., HATANO, Y., YOSHINO, H., ATSUMI, M., KITAGUCHI, M., SASAKI, S., KAWAGUCHI, S., MIYAJIMA, H., TODA, T., MIZUNO, Y. & HATTORI, N. 2005. Clinicogenetic study of PINK1 mutations in autosomal recessive early-onset parkinsonism. *Neurology,* 64**,** 1955-7.

LI, Z., OKAMOTO, K., HAYASHI, Y. & SHENG, M. 2004. The importance of dendritic mitochondria in the morphogenesis and plasticity of spines and synapses. *Cell,* 119**,** 873-87.

LIANG, C. L., WANG, T. T., LUBY-PHELPS, K. & GERMAN, D. C. 2007. Mitochondria mass is low in mouse substantia nigra dopamine neurons: implications for Parkinson's disease. *Exp Neurol,* 203**,** 370-80.

LIN, S. & FU, X. D. 2007. SR proteins and related factors in alternative splicing. *Adv Exp Med Biol,* 623**,** 107-22.

LITTLE, J. P., SAFDAR, A., BENTON, C. R. & WRIGHT, D. C. 2011. Skeletal muscle and beyond: the role of exercise as a mediator of systemic mitochondrial biogenesis. *Appl Physiol Nutr Metab,* 36**,** 598-607.

LOCKHART, P. J., LINCOLN, S., HULIHAN, M., KACHERGUS, J., WILKES, K., BISCEGLIO, G., MASH, D. C. & FARRER, M. J. 2004. DJ-1 mutations are a rare

cause of recessively inherited early onset parkinsonism mediated by loss of protein function. *J Med Genet,* 41**,** e22.

LOPEZ-BIGAS, N., AUDIT, B., OUZOUNIS, C., PARRA, G. & GUIGO, R. 2005. Are splicing mutations the most frequent cause of hereditary disease? *FEBS Lett,* 579**,** 1900-3.

LORSON, C. L., HAHNEN, E., ANDROPHY, E. J. & WIRTH, B. 1999. A single nucleotide in the SMN gene regulates splicing and is responsible for spinal muscular atrophy. *Proc Natl Acad Sci U S A,* 96**,** 6307-11.

LOTHARIUS, J. & BRUNDIN, P. 2002. Pathogenesis of Parkinson's disease: dopamine, vesicles and alpha-synuclein. *Nat Rev Neurosci,* 3**,** 932-42.

LUCAS, J. I. & MARIN, I. 2007. A new evolutionary paradigm for the Parkinson disease gene DJ-1. *Mol Biol Evol,* 24**,** 551-61.

LUCKING, C. B., DURR, A., BONIFATI, V., VAUGHAN, J., DE MICHELE, G., GASSER, T., HARHANGI, B. S., MECO, G., DENEFLE, P., WOOD, N. W., AGID, Y., BRICE, A., FRENCH PARKINSON'S DISEASE GENETICS STUDY, G. & EUROPEAN CONSORTIUM ON GENETIC SUSCEPTIBILITY IN PARKINSON'S, D. 2000. Association between early-onset Parkinson's disease and mutations in the parkin gene. *N Engl J Med,* 342**,** 1560-7.

LUTZ, A. K., EXNER, N., FETT, M. E., SCHLEHE, J. S., KLOOS, K., LAMMERMANN, K., BRUNNER, B., KURZ-DREXLER, A., VOGEL, F., REICHERT, A. S., BOUMAN, L., VOGT-WEISENHORN, D., WURST, W., TATZELT, J., HAASS, C. & WINKLHOFER, K. F. 2009. Loss of parkin or PINK1 function increases Drp1-dependent mitochondrial fragmentation. *J Biol Chem,* 284**,** 22938-51.

MA, S. Y., ROYTTA, M., RINNE, J. O., COLLAN, Y. & RINNE, U. K. 1997. Correlation between neuromorphometry in the substantia nigra and clinical features in Parkinson's disease using disector counts. *J Neurol Sci,* 151**,** 83-7.

MACEDO, M. G., VERBAAN, D., FANG, Y., VAN ROODEN, S. M., VISSER, M., ANAR, B., URAS, A., GROEN, J. L., RIZZU, P., VAN HILTEN, J. J. & HEUTINK, P. 2009. Genotypic and phenotypic characteristics of Dutch patients with early onset Parkinson's disease. *Mov Disord,* 24**,** 196-203.

MACLEOD, A. D., TAYLOR, K. S. & COUNSELL, C. E. 2014. Mortality in Parkinson's disease: a systematic review and meta-analysis. *Mov Disord,* 29**,** 1615-22.

MACLEOD, D., DOWMAN, J., HAMMOND, R., LEETE, T., INOUE, K. & ABELIOVICH, A. 2006. The familial Parkinsonism gene LRRK2 regulates neurite process morphology. *Neuron,* 52**,** 587-93.

MADHANI, H. D. & GUTHRIE, C. 1994. Dynamic RNA-RNA interactions in the spliceosome. *Annu Rev Genet,* 28**,** 1-26.

MALI, P., YANG, L., ESVELT, K. M., AACH, J., GUELL, M., DICARLO, J. E., NORVILLE, J. E. & CHURCH, G. M. 2013. RNA-guided human genome engineering via Cas9. *Science,* 339**,** 823-6.

MALIK, N., EFTHYMIOU, A. G., MATHER, K., CHESTER, N., WANG, X., NATH, A., RAO, M. S. & STEINER, J. P. 2014. Compounds with species and cell type specific toxicity identified in a 2000 compound drug screen of neural stem cells and rat mixed cortical neurons. *Neurotoxicology,* 45**,** 192-200.

MANN, V. M., COOPER, J. M., DANIEL, S. E., SRAI, K., JENNER, P., MARSDEN, C. D. & SCHAPIRA, A. H. 1994. Complex I, iron, and ferritin in Parkinson's disease substantia nigra. *Ann Neurol,* 36**,** 876-81.

MANOLIO, T. A., COLLINS, F. S., COX, N. J., GOLDSTEIN, D. B., HINDORFF, L. A., HUNTER, D. J., MCCARTHY, M. I., RAMOS, E. M., CARDON, L. R., CHAKRAVARTI, A., CHO, J. H., GUTTMACHER, A. E., KONG, A., KRUGLYAK, L., MARDIS, E., ROTIMI, C. N., SLATKIN, M., VALLE, D., WHITTEMORE, A. S., BOEHNKE, M., CLARK, A. G., EICHLER, E. E., GIBSON, G., HAINES, J. L., MACKAY, T. F., MCCARROLL, S. A. & VISSCHER, P. M. 2009. Finding the missing heritability of complex diseases. *Nature,* 461**,** 747-53.

MARCHETTO, M. C., CARROMEU, C., ACAB, A., YU, D., YEO, G. W., MU, Y., CHEN, G., GAGE, F. H. & MUOTRI, A. R. 2010. A model for neural development and treatment of Rett syndrome using human induced pluripotent stem cells. *Cell,* 143**,** 527-39.

MARTINEZ-CONTRERAS, R., CLOUTIER, P., SHKRETA, L., FISETTE, J. F., REVIL, T. & CHABOT, B. 2007. hnRNP proteins and splicing control. *Adv Exp Med Biol,* 623**,** 123-47.

MASUI, S., NAKATAKE, Y., TOYOOKA, Y., SHIMOSATO, D., YAGI, R., TAKAHASHI, K., OKOCHI, H., OKUDA, A., MATOBA, R., SHAROV, A. A., KO, M. S. & NIWA, H. 2007. Pluripotency governed by Sox2 via regulation of Oct3/4 expression in mouse embryonic stem cells. *Nat Cell Biol,* 9**,** 625-35.

MAUGER, D. M., LIN, C. & GARCIA-BLANCO, M. A. 2008. hnRNP H and hnRNP F complex with Fox2 to silence fibroblast growth factor receptor 2 exon IIIc. *Mol Cell Biol,* 28**,** 5403-19.

MENOTTA, M., BIAGIOTTI, S., BIANCHI, M., CHESSA, L. & MAGNANI, M. 2012. Dexamethasone partially rescues ataxia telangiectasia-mutated (ATM) deficiency in ataxia telangiectasia by promoting a shortened protein variant retaining kinase activity. *J Biol Chem,* 287**,** 41352-63.

MENZIES, F. M., YENISETTI, S. C. & MIN, K. T. 2005. Roles of Drosophila DJ-1 in survival of dopaminergic neurons and oxidative stress. *Curr Biol,* 15**,** 1578-82.

MEULENER, M., WHITWORTH, A. J., ARMSTRONG-GOLD, C. E., RIZZU, P., HEUTINK, P., WES, P. D., PALLANCK, L. J. & BONINI, N. M. 2005. Drosophila DJ-1 mutants are selectively sensitive to environmental toxins associated with Parkinson's disease. *Curr Biol,* 15**,** 1572-7.

MEULENER, M. C., XU, K., THOMSON, L., ISCHIROPOULOS, H. & BONINI, N. M. 2006. Mutational analysis of DJ-1 in Drosophila implicates functional inactivation by oxidative damage and aging. *Proc Natl Acad Sci U S A,* 103**,** 12517-22.

MILLER, J. D., GANAT, Y. M., KISHINEVSKY, S., BOWMAN, R. L., LIU, B., TU, E. Y., MANDAL, P. K., VERA, E., SHIM, J. W., KRIKS, S., TALDONE, T., FUSAKI, N., TOMISHIMA, M. J., KRAINC, D., MILNER, T. A., ROSSI, D. J. & STUDER, L. 2013. Human iPSC-based modeling of late-onset disease via progerin-induced aging. *Cell Stem Cell,* 13**,** 691-705.

MIZUNO, Y., OHTA, S., TANAKA, M., TAKAMIYA, S., SUZUKI, K., SATO, T., OYA, H., OZAWA, T. & KAGAWA, Y. 1989. Deficiencies in complex I subunits of the respiratory chain in Parkinson's disease. *Biochem Biophys Res Commun,* 163**,** 1450-5.

MOHAMMAD ALINOOR RAHMAN, F. N., AKIO MASUDA, KINJI OHNO 2015. Decoding abnormal splicing code in human diseases. *Journal of Investigative Genomics,* 2.

MONANI, U. R., LORSON, C. L., PARSONS, D. W., PRIOR, T. W., ANDROPHY, E. J., BURGHES, A. H. & MCPHERSON, J. D. 1999. A single nucleotide difference that alters splicing patterns distinguishes the SMA gene SMN1 from the copy gene SMN2. *Hum Mol Genet,* 8**,** 1177-83.

MOORE, D. J., ZHANG, L., DAWSON, T. M. & DAWSON, V. L. 2003. A missense mutation (L166P) in DJ-1, linked to familial Parkinson's disease, confers reduced protein stability and impairs homo-oligomerization. *J Neurochem,* 87**,** 1558-67.

MOORE, D. J., ZHANG, L., TRONCOSO, J., LEE, M. K., HATTORI, N., MIZUNO, Y., DAWSON, T. M. & DAWSON, V. L. 2005. Association of DJ-1 and parkin mediated by pathogenic DJ-1 mutations and oxidative stress. *Hum Mol Genet,* 14**,** 71-84.

MORETTI, A., BELLIN, M., WELLING, A., JUNG, C. B., LAM, J. T., BOTT-FLUGEL, L., DORN, T., GOEDEL, A., HOHNKE, C., HOFMANN, F., SEYFARTH, M., SINNECKER, D., SCHOMIG, A. & LAUGWITZ, K. L. 2010. Patient-specific induced pluripotent stem-cell models for long-QT syndrome. *N Engl J Med,* 363**,** 1397-409.

MORTIBOYS, H., THOMAS, K. J., KOOPMAN, W. J., KLAFFKE, S., ABOU-SLEIMAN, P., OLPIN, S., WOOD, N. W., WILLEMS, P. H., SMEITINK, J. A., COOKSON, M. R. & BANDMANN, O. 2008. Mitochondrial function and morphology are impaired in parkin-mutant fibroblasts. *Ann Neurol,* 64**,** 555-65.

MOSCOU, M. J. & BOGDANOVE, A. J. 2009. A simple cipher governs DNA recognition by TAL effectors. *Science,* 326**,** 1501.

MUANGPAISAN, W., MATHEWS, A., HORI, H. & SEIDEL, D. 2011. A systematic review of the worldwide prevalence and incidence of Parkinson's disease. *J Med Assoc Thai,* 94**,** 749-55.

MULLETT, S. J. & HINKLE, D. A. 2011. DJ-1 deficiency in astrocytes selectively enhances mitochondrial Complex I inhibitor-induced neurotoxicity. *J Neurochem,* 117**,** 375-87.

NAGAKUBO, D., TAIRA, T., KITAURA, H., IKEDA, M., TAMAI, K., IGUCHI-ARIGA, S. M. & ARIGA, H. 1997. DJ-1, a novel oncogene which transforms mouse NIH3T3 cells in cooperation with ras. *Biochem Biophys Res Commun,* 231**,** 509-13.

NAKAI, K. & SAKAMOTO, H. 1994. Construction of a novel database containing aberrant splicing mutations of mammalian genes. *Gene,* 141**,** 171-7.

NALLS, M. A. 2011. Imputation of sequence variants for identification of genetic risks for Parkinson's disease: a meta-analysis of genome-wide association studies. *Lancet,* 377**,** 641-649.

NALLS, M. A., PANKRATZ, N., LILL, C. M., DO, C. B., HERNANDEZ, D. G., SAAD, M., DESTEFANO, A. L., KARA, E., BRAS, J., SHARMA, M., SCHULTE, C., KELLER, M. F., AREPALLI, S., LETSON, C., EDSALL, C., STEFANSSON, H., LIU, X., PLINER, H., LEE, J. H., CHENG, R., INTERNATIONAL PARKINSON'S DISEASE GENOMICS, C., PARKINSON'S STUDY GROUP PARKINSON'S RESEARCH: THE ORGANIZED, G. I., ANDME, GENEPD, NEUROGENETICS RESEARCH, C., HUSSMAN INSTITUTE OF HUMAN, G., ASHKENAZI JEWISH DATASET, I., COHORTS FOR, H., AGING RESEARCH IN GENETIC, E., NORTH AMERICAN BRAIN EXPRESSION, C., UNITED KINGDOM BRAIN EXPRESSION, C., GREEK PARKINSON'S DISEASE, C., ALZHEIMER GENETIC ANALYSIS, G., IKRAM, M. A., IOANNIDIS, J. P., HADJIGEORGIOU, G. M., BIS, J. C., MARTINEZ, M., PERLMUTTER, J. S., GOATE, A., MARDER, K., FISKE, B., SUTHERLAND, M., XIROMERISIOU, G., MYERS, R. H., CLARK, L. N., STEFANSSON, K., HARDY, J. A., HEUTINK, P., CHEN, H., WOOD, N. W., HOULDEN, H., PAYAMI, H., BRICE, A., SCOTT, W. K., GASSER, T., BERTRAM, L., ERIKSSON, N., FOROUD, T. & SINGLETON, A. B. 2014. Large-scale meta-analysis of genome-wide association data identifies six new risk loci for Parkinson's disease. *Nat Genet,* 46**,** 989-93.

NARENDRA, D., TANAKA, A., SUEN, D. F. & YOULE, R. J. 2008. Parkin is recruited selectively to impaired mitochondria and promotes their autophagy. *J Cell Biol,* 183**,** 795-803.

NARENDRA, D. P., JIN, S. M., TANAKA, A., SUEN, D. F., GAUTIER, C. A., SHEN, J., COOKSON, M. R. & YOULE, R. J. 2010. PINK1 is selectively stabilized on impaired mitochondria to activate Parkin. *PLoS Biol,* 8**,** e1000298.

NEUMANN, M., MULLER, V., GORNER, K., KRETZSCHMAR, H. A., HAASS, C. & KAHLE, P. J. 2004. Pathological properties of the Parkinson's disease-associated protein DJ-1 in alpha-synucleinopathies and tauopathies: relevance for multiple system atrophy and Pick's disease. *Acta Neuropathol,* 107**,** 489-96.

NGUYEN, H. N., BYERS, B., CORD, B., SHCHEGLOVITOV, A., BYRNE, J., GUJAR, P., KEE, K., SCHULE, B., DOLMETSCH, R. E., LANGSTON, W., PALMER, T. D. & PERA, R. R. 2011. LRRK2 mutant iPSC-derived DA neurons demonstrate increased susceptibility to oxidative stress. *Cell Stem Cell,* 8**,** 267-80.

NICKLAS, W. J., VYAS, I. & HEIKKILA, R. E. 1985. Inhibition of NADH-linked oxidation in brain mitochondria by 1-methyl-4-phenyl-pyridine, a metabolite of the neurotoxin, 1-methyl-4-phenyl-1,2,5,6-tetrahydropyridine. *Life Sci,* 36**,** 2503-8.

NIKI, T., TAKAHASHI-NIKI, K., TAIRA, T., IGUCHI-ARIGA, S. M. & ARIGA, H. 2003. DJBP: a novel DJ-1-binding protein, negatively regulates the androgen receptor by recruiting histone deacetylase complex, and DJ-1 antagonizes this inhibition by abrogation of this complex. *Mol Cancer Res,* 1**,** 247-61.

NILSEN, T. W. 1994. RNA-RNA interactions in the spliceosome: unraveling the ties that bind. *Cell,* 78**,** 1-4.

NIWA, H., MIYAZAKI, J. & SMITH, A. G. 2000. Quantitative expression of Oct-3/4 defines differentiation, dedifferentiation or self-renewal of ES cells. *Nat Genet,* 24**,** 372-6.

NUYTEMANS, K., THEUNS, J., CRUTS, M. & VAN BROECKHOVEN, C. 2010. Genetic etiology of Parkinson disease associated with mutations in the SNCA, PARK2, PINK1, PARK7, and LRRK2 genes: a mutation update. *Hum Mutat,* 31**,** 763-80.

OLSEN, A., SIBOSKA, G. E., CLARK, B. F. & RATTAN, S. I. 1999. N(6)-Furfuryladenine, kinetin, protects against Fenton reaction-mediated oxidative damage to DNA. *Biochem Biophys Res Commun,* 265**,** 499-502.

OLZMANN, J. A., BROWN, K., WILKINSON, K. D., REES, H. D., HUAI, Q., KE, H., LEVEY, A. I., LI, L. & CHIN, L. S. 2004. Familial Parkinson's disease-associated L166P mutation disrupts DJ-1 protein folding and function. *J Biol Chem,* 279**,** 8506-15.

ORSUCCI, D., CALDARAZZO IENCO, E., MANCUSO, M. & SICILIANO, G. 2011. POLG1-related and other "mitochondrial Parkinsonisms": an overview. *J Mol Neurosci,* 44**,** 17-24.

OTTOLINI, D., CALI, T., NEGRO, A. & BRINI, M. 2013. The Parkinson disease-related protein DJ-1 counteracts mitochondrial impairment induced by the tumour suppressor protein p53 by enhancing endoplasmic reticulum-mitochondria tethering. *Hum Mol Genet,* 22**,** 2152-68.

PAGANI, F., BURATTI, E., STUANI, C., ROMANO, M., ZUCCATO, E., NIKSIC, M., GIGLIO, L., FARAGUNA, D. & BARALLE, F. E. 2000. Splicing factors induce cystic fibrosis transmembrane regulator exon 9 skipping through a nonevolutionary conserved intronic element. *J Biol Chem,* 275**,** 21041-7.

PAISAN-RUIZ, C., BHATIA, K. P., LI, A., HERNANDEZ, D., DAVIS, M., WOOD, N. W., HARDY, J., HOULDEN, H., SINGLETON, A. & SCHNEIDER, S. A. 2009. Characterization of PLA2G6 as a locus for dystonia-parkinsonism. *Ann Neurol,* 65**,** 19-23.

PAN, Q., SHAI, O., LEE, L. J., FREY, B. J. & BLENCOWE, B. J. 2008. Deep surveying of alternative splicing complexity in the human transcriptome by high-throughput sequencing. *Nat Genet,* 40**,** 1413-5.

PANKRATZ, N., NICHOLS, W. C., UNIACKE, S. K., HALTER, C., RUDOLPH, A., SHULTS, C., CONNEALLY, P. M., FOROUD, T. & PARKINSON STUDY, G. 2002. Genome screen to identify susceptibility genes for Parkinson disease in a sample without parkin mutations. *Am J Hum Genet,* 71**,** 124-35.

PARK, I. H., ARORA, N., HUO, H., MAHERALI, N., AHFELDT, T., SHIMAMURA, A., LENSCH, M. W., COWAN, C., HOCHEDLINGER, K. & DALEY, G. Q. 2008. Disease-specific induced pluripotent stem cells. *Cell,* 134**,** 877-86.

PARK, J., KIM, S. Y., CHA, G. H., LEE, S. B., KIM, S. & CHUNG, J. 2005. Drosophila DJ-1 mutants show oxidative stress-sensitive locomotive dysfunction. *Gene,* 361**,** 133-9.

PARKER, W. D., JR., PARKS, J. K. & SWERDLOW, R. H. 2008. Complex I deficiency in Parkinson's disease frontal cortex. *Brain Res,* 1189**,** 215-8.

PARKINSON, J. 2002. An essay on the shaking palsy. 1817. *J. Neuropsychiatry Clin. Neurosci.,* 14**,** 223-236.

PERIER, C., BENDER, A., GARCIA-ARUMI, E., MELIA, M. J., BOVE, J., LAUB, C., KLOPSTOCK, T., ELSTNER, M., MOUNSEY, R. B., TEISMANN, P., PROLLA, T., ANDREU, A. L. & VILA, M. 2013. Accumulation of mitochondrial DNA

deletions within dopaminergic neurons triggers neuroprotective mechanisms. *Brain,* 136**,** 2369-78.

PESCE, M. & SCHOLER, H. R. 2001. Oct-4: gatekeeper in the beginnings of mammalian development. *Stem Cells,* 19**,** 271-8.

PHAM, T. T., GIESERT, F., ROTHIG, A., FLOSS, T., KALLNIK, M., WEINDL, K., HOLTER, S. M., AHTING, U., PROKISCH, H., BECKER, L., KLOPSTOCK, T., HRABE DE ANGELIS, M., BEYER, K., GORNER, K., KAHLE, P. J., VOGT WEISENHORN, D. M. & WURST, W. 2010. DJ-1-deficient mice show less TH-positive neurons in the ventral tegmental area and exhibit non-motoric behavioural impairments. *Genes Brain Behav,* 9**,** 305-17.

PICCONI, B., PICCOLI, G. & CALABRESI, P. 2012. Synaptic dysfunction in Parkinson's disease. *Adv Exp Med Biol,* 970**,** 553-72.

PISSADAKI, E. K. & BOLAM, J. P. 2013. The energy cost of action potential propagation in dopamine neurons: clues to susceptibility in Parkinson's disease. *Front Comput Neurosci,* 7**,** 13.

POLYMEROPOULOS, M. H. 1997. Mutation in the α-synuclein gene identified in families with Parkinson's disease. *Science,* 276**,** 2045-2047.

POOLE, A. C., THOMAS, R. E., ANDREWS, L. A., MCBRIDE, H. M., WHITWORTH, A. J. & PALLANCK, L. J. 2008. The PINK1/Parkin pathway regulates mitochondrial morphology. *Proc Natl Acad Sci U S A,* 105**,** 1638-43.

PRIGIONE, A. & CORTOPASSI, G. 2007. Mitochondrial DNA deletions induce the adenosine monophosphate-activated protein kinase energy stress pathway and result in decreased secretion of some proteins. *Aging Cell,* 6**,** 619-30.

PRIGIONE, A., FAULER, B., LURZ, R., LEHRACH, H. & ADJAYE, J. 2010. The senescence-related mitochondrial/oxidative stress pathway is repressed in human induced pluripotent stem cells. *Stem Cells,* 28**,** 721-33.

PRINGSHEIM, T., JETTE, N., FROLKIS, A. & STEEVES, T. D. 2014. The prevalence of Parkinson's disease: a systematic review and meta-analysis. *Mov Disord,* 29**,** 1583-90.

PROS, E., FERNANDEZ-RODRIGUEZ, J., BENITO, L., RAVELLA, A., CAPELLA, G., BLANCO, I., SERRA, E. & LAZARO, C. 2010. Modulation of aberrant NF1 pre-mRNA splicing by kinetin treatment. *Eur J Hum Genet,* 18**,** 614-7.

QUADRI, M., FANG, M., PICILLO, M., OLGIATI, S., BREEDVELD, G. J., GRAAFLAND, J., WU, B., XU, F., ERRO, R., AMBONI, M., PAPPATA, S., QUARANTELLI, M., ANNESI, G., QUATTRONE, A., CHIEN, H. F., BARBOSA, E. R., INTERNATIONAL PARKINSONISM GENETICS, N., OOSTRA, B. A., BARONE, P., WANG, J. & BONIFATI, V. 2013. Mutation in the SYNJ1 gene associated with autosomal recessive, early-onset Parkinsonism. *Hum Mutat,* 34**,** 1208-15.

RAHMAN, M., NASRIN, F., MASUDA, A. & OHNO, K. 2015. Decoding Abnormal Splicing Code in Human Diseases. *Journal of Investigative Genomics,* 2.

RAMIREZ, A., HEIMBACH, A., GRUNDEMANN, J., STILLER, B., HAMPSHIRE, D., CID, L. P., GOEBEL, I., MUBAIDIN, A. F., WRIEKAT, A. L., ROEPER, J., AL-DIN, A., HILLMER, A. M., KARSAK, M., LISS, B., WOODS, C. G., BEHRENS, M. I. & KUBISCH, C. 2006. Hereditary parkinsonism with dementia is caused by mutations in ATP13A2, encoding a lysosomal type 5 P-type ATPase. *Nat Genet,* 38**,** 1184-91.

RAO, M. S. & MALIK, N. 2012. Assessing iPSC reprogramming methods for their suitability in translational medicine. *J Cell Biochem,* 113**,** 3061-8.

RASMUSSEN R., M. S., WITTWER,C. AND NAKAGAWARA,K. 2001. *Rapid Cycle Real-Time PCR: Methods and Applications. Quantification on the LightCycler instrument.,* Heidelberg, Springer Press.

RATTAN, S. I. & CLARK, B. F. 1994. Kinetin delays the onset of ageing characteristics in human fibroblasts. *Biochem Biophys Res Commun,* 201**,** 665-72.

REEVE, A., SIMCOX, E. & TURNBULL, D. 2014. Ageing and Parkinson's disease: why is advancing age the biggest risk factor? *Ageing Res Rev,* 14**,** 19-30.

REEVE, A. K., KRISHNAN, K. J. & TURNBULL, D. 2008. Mitochondrial DNA mutations in disease, aging, and neurodegeneration. *Ann N Y Acad Sci,* 1147**,** 21-9.

REINHARDT, P., GLATZA, M., HEMMER, K., TSYTSYURA, Y., THIEL, C. S., HOING, S., MORITZ, S., PARGA, J. A., WAGNER, L., BRUDER, J. M., WU, G., SCHMID, B., ROPKE, A., KLINGAUF, J., SCHWAMBORN, J. C., GASSER, T., SCHOLER, H. R. & STERNECKERT, J. 2013a. Derivation and expansion using only small molecules of human neural progenitors for neurodegenerative disease modeling. *PLoS One,* 8**,** e59252.

REINHARDT, P., SCHMID, B., BURBULLA, L. F., SCHONDORF, D. C., WAGNER, L., GLATZA, M., HOING, S., HARGUS, G., HECK, S. A., DHINGRA, A., WU, G., MULLER, S., BROCKMANN, K., KLUBA, T., MAISEL, M., KRUGER, R., BERG, D., TSYTSYURA, Y., THIEL, C. S., PSATHAKI, O. E., KLINGAUF, J., KUHLMANN, T., KLEWIN, M., MULLER, H., GASSER, T., SCHOLER, H. R. & STERNECKERT, J. 2013b. Genetic correction of a LRRK2 mutation in human iPSCs links parkinsonian neurodegeneration to ERK-dependent changes in gene expression. *Cell Stem Cell,* 12**,** 354-67.

RIZZU, P., HINKLE, D. A., ZHUKAREVA, V., BONIFATI, V., SEVERIJNEN, L. A., MARTINEZ, D., RAVID, R., KAMPHORST, W., EBERWINE, J. H., LEE, V. M., TROJANOWSKI, J. Q. & HEUTINK, P. 2004. DJ-1 colocalizes with tau inclusions: a link between parkinsonism and dementia. *Ann Neurol,* 55**,** 113-8.

ROCA, X., SACHIDANANDAM, R. & KRAINER, A. R. 2003. Intrinsic differences between authentic and cryptic 5' splice sites. *Nucleic Acids Res,* 31**,** 6321-33.

ROGAEVA, E., JOHNSON, J., LANG, A. E., GULICK, C., GWINN-HARDY, K., KAWARAI, T., SATO, C., MORGAN, A., WERNER, J., NUSSBAUM, R., PETIT, A., OKUN, M. S., MCINERNEY, A., MANDEL, R., GROEN, J. L., FERNANDEZ, H. H., POSTUMA, R., FOOTE, K. D., SALEHI-RAD, S., LIANG, Y., REIMSNIDER, S., TANDON, A., HARDY, J., ST GEORGE-HYSLOP, P. & SINGLETON, A. B. 2004. Analysis of the PINK1 gene in a large cohort of cases with Parkinson disease. *Arch Neurol,* 61**,** 1898-904.

RONY, I. K., BATEN, A., BLOOMFIELD, J. A., ISLAM, M. E., BILLAH, M. M. & ISLAM, K. D. 2015. Inducing pluripotency in vitro: recent advances and highlights in induced pluripotent stem cells generation and pluripotency reprogramming. *Cell Prolif,* 48**,** 140-56.

ROSS, G. W. & ABBOTT, R. D. 2014. Living and dying with Parkinson's disease. *Mov Disord,* 29**,** 1571-3.

ROSS, G. W., ABBOTT, R. D., PETROVITCH, H., MORENS, D. M., GRANDINETTI, A., TUNG, K. H., TANNER, C. M., MASAKI, K. H., BLANCHETTE, P. L., CURB, J. D., POPPER, J. S. & WHITE, L. R. 2000. Association of coffee and caffeine intake with the risk of Parkinson disease. *JAMA,* 283**,** 2674-9.

ROUSSEAUX, M. W., MARCOGLIESE, P. C., QU, D., HEWITT, S. J., SEANG, S., KIM, R. H., SLACK, R. S., SCHLOSSMACHER, M. G., LAGACE, D. C., MAK, T. W. & PARK, D. S. 2012. Progressive dopaminergic cell loss with unilateral-to-bilateral progression in a genetic model of Parkinson disease. *Proc Natl Acad Sci U S A,* 109**,** 15918-23.

SAHASHI, K., MASUDA, A., MATSUURA, T., SHINMI, J., ZHANG, Z., TAKESHIMA, Y., MATSUO, M., SOBUE, G. & OHNO, K. 2007. In vitro and in silico analysis reveals an efficient algorithm to predict the splicing consequences of mutations at the 5' splice sites. *Nucleic Acids Res,* 35**,** 5995-6003.

SAHIN, E. & DEPINHO, R. A. 2010. Linking functional decline of telomeres, mitochondria and stem cells during ageing. *Nature,* 464**,** 520-8.

SAKLA, M. S. & LORSON, C. L. 2008. Induction of full-length survival motor neuron by polyphenol botanical compounds. *Hum Genet,* 122**,** 635-43.

SANCHEZ-DANES, A., RICHAUD-PATIN, Y., CARBALLO-CARBAJAL, I., JIMENEZ-DELGADO, S., CAIG, C., MORA, S., DI GUGLIELMO, C., EZQUERRA, M., PATEL, B., GIRALT, A., CANALS, J. M., MEMO, M., ALBERCH, J., LOPEZ-

BARNEO, J., VILA, M., CUERVO, A. M., TOLOSA, E., CONSIGLIO, A. & RAYA, A. 2012. Disease-specific phenotypes in dopamine neurons from human iPS-based models of genetic and sporadic Parkinson's disease. *EMBO Mol Med,* 4**,** 380-95.

SANGER, F., NICKLEN, S. & COULSON, A. R. 1977. DNA sequencing with chain-terminating inhibitors. *Proc Natl Acad Sci U S A,* 74**,** 5463-7.

SARRAF, S. A., RAMAN, M., GUARANI-PEREIRA, V., SOWA, M. E., HUTTLIN, E. L., GYGI, S. P. & HARPER, J. W. 2013. Landscape of the PARKIN-dependent ubiquitylome in response to mitochondrial depolarization. *Nature,* 496**,** 372-6.

SATAKE, W., NAKABAYASHI, Y., MIZUTA, I., HIROTA, Y., ITO, C., KUBO, M., KAWAGUCHI, T., TSUNODA, T., WATANABE, M., TAKEDA, A., TOMIYAMA, H., NAKASHIMA, K., HASEGAWA, K., OBATA, F., YOSHIKAWA, T., KAWAKAMI, H., SAKODA, S., YAMAMOTO, M., HATTORI, N., MURATA, M., NAKAMURA, Y. & TODA, T. 2009. Genome-wide association study identifies common variants at four loci as genetic risk factors for Parkinson's disease. *Nat Genet,* 41**,** 1303-7.

SAXTON, W. M. & HOLLENBECK, P. J. 2012. The axonal transport of mitochondria. *J Cell Sci,* 125**,** 2095-104.

SAYRE, L. M., PERRY, G. & SMITH, M. A. 2008. Oxidative stress and neurotoxicity. *Chem Res Toxicol,* 21**,** 172-88.

SCHAPIRA, A. H. 1999. Mitochondria in the aetiology and pathogenesis of Parkinson's disease. *Parkinsonism Relat Disord,* 5**,** 139-43.

SCHAPIRA, A. H. 2008. Mitochondria in the aetiology and pathogenesis of Parkinson's disease. *Lancet Neurol,* 7**,** 97-109.

SCHAPIRA, A. H., COOPER, J. M., DEXTER, D., CLARK, J. B., JENNER, P. & MARSDEN, C. D. 1990. Mitochondrial complex I deficiency in Parkinson's disease. *J Neurochem,* 54**,** 823-7.

SCHAPIRA, A. H., COOPER, J. M., DEXTER, D., JENNER, P., CLARK, J. B. & MARSDEN, C. D. 1989. Mitochondrial complex I deficiency in Parkinson's disease. *Lancet,* 1**,** 1269.

SCHONDORF, D. C., AURELI, M., MCALLISTER, F. E., HINDLEY, C. J., MAYER, F., SCHMID, B., SARDI, S. P., VALSECCHI, M., HOFFMANN, S., SCHWARZ, L. K., HEDRICH, U., BERG, D., SHIHABUDDIN, L. S., HU, J., PRUSZAK, J., GYGI, S. P., SONNINO, S., GASSER, T. & DELEIDI, M. 2014. iPSC-derived neurons from GBA1-associated Parkinson's disease patients show autophagic defects and impaired calcium homeostasis. *Nat Commun,* 5**,** 4028.

SCHWARZ, J. M., RODELSPERGER, C., SCHUELKE, M. & SEELOW, D. 2010. MutationTaster evaluates disease-causing potential of sequence alterations. *Nat Methods,* 7**,** 575-6.

SEIBLER, P., GRAZIOTTO, J., JEONG, H., SIMUNOVIC, F., KLEIN, C. & KRAINC, D. 2011. Mitochondrial Parkin recruitment is impaired in neurons derived from mutant PINK1 induced pluripotent stem cells. *J Neurosci,* 31**,** 5970-6.

SEKITO, A., KOIDE-YOSHIDA, S., NIKI, T., TAIRA, T., IGUCHI-ARIGA, S. M. & ARIGA, H. 2006. DJ-1 interacts with HIPK1 and affects H2O2-induced cell death. *Free Radic Res,* 40**,** 155-65.

SHAPIRO, M. B. & SENAPATHY, P. 1987. RNA splice junctions of different classes of eukaryotes: sequence statistics and functional implications in gene expression. *Nucleic Acids Res,* 15**,** 7155-74.

SHARMA, S. P., KAUR, P. & RATTAN, S. I. 1995. Plant growth hormone kinetin delays ageing, prolongs the lifespan and slows down development of the fruitfly Zaprionus paravittiger. *Biochem Biophys Res Commun,* 216**,** 1067-71.

SHEN, H. & GREEN, M. R. 2004. A pathway of sequential arginine-serine-rich domain-splicing signal interactions during mammalian spliceosome assembly. *Mol Cell,* 16**,** 363-73.

SHEN, H., KAN, J. L. & GREEN, M. R. 2004. Arginine-serine-rich domains bound at splicing enhancers contact the branchpoint to promote prespliceosome assembly. *Mol Cell,* 13**,** 367-76.

SHENDELMAN, S., JONASON, A., MARTINAT, C., LEETE, T. & ABELIOVICH, A. 2004. DJ-1 is a redox-dependent molecular chaperone that inhibits alpha-synuclein aggregate formation. *PLoS Biol,* 2**,** e362.

SHENG, C., HENG, X., ZHANG, G., XIONG, R., LI, H., ZHANG, S. & CHEN, S. 2013. DJ-1 deficiency perturbs microtubule dynamics and impairs striatal neurite outgrowth. *Neurobiol Aging,* 34**,** 489-98.

SHINBO, Y., TAIRA, T., NIKI, T., IGUCHI-ARIGA, S. M. & ARIGA, H. 2005. DJ-1 restores p53 transcription activity inhibited by Topors/p53BP3. *Int J Oncol,* 26**,** 641-8.

SHINO, M. Y., MCGUIRE, V., VAN DEN EEDEN, S. K., TANNER, C. M., POPAT, R., LEIMPETER, A., BERNSTEIN, A. L. & NELSON, L. M. 2010. Familial aggregation of Parkinson's disease in a multiethnic community-based case-control study. *Mov Disord,* 25**,** 2587-94.

SIDRANSKY, E., NALLS, M. A., AASLY, J. O., AHARON-PERETZ, J., ANNESI, G., BARBOSA, E. R., BAR-SHIRA, A., BERG, D., BRAS, J., BRICE, A., CHEN, C. M., CLARK, L. N., CONDROYER, C., DE MARCO, E. V., DURR, A., EBLAN, M. J., FAHN, S., FARRER, M. J., FUNG, H. C., GAN-OR, Z., GASSER, T., GERSHONI-BARUCH, R., GILADI, N., GRIFFITH, A., GUREVICH, T., JANUARIO, C., KROPP, P., LANG, A. E., LEE-CHEN, G. J., LESAGE, S., MARDER, K., MATA, I. F., MIRELMAN, A., MITSUI, J., MIZUTA, I., NICOLETTI, G., OLIVEIRA, C., OTTMAN, R., ORR-URTREGER, A., PEREIRA, L. V., QUATTRONE, A., ROGAEVA, E., ROLFS, A., ROSENBAUM, H., ROZENBERG, R., SAMII, A., SAMADDAR, T., SCHULTE, C., SHARMA, M., SINGLETON, A., SPITZ, M., TAN, E. K., TAYEBI, N., TODA, T., TROIANO, A. R., TSUJI, S., WITTSTOCK, M., WOLFSBERG, T. G., WU, Y. R., ZABETIAN, C. P., ZHAO, Y. & ZIEGLER, S. G. 2009. Multicenter analysis of glucocerebrosidase mutations in Parkinson's disease. *N Engl J Med,* 361**,** 1651-61.

SIM, C. H., LIO, D. S., MOK, S. S., MASTERS, C. L., HILL, A. F., CULVENOR, J. G. & CHENG, H. C. 2006. C-terminal truncation and Parkinson's disease-associated mutations down-regulate the protein serine/threonine kinase activity of PTEN-induced kinase-1. *Hum Mol Genet,* 15**,** 3251-62.

SIMON-SANCHEZ, J., SCHULTE, C., BRAS, J. M., SHARMA, M., GIBBS, J. R., BERG, D., PAISAN-RUIZ, C., LICHTNER, P., SCHOLZ, S. W., HERNANDEZ, D. G., KRUGER, R., FEDEROFF, M., KLEIN, C., GOATE, A., PERLMUTTER, J., BONIN, M., NALLS, M. A., ILLIG, T., GIEGER, C., HOULDEN, H., STEFFENS, M., OKUN, M. S., RACETTE, B. A., COOKSON, M. R., FOOTE, K. D., FERNANDEZ, H. H., TRAYNOR, B. J., SCHREIBER, S., AREPALLI, S., ZONOZI, R., GWINN, K., VAN DER BRUG, M., LOPEZ, G., CHANOCK, S. J., SCHATZKIN, A., PARK, Y., HOLLENBECK, A., GAO, J., HUANG, X., WOOD, N. W., LORENZ, D., DEUSCHL, G., CHEN, H., RIESS, O., HARDY, J. A., SINGLETON, A. B. & GASSER, T. 2009. Genome-wide association study reveals genetic risk underlying Parkinson's disease. *Nat Genet,* 41**,** 1308-12.

SINGLETON, A. B., FARRER, M., JOHNSON, J., SINGLETON, A., HAGUE, S., KACHERGUS, J., HULIHAN, M., PEURALINNA, T., DUTRA, A., NUSSBAUM, R., LINCOLN, S., CRAWLEY, A., HANSON, M., MARAGANORE, D., ADLER, C., COOKSON, M. R., MUENTER, M., BAPTISTA, M., MILLER, D., BLANCATO, J., HARDY, J. & GWINN-HARDY, K. 2003. alpha-Synuclein locus triplication causes Parkinson's disease. *Science,* 302**,** 841.

SINGLETON, A. B., FARRER, M. J. & BONIFATI, V. 2013. The genetics of Parkinson's disease: progress and therapeutic implications. *Mov Disord,* 28**,** 14-23.

SLAUGENHAUPT, S. A., BLUMENFELD, A., GILL, S. P., LEYNE, M., MULL, J., CUAJUNGCO, M. P., LIEBERT, C. B., CHADWICK, B., IDELSON, M., REZNIK,

5 References

L., ROBBINS, C., MAKALOWSKA, I., BROWNSTEIN, M., KRAPPMANN, D., SCHEIDEREIT, C., MAAYAN, C., AXELROD, F. B. & GUSELLA, J. F. 2001. Tissue-specific expression of a splicing mutation in the IKBKAP gene causes familial dysautonomia. *Am J Hum Genet,* 68**,** 598-605.

SLAUGENHAUPT, S. A., MULL, J., LEYNE, M., CUAJUNGCO, M. P., GILL, S. P., HIMS, M. M., QUINTERO, F., AXELROD, F. B. & GUSELLA, J. F. 2004. Rescue of a human mRNA splicing defect by the plant cytokinin kinetin. *Hum Mol Genet,* 13**,** 429-36.

SMITH, P. J., ZHANG, C., WANG, J., CHEW, S. L., ZHANG, M. Q. & KRAINER, A. R. 2006. An increased specificity score matrix for the prediction of SF2/ASF-specific exonic splicing enhancers. *Hum Mol Genet,* 15**,** 2490-508.

SOKOLOFF, L., REIVICH, M., KENNEDY, C., DES ROSIERS, M. H., PATLAK, C. S., PETTIGREW, K. D., SAKURADA, O. & SHINOHARA, M. 1977. The [14C]deoxyglucose method for the measurement of local cerebral glucose utilization: theory, procedure, and normal values in the conscious and anesthetized albino rat. *J Neurochem,* 28**,** 897-916.

SOLDNER, F., HOCKEMEYER, D., BEARD, C., GAO, Q., BELL, G. W., COOK, E. G., HARGUS, G., BLAK, A., COOPER, O., MITALIPOVA, M., ISACSON, O. & JAENISCH, R. 2009. Parkinson's disease patient-derived induced pluripotent stem cells free of viral reprogramming factors. *Cell,* 136**,** 964-77.

SOLDNER, F., LAGANIERE, J., CHENG, A. W., HOCKEMEYER, D., GAO, Q., ALAGAPPAN, R., KHURANA, V., GOLBE, L. I., MYERS, R. H., LINDQUIST, S., ZHANG, L., GUSCHIN, D., FONG, L. K., VU, B. J., MENG, X., URNOV, F. D., REBAR, E. J., GREGORY, P. D., ZHANG, H. S. & JAENISCH, R. 2011. Generation of isogenic pluripotent stem cells differing exclusively at two early onset Parkinson point mutations. *Cell,* 146**,** 318-31.

SPILLANTINI, M. G., SCHMIDT, M. L., LEE, V. M., TROJANOWSKI, J. Q., JAKES, R. & GOEDERT, M. 1997. Alpha-synuclein in Lewy bodies. *Nature,* 388**,** 839-40.

STENSON, P. D., BALL, E. V., MORT, M., PHILLIPS, A. D., SHIEL, J. A., THOMAS, N. S., ABEYSINGHE, S., KRAWCZAK, M. & COOPER, D. N. 2003. Human Gene Mutation Database (HGMD): 2003 update. *Hum Mutat,* 21**,** 577-81.

STERKY, F. H., LEE, S., WIBOM, R., OLSON, L. & LARSSON, N. G. 2011. Impaired mitochondrial transport and Parkin-independent degeneration of respiratory chain-deficient dopamine neurons in vivo. *Proc Natl Acad Sci U S A,* 108**,** 12937-42.

STERN, G. 1989. Did parkinsonism occur before 1817? *J Neurol Neurosurg Psychiatry,* Suppl**,** 11-2.

STRAUSS, K. M., MARTINS, L. M., PLUN-FAVREAU, H., MARX, F. P., KAUTZMANN, S., BERG, D., GASSER, T., WSZOLEK, Z., MULLER, T., BORNEMANN, A., WOLBURG, H., DOWNWARD, J., RIESS, O., SCHULZ, J. B. & KRUGER, R. 2005. Loss of function mutations in the gene encoding Omi/HtrA2 in Parkinson's disease. *Hum Mol Genet,* 14**,** 2099-111.

SUGIOKA, K., NAKANO, M., TOTSUNE-NAKANO, H., MINAKAMI, H., TERO-KUBOTA, S. & IKEGAMI, Y. 1988. Mechanism of O2- generation in reduction and oxidation cycle of ubiquinones in a model of mitochondrial electron transport systems. *Biochim Biophys Acta,* 936**,** 377-85.

SUHR, S. T., CHANG, E. A., TJONG, J., ALCASID, N., PERKINS, G. A., GOISSIS, M. D., ELLISMAN, M. H., PEREZ, G. I. & CIBELLI, J. B. 2010. Mitochondrial rejuvenation after induced pluripotency. *PLoS One,* 5**,** e14095.

SULZER, D., BOGULAVSKY, J., LARSEN, K. E., BEHR, G., KARATEKIN, E., KLEINMAN, M. H., TURRO, N., KRANTZ, D., EDWARDS, R. H., GREENE, L. A. & ZECCA, L. 2000. Neuromelanin biosynthesis is driven by excess cytosolic catecholamines not accumulated by synaptic vesicles. *Proc Natl Acad Sci U S A,* 97**,** 11869-74.

SUMNER, C. J., HUYNH, T. N., MARKOWITZ, J. A., PERHAC, J. S., HILL, B., COOVERT, D. D., SCHUSSLER, K., CHEN, X., JARECKI, J., BURGHES, A. H., TAYLOR, J. P. & FISCHBECK, K. H. 2003. Valproic acid increases SMN levels in spinal muscular atrophy patient cells. *Ann Neurol,* 54**,** 647-54.

SUN, H. & CHASIN, L. A. 2000. Multiple splicing defects in an intronic false exon. *Mol Cell Biol,* 20**,** 6414-25.

TAIRA, T., IGUCHI-ARIGA, S. M. & ARIGA, H. 2004a. Co-localization with DJ-1 is essential for the androgen receptor to exert its transcription activity that has been impaired by androgen antagonists. *Biol Pharm Bull,* 27**,** 574-7.

TAIRA, T., SAITO, Y., NIKI, T., IGUCHI-ARIGA, S. M., TAKAHASHI, K. & ARIGA, H. 2004b. DJ-1 has a role in antioxidative stress to prevent cell death. *EMBO Rep,* 5**,** 213-8.

TAKAHASHI, K., TAIRA, T., NIKI, T., SEINO, C., IGUCHI-ARIGA, S. M. & ARIGA, H. 2001. DJ-1 positively regulates the androgen receptor by impairing the binding of PIASx alpha to the receptor. *J Biol Chem,* 276**,** 37556-63.

TAKAHASHI, K., TANABE, K., OHNUKI, M., NARITA, M., ICHISAKA, T., TOMODA, K. & YAMANAKA, S. 2007. Induction of pluripotent stem cells from adult human fibroblasts by defined factors. *Cell,* 131**,** 861-72.

TAKAHASHI, K. & YAMANAKA, S. 2006. Induction of pluripotent stem cells from mouse embryonic and adult fibroblast cultures by defined factors. *Cell,* 126**,** 663-76.

TANG, B., XIONG, H., SUN, P., ZHANG, Y., WANG, D., HU, Z., ZHU, Z., MA, H., PAN, Q., XIA, J. H., XIA, K. & ZHANG, Z. 2006. Association of PINK1 and DJ-1 confers digenic inheritance of early-onset Parkinson's disease. *Hum Mol Genet,* 15**,** 1816-25.

TAO, X. & TONG, L. 2003. Crystal structure of human DJ-1, a protein associated with early onset Parkinson's disease. *J Biol Chem,* 278**,** 31372-9.

THOMAS, K. J., MCCOY, M. K., BLACKINTON, J., BEILINA, A., VAN DER BRUG, M., SANDEBRING, A., MILLER, D., MARIC, D., CEDAZO-MINGUEZ, A. & COOKSON, M. R. 2011. DJ-1 acts in parallel to the PINK1/parkin pathway to control mitochondrial function and autophagy. *Hum Mol Genet,* 20**,** 40-50.

TILLMAN, J. E., YUAN, J., GU, G., FAZLI, L., GHOSH, R., FLYNT, A. S., GLEAVE, M., RENNIE, P. S. & KASPER, S. 2007. DJ-1 binds androgen receptor directly and mediates its activity in hormonally treated prostate cancer cells. *Cancer Res,* 67**,** 4630-7.

TRETIAKOFF, C. 1919. Contribution a l'etude de l'anatomie pathologique du locus niger de Soemmering avec quelques deductions relatives a la athogenie des troubles du tonus musculaire et de la maladie de Parkinson.

TRIFUNOVIC, A., WREDENBERG, A., FALKENBERG, M., SPELBRINK, J. N., ROVIO, A. T., BRUDER, C. E., BOHLOOLY, Y. M., GIDLOF, S., OLDFORS, A., WIBOM, R., TORNELL, J., JACOBS, H. T. & LARSSON, N. G. 2004. Premature ageing in mice expressing defective mitochondrial DNA polymerase. *Nature,* 429**,** 417-23.

TRINH, J. & FARRER, M. 2013. Advances in the genetics of Parkinson disease. *Nat Rev Neurol,* 9**,** 445-54.

TURRENS, J. F. & BOVERIS, A. 1980. Generation of superoxide anion by the NADH dehydrogenase of bovine heart mitochondria. *Biochem J,* 191**,** 421-7.

TWELVES, D., PERKINS, K. S. & COUNSELL, C. 2003. Systematic review of incidence studies of Parkinson's disease. *Mov Disord,* 18**,** 19-31.

ULE, J., STEFANI, G., MELE, A., RUGGIU, M., WANG, X., TANERI, B., GAASTERLAND, T., BLENCOWE, B. J. & DARNELL, R. B. 2006. An RNA map predicting Nova-dependent splicing regulation. *Nature,* 444**,** 580-6.

ULMER, T. S., BAX, A., COLE, N. B. & NUSSBAUM, R. L. 2005. Structure and dynamics of micelle-bound human alpha-synuclein. *J Biol Chem,* 280**,** 9595-603.

VALENTE, E. M., ABOU-SLEIMAN, P. M., CAPUTO, V., MUQIT, M. M., HARVEY, K., GISPERT, S., ALI, Z., DEL TURCO, D., BENTIVOGLIO, A. R., HEALY, D. G., ALBANESE, A., NUSSBAUM, R., GONZALEZ-MALDONADO, R., DELLER, T.,

5 References

SALVI, S., CORTELLI, P., GILKS, W. P., LATCHMAN, D. S., HARVEY, R. J., DALLAPICCOLA, B., AUBURGER, G. & WOOD, N. W. 2004a. Hereditary early-onset Parkinson's disease caused by mutations in PINK1. *Science,* 304**,** 1158-60.

VALENTE, E. M., SALVI, S., IALONGO, T., MARONGIU, R., ELIA, A. E., CAPUTO, V., ROMITO, L., ALBANESE, A., DALLAPICCOLA, B. & BENTIVOGLIO, A. R. 2004b. PINK1 mutations are associated with sporadic early-onset parkinsonism. *Ann Neurol,* 56**,** 336-41.

VALKO, M., IZAKOVIC, M., MAZUR, M., RHODES, C. J. & TELSER, J. 2004. Role of oxygen radicals in DNA damage and cancer incidence. *Mol Cell Biochem,* 266**,** 37-56.

VAN DEN EEDEN, S. K., TANNER, C. M., BERNSTEIN, A. L., FROSS, R. D., LEIMPETER, A., BLOCH, D. A. & NELSON, L. M. 2003. Incidence of Parkinson's disease: variation by age, gender, and race/ethnicity. *Am J Epidemiol,* 157**,** 1015-22.

VAN LAAR, V. S. & BERMAN, S. B. 2013. The interplay of neuronal mitochondrial dynamics and bioenergetics: implications for Parkinson's disease. *Neurobiol Dis,* 51**,** 43-55.

VARUM, S., RODRIGUES, A. S., MOURA, M. B., MOMCILOVIC, O., EASLEY, C. A. T., RAMALHO-SANTOS, J., VAN HOUTEN, B. & SCHATTEN, G. 2011. Energy metabolism in human pluripotent stem cells and their differentiated counterparts. *PLoS One,* 6**,** e20914.

VED, R., SAHA, S., WESTLUND, B., PERIER, C., BURNAM, L., SLUDER, A., HOENER, M., RODRIGUES, C. M., ALFONSO, A., STEER, C., LIU, L., PRZEDBORSKI, S. & WOLOZIN, B. 2005. Similar patterns of mitochondrial vulnerability and rescue induced by genetic modification of alpha-synuclein, parkin, and DJ-1 in Caenorhabditis elegans. *J Biol Chem,* 280**,** 42655-68.

VILARINO-GUELL, C., RAJPUT, A., MILNERWOOD, A. J., SHAH, B., SZU-TU, C., TRINH, J., YU, I., ENCARNACION, M., MUNSIE, L. N., TAPIA, L., GUSTAVSSON, E. K., CHOU, P., TATARNIKOV, I., EVANS, D. M., PISHOTTA, F. T., VOLTA, M., BECCANO-KELLY, D., THOMPSON, C., LIN, M. K., SHERMAN, H. E., HAN, H. J., GUENTHER, B. L., WASSERMAN, W. W., BERNARD, V., ROSS, C. J., APPEL-CRESSWELL, S., STOESSL, A. J., ROBINSON, C. A., DICKSON, D. W., ROSS, O. A., WSZOLEK, Z. K., AASLY, J. O., WU, R. M., HENTATI, F., GIBSON, R. A., MCPHERSON, P. S., GIRARD, M., RAJPUT, M., RAJPUT, A. H. & FARRER, M. J. 2014. DNAJC13 mutations in Parkinson disease. *Hum Mol Genet,* 23**,** 1794-801.

VOGEL, G. 2010. Stem cells. Diseases in a dish take off. *Science,* 330**,** 1172-3.

VON CAMPENHAUSEN, S., BORNSCHEIN, B., WICK, R., BOTZEL, K., SAMPAIO, C., POEWE, W., OERTEL, W., SIEBERT, U., BERGER, K. & DODEL, R. 2005. Prevalence and incidence of Parkinson's disease in Europe. *Eur Neuropsychopharmacol,* 15**,** 473-90.

WAGENFELD, A., GROMOLL, J. & COOPER, T. G. 1998. Molecular cloning and expression of rat contraception associated protein 1 (CAP1), a protein putatively involved in fertilization. *Biochem Biophys Res Commun,* 251**,** 545-9.

WANG, E. T., SANDBERG, R., LUO, S., KHREBTUKOVA, I., ZHANG, L., MAYR, C., KINGSMORE, S. F., SCHROTH, G. P. & BURGE, C. B. 2008. Alternative isoform regulation in human tissue transcriptomes. *Nature,* 456**,** 470-6.

WANG, Y., MA, M., XIAO, X. & WANG, Z. 2012a. Intronic splicing enhancers, cognate splicing factors and context-dependent regulation rules. *Nat Struct Mol Biol,* 19**,** 1044-52.

WANG, Y., NARTISS, Y., STEIPE, B., MCQUIBBAN, G. A. & KIM, P. K. 2012b. ROS-induced mitochondrial depolarization initiates PARK2/PARKIN-dependent mitochondrial degradation by autophagy. *Autophagy,* 8**,** 1462-76.

WEI, Y. H. 1998. Oxidative stress and mitochondrial DNA mutations in human aging. *Proc Soc Exp Biol Med,* 217**,** 53-63.

WEI, Z., YANG, Y., ZHANG, P., ANDRIANAKOS, R., HASEGAWA, K., LYU, J., CHEN, X., BAI, G., LIU, C., PERA, M. & LU, W. 2009. Klf4 interacts directly with Oct4 and Sox2 to promote reprogramming. *Stem Cells,* 27**,** 2969-78.

WEISSCHUH, N., WISSINGER, B. & GRAMER, E. 2012. A splice site mutation in the PAX6 gene which induces exon skipping causes autosomal dominant inherited aniridia. *Mol Vis,* 18**,** 751-7.

WELCH, J. E., BARBEE, R. R., ROBERTS, N. L., SUAREZ, J. D. & KLINEFELTER, G. R. 1998. SP22: a novel fertility protein from a highly conserved gene family. *J Androl,* 19**,** 385-93.

WESTERLUND, M., HOFFER, B. & OLSON, L. 2010. Parkinson's disease: Exit toxins, enter genetics. *Prog Neurobiol,* 90**,** 146-56.

WILSON, M. A., COLLINS, J. L., HOD, Y., RINGE, D. & PETSKO, G. A. 2003. The 1.1-A resolution crystal structure of DJ-1, the protein mutated in autosomal recessive early onset Parkinson's disease. *Proc Natl Acad Sci U S A,* 100**,** 9256-61.

WILSON, M. A., RINGE, D. & PETSKO, G. A. 2005. The atomic resolution crystal structure of the YajL (ThiJ) protein from Escherichia coli: a close prokaryotic homologue of the Parkinsonism-associated protein DJ-1. *J Mol Biol,* 353**,** 678-91.

WINKLER-STUCK, K., WIEDEMANN, F. R., WALLESCH, C. W. & KUNZ, W. S. 2004. Effect of coenzyme Q10 on the mitochondrial function of skin fibroblasts from Parkinson patients. *J Neurol Sci,* 220**,** 41-8.

XU, J., ZHONG, N., WANG, H., ELIAS, J. E., KIM, C. Y., WOLDMAN, I., PIFL, C., GYGI, S. P., GEULA, C. & YANKNER, B. A. 2005. The Parkinson's disease-associated DJ-1 protein is a transcriptional co-activator that protects against neuronal apoptosis. *Hum Mol Genet,* 14**,** 1231-41.

YAHATA, N., ASAI, M., KITAOKA, S., TAKAHASHI, K., ASAKA, I., HIOKI, H., KANEKO, T., MARUYAMA, K., SAIDO, T. C., NAKAHATA, T., ASADA, T., YAMANAKA, S., IWATA, N. & INOUE, H. 2011. Anti-Abeta drug screening platform using human iPS cell-derived neurons for the treatment of Alzheimer's disease. *PLoS One,* 6**,** e25788.

YAKES, F. M. & VAN HOUTEN, B. 1997. Mitochondrial DNA damage is more extensive and persists longer than nuclear DNA damage in human cells following oxidative stress. *Proc Natl Acad Sci U S A,* 94**,** 514-9.

YAMAGUCHI, H. & SHEN, J. 2007. Absence of dopaminergic neuronal degeneration and oxidative damage in aged DJ-1-deficient mice. *Mol Neurodegener,* 2**,** 10.

YANG, Y., GEHRKE, S., HAQUE, M. E., IMAI, Y., KOSEK, J., YANG, L., BEAL, M. F., NISHIMURA, I., WAKAMATSU, K., ITO, S., TAKAHASHI, R. & LU, B. 2005. Inactivation of Drosophila DJ-1 leads to impairments of oxidative stress response and phosphatidylinositol 3-kinase/Akt signaling. *Proc Natl Acad Sci U S A,* 102**,** 13670-5.

YAZAWA, M., HSUEH, B., JIA, X., PASCA, A. M., BERNSTEIN, J. A., HALLMAYER, J. & DOLMETSCH, R. E. 2011. Using induced pluripotent stem cells to investigate cardiac phenotypes in Timothy syndrome. *Nature,* 471**,** 230-4.

YEO, G. W., COUFAL, N. G., LIANG, T. Y., PENG, G. E., FU, X. D. & GAGE, F. H. 2009. An RNA code for the FOX2 splicing regulator revealed by mapping RNA-protein interactions in stem cells. *Nat Struct Mol Biol,* 16**,** 130-7.

YOKOTA, T., SUGAWARA, K., ITO, K., TAKAHASHI, R., ARIGA, H. & MIZUSAWA, H. 2003. Down regulation of DJ-1 enhances cell death by oxidative stress, ER stress, and proteasome inhibition. *Biochem Biophys Res Commun,* 312**,** 1342-8.

YOULE, R. J. & VAN DER BLIEK, A. M. 2012. Mitochondrial fission, fusion, and stress. *Science,* 337**,** 1062-5.

YU, W., SUN, Y., GUO, S. & LU, B. 2011. The PINK1/Parkin pathway regulates mitochondrial dynamics and function in mammalian hippocampal and dopaminergic neurons. *Hum Mol Genet,* 20**,** 3227-40.

ZHANG, L., SHIMOJI, M., THOMAS, B., MOORE, D. J., YU, S. W., MARUPUDI, N. I., TORP, R., TORGNER, I. A., OTTERSEN, O. P., DAWSON, T. M. & DAWSON,

V. L. 2005. Mitochondrial localization of the Parkinson's disease related protein DJ-1: implications for pathogenesis. *Hum Mol Genet,* 14**,** 2063-73.

ZHENG, G. Q. 2009. Therapeutic history of Parkinson's disease in Chinese medical treatises. *J Altern Complement Med,* 15**,** 1223-30.

ZHOU, P., QIAN, L., CHOU, T. & IADECOLA, C. 2008. Neuroprotection by PGE2 receptor EP1 inhibition involves the PTEN/AKT pathway. *Neurobiol Dis,* 29**,** 543-51.

ZHOU, W. & FREED, C. R. 2005. DJ-1 up-regulates glutathione synthesis during oxidative stress and inhibits A53T alpha-synuclein toxicity. *J Biol Chem,* 280**,** 43150-8.

ZHOU, W., ZHU, M., WILSON, M. A., PETSKO, G. A. & FINK, A. L. 2006. The oxidation state of DJ-1 regulates its chaperone activity toward alpha-synuclein. *J Mol Biol,* 356**,** 1036-48.

ZIMPRICH, A., BENET-PAGES, A., STRUHAL, W., GRAF, E., ECK, S. H., OFFMAN, M. N., HAUBENBERGER, D., SPIELBERGER, S., SCHULTE, E. C., LICHTNER, P., ROSSLE, S. C., KLOPP, N., WOLF, E., SEPPI, K., PIRKER, W., PRESSLAUER, S., MOLLENHAUER, B., KATZENSCHLAGER, R., FOKI, T., HOTZY, C., REINTHALER, E., HARUTYUNYAN, A., KRALOVICS, R., PETERS, A., ZIMPRICH, F., BRUCKE, T., POEWE, W., AUFF, E., TRENKWALDER, C., ROST, B., RANSMAYR, G., WINKELMANN, J., MEITINGER, T. & STROM, T. M. 2011. A mutation in VPS35, encoding a subunit of the retromer complex, causes late-onset Parkinson disease. *Am J Hum Genet,* 89**,** 168-75.

ZIMPRICH, A., BISKUP, S., LEITNER, P., LICHTNER, P., FARRER, M., LINCOLN, S., KACHERGUS, J., HULIHAN, M., UITTI, R. J., CALNE, D. B., STOESSL, A. J., PFEIFFER, R. F., PATENGE, N., CARBAJAL, I. C., VIEREGGE, P., ASMUS, F., MULLER-MYHSOK, B., DICKSON, D. W., MEITINGER, T., STROM, T. M., WSZOLEK, Z. K. & GASSER, T. 2004a. Mutations in LRRK2 cause autosomal-dominant parkinsonism with pleomorphic pathology. *Neuron,* 44**,** 601-7.

ZIMPRICH, A., MULLER-MYHSOK, B., FARRER, M., LEITNER, P., SHARMA, M., HULIHAN, M., LOCKHART, P., STRONGOSKY, A., KACHERGUS, J., CALNE, D. B., STOESSL, J., UITTI, R. J., PFEIFFER, R. F., TRENKWALDER, C., HOMANN, N., OTT, E., WENZEL, K., ASMUS, F., HARDY, J., WSZOLEK, Z. & GASSER, T. 2004b. The PARK8 locus in autosomal dominant parkinsonism: confirmation of linkage and further delineation of the disease-containing interval. *Am J Hum Genet,* 74**,** 11-9.